Transactions

of the

ASME

April, 1949

VOL. 71, NO. 3

Transactions

of The American Society of Mechanical Engineers

Published on the tenth of every month, except March, June, September, and December

---

Published monthly by The American Society of Mechanical Engineers. Publication office at 20th and Northampton Streets, Easton, Pa. The editorial department is located at the headquarters of the Society, 29 West Thirty-Ninth Street, New York 18, N. Y. Cable address, "Dynamic," New York. Price $1.50 a copy, $12.00 a year for Transactions and the *Journal of Applied Mechanics*, to members and affiliates, $1.00 a copy, $6.00 a year. Changes of address must be received at Society headquarters three weeks before they are to be effective on the mailing list. Please send old as well as new address.... By-Law: The Society shall not be responsible for statements or opinions advanced in papers or...printed in its publications (B13, Par. 4)....Entered as second-class matter March 2, 1928, at the Post Office at Easton, Pa., under the Act of August 24, 1912....

Thermal Environment of Railroad Passenger Cars

By K. A. BROWNE[1] and S. G. GUINS,[2] CLEVELAND, OHIO

Appreciating the limitations imposed by conventional railroad heating and air-conditioning equipment on thermal environment from the passenger viewpoint, the Chesapeake and Ohio Railway undertook a research program to develop means for improving substantially the thermal comfort in cars. Various controls and their components were investigated. Radiant panel and floor heating and cooling were tested in a car in the Budd Company cold room and on the road. Then the car was completely re-equipped with means for accomplishing the objective and put into service test. It features effective control of humidity in the summer, no recirculating air in the overhead system, forced-convection heating and cooling panels, low temperature gradients, and lack of draft. This paper is a progress report on the project, which is continuing.

At the time when the Chesapeake and Ohio Railway placed inquiries for extensive replacement of passenger cars, investigation was made of the major manufacturers of heating and air-conditioning equipment as to their latest developments. Of the responses received, equipment by Vapor Car Heating Company and Minneapolis-Honeywell Regulator Company was available for immediate comparison. Additionally, their systems incorporated new trends of thinking in respect to air conditioning and controls compared to prewar installations; consequently a test program was decided upon to evaluate the merits of each system, utilizing C and O Coach No. 830 for the heating tests. To save time, the car was divided laterally by a partition running from floor to ceiling and the vapor system was installed at the *A* end of the car, while Minneapolis-Honeywell was located at the opposite end. Both applications were made by Pullman-Standard Car Manufacturing Company, and, for simplicity of installation, certain items were carried throughout the length of the car. The distinguishing feature was the modification of the side heater box. The side-wall surfaces were enclosed in side-wall convectors which also acted as radiant surfaces, although the actual amount of radiant heat was small compared to the total heat output of the convectors, shown diagrammatically in Fig. 1. The floor was provided with a separate heat source, because the side heat elements were completely enclosed thus cutting off the usual radiation to the floor.

The Vapor Car Heating Company installed an improved version of its cycle-modulation system in operation on many postwar passenger cars. The side-wall surfaces were of the unit radiation type, consisting of an inner pipe to which steam was admitted and an outer pipe with fins through which the steam condensate was returned. In order to achieve a wide range of temperature control of the side-wall surfaces, steam condensate was retained in the outer pipe, and its temperature was controlled by metering steam by slugs to the inner pipe, thus affording temperature range of from 120 F to 200 F. The same pipes, less fins, were placed under the floor, see Fig. 2 (*a*). The system as a whole was regulated by an automatic-control panel which included an interlocking arrangement with the refrigeration cycle, so that cooling or heating could be supplied automatically without attention from the crew. The cycle modulation control, shown in Fig. 3 diagrammatically, provides a means of metering steam into any heating surface by intermittent on-off action with a variable division of time between action to control the total heat admitted.

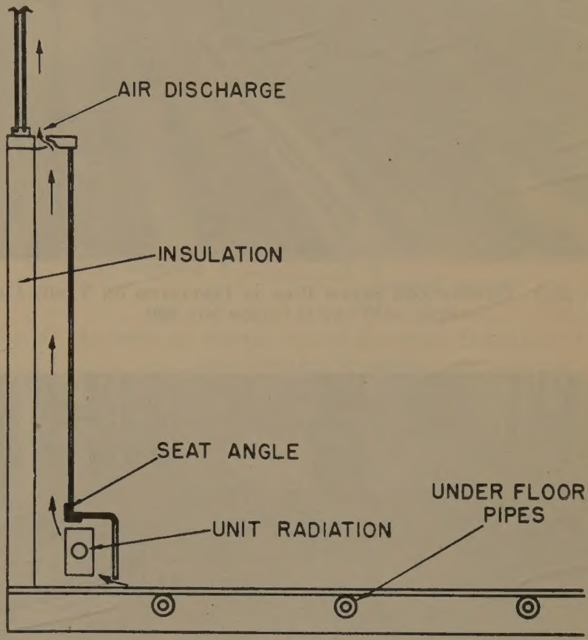

Fig. 1 Side-Wall Convector Construction Diagram

The Minneapolis-Honeywell Regulator Company system was similar to that of Vapor Car Company's in its use of side-wall paneling and underfloor piping, Fig. 2 (*b*), the rest of the application being entirely different.

The heating medium of the Minneapolis-Honeywell system was a circulating liquid (tetracresyl silicate) to allow a very uniform and close control of temperature. The side-wall surface had a large fin area to permit lower liquid temperatures, and yet supply the required thermal output. A 9-ft model of the side wall was tested by The Trane Company of LaCrosse, Wis., to determine proper capacity, air flow, and air-discharge temperatures. On the basis of The Trane Company tests, the side-wall panel in Car 830 was designed and installed by Pullman-Standard. Fig. 4 shows the laboratory installation of the side panels, with galvanized tanks packed with ice to simulate cold windows. One of the interesting results of this test was that the panel temperature varied only slightly over the entire range of convector output. The information given in Fig. 5 indicates the fallacy of trying to control space temperature solely by sensing panel temperature, as

[1] Research Consultant, President's Office, The Chesapeake and Ohio Railway Company. Mem. ASME.

[2] Project Engineer, Office of Research Consultant, The Chesapeake and Ohio Railway Company. Jun. ASME.

Contributed by the Railroad Division and presented at the Semi-Annual Meeting, Milwaukee, Wis., May 30–June 5, 1948, of The American Society of Mechanical Engineers.

Note: Statements and opinions advanced in papers are to be understood as individual expressions of their authors and not those of the Society. Paper No. 48—SA-45.

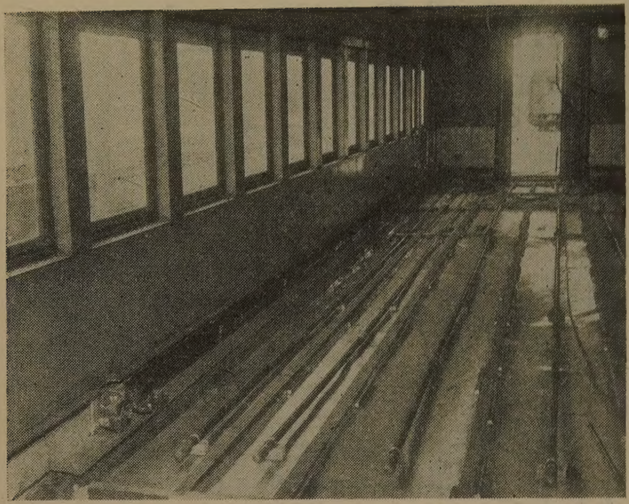

Fig. 2(*a*) Underfloor Steam Pipe as Installed on Vapor Car Side of C and O Coach No. 830

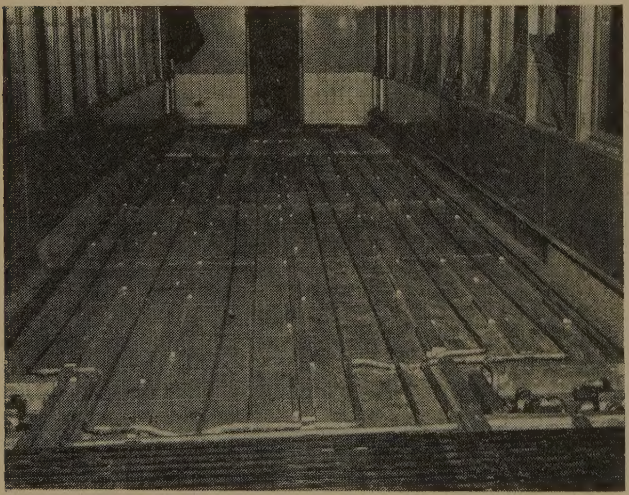

Fig. 2(*b*) Underfloor Liquid-Carrying Heating Pipes on Minneapolis-Honeywell Side of C and O Coach No. 830

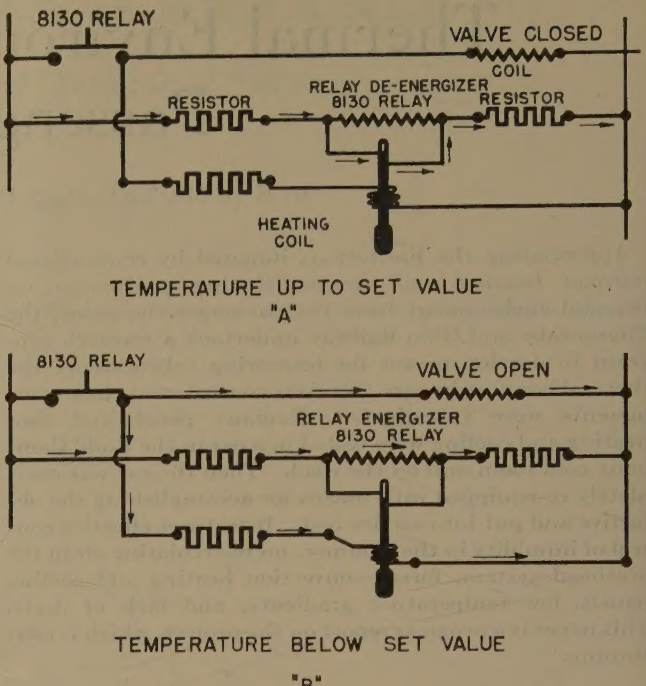

Fig. 3 Vapor Circuit for Cycle Modulation

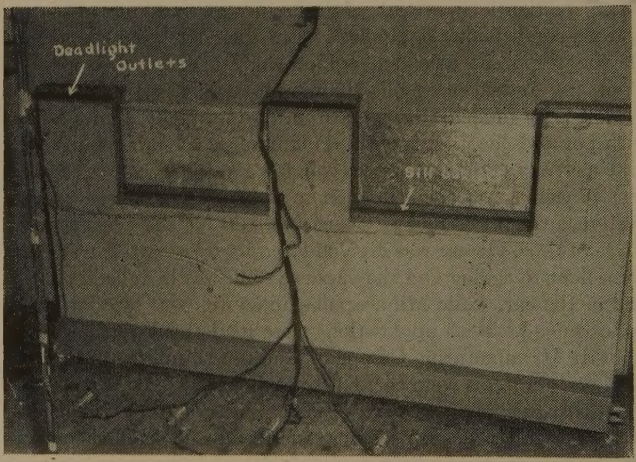

Fig. 4 Original Test Panel as Installed at Trane Company Plant

attempted on the first test runs. Fig. 6 shows schematically the cycle of liquid flow. A pump and a steam-to-liquid heat exchanger, located under the car, provided forced circulation and heat source. An electrically operated mixing valve determined the addition of heat from the exchanger and established the liquid circuit temperature. Independent control was applied to each side wall and floor from one exchanger.

Minneapolis-Honeywell controls are designed around the principle of a Wheatstone bridge; hence it uses resistance-wire thermostats instead of the usual mercury tubes. An example of a Minneapolis-Honeywell control circuit is presented in Fig. 7. The bridge itself consists of four legs connecting at points *A*, *B*, *C*, and *D;* the legs *A D* and *B C* are formed by the thermostats, the resistance of which changes with surrounding temperature. The other two legs con ist of fixed and adjustable resistances, one of the adjustable resistances being located on the panel and used to change the control settings if it is desirable, and the other is adjusted by the position of the motor so that the motor opens only enough to supply the necessary heat. When the temperature is below or above that for which the controls are set, the bridge becomes unbalanced and the current flows through points *B* and *D* to the amplifier and energizes the relay *E* or *F* to change the position of the motor-operated valve to adjust the supply of heat into the surfaces. Depending upon the way the bridge is unbalanced, the direction of the current to the amplifier is determined, and the proper relay is energized. The resistances in the bridge are so selected as to distribute the authority between the thermostats used.

Additionally, the two systems differed in the distribution of control zones. Vapor was zoned for lower temperature in the men's room, higher in women's lounge, and a third different temperature in the car body. The Minneapolis-Honeywell Company divided the car into two zones lengthwise, each side of the car with its own independent set of controls, in order to compensate for solar gain and wind effect. Our first series of tests did not give sufficient data to determine the effect of compensation for the solar gain.

The overhead equipment was common to both systems; how-

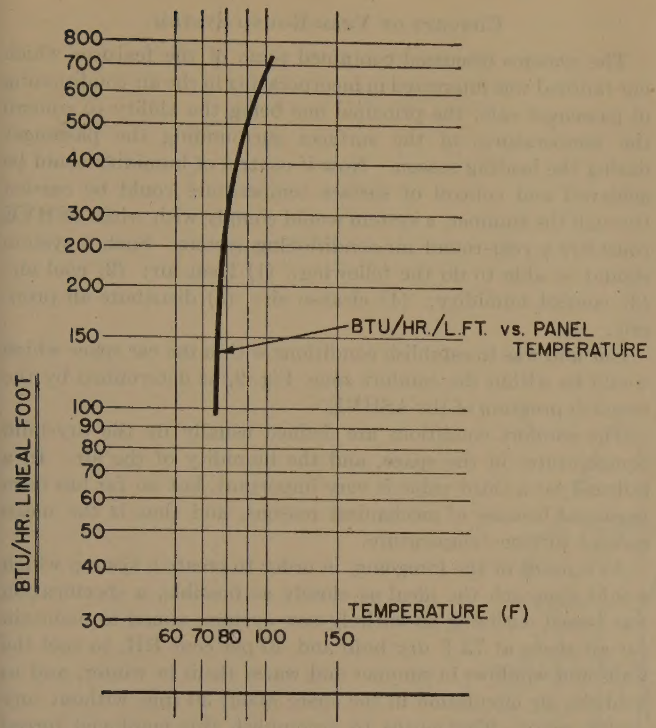

Fig. 5 Btu per Hour per Lineal Foot Versus Panel Temperature

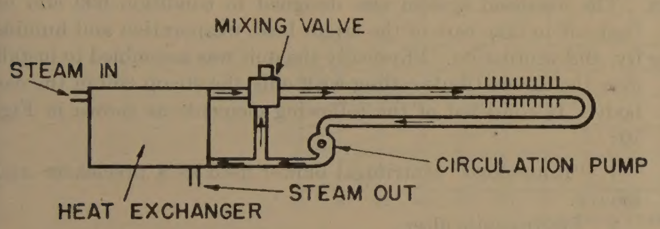

Fig. 6 Diagram of Minneapolis-Honeywell Heating Equipment Utilizing Liquids as Heating Media

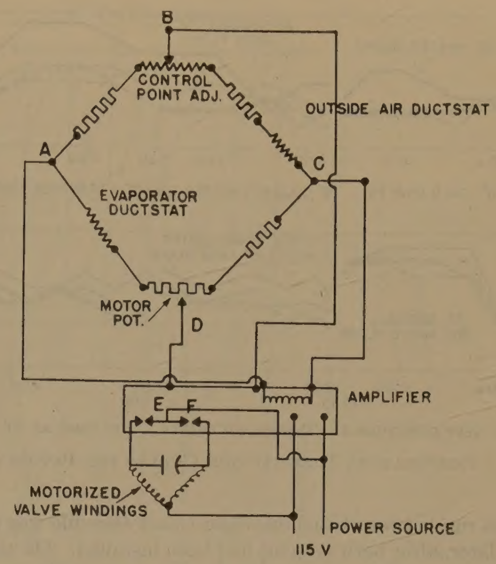

Fig. 7 Example of Minneapolis-Honeywell Regulator Company Control Diagram

ever, an arrangement was made to enable independent use of several different control valves. In addition to the Vapor and Minneapolis, a Fulton-Sylphon self-contained valve was installed; thus a comparison was made between the performance of all the valves then available.

Instrumentation

In order to get a good check on temperature distribution throughout the car space, and also to record temperature changes on the heating surfaces, a Brown Instrument Company recording potentiometer was used. The car was divided into planes $^1/_6$, $^1/_3$, $^2/_3$, and $^5/_6$ of the length of the car, measuring from the blower end of the car. This arrangement gave two check planes in each half of the car. In each plane, thermocouples were located 6 in., 48 in., and 60 in. from the floor, 6 in. away from the wall, on both sides of the car. Thermocouples were also located under the seats near the aisles. The foregoing arrangement gave checks on temperature distribution in planes that were longitudinal, lateral, and vertical. Additional couples were placed on the heating surfaces, at all thermostat locations, and in outdoor air. In all, there were 96 thermocouples placed on the car, with 48 couples devoted to each system. The temperatures at each thermocouple location were recorded at about five-minute intervals on a continuous tape. A steam pressure gage was used as a check on steam supply and a humidity recorder was used with little result.

Test Procedure

Road tests were made between Chicago, Ill., and Petosky, Mich., and between Cincinnati, Ohio, and Charlottesville, Va. As both installations were not completed at the same time, only Vapor Car Heating Company system was tested on the run to Petosky. Two round trips were made. The first day the weather was very bright and warm, no heat being required until late in the evening. At that time performance was similar to that of a standard system with a noticeable temperature difference between floor and ceiling.

The second day the temperature was dropping continuously from 60 F to 15 F, providing good test conditions.

Table 1 gives temperature settings in the car, which were made in an attempt to determine ultimate settings of various control points and the quantity of circulated air required.

TABLE 1 TEMPERATURE SETTINGS

			Overhead air		
Floor temp, deg F	Panel temp, deg F	Overhead-air temp, deg F	Fresh, cfm	Recirculating, cfm	Remarks
A 85	85	65	600	1200	Cold
B 80	85	68	600	1200	Cool and drafty
C 80	85	70	600	1200	Warm but drafty
D 80	85	..	0	0	Very comfortable
E 80	85	70	600	0	Cool draft
F 80	85	75	600	0	Very comfortable
G Off	85	75	600	0	...

As shown by the curves, Fig. 8, there is a scattering of space temperatures for settings *B* and *C*; setting *D* gave a remarkable feeling of comfort, but no ventilation. To determine the overhead-air temperatures that would simulate comfort conditions of setting *D*, settings *E* and *F* were then tried, providing a conventional amount of outdoor air, but with no recirculation, setting *F* giving the better result.

Setting *G* was tried to find out if side walls alone could supply sufficient heat to maintain car temperature. Unfortunately this was done at night between Grand Rapids and Chicago, the train line being broken for three 20-minute periods. Because the overhead blowers were not shut off, the car was overcooled and no conclusion could be made.

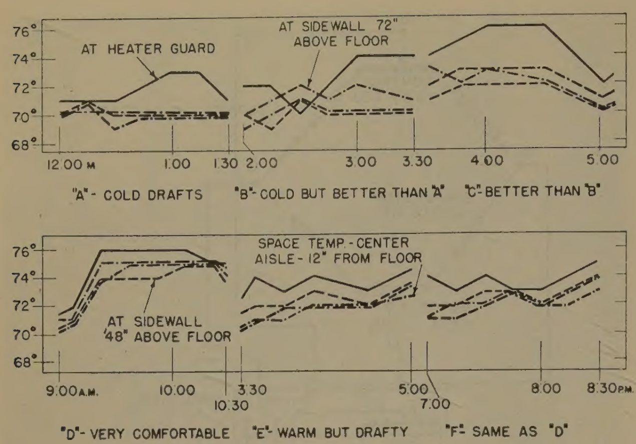

Fig. 8 Temperature-Distribution Curves for Petosky Run

A test run between Cincinnati and Charlottesville was made a month later, after both systems had been installed. On that run it was raining and the temperature was around 50 F most of the time, except for an hour in the mountains near Hinton, W. Va., when it dropped to 32 F. Only two conclusions could be made from that run:

1 That, regardless of type of control system, if the overhead air entered the car at other than car-space temperature, the evenness of space temperature was upset, which resulted in stratification.

2 That if a temperature for the overhead is selected and is to be kept constant, any one of the three available control valves performs equally well in maintaining that temperature.

Cold-Room Tests

After the Charlottesville run, it was decided that the weather was such that no successful heating tests could be conducted on the road. Consequently an arrangement was made to send the car to the Budd Company's cold room in Philadelphia where the temperatures could be controlled, and tests could be made at temperatures of 0 F, even in summer months. In the cold room, two series of tests were conducted: (1) Heat required to maintain set temperature conditions within the car were determined at several outdoor temperatures. These tests gave the steam requirements of both systems and its distribution to various components. From these data a plot was made from which heating requirements for any desired condition could be determined and, inasmuch as this plot is a straight line, cooling requirements could be obtained from the same information by extending the line to the cooling region.

Series (2) tests gave us a study of control response. The controls were set to maintain a given space condition and then the outdoor temperature was changed from 70 F to 0 F within 4 hr, or as quickly as the refrigeration equipment of the cold room would permit. The cold-room temperature was then allowed to drift up to 70 F.

These tests indicated that controls of both systems responded equally well, which led to a general conclusion that in so far as heating is concerned, there is little to choose between the two proposed systems. The radiant convector which was placed over the heating surfaces in both cases seemed to act as a lag-controlling device; this levels the changes in the temperatures of the heating surface into which steam is injected periodically and improves the slow response inherent in a system with large body, such as a liquid system, and what is really important, makes the car more comfortable to the passenger.

Concept of Year-Round System

The systems discussed contained some of the features which our railroad was interested in incorporating in the air conditioning of passenger cars, the principal one being the ability to control the temperatures of the surfaces surrounding the passenger during the heating season. Now if control of humidity could be achieved and control of surface temperature could be carried through the summer, a system would comply with what ASHVE considers a year-round air-conditioning system. Such a system should be able to do the following: (1) Heat air; (2) cool air; (3) control humidity; (4) cleanse air; (5) distribute air properly.

Our aim was to establish conditions within the car space which would be within the comfort zone, Fig. 9, as determined by the research program of the ASHVE.

The comfort conditions are defined usually by the dry-bulb temperatures in the space, and the humidity of the air. In a railroad car a third value is very important, but so far has been neglected because of mechanical reasons, and that is the mean radiant surface temperature.

As a result of the foregoing, in order to create a system which would approach the ideal as closely as possible, a specification was issued outlining an entirely new system, aimed to maintain car air space at 75 F dry bulb and 40 per cent RH, to cool the walls and windows in summer and warm them in winter, and to hold the air circulation in the space about 30 fpm without any drafty spots. The means to accomplish this employed forced convection in the walls and over the windows with overhead air supply of fresh air only.

The overhead system was designed to condition 600 cfm of fresh air to take care of the latent load, evaporation and humidity, and ventilation. Physically the unit was assembled to install over the car-vestibule ceiling with only the steam coil in the car body. It consisted of the following elements as shown in Fig. 10:

1 "Roto-clone" centrifugal blower used as a precleaner and blower.
2 Electrostatic filter.
3 Air-to-air heat exchanger.
4 Evaporator coil (direct-expansion coil).
5 Steam-heating coil.

The capacity of the evaporator coil was such that air passing through it was cooled to 41 to 45 F, which, when reheated by the exchanger and steam coil to 75 F, resulted in air entering the car body at 30 per cent to 38 per cent RH. Consequently this air was capable of absorbing moisture discharged by the passengers into the car body and still maintain the space relative humidity below 50 per cent.

Two alternatives were considered for absorbing the sensible-heat load by the side walls: (1) Separate surfaces, one for heating with steam direct and the other for cooling, and both in series to the air flow is obvious. (2) A method using circulating liquid for both the heating and cooling operation, thus utilizing the same side-wall surface. This approach was adopted because it offered stability and refinement of temperature control. A special air-induction system was designed to maintain a steady upward flow of air through the side-wall convectors regardless of the temperature of the heat-exchanger surface, Fig. 11. Side walls, designed to be completely independent from each other, consisted of the following, Fig. 12: (1) Side-wall surfaces; (2) circulating pump; (3) liquid chiller (Freon used for coolant); (4) steam heat exchanger; (5) primary-air blower; (6) primary-air duct and jets. Items 2, 3, 4, and 5 were mounted in a special cabinet under the car, together with control valves for the heat exchangers. Fig. 13 shows the actual cabinet assembly.

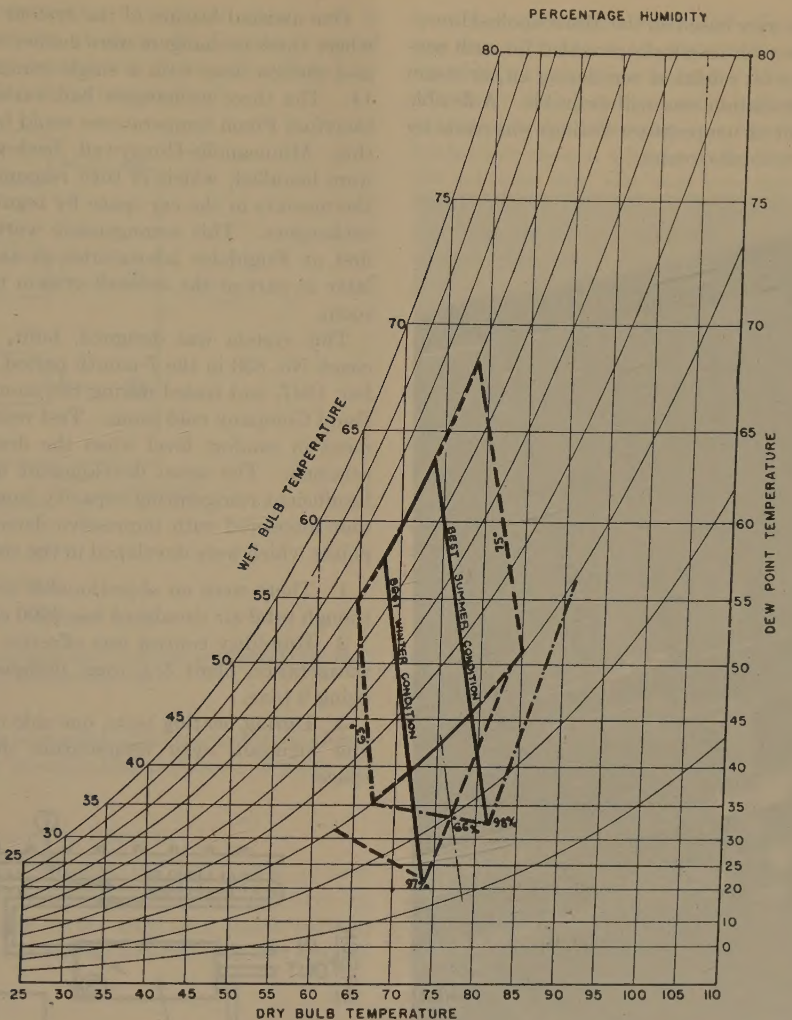

Fig. 9 Comfort Limits as Defined by ASHVE Superimposed on Psychrometer Chart

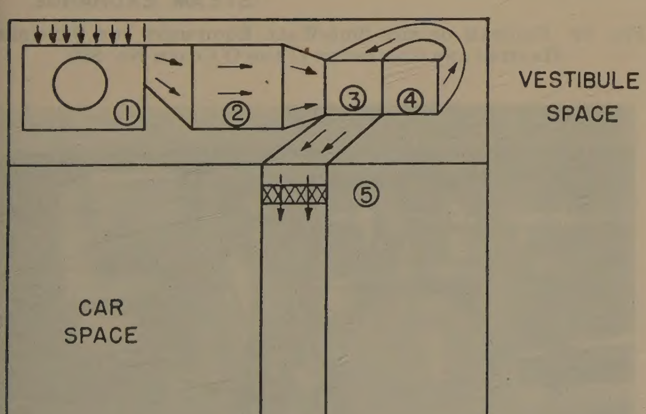

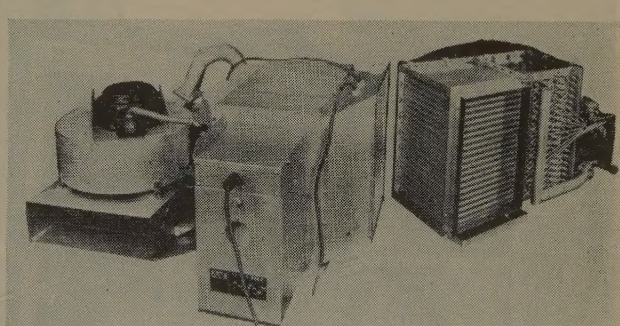

Fig. 10 Overhead Equipment for C and O Coach No. 830
(Actual weight of assembly = 275 lb.)

Controls for this system were based on the Minneapolis-Honeywell Company's principles with interlocks provided for such contingencies as lack of steam for reheat of ventilating air, or steam failure in winter when ventilation was still desirable. A flexible arrangement in adjustment of temperature settings was made by placing variable resistances in all circuits.

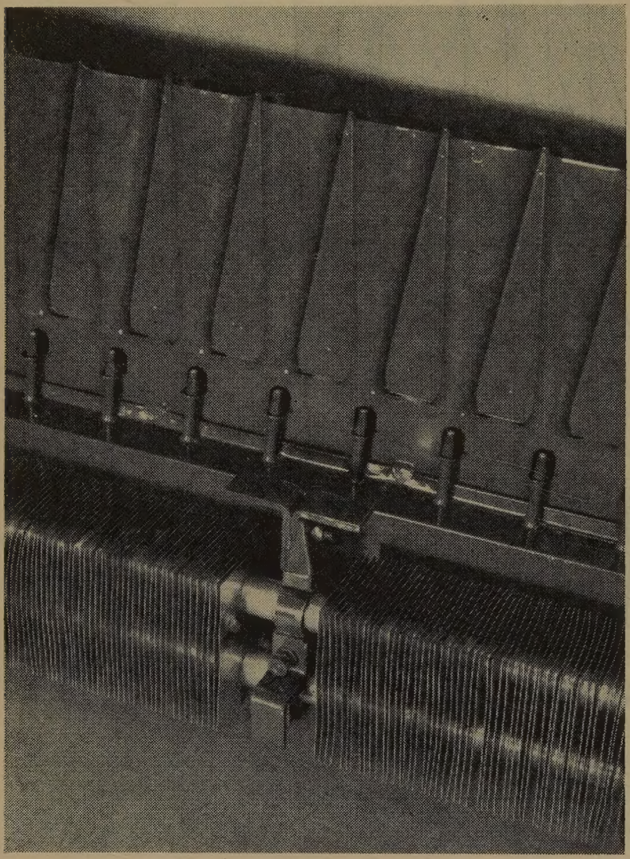

Fig. 11 Side-Wall Equipment Showing Air-Induction System Used in Present Installation of C and O Coach No. 830

One unusual feature of the system was the refrigeration cycle, where three exchangers were connected to the same Freon liquid and suction lines with a single compressor-condenser unit, Fig. 14. The three exchangers had variable-load requirements and therefore Freon temperatures could be different. To accomplish this, Minneapolis-Honeywell back-pressure motorized valves were installed, which in turn responded to the demands of the thermostats in the car space by regulating Freon pressure in the exchangers. This arrangement worked out quite successfully, first at Frigidaire laboratories as an independent system, and later as part of the over-all system in the Budd Company cold room.

This system was designed, built, and installed in C and O coach No. 830 in the 7-month period between June and December, 1947, and tested during the month of January, 1948, in the Budd Company cold room. Test results confirmed the improvement in comfort level when the desired space conditions were attained. The usual development difficulties with details and insufficient refrigerating capacity from the Model D Waukeshaw unit interfered with impressive demonstrations. The favorable points which were developed in the cold-room tests are as follows:

1 There were no objectionable drafts in the car space, even though total air circulated was 3000 cfm.

2 Humidity control was effective within the capacity of the refrigeration plant $5^1/_2$ tons, designed capacity for the system being 9 tons.

3 During heating tests, one side can carry total heating load and maintain even temperature distribution within the car space.

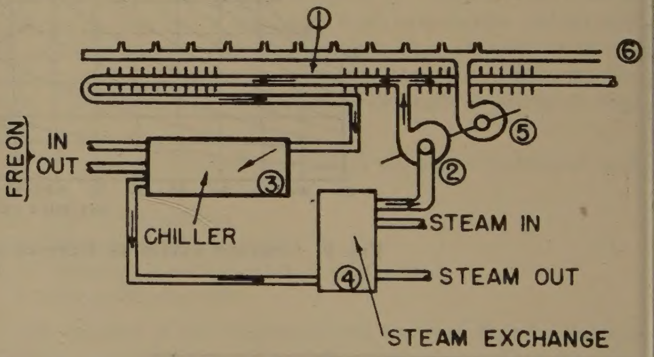

Fig. 12 Diagram of the Side-Wall Equipment for Sensible Heating and Cooling in C and O Coach No. 830

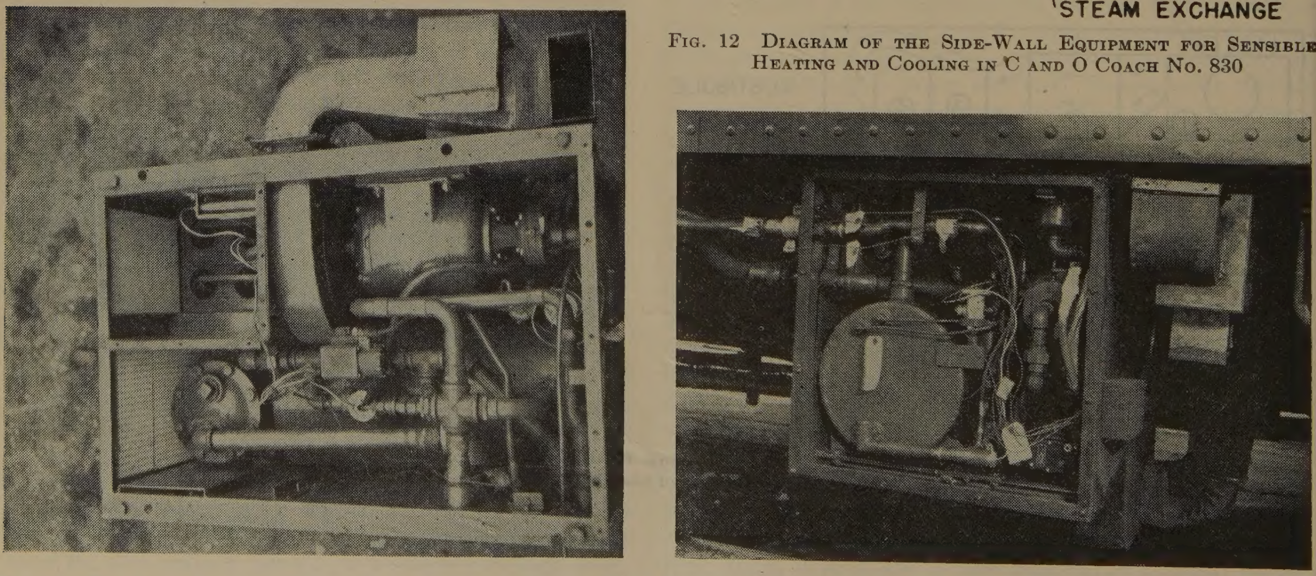

Fig. 13 Undercar Cabinet Giving Disposition of Motor With Pump and Blower and Chiller Both Mounted Horizontally; Steam Heat Exchanger Mounted Vertically in Back and Control Valves

The system failed in its stand-by requirements, which were to maintain car-space temperature at about 60 F without use of electrical energy. Stand-by heating was to be accomplished by gravity flow of hot liquid, but never materialized.

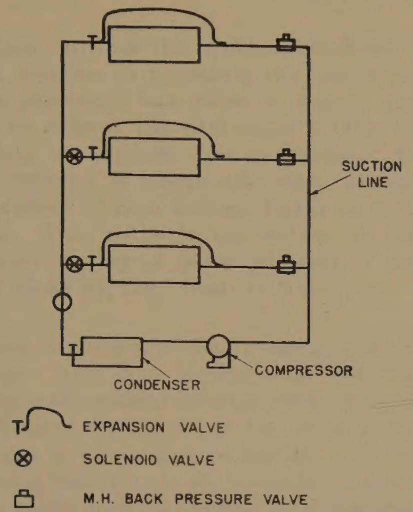

FIG. 14 DIAGRAM OF REFRIGERATION CIRCUIT AS INSTALLED IN C AND O COACH No. 830

The assignment of the car to regular passenger service is affording an opportunity to study the operating problem and passenger reactions.

Discussion of Results

The induced air circulation through the wall panels on each side of the car produces a definite flow up the walls and over the ceiling, producing a down-flow in the aisle area, which parts at the floor and moves across the floor at 10 to 20 fpm, and into the heating surface at the wall. The effectiveness of this circulation was unanticipated and it was found unnecessary to supply additional heat in the pipes under the floor as this was demonstrated effectively during the test, when one side of the car had no heat supply and the other side was carrying the entire load. The heated side showed a floor temperature only 3 deg F higher than the unheated side, and both were maintained at a comfortable level. This circulation is unnoticeable as a draft to passengers anywhere in the car, although there is a local draft over the window glass which can be felt if the hand is placed near the glass.

It is no news that dry air is more comfortable than cooler but humid air and this system has definitely accomplished the former with results that the car-space conditions have been noticeaby improved even at space temperature of 80 F. The circulation within the body is sufficient to provide evaporative cooling but it is not noticeable as a draft. The automatic transition from heating to cooling is effective without any notice on the part of the passengers and hardly any indication on recordings. The feel of thermal environment is definitely improved over that of the conventional system where all cooling load is handled by an overhead system of opposite circulation, and heating is handled by "hot boxes" along the floor.

It is freely admitted that the system now installed on Car 830 is complicated and relatively expensive; however, the system is now undergoing redesign to simplify the equipment drastically without losing any of the advantages obtained and provide adequate stand-by and emergency heating.

Acknowledgment

We wish to express thanks to the engineering departments of The Trane Company and Minneapolis-Honeywell Regulator Company for their valuable assistance in making our latest installation possible, and to Mr. H. F. Peterson of the Pullman-Standard Car Manufacturing Company for his valuable advice and assistance in adapting our ideas for installation.

Visual Passenger Comfort

By Brooks Stevens,[1] Milwaukee, Wis.

The author outlines the problem confronting the railroad-train designer in providing the comfort and beauty which the passenger has come to expect, and which is necessary to attract his patronage in the highly competitive field of modern transportation. The over-all design conception is discussed, with decorative treatments described of such famous trains as the Olympian-Hiawathas. The author's conception is given of the facilities and styling of passenger cars of various types which will make up the "train of tomorrow."

In treating the subject of visual passenger comfort, or railroad passenger equipment styling, the industrial designer, counseling the railroad industry today, feels called upon to cite the stringent limitations of the problem at the outset. Working alone or with a staff, he becomes only one link in the chain of events leading up to the complete design of any product. He depends wholly upon the co-operation and support of management, engineering, production, sales, and advertising. Without them, and their knowledge and experience pertinent to their own problems, he could never make his contribution to the ultimate solution.

The Hold to Tradition

The industrial designer's first step in any program is to consult with these important departments for an accurate idea of the limitations and the latitudes. As important as is this initial knowledge of limitations, the designer must approach this meeting and discussion with a great deal of tact and diplomacy. He must be extremely careful to prevent this open discussion of limitations from being so complete that there is no latitude for change over that which has always been done before. A certain amount of this conservatism and reluctance to change occurs in any product-design picture, but it must be said that in the railroad field this characteristic is particularly pronounced. In general, the limitations which must be considered in the design of railroad passenger equipment and the styling of locomotives, are the materials involved, initial costs, safety, maintenance, traffic handling, legal complexities, tradition, and obsolescence.

The Train-Styling Problem

In the general architecture of the railroad train as a whole, and the railroad passenger car individually, the designer must deal with a rather inflexible set of dimensions and proportions. The railroad car is long and narrow, mounted relatively high on swivel trucks, and a necessary gap exists where cars are coupled together in a train. The cross-sectional contours cannot be deviated from too widely, and a definite and general similarity with older equipment must be maintained so as not to make obsolete cars 10 and 20 years old which are still serviceable. It is naturally the designer's dream, in the creation of a new train, to give it a theme, design it as a unit, and have it remain intact during its service. However, unavoidable situations occur in railroading today, demanding the occasional use of older equipment in emergencies, and this causes an aesthetic jolt in many of our up-to-date trains.

In discussing the limitations of the exterior design as it pertains to eye appeal or passenger appeal, the designer can work with the surface styling of the outer skin by the use of corrugated sections, stainless steel, applied trim, skirt contours, window spacings and shapes, and colors. The more modern trains today have fallen roughly into two categories, namely, the bright, stainless-steel treatment, fluted or otherwise, and the painted steel car. One manufacturer has practically established a trade-mark with the use of fluted stainless side walls. In the painted steel versions, we have fallen into a logical but rather stereotyped pattern of horizontal bands of color, beginning with the traditional letterboard and varying in width and proportion over the rest of the surface. By now, most of the top trains in the country are following the general pattern of horizontal stripes running through the windows and letter board, leaving only a color scheme for individual identity.

Although I do not believe in pseudo-streamlined garish paint schemes as the answer, I feel that infinitely more individual identity and passenger appeal can be injected into the railroad-car paint styling today. In the design of the new Olympian-Hiawathas for the Chicago, Milwaukee, St. Paul and Pacific, we have injected a "new look" in paint styling. Those who as yet are not familiar with this new equipment will be interested to know that we have departed from the traditional horizontal bands, and in working with the colors of the Milwaukee Road—harvest orange and royal maroon—we have created individual identity that will become recognizable on the spot as the trade-mark of the Olympian-Hiawatha trains. The principle of the paint scheme is based upon the fact that visually it tells the story of the interior, architecturally, of the car. The average car is broken up into three areas, i.e., the large central area, being the passenger area, with coach seats, sleeping sections in the Tour-a-lux car and roomettes, bedrooms, and compartments. The areas at each end are generally allocated to men's and women's lounges, and passageways from vestibules to the central passenger area.

The window pattern has been changed between the passenger area and what the designer refers to as the "utility" area. Rectangular windows are used in the passenger area, contrasting with portholes and elongated portholes in the vestibules and lounge rooms. The maroon horizontal panel embracing the main central passenger area is thereby divorced from the two end areas, which remain in the over-all orange field. A wide trim stripe, beginning under the portholes in the utility area, rises upward and over the central maroon panel, to return down again and carry under the portholes of the opposite end utility urea. With two cars butting together at the vestibules, we find an obvious continuous pattern of portholes or utility-type windows joining visually together, as well as the joining of the trim stripe. This combining of similar porthole patterns minimizes the necessary joint between the cars, making the surface appear more continuous. The reoccurrence of this pattern from car to car in a long train relieves the monotony of the already exaggerated continuous length of a group of cars, and, in turn, we have a strong individual pattern entirely original with this new train. At each vestibule door a large aluminum and maroon emblem is employed, carrying out the symbolic figure of Hiawatha.

[1] Industrial Designer, Brooks Stevens Associates.

Contributed by the Railroad Division and presented at the Semi-Annual Meeting, Milwaukee, Wis., May 30–June 5, 1948, of The American Society of Mechanical Engineers.

Individual car names are carried out in gold leaf and maroon edging in bold, modern script comparable to the locomotive lettering "Olympian-Hiawatha." All of the roofs of the equipment are painted in a dark sandy gray to offer the least possible change in appearance from dirt and weathering. The trucks and entire underbody are painted out in a dull shadow black to minimize their irregularity, which normally would detract from the sleekness of the upper car body. Deep superfluous sheet-metal skirting has been eliminated from these cars entirely in favor of maintenance, continued good appearance, and the elimination of the unnecessary load of ice and snow during the winter months.

Construction Costs, Safety, and Maintenance

To carry on with the limitations necessarily placed upon the designer, it is almost needless to point out that car costs must be held within reason. Many things, interesting and unique to the public, could be done with carte blanche or unlimited initial expense.

Safety must certainly come into the industrial designer's approach to the problem. His goal is to intrigue and please the passenger with the equipment, but it should not be at the expense of their safety and well-being. Many dangers lurk in the more aesthetic ways of styling lounge cars, diners, and even coaches. With the high speeds of today, we have sway, despite our great improvements in riding qualities and suspension design. Passengers may still be thrown against bulkheads, partitions, and furniture. One must be tremendously careful with the use of glass, sharp-cornered appendages, doorways, and the like. It is on important matters such as these that the designer depends heavily upon the experience and knowledge of the operating departments and the car builders' engineers.

The public can never know how important the consideration of maintenance must be in the design of this equipment. Some of the most beautiful things on paper will even pass the pilot-model stage successfully, only to become a miserable eyesore after a few thousand miles of use. Car-cleaning departments can be compared to professional dishwashers in a large restaurant, they never complete their task. They must do their work quickly and well in order to return an expensive piece of equipment to profitable operation in the shortest period of time. The same passenger who would be intrigued and overwhelmed with the beauty of certain interiors would be the first to scorn and criticize its shopworn appearance after it could not "stand the gaff" of disinterested public riders who had purchased tickets but who have very little interest in the railroad which owns the equipment. Railroad studies to date on passenger behavior reveal astounding facts. The habits and actions on the part of some passengers would be unbelievable if advertised to the general public.

Interior Design

Problems with traffic go further than riding habits and disregard of property. Great care must be given to seating comfort and interior design to minimize the risks of dissatisfaction, complaint with regard to lounging facilities, food and beverage serving, attendant behavior, and the like. Legal complications and lawsuits can arise from seemingly minor errors in design and construction. We must contend, too, with the fact that some human beings are so constituted as to provoke situations which would result in suit for financial gain.

Last but not least, in the limitation picture, we have tradition—something which I shall call "*train*dition" (precedent adherence). There is a definite leaning toward approaching the new car-design problem from the standpoint of materials, methods, and even shapes, with which there has been a long record of tried and proved experience and a definite desire to hold on to; to do it that way again—but just to change the color.

As an interesting and stimulating battle between tradition, convention, and the "new look" goes on, we find definite passenger acceptance of much of our good-looking equipment of today. In general, there is some flexibility in the interior plan of each car, based of course primarily upon maximum pay load with maximum comfort. The passenger today is not going to be satisfied with drab, monotonous, purely mechanical interiors which represent the zenith in fabrication, simplicity, and maintenance ease. The dark glossy woods of the past, with a shiny layer of varnish, drab plush fabrics, and "busy" flowered rug patterns, have given way to a greater use of color, woven patterned fabrics simplified-pattern carpeting, rubber tiles, linoleums, and individuality in color schemes between cars. Lounge areas for women can take on an individualized, feminine appearance, or the powder-room atmosphere; and for the men, the denlike masculinity of the club.

Homelike Atmosphere Desirable

Railroad-car equipment today can borrow, in a sense, from two other sources appealing to the passenger—the home, and some of the brilliant styling of the motorcar. A cross between these can be cleverly woven into the scheme so that the warmth and cheerfulness of the home, coupled with a dash of our most popular means of transportation, can combine to be both practical and attractive. The occasional use of carefully selected pictorial subjects for lounge-room areas, as well as passageways and bulkheads, can brighten and individualize any interior. It may be interesting in the future approach to coach bulkheads to use an etched plastic map of the route of the particular train, showing the key cities of interest, the stops, edge-lighted and with a light source following the route of the train slowed down to show the actual progress to scale, or with the city designation lighting up a few moments before each arrival. This would be very informative and useful to the passenger, as well as having definite decorative possibilities without extreme cost or mechanical problems.

The tendency for regimentation of seating is required functionally in the coach of today, but there are possibilities for breaking the monotony of the long narrow room with wall treatments, window spacings and shapes, and even color schemes of certain groups of seats. The latitude in wall coverings is expanding tremendously with the introduction of low-maintenance synthetic materials of the decorative melamine laminate types, as well as impregnated cloths, vinyl leather simulations, and many types of floor coverings. I do not believe in the use of high-gloss, hard-surfaced, enamel panels, or plastics, studded with stainless decorative moldings over every seam and joint. Despite the chances to use warm pastel colors, these interiors are apt to become cold and kitchenlike in their appearance. Wood grains in the blond finishes can go a long way toward softening this effect and increasing the homelike character, but the use of genuine wood with lacquered or varnished surfaces is obviously subject to brutal wear and tear. Melamine laminates can be obtained in a tremendous variety of wood grains and patterns which have the surface toughness to withstand hobnailed boots, metal-cornered suitcases, and other damaging forces.

Lighting can play a most important part in the interior aesthetic scheme, both from the standpoint of function and decoration, and I believe that the surface has only been scratched in this particular category. In connection with light and vision, it is felt that we will continue to increase the size of windows and minimize the width of intermediate pillar posts. We have seen experimental samples of economically heated window glass which will probably become available in the future as a means of doing away with the "cold shoulder."

In lounge and club cars today there is a tremendous opportunity for individual styling. Seating need not be regimented with chairs lined upon both sides of an aisle,but can be arranged in the smartest restaurant and night-club groupings, with changes in fabric and color schemes so planned as to offer privacy, different-sized groupings, and even improved scenery appreciation. The use of living plants and hardy green foliage can go a long way toward styling and softening the interiors of observation and club cars. Edge-lighted plastics, decorative lighting, colorful and cheerful patterns in fabric, and interesting architectural treatments can make the lounge car a great part of the answer to the threat of high-speed air transport. The traveler who is on a semi-pleasure trip and does not have to rush to make a business appointment at a distant point, as well as those who "have to be there" at an appointed time, can enjoy the luxuries of a well-appointed train.

In the ultimate styling of the entertainment car, it is this designer's opinion that uniforms be designed to harmonize with the general theme. The treatment of menus, napkins, and even beverage coasters, can all be made to blend to tell a given story. Radio reception, recorded music selections, and news announcements already are realities. Ship-to-shore telephone facilities are on the horizon, and we have had motion-picture cars in experimental stages for some time. No doubt the near future will bring even television to mobile rail equipment.

Styling the Dining Car

Dining cars can also take on a higher degree of style and cleverness in design, as compared to the standard coaches. Again, the regimentation of conventional seating can be varied for more interesting effects to increase scenic vision and the accessibility for entry and exit. All of the latitudes of architecture, materials, colors, lighting, and the like, are equally applicable to the modern diner. It might be interesting to prophesy that with some of the functional beauty of the modern stainless-steel galley, we might arrange for windowed passageways through which passengers could observe the preparation of food. In many a fashionable restaurant today, the open-to-vision barbecue and food preparation is capitalized upon by the management which is proud of its cuisine.

The Sleeping Car of Tomorrow

In the sleeping car of tomorrow, the designer must work with the usual limitations of space and flexibility, but with a definite goal of creating a pleasant individualized interior and a definite departure from the cell-like appearance of many cars today. In the room car of tomorrow, it is this designer's opinion that each room could have its own color scheme, fabric patterns, and pictorial theme. It even would be possible and advisable to take the most predominating color and bring it outside the room on the surface of the door to individualize and eliminate the monotony of the long narrow hallway. This, too, would go beyond just the numbers or letters for room identification.

Berth mechanisms will be simplified and improved, and the use of folding individual chairs is becoming more popular. Toilet-facility annexes are welcome realities. Observation lounge-car areas can be treated in much the same manner as a club car, but with even greater emphasis on vision. The new solar lounge for the Olympian-Hiawatha and the Twin Cities Hiawatha trains features one solution to this problem with its aerodynamically contoured safety-glass dome, built into the single level contours of the conventional car, offering 180 degrees panoramic vision in the horizontal plane to the rear, and 180-degrees in the vertical plane, with sufficient structural strength to combat roll-over and rear-end collision. The use of heat and glare-resistant glass will minimize the conditions in bright weather and offer the maximum visibility for an appreciation of the countryside.

Other Features to Be Expected

A further use of transparent roof areas might also be used in dining cars or lounge cars by fitting similar heat and glare-resistant glass into the cove area of the roof only, which would not remove the center air-conditioning duct work from the car, yet would allow passengers to glance upward to view mountainous scenic areas, cloud formations, and the like. This treatment could be used in portions of the lounge cars and diners only, to allow it to be there for those who wish to make use of it and to have more sheltered areas in the same car for others.

Soft cove lighting, centrally located on the wall, in the down direction only, will offer reading light without making mirrors of the ceiling glass areas at night. Rheostating of this light will permit full damping for moonlight observation at night, with low courtesy lights built into the furniture for passenger safety.

Railroad travel should be made as interesting and pleasant as possible at the lowest possible cost. If the surroundings are pleasant, the service and facilities good, there should be a proportionate share of allegiance and attendance on the part of the public which would choose this pleasant means of relaxation as compared to high-speed air transport. Railroad equipment is sizable, expensive, and must be used profitably over a long period. It should not be freakish in design, and should not involve momentary fads and trends in its execution because of the obsolescence problem.

Railroad Passenger Comfort—Decibel Level

By W. A. JACK,[1] MANVILLE, N. J.

Improvement in comfort may be realized by lowering the noise level to which the passenger is subjected. The author outlines the scientific approach to the noise problem, giving the analytical formulas essential to its study. These principles are then applied to railroad transportation problems.

Introduction

ORIGINALLY the passenger sought transportation at a speed faster than walking. Given a mode of travel which he knew to be as fast as possible for the age, or as fast as his purse would allow, he began to be interested in other aspects of the conveyance than its mere speed. The railroad passenger of today knows that modern techniques and materials are available to give him transportation in comfort. Whether he chooses instead to use an airplane, bus, or private automobile depends on the facilities available, the ease and pleasure with which he can use them, and the cost to him in time and money. Competition between the different types of transportation, and between operators of the same type, makes it pertinent to examine all phases of the demands of the traveling public. The average passenger may consciously want something that he knows about, such as a comfortable seat like the one at home, or he may be won over by something demonstrated to him that he had not particularly thought about, such as a train ride super-quiet by present standards.

This paper is partially concerned with mechanical vibrations, but only for those higher than 30 cycles per sec (cps). Air-borne sound caused by them, when heard by the passenger, constitutes a portion of the acoustical problem. At frequencies lower than 30 cps we are in the region of the riding-comfort problem. Not all air-borne sounds come from mechanical vibrations, but are formed directly in air. We will see that, by ordinary standards, the amplitudes of mechanical motion which generate troublesome sounds can be very small. Because of this the remedy usually does not lie in the field of closer tolerances, but the problem can be controlled by certain techniques of the acoustical engineer.

Air-borne sound is generated underneath the coach by (*a*) rolling and jumping of wheels on rails, (*b*) bumping in the spring-truck system, (*c*) auxiliary units such as a compressor, (*d*) wind noise; at the ends of the coach by (*a*) couplings, (*b*) loose vestibule doors and latches; inside the coach by (*a*) vibration of all interior surfaces, (*b*) ventilation system, (*c*) loose fixtures, (*d*) leakage sounds from any outside air-borne source. There are many possible ways by which the sound level, which the passenger hears, is built up. Acoustical theory and experience demonstrate that all important components must be controlled to obtain a significant noise reduction. There is no attempt in this paper to compare different types of coaches. The figures presented are from rather extensive investigations but are used in an illustrative rather than a comparative way.

[1] Chief, Acoustical Engineering Section, Johns-Manville Research Center.

Contributed by the Railroad Division and presented at the Semi-Annual Meeting, Milwaukee, Wis., May 30–June 5, 1948, of The American Society of Mechanical Engineers.

Fundamentals of Sound and Vibration

Sound in Air. Before giving figures on sound levels representative of the problem, a statement of the pertinent fundamentals is in order. This section is concerned with the physical aspects of sound in air. There will be references to the sense of hearing, but how the ear interprets this will be discussed separately. When a sound wave passes a given point the barometric pressure fluctuates above and below normal atmospheric pressure. A simple source, such as a gently struck tuning fork, vibrates with a harmonic motion and generates a pure tone. The pressure fluctuation as a function of time is sinusoidal. Complicated sources, such as those found in transportation, cause pressure fluctuations which may be quite complex. Using a 1000-cps pure tone, it has been determined that the average ear can just hear as sound a root-mean-square (rms) pressure variation of 2.04×10^{-4} dynes per sq cm. The pressure variation is usually called the sound pressure. The ear still gives the sensation of sound, with some discomfort, at 1000 cps for a pressure as high as 6.45×10^3 dynes per sq cm rms. Above that the chief sensation is pain.

Decibels. In communication engineering the concept of the decibel was first formulated. Given two amounts of power, W_2 and W_1, W_2 being the larger, we have the definition

$$\text{Decibel difference} = 10 \log_{10} \frac{W_2}{W_1}$$

It may be shown, for conditions that are nearly always fulfilled in noise-control problems, that given two sound pressures, P_2 and P_1, P_2 being the larger

$$\text{Decibel difference} = 20 \log_{10} \frac{P_2}{P_1}$$

The decibel always involves a ratio. When a train noise is said to be 80 decibels, it refers to 80 decibels above some reference pressure. The reference pressure has now been standardized at 2.04×10^{-4} dynes per sq cm. Given a sound pressure P expressed in dynes per sq cm rms we have the definition

$$\text{Pressure level in decibels} = 20 \log_{10} \frac{P}{2.04 \times 10^{-4}}$$

The range of the ear, just referred to, is 0 to 150 decibels (db) pressure level. While it is sometimes useful for computational purposes to know the sound pressure, for most applications the decibel concept is sufficient. Sound-level meters ordinarily read in decibels. When in calibration, or when the proper correction factor is added, the value obtained is pressure level in decibels.

Mechanical Vibrations as Sound Sources. Given a vibrating surface which acts as a sound source, it may be shown that the air particles near-by move in phase with the surface and at the same velocity. As the sound pressure is a linear function of the air-particle velocity, it is convenient to rate a vibration in terms similar to those discussed. When the vibrating surface, at 1000 cps, moves with a velocity of 4.87×10^{-6} cm per sec rms, the near-by sound pressure is 2.04×10^{-4} dynes per sq cm rms. Accordingly, given a velocity V expressed in cm per sec rms we have the definition

$$\text{Vibration velocity level in decibels} = 20 \log_{10} \frac{V}{4.87 \times 10^{-6}}$$

TABLE 1 FREQUENCY AND DECIBEL LEVEL RANGES

Frequency	0 decibels		80 decibels		150 decibels	
	D	V	D	V	D	V
30	2.59×10^{-8}	4.87×10^{-6}	2.59×10^{-4}	4.87×10^{-2}	8.19×10^{-1}	1.54×10^{2}
100	7.76×10^{-9}	4.87×10^{-6}	7.76×10^{-5}	4.87×10^{-2}	2.45×10^{-1}	1.54×10^{2}
500	1.55×10^{-9}	4.87×10^{-6}	1.55×10^{-5}	4.87×10^{-2}	4.90×10^{-2}	1.54×10^{2}
1000	7.76×10^{-10}	4.87×10^{-6}	7.76×10^{-6}	4.87×10^{-2}	2.45×10^{-2}	1.54×10^{2}
4000	1.94×10^{-10}	4.87×10^{-6}	1.94×10^{-6}	4.87×10^{-2}	6.14×10^{-3}	1.54×10^{2}

D = Displacement; cm, rms; V = vibration velocity, cm per sec., rms

If a surface has a vibration velocity level of 80 db, it will generate near it a pressure level of 80 db, for example. In Table 1 are given displacements in "cm rms" and velocities in "cm per sec rms" for the frequency and decibel level ranges of interest.

Multiple Sources and Adding Decibels. Suppose at a point of observation that a source of sound creates a pressure P_1, that a second source, when it alone is emitting, creates a pressure P_2. For the random-phase relationships which occur with multiple-wall reflections and radiation from complex sources, it may be shown that the total pressure P_t, when the sources emit simultaneously, is $\sqrt{P_1^2 + P_2^2}$. For the case where $P_1 = P_2$, we obtain $P_t = \sqrt{2}\, P_1$. Applying the definition of decibel difference, P_t turns out to be 3 db more than P_1. In Table 2 are given this and other addition factors found by such an analysis.

TABLE 2 FACTORS TO ADD IN DECIBEL DETERMINATIONS

Db difference in two levels	Db to add to larger level
0	3.0
1	2.5
2	2.1
3	1.8
4	1.5
5	1.2
6	1.0
7	0.8
8	0.6
9	0.5
10	0.4

Sound in a Closed Space. For a source inside any space the pressure level which establishes itself as steady is the one where the rate of sound-energy removal is just equal to the rate of sound energy emitted by the source. Sound energy is incident typically upon walls, sound-absorbing materials, and openings. The absorption coefficient may be thought of as the percentage of sound energy absorbed at one incidence when a ray of sound strikes the surface at a random angle. If an area of S_1 sq ft has an absorption coefficent of α_1, this area is said to have $\alpha_1 S_1$ units of absorption measured in sabines. The total sabines are obtained by summing all the αS values in the enclosure. For practical purposes the equivalent sabines of an open window are obtained by considering its "absorption coefficient" as 1. In some applications the sabines contributed by relatively nonabsorbing surfaces, such as walls or floors, may be important because of the area factor. With a constant source, if a_j sabines are initially present and a_k sabines are present after the introduction of sound-absorbing material, the decibel reduction in pressure level will be

$$10 \log_{10} \frac{a_k}{a_j}$$

In an enclosure subjected to air-borne sound striking the outside, the pressure level established inside will be

$$PL_i = PL_q - TL - 10 \log_{10} \frac{a}{A}$$

where

PL_i = average inside pressure level
PL = pressure level of sound outside striking transmitting area A
TL = transmission loss of area A
a = total sabines absorption inside enclosure
A = transmitting area, sq ft

Transmission loss is the decibel drop produced on air-borne sound of random angle of incidence by a sound barrier, measured close to each side, under conditions which discount the effect of reflected waves.

Vibration Isolation. Usually, when a structure of appreciable weight is found to be in vibration, the addition of extra weight causes little change in the vibration of the original structure. If the addition is rigidly fastened it partakes in the vibratory motion exactly. If the addition is compliantly fastened by a spring or a rubber mounting, the decibel difference between the vibration velocity level of the structure and the vibration velocity level of the addition is

$$10 \log_{10} \frac{(c\omega)^2 + (k - m\omega^2)^2}{(c\omega)^2 + k^2}$$

where

m = mass of addition (W lb/386)
k = pounds to produce 1 in. deflection in compliance
c = pounds force required to maintain velocity of 1 in. per sec
ω = $2\pi f$, where f is driving frequency in cps

Pressure Level and Sense of Hearing. We have been discussing sound mainly from the physical viewpoint and have referred to the ear only in terms of the threshold of hearing—0 db, and the pressure level at which pain begins—150 db. By definition, the loudness level of a pure tone is the pressure level of an equally loud 1000-cps tone, as decided by a sound jury. The unit of loudness level is the phon. For a 1000-cps tone the loudness level in phons is the same as the pressure level in decibels for any value of pressure level. Due to the peculiarities of the ear, which, in general, lacks acuity at low frequencies and low pressure levels, the relation between loudness level and pressure level is a complicated function of both frequency and pressure level. In Table 3 are given pressure levels at different frequencies required to evoke the sensation of 0, 40, 70, and 100 phons loudness level.

When the pressure level at the frequency under consideration rises to that shown in the "0 phons" column, the ear can just detect it. For example, at 50 cps, a pressure level of 53 db is necessary before the sensation of hearing is evoked . At 500 cps, the ear detects a pressure level of 6 db. At 3500 cps, the ear is most acute, detecting a pressure level 8 db below 2.04×10^{-4} dynes per sq cm. At high pressure levels the ear has a relatively even

TABLE 3 PRESSURE LEVELS AT VARIOUS FREQUENCIES

Frequency, cps	Loudness level, phons			
	0	40	70	100
50	53	72	82	100
100	36	62	78	100
250	18	49	72	100
500	6	42	70	101
1000	0	40	70	100
1500	—2	40	70	98
2000	—4	39	69	97
2500	—6	38	68	95
3000	—7	37	67	93
3500	—8	37	67	92
4000	—7	38	67	92
5000	—5	39	69	95
7500	6	51	81	105
10000	8	52	82	105

response over the frequency range, as shown by the "100 phons" column. In communication-engineering parlance this is known as a "flat" response.

Noise Reduction Required to Be Significant. If a typical industrial or transportation noise is reduced 25 phons, the usual reaction is that most of it has been eliminated. If reduced by 20 phons, the improvement is considered outstanding. If reduced by 10 phons, it is usually judged worth considerable expenditure. A 5-phon reduction is recognized as a definite improvement, but a 1-phon reduction is barely detectable. There are no hard and fast rules, as the worth of a noise reduction depends, among other things, on what the customer expects and what is to be achieved by the reduction. The values, as given, are fairly applicable in the range of 60 phons to 90 phons, where most noise-quieting problems lie. In a weaving shed where a loudness level of 110 phons may exist, conversation is virtually impossible. A reduction of 10 phons in this instance might not be judged worth while because conversation cannot be carried on except with considerable discomfort at 100-phons loudness level.

Sources Emitting Many Frequencies. A complex noise source produces sound energy at many different frequencies over the audible range. It is comparable to an aggregation of simple sources each giving a pure tone at a different frequency. The effect of adding multiple sources has already been discussed, although nothing was said about frequency. In a similar way, when a complex source has a 90-db component at 100 cps, and an 80-db component at 500 cps, the total pressure level is 90.4 db. The complete elimination of the 500-cps component would reduce the total pressure level by only 0.4 db, an insignificant amount. Those sound-level meters, which indicate only total level, would show no experimentally detectable change. What is needed is a frequency analyzer in conjunction with a sound-level meter. By tuning in the two component frequencies individually, the pressure levels of each can be measured. As the ear is capable of such frequency discriminations, it is usually important in transportation noise problems to make a frequency analysis. It oftens happens that noise-control methods give significant reductions in the middle and high-frequency components only. In cases where the total pressure level before treatment is due primarily to the low-frequency components, the total pressure level after treatment will also be due to them, and there will be no detectable change in the total. However, a frequency analysis in octave bands shows the reductions where they have occurred, and these readings, converted to phons loudness level, give values in accord with ear judgment.

Application to Transportation Problems

Noise in a Coach. A noise survey using a microphone underneath the coach, suitably protected from windage noise, at 60 mph, gave the analysis in Table 4.

When it is considered that representative conversation (male voice) in a quiet place at a distance of 4 ft has the analysis shown in Table 5, it is apparent that a good sound barrier must be interposed if levels of the order of Table 5 are to be obtained. The transmission loss of one type of typical coach floor, measured in the laboratory, is given in Table 6.

Given the noise spectrum of Table 6 on the sending side, such a floor would produce, on the receiving side, measured at a point near the floor, the pressure levels of Table 7. At the passenger's ear the pressure levels would be of the order of 4 db less than the pressure levels near the floor, but it is apparent that even at this point the pressure levels are substantially higher than Table 5 in many bands.

Despite the spring system, the coach structural members vibrate from the shocks of rolling, the jars of pulling one car with another, and the forces transmitted from a unit such as a compressor directly attached to the frame. With conventional rigid methods of attachment, these vibrations travel into the floor, side-trim panels, windows, and head lining. The passenger is surrounded by sound-generating surfaces. Proper methods of attaching the interior surfaces must be adopted if an important improvement is to be obtained.

TABLE 4 RESULTS OF NOISE SURVEY UNDERNEATH PASSENGER CAR

Frequency band, cps	Pressure level, db	Loudness level, phons
0– 50	80	42
50– 100	81	74
100– 200	83	81
200– 400	94	94
400– 800	111	111
800–1600	108	108
1600–3200	98	98
2400–4800	95	95
4800 +	86	86
Total	113	113

TABLE 5 ANALYSIS OF REPRESENTATIVE CONVERSATION: MALE VOICE AT 4 FT

Frequency band, cps	Pressure level, db	Loudness level, phons
0– 50	..	..
50– 100	50	7
100– 200	59	45
200– 400	57	53
400– 800	61	61
800–1600	54	54
1600–3200	48	48
2400–4800	42	42
4800 +	40	40
Total	64	63

TABLE 6 TRANSMISSION LOSS OF TYPICAL COACH FLOOR

Frequency, cps	Transmission loss, db
30	18
75	26
150	28
300	25
600	27
1200	28
2400	36
3600	43
6000	45

TABLE PRESSURE LEVELS ON RECEIVING SIDE OF FLOOR OF COACH IN TABLE 6

Frequency, cps	Pressure level, db
0– 50	62
50– 100	55
100– 200	55
200– 400	69
400– 800	84
800–1600	80
1600–3200	62
2400–4800	52
4800 +	41
Total	86

Improving Floor Transmission Loss. Using structures with substantially rigid connections throughout, experiment has shown that, averaged over the nine frequencies commonly used to cover the audible range, the transmission loss is represented by

$$TL = 22.4 + 14.3 \log_{10} w$$

where w is the weight in pounds per square foot of the panel or wall. The equation describes the average of many tests. Individual panels may vary as much as 6 db from this. In general, however, the average TL for a 10-lb per sq ft panel, typical of coach floors, is 37 db. This average is also approximately the transmission loss at 1024 cps. With a fixed weight the transmission loss increases about 4 db per octave. For a fixed frequency it increases about 4 db every time the weight is doubled. There are important considerations from this "weight law," as the prohibitive weight of 50 lb per sq ft is indicated if we are to increase TL by 10 db. Fortunately, the vibration-isolation principle used for many years in broadcasting-studio constructions is equally applicable here. By the weight law, the TL of a 3-lb per sq ft panel is 29 db. Under suitable conditions, such as the large spacing possible in the entrance and exit doors of a sound lock, the TL of a 10-lb and 3-lb two-barrier system is ap-

proximately the sum of the TL's of the individual components or 66 db. In a coach floor a 3-lb per sq ft deafening plate, for example, must be used near the floor structure and must be carried by it. However, by attaching the deafening plate with rubber isolators and using a rock-wool blanket between the two panels, a TL of 48 may be obtained. Table 8 gives the improvement in transmission loss by attaching such a construction, measured in the laboratory.

TABLE 8 IMPROVEMENT IN TRANSMISSION LOSS BY ADDING DEAFENING PLATE

Frequency, cps	Transmission-loss increase, db
150	0
300	3
600	15
1200	12
2400	18
4800	20

Vibration Isolation of Equipment. A typical piece of equipment, such as a compressor, may be surrounded with a housing, and a floor may be interposed, giving more than enough of a sound barrier to keep its air-borne noise from reaching the inside of the coach. With present floor construction, however, enough energy may be transmitted directly from the compressor through the structure to vibrate the floor sufficiently to radiate an important amount of air-borne sound to the passenger. This can be remedied by mounting the compressor on rubber or spring isolators. Using the equation given under "Vibration Isolation," it turns out that isolation is obtained when the natural frequency of the equipment on the mounting is low compared to the frequency of the driving force. It is common practice to use mountings soft enough to deflect $^1/_8$ in. or more under the static load of the equipment. This means that the natural frequency is 9 cps or less, and good isolation is obtained for driving frequencies of 50 cps and higher.

Over-All Improvement of Interior Surfaces. The compliant mounting of the deafening plate mentioned, is an application of this principle, used to increase the barrier effect of the floor against air-borne sound. This is important because there is intense noise under the floor. The floor also radiates noise to the interior of the coach via its rigid connection to the frame. This situation involves, in effect, two sources, and it is useless to lessen the weaker one. For best results, the entire floor should be isolated from the structure so that both paths of energy transfer to the interior coach surface will be dealt with. Field measurements have shown that, given a choice, the floor should be controlled first. However, once it has been reduced to the vibration velocity level of the remaining interior surfaces, all surfaces must then be considered if a further reduction in pressure level is to be attained.

Miscellaneous Noise Sources and Methods of Control. Noise from a ventilating system can be controlled by the usual techniques of low air velocity and a sound-absorbing lining in the ducts. Ventilating noise which cannot be heard when the coach is in operation can be troublesome when the train is stationary and other sources are quiet. For detection and correction of trouble from open ventilators, loose-fitting doors, open drains, and the like, an acoustical engineer is not needed, but careful attention to both scientific and common-sense methods will result in new standards of quiet railroad transportation.

Truck Riding Comfort

By K. F. Nystrom,[1] Milwaukee, Wis.

The author feels that in creating luxurious passenger cars, economical limits have been exceeded by introducing costly, complicated, and over-engineered appurtenances. The same criticism applies to truck design. Excessive weight and complications militate against long life of truck and track, and maintenance costs are high. He analyzes the components of the truck and points out where improvements can be made, finally suggesting the characteristics of the passenger-car truck of the future.

As the weight of a car set of passenger trucks is approximately one third of the entire weight of the car, it is difficult to consider it as a separate unit since its function is, generally, threefold, namely, to carry the weight of the car body, to generate enough friction to stop the moving car at will and, in most instances, to generate electric power for light, air conditioning, and other appurtenances.

Considerable progress has been made from an aesthetic point of view both in interior and exterior appointments of passenger cars. In connection with the latter, streamlining has run ahead of functional progress, resulting in increased cost of maintenance and more difficult inspection, especially in severe winter weather when a large amount of snow and ice is accumulated by the shrouding. This problem has been recognized by some railroads and corrected.

In creating luxurious passenger cars we have gone beyond the economical limits by introducing costly, complicated, and, in many instances, over-engineered appurtenances which have to be simplified greatly and reduced both in cost and weight to meet the competition of other forms of transportation. While this paper is confined to passenger-car trucks, it is considered pertinent to dwell briefly upon the elements placed in or underneath the car body, which introduce problems when endeavoring to design a safe, economical, and easy-riding truck. These elements are excessive weight, cumbersome brake equipment, and too great electric-power requirement.

In regard to excessive weight, the engineer is very much circumscribed as he can save very little weight in the body structure itself without sacrificing strength as long as he is forced to load the car with heavy equipment such as seats, air-conditioning units, and the like, and has to design the car body to carry this weight.

Lighter Brakes Needed

The high-speed brake with electrical control is heavy, cumbersome, and complicated. A simplified, powerful, and foolproof brake, even at the expense of sacrificing some efficiency, seems desirable.

The truck brake, known as the "clasp" brake, was developed about 30 years ago and does not meet the exacting requirements of high-speed service because of the rapid wear of its parts, as well as brake shoes and wheels. There is a need for a lighter and more efficient truck brake when consideration is given to the fact that a car set of clasp brakes weighs 5300 lb complete with cylinders and slack adjusters, and that under favorable conditions from a speed of 100 mph a train cannot be stopped in much less than 3600 ft. It is hard to conceive why we have lived with this condition up to the present time.

The so-called disk brake, as developed up to the present time, is an improved method of braking, but the braking disks have blades which act as cooling fans for dissipating the maximum anticipated heat generated under most severe conditions by drag-braking, or in other words, braking down heavy grades, a practice which few railroads use with modern Diesel-powered trains. The resistance of these blades consumes considerable power at high speeds and from experience obtained this resistance probably could be reduced. Considerable progress has been made recently in increasing the service life of the brake shoe and and we feel the disk brake holds considerable promise for the future.

W. S. Graff-Baker, chief mechanical engineer (Railway), London Transport Executive, London, England, in co-operation with the Westinghouse Limited, has worked out an interesting truck-brake application as shown in Fig. 1. In corresponding with Mr. Graff-Baker, he comments on this subject as follows: "The unit was developed at my instance as I became very dissatisfied with the amount of brake rigging carried on either the truck or the body. It is very surprising that engineers have been content to put a mechanism on bodies and trucks of a crudeness which they would not contemplate anywhere else." The Milwaukee Railroad has developed a hydraulic brake as shown in Fig. 2 but due to lack of time and outside interests the device is, for the present, lying dormant.

Wheels and Axles Need Attention

While on the side of criticism, the wheels and axles must not be overlooked. There has been but little improvement in wheels with the result that, with the increased speed and braking forces, the life of a wheel under a passenger car is very unsatisfactory. There was a time when 75,000 miles could be attained between each wheel-turning without creating rough riding, but it is doubtful if one half of the foregoing mileage is obtained by any railroad operating high-speed trains. Besides the unsatisfactory mileage, the wheel is too heavy.

The axle situation is even worse. Some years ago one of our railroads had an unfortunate accident, resulting from a broken axle, which led to a further increase in the weight of the axle, instead of to a careful study and development of a design and specification for suitable steel to reduce the weight and provide a stronger axle.

The principal roller-bearing manufacturers have perfected their product so that bearings today are almost trouble-free. Notwithstanding the fact that all basic patents on roller bearings have expired, we have not taken advantage of this situation by designing a standard axle or one standard bearing for all passenger cars.

The foregoing criticisms or facts should prove that we still have a long way to go before we can take much comfort in so far as progress is concerned.

Improvements in Spring Suspensions

On the other hand, since streamlined trains were introduced we have made some improvement or, more correctly stated, made some attempts in that direction and, either by luck or some ingenuity, have succeeded in improving the riding of passenger cars

[1] Chief Mechanical Officer, Chicago, Milwaukee, St. Paul & Pacific Railroad Company. Fellow ASME.

Contributed by the Railroad Division and presented at the Semi-Annual Meeting, Milwaukee, Wis., May 30–June 5, 1948, of The American Society of Mechanical Engineers.

by introducing more flexible springs. While riding has been improved, by increasing spring deflection we have encountered undesirable features such as vertical and horizontal oscillation and car-body rolling, which have necessitated the application of snubbers and levelizing bars, the use of rubber, and the like. These devices, although helpful, have increased the first cost as well as maintenance cost.

The Milwaukee Railroad has made some attempt to reduce maintenance cost by introducing a rubber mat in the truck center plate, thereby practically eliminating wear between body an truck center plates. It has taken away the spring plank, swin hangers, pins and axles, and with their elimination has solve automatically the problem of severe wear on these parts. Th equalizers have been extended to form pedestal guides, and as th pedestal follows the movement of the journal boxes, there i practically no wear on these parts. This truck is shown in Fig. 3

In connection with the wear of swing hangers and pins, it wa discovered that when the Milwaukee Railroad introduced th

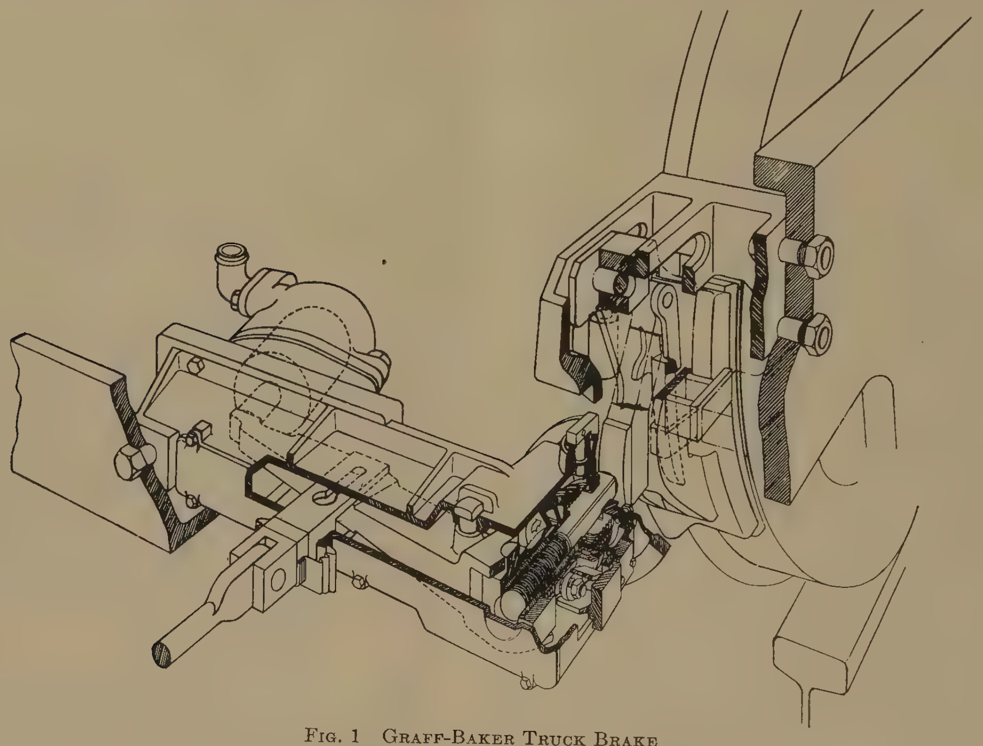

Fig. 1 Graff-Baker Truck Brake

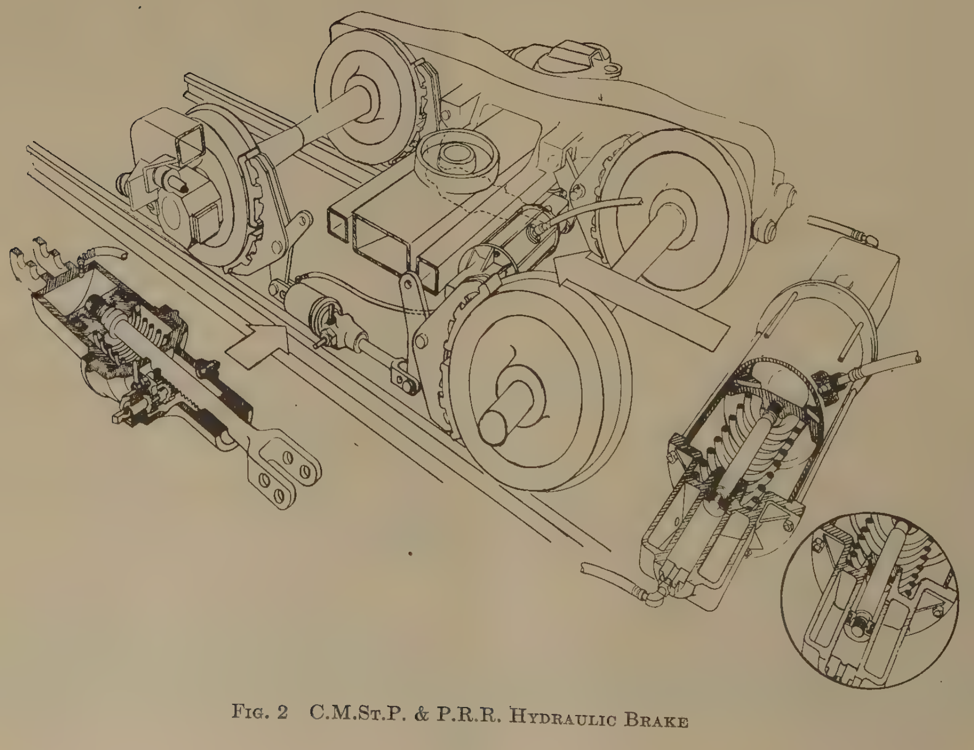

Fig. 2 C.M.St.P. & P.R.R. Hydraulic Brake

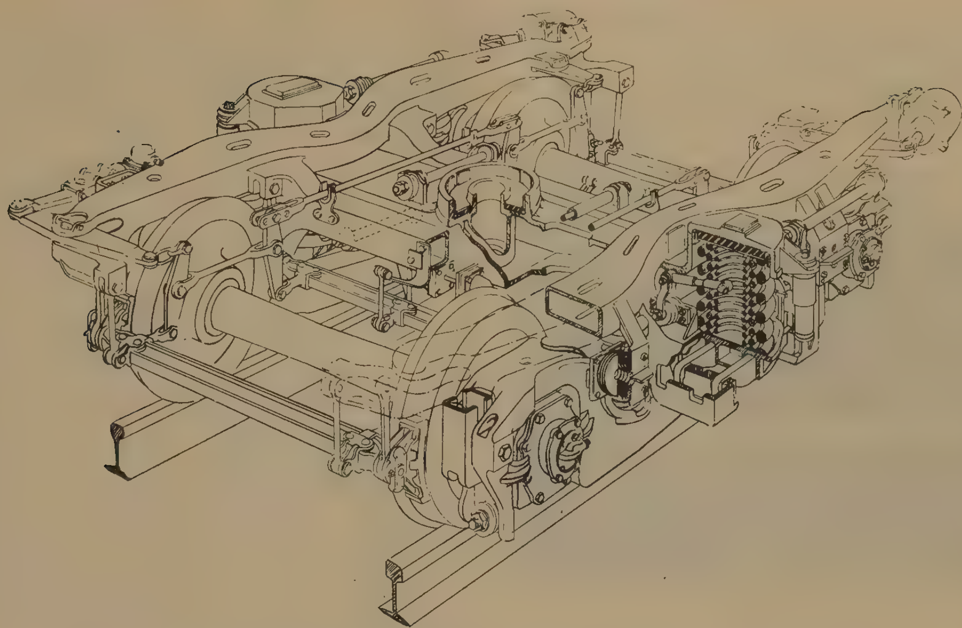

Fig. 3 Milwaukee Railroad Design Featuring Rubber Mat in Center Plate

large bolster coil springs having $13^3/_4$-in. OD, the wear was reduced materially because of the fact that this large-diameter spring, in itself, acted as a pendulum, thereby reducing the movement in the swing hanger. This experience led to the complete elimination of swing hangers and associated parts and, by moving the bolster spring from its conventional location inside the equalizer to a location outside the truck frame, elimination of the afore-mentioned wear was accomplished. In addition, by widening the base of the bolster springs, the stability of the car body was increased to such a point that roll stabilizers were no longer required.

Many attempts have been made with different types of springs, but all attempts seem to lead to one thing and that is, the more deflection which can be introduced and controlled, the smoother the riding.

In cars built in 1942 by the Milwaukee Railroad, the pedestal guides were integral with equalizer, as shown in Fig. 4, and this arrangement, together with end tie bars fixing the relation between truck frame and the equalizer, has proved a success. From a number of tests made several years ago with wheel bases varying from 5 ft 6 in. to 11 ft, we came to the conclusion that the wheel base had no function in good riding, and therefore in cars built in 1946, the wheel base was shortened from 8 ft to 7 ft. With this change the swing hangers mentioned previously were eliminated and the bolster springs moved outside the truck frame. Although we had made extensive and satisfactory tests with a truck so equipped with 8-ft wheel base, when the shorter-wheel-base truck was introduced in regular service, an undesirable shimmy developed at certain speeds and track conditions. A large number of tests were made both in road service and in the laboratory before this shimmy was eliminated at all speeds and under all track conditions. The remedy was the introduction of what we call lateral-control sandwiches between the truck frame and the equalizer as shown in Fig. 5.

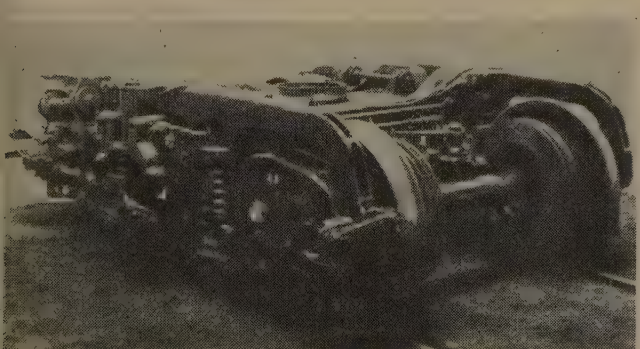

Fig. 4 Pedestal Guides Integral With Equalizer

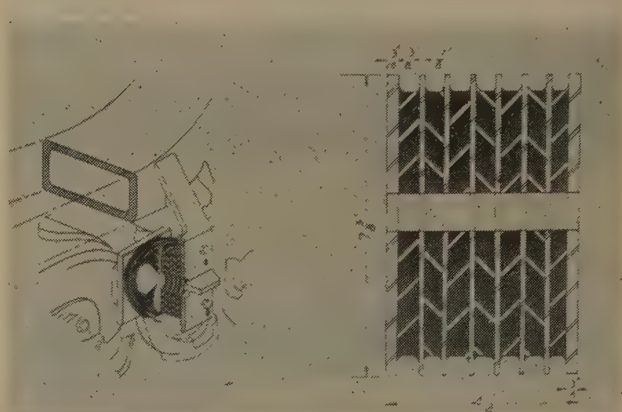

Fig. 5 Lateral-Control Sandwiches Between Truck and Frame

Individual tests were made also with wheels having AAR standard as well as cylindrical contour. It was found that both the riding qualities as well as the tread wear were improved by the cylindrical-contoured wheels, and these were adopted as standard for high-speed trains. To eliminate excessive lateral movements of the truck bolster as well as excessively high torsion stresses in the bolster springs, an automotive type of rubber bumper was introduced between the bolster and transom. The location of this bumper is shown in Fig. 6.

Combination Helical and Elliptical Spring

The Pennsylvania Railroad has introduced a combination helical and elliptical bolster spring which, it is claimed, has materially improved the riding qualities as the friction of the

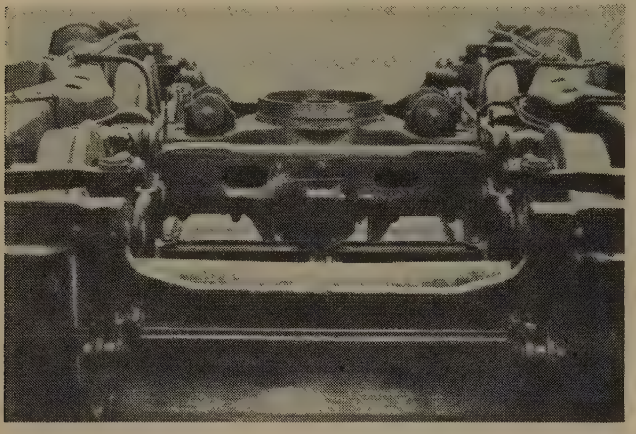

Fig. 6 Automotive-Type Rubber Bumper Between Bolster and Transom

elliptical spring introduces a stabilizing influence which provides an opportunity to eliminate the hydraulic shock absorbers which are costly to maintain. The passenger truck most commonly used today, which is called the General Steel Castings Corporation's basic truck, is shown in Fig. 7.

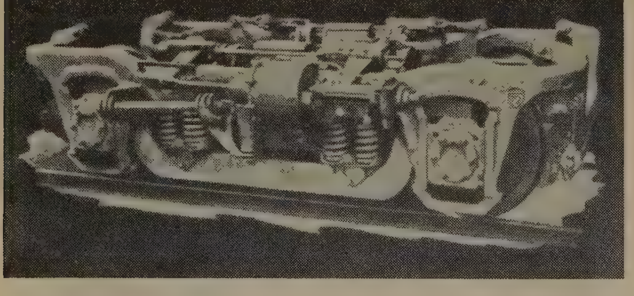

Fig. 7 Combination Helical and Elliptical Bolster and Spring

Fig. 8 Copy of Goerlitz Truck Made in the United States

The majority of truck designs used in Europe have no equalizers, but carry the load from the truck frame to the journal by means of springs either directly above or at the journal boxes. In this country, we have never been successful in such grouping of springs, although several attempts have been made even to the extent of copying a European truck known as the Goerlitz truck shown in Fig. 8. The advantage of this type of truck is that the unsprung weight is reduced to a minimum.

European Developments

Some interesting developments are being made in Europe; for instance, Mr. Graff-Baker, previously mentioned, has designed a passenger truck, substituting rubber sandwiches for the conventional bolster springs, as shown in Fig. 9. It will be noted that this design is patented, but it promises interesting possibilities. The Brown, Boveri Corporation has introduced two outstanding truck designs: One arrangement is shown in Fig. 10 in which has been solved the problem of the wear on journal boxes and pedestal guides by combining journal boxes with a radius arm fastened to the truck frame, by vertical spindles at the side adjoining the bolster and by horizontal links at the outer ends. Another feature of this truck is carrying the weight of the car body from the side sill directly to the truck bolster rather than through the conventional center plate. Another arrangement, shown in Fig. 11, is an even more interesting design in that the weight of the car body is carried entirely on torsion bars. This design introduces a large number of special bushings which probably would be as troublesome as the parts they eliminated from the conventional design; however, the construction is novel and noteworthy.

In addition to Mr. Graff-Baker's novel introduction previously mentioned, wherein the rubber carries the load from the bolster to the truck frame, he has also developed the truck shown in Fig. 12 which may be described as follows: The frame is a weldment built of plates and channels. The wheel base is 6 ft $4^1/_2$ in. with the bolster 2 ft $9^3/_4$ in. from the motored axle to increase the weight on this axle. The semielliptical springs over the journals are exceptionally long, being 48 in. over the motored axle and 57 in. over the idler axle. The springs are not symmetrical due to the bolster being off center. The ends of the semielliptical springs are secured to the truck frame by rubber compression springs. The coil bolster springs are placed outside of the truck frame. The truck bolster is of an articulated construction. The main truck bolster is short and sits between the truck-frame wheel pieces, the ends of which are carried by swing hangers. The swing hangers are supported by two parallel bars which in turn are supported by the coil bolster springs. The foundation brake rigging is of the unit type in which the cylinder, lever, and slack adjuster are all encased in a unit enclosure. The truck is very low, the highest part being the wheels, and the highest part of the truck frame being 2 ft $3^3/_4$ in. above the rail.

Earlier in this paper the specialty manufacturers were criticized for introducing heavy, cumbersome, and complicated devices, but in so far as the development of the passenger truck is concerned, we have not done much better as it is still heavy and cumbersome.

Future Passenger-Car Trucks

The author ventures to forecast that the future passenger-car truck will be radically different from what we are now using and probably along the following lines: There will be no axle-driven generator, but a self-contained power unit for each individual car or a head-end power plant furnishing 220 volts or higher; hydraulic brakes; no springs as we know them today, but the weight will be carried on rubber sandwiches or on torsion bars; inboard roller bearings with tubular axles, and the wheels will be considerably lighter with twice their present life. This future truck would be, in itself, simple, compact and streamlined, so dirt, snow, and ice could not accumulate under the most adverse weather conditions. Such a truck would need to be serviced only every 10,000 miles.

Conclusion

In closing, it is desirable to call attention to the craze for speed. The author went on record some years ago to the effect that a

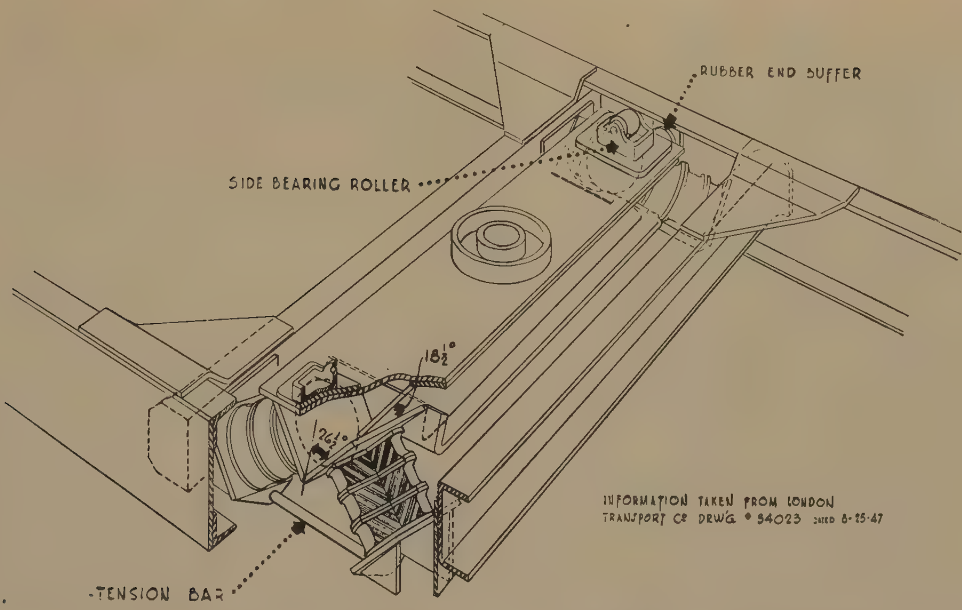

FIG. 9 PERSPECTIVE OF BONDED-RUBBER BOLSTER-SUSPENSION ARRANGEMENT

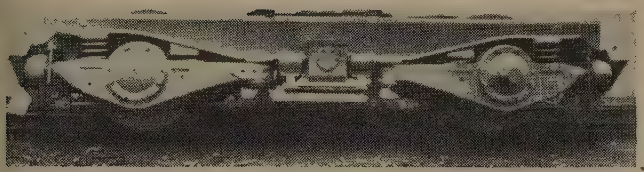

FIG. 10 BROWN BOVERI TRUCK

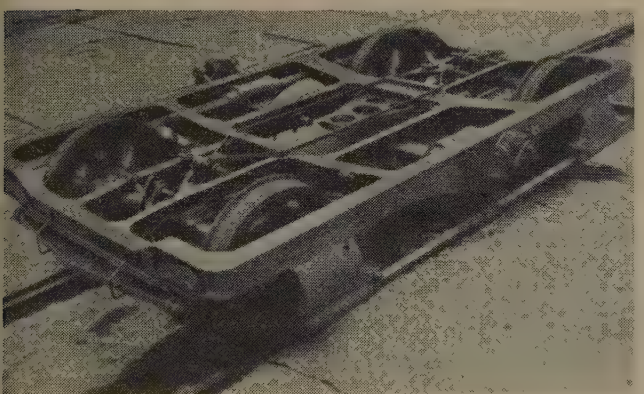

FIG. 11 ANOTHER BROWN BOVERI DESIGN

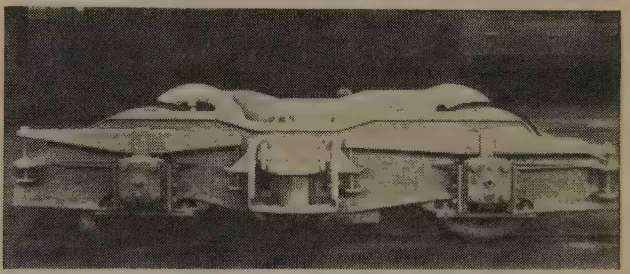

FIG. 12 UNUSUAL DESIGN BY GRAFF-BAKER

truck can be built to operate at a speed of 150 mph on straight tangent track in safety and he is still of the same opinion, but seriously questions whether in the future we can afford to operate at much more than half that speed.

Fig. 13 shows the train resistance from 10 to 150 mph on level tangent track, and tractive effort and drawbar pull for a 2000-hp Electro-Motive Diesel, a 4000-hp Electro-Motive Diesel, and a 6000-hp Fairbanks-Morse Diesel. It will be noted that a 2000-hp Diesel could handle 16 cars weighing 60 tons each at 70 mph. The same Diesel could handle 8 cars at 90 mph, 4 cars at 108 mph, one car at 130 mph, and would absorb all energy in pulling itself at slightly over 140 mph.

Expressing the same thing in another way: A 1000-hp Diesel could pull a 12-car train at 52 mph, while 4000 hp would be required to pull the same train at 104 mph. In other words, the horsepower requirement increases with the square of the speed. The same applies to a modern steam locomotive, but speeds above 100 mph are disastrous to the locomotive as well as to the rails.

We know that the horsepower requirement is a function of approximately the square of the velocity, and, from observation, we know that the wear and tear of motive power and rolling stock increases very rapidly with higher speed. Shipowners years ago, through experience, found that they could not operate a steamship economically above a certain speed. We also have to learn what is the economical speed and weight limit for both passenger and freight trains. Any automobile owner knows that high speed shortens the life of the automobile, not to mention the greater driving risk.

If we recognize other forms of transportation, particularly airborne, then we must admit that railroads cannot compete with airplanes in so far as speed is concerned. Recognizing this fact, a few minutes on a short trip or even a couple of hours on a transcontinental trip would not make much difference to the majority of the traveling public, but we would increase the safety materially and would substantially reduce the maintenance cost of both equipment and roadbed, not to mention the great saving in fuel.

The American railroads are spending millions of dollars for new power and on roadbeds for the purpose of increasing speed, and it is questionable whether we have taken full account of the fact that by increasing the speed substantially we are pyramiding the maintenance cost of both roadbed and equipment. It is doubtful

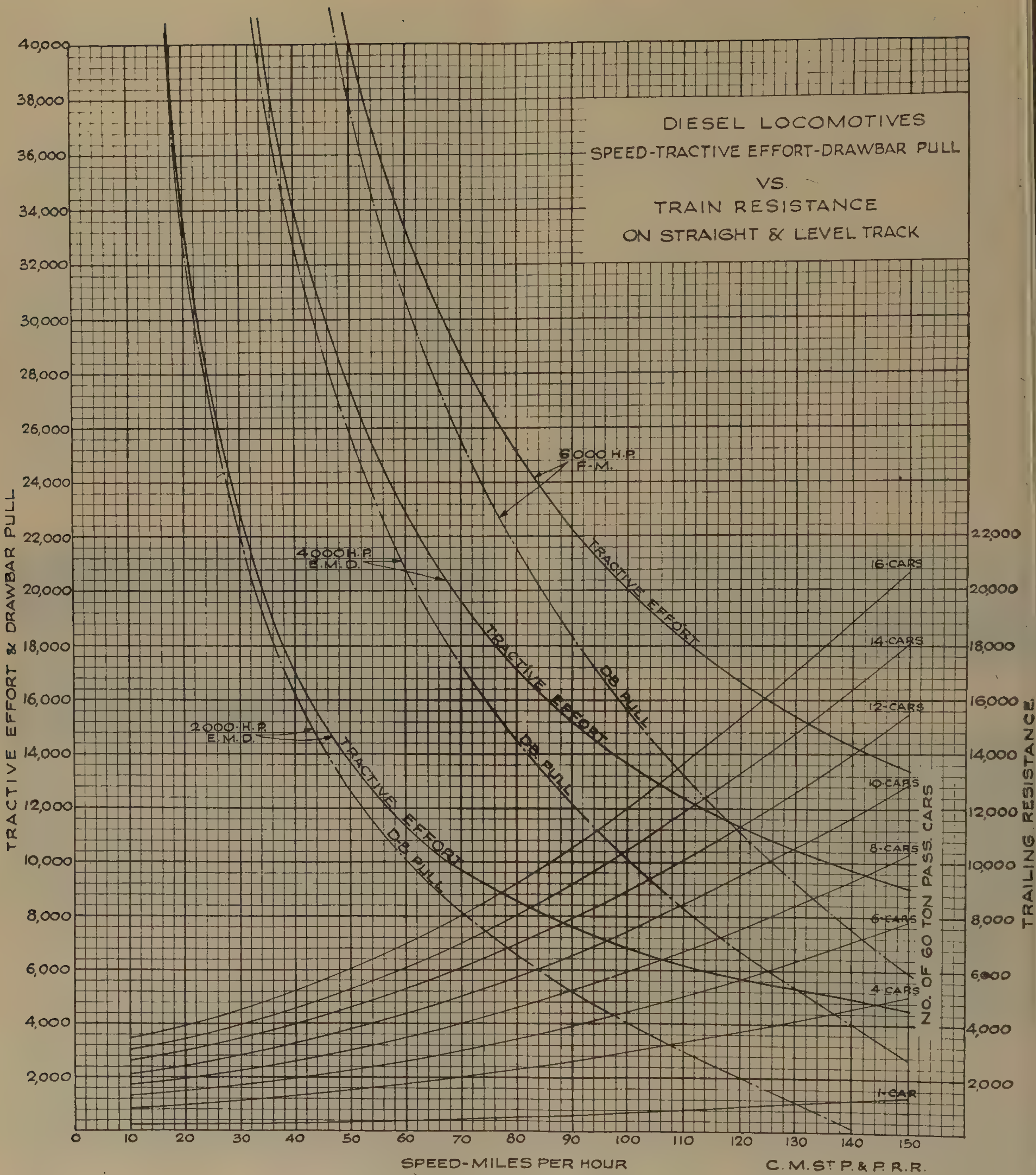

Fig. 13 Diesel-Locomotive Performance Curves

if freight trains can be operated economically over 50 mph and passenger trains over 90 mph. In connection with freight trains, the horsepower required between 30 mph and 52 mph is approximately doubled, and between 52 mph and 91 mph is tripled. If the speed were held to the limits suggested, most of our vexing problems would be eliminated.

Railroad Passenger-Car Comfort Discussion[1]

J. D. Loftis.[2] The paper presented by W. A. Jack is an excellent theoretical treatise from which the practical application engineer should be able to progress toward the main problem, which is the elimination of the harmful vibration and noise. It is indeed unfortunate that with the theories developed and expounded by this author, we have not been able to secure the interest of application engineers in the elimination of these vibrations. To construct moving vehicles, such as railroad passenger cars, with the sound and vibration-dampening qualities found in broadcasting studios is impractical. Therefore it is necessary for the application engineer to find the happy medium whereby sound and vibration-dampening qualities may be included to the fullest extent without excessive cost, without exceeding weight and dimension limitations, and without falling below necessary strength requirements.

Mr. Jack has developed and expanded the problems presented in railroad-car operation from an acoustical standpoint, and it is expected that the leading manufacturers of insulation and sound-deadening material, in the near future, will make practical applications of their products to railroad-car construction to eliminate noise and vibration.

The need for industrial design in railroad equipment as indicated by Brooks Stevens, has long been realized, but it is essential that the industrial designer furnish that which pleases the majority.

The popular present-day concept of industrial design is not the answer. It is true that we are interested in visual passenger comfort, but we also look to the industrial designer to tell us far more than color schemes or the tasteful arrangement of seats and furniture. The industrial designer should include such items as the rounding of corners, the elimination of dirt-catching spaces, and the provision of easily cleaned surfaces and areas, because dirt detracts from the visual comfort of the passenger.

It is only natural that those who are responsible for maintenance of equipment wish to make it as simple and as easy to maintain as possible. It is up to the industrial designer to give the advantages of bull-nose construction, upholstery that can be removed easily for cleaning, and other items which initially might cost a little more but, with proper design, not only will make the maintenance task easier but also will continue the initial eye-appeal.

A great deal of comment is given to the limitations imposed upon the industrial designer by hesitancy of the railroads in departing from tried and true structure and methods. This hesitancy on the part of the railroads is not because they lack foresight but because they have had their fingers burned by so-called new and improved designs. A passenger car must still be built to withstand the requirements of high-speed service with little time for maintenance at turn-around points and must last long enough to pay off the original investment. Items which look shoddy in a few years have no place in a railroad car; unusual windows, however eye-appealing initially, certainly have no appeal to the traveling public if the cleaning of these windows on the inside surfaces is impossible and they are continually fogging; plastic light fixtures which require frequent cleaning should not be considered, regardless of how much initial appeal they have.

Visual passenger comfort is far more than interior decoration, but the writer is afraid most people still consider it as such. Because of the limited space in passenger trains, it is often necessary that space be used for dual purposes. Therefore it becomes apparent that illumination must be useful as well as decorative. Useful illumination can be decorative, but much of the decorative illumination is not useful. Sufficient lighting with well-designed and well-placed fixtures must be given the passenger as a primary requirement affecting his comfort. In the period of a few short years we have all seen illumination levels of 10–12 ft-c increase to 20–25 and even 30 ft-c. We still have not reached the limit of lighting. It may be that we are approaching desirable foot-candle levels, but, certainly, a great deal can be done toward better diffusion and arrangement of this lighting.

Of equal importance to passenger comfort is a complete air-conditioning system, including completely automatic heating and cooling, which not only will operate free of mechanical difficulties and failures but will also give the passenger the maximum in comfort. Present-day air conditioning, regardless of the initial source of cooling, is dependent primarily on an overhead air-distribution system. While this system controls the temperature of the car, it has many limitations with respect to complete passenger comfort. We are all aware that a passenger seated on the sunny side of the car may be uncomfortably warm while a passenger on the shady side of the car may be too cool.

It is interesting to note from the paper by K. A. Brown that the C&O, recognizing this problem, is making a practical application of theories which indicates that the problem may be solved. It can be expected that the absorption or emission of heat from large panels, such as the side walls of a railroad passenger car, will produce far more comfort as it takes into account the radiation of heat from and to the human body.

While Mr. Brown's paper is only an interim report, based upon stationary tests, several specific conclusions can be reached which will advance the art of air conditioning to passenger cars, the principal one of which is the use of side-wall panels for radiation of heat. It is noted that there is very little variation in temperatures throughout the car, that drafts are held to a minimum even though large volumes of air are handled, and that radiant heating of the floor surface is not required.

It can be expected that with further developments the same comfort will be obtained when the side walls are used for cooling as has been attained with heating. It was unfortunate that sufficient refrigeration capacity was not available for these tests, but results which were obtained indicate that the type of system being developed by the C&O shows promise of a very great improvement in passenger comfort.

It is hoped that sufficient development work will be done so that, when service application of a system of this type is made, mechanical details will not interfere with its progress.

It is anticipated that developments of this type will be continued by the railroads and equipment manufacturers until a system is perfected which will present a practical solution to our

[1] Discussion applies to one or all of the following papers, published in this issue of the Transactions: "Thermal Environment of Railroad Passenger Cars," by K. A. Browne and S. G. Guins, pp. 185–191; "Visual Passenger Comfort," by Brooks Stevens, pp. 193–195; "Railroad Passenger Comfort—Decibel Level," by W. A. Jack, pp. 197–200, and "Truck Riding Comfort," by K. F. Nystrom, pp. 201–206.

[2] Chief of Motive Power and Equipment, Atlantic Coast Line Railroad Company, Wilmington, N. C.

present problems of cold and hot side walls, drafts, and air stratification.

In his paper on truck riding comfort, K. F. Nystrom has touched the keynote that should be a part of all papers on improvement, that is, whether the expenditures necessary to make the improvements are economically justifiable. It is true that in so far as elapsed time is involved, railroads will never be in a position to compete with air traffic. This has very little bearing on trips involving 200 to 700 miles, as in most cases these trips can be made overnight by rail. Convenience, comfort, and on-time performance then become greater factors than elapsed time.

It is quite definite that the core of passenger comfort starts with the truck, and it is evident, from the study given the matter by Mr. Nystrom, that this factor is not only recognized but action is being taken to improve the situation.

With the research that has been given the problem on the Atlantic Coast Line, we have come to the conclusion that the outside-swing-hanger truck, similar to that used on the "Train of Tomorrow," contributes the greatest to passenger comfort of any of the trucks now in use. It also has many advantages over the so-called basic truck in ease of maintenance and inspection. However, from an analysis of the truck developed by the Milwaukee Railroad and described by Mr. Nystrom, it would appear that he has accomplished the same purpose with the elimination of wearing parts incorporated in the outside swing hanger. If this is the situation, a great contribution has been made by Mr. Nystrom and the Milwaukee Railroad.

In the conclusion of his paper Mr. Nystrom touches upon a very important factor in rail operation, namely, the question of the economics of further increasing speeds. Widespread recognition has been given to the increase in costs of operation as speeds are increased yet very little recognition has been given to the effect on average speed by interruptions to normal operating speeds. Until full utilization has been made with existing top operating speeds it is questionable as to the over-all gain to be experienced in increasing maximum speeds. Speed restrictions through towns, over railroad crossings, through interlocking plants, over bridges, through curves, and through other speed-restricting territories, often have the effect of nullifying the advantage of high-speed operation. If, however, these nullifying effects are eliminated, then consideration can be given to increasing maximum speeds. In freight-train operation, these restrictions are even more apparent than in passenger-train operation. The delays incident to switching, icing, and other yard operations have the effect of reducing almost to 50 per cent the average speed under that of the authorized maximum speed. Therefore it is readily apparent that the greatest gain can be accomplished by eliminating these factors, rather than increasing maximum speeds, which results in greatly increasing maintenance and operating costs.

A common theme is apparent in the three papers presented by Messrs. Nystrom, Brown, and Stevens, which, while only inferred by Messrs. Stevens and Brown, was stated by Mr. Nystrom. This is the requirement of a dependable power supply of ample capacity which does not utilize axle generation.

Good lighting, as well as efficient air conditioning, requires a dependable power plant of ample continuous capacity. Direct-current systems of varying voltages cannot meet the demands of present-day electrical-power requirements. In addition to the lack of capacity, mechanical difficulties, such as were brought out by Mr. Nystrom are apparent. The need of a different type system is recognized but, in general, little effort is being made toward applying such a system. Head-end power is the ideal source of electrical energy for modern passenger cars and ultimately will be adopted. However, at this time there is a great hesitancy to take such a far-reaching step because of the expected restrictions in operating flexibility. Several roads have installed individual Diesel power plants generating 220-volt, 3-phase a-c power. While these installations do not have a large amount of operating experience, a sufficient amount has been gained to show this type of equipment is not only feasible but practical.

Recently, eight railroads jointly agreed upon specifications covering new equipment which included the use of Diesel-engine alternators continuously trainlined, hermetically sealed air-conditioning units, and electrical and Diesel exhaust heating for cars, proposed to be operated in joint service. In this discussion it appeared that the Diesel-engine alternators are a necessary interim step between present direct-current electrical systems and head-end power.

The advantages of three-phase alternating-current power for electric heating, totally enclosed three-phase motors, and hermetically sealed compressors are well recognized. With an adequate supply of alternating-current power, either from the individual Diesel-engine alternator or from head-end power, these advantages can be utilized to their fullest extent.

As an item of interest, in bidding on cars with individual Diesel-engine alternators continuously trainlined, a car-builder estimated the weight of car at 5000 lb less than a car equipped with a present conventional direct-current electrical system.

A. M. Miers.[3] When transportation by steam railroad first was introduced about a century and a quarter ago, the advantages offered over the then best forms of overland travel were so great that almost any degree of discomfort was acceptable without undue complaint, but over the succeeding decades, the desire of freemen for progress, accelerated speeds, and discrimination of railroad patrons have brought about constant and progressive revision in performance standards in which the passenger truck continues to be one of the foremost factors. This never-ending urge and need for improvement has been responsible for the development of truck detail which has greatly narrowed the gap between the normally opposed objectives of speed and riding comfort.

Although the subject of passenger-car trucks is very broad and involved, progressive results have been accomplished with different designs which successively have been reduced to practice, and as a further contribution of possible interest and value to the general subject of "Passenger Riding Comfort," discussed by K. F. Nystrom, the purpose of this comment is to examine in some detail the salient features of one of the latest and most widely and successfully used designs, even though it is realized that this particular truck, generally illustrated by Mr. Nystrom's Fig. 7, is quite well known. Further, the writer will discuss an outstandingly important functional characteristic of this and other passenger trucks which it is essential further to improve, and finally to outline the experience and views of the engineering organization with which the writer is connected, on the important question of developing and recording test results.

The truck here referred to is illustrated by Figs. 1 and 2, and embodies the results of experience with similar designs extending over a period of several years and the related over-all developments accomplished to date. While the basic arrangement follows the four-wheel drop-equalizer swing-motion bolster pattern of former standards, several important engineering advantages are incorporated therein which have provided a materially raised base line of riding performance with respect to vertical and lateral action and have resulted in a lowered operating noise level.

Spring Suspension. Elliptical springs, unless lubricated and properly encased, both offering numerous maintenance difficulties, have unstable characteristics caused by changes in interleaf friction through the formation of rust and penetration of other

[3] Assistant Engineer on Rolling Stock, New York Central System.

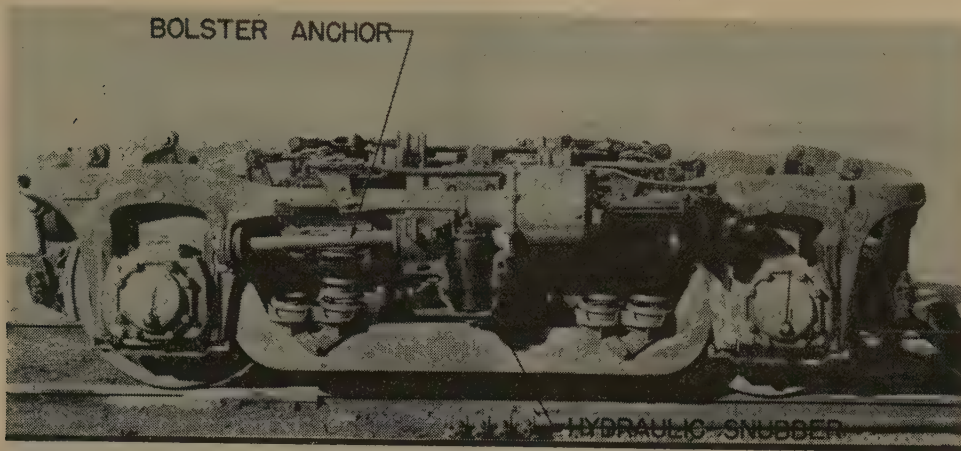

Fig. 1 New York Central Railroad Four-Wheel Passenger Car Truck

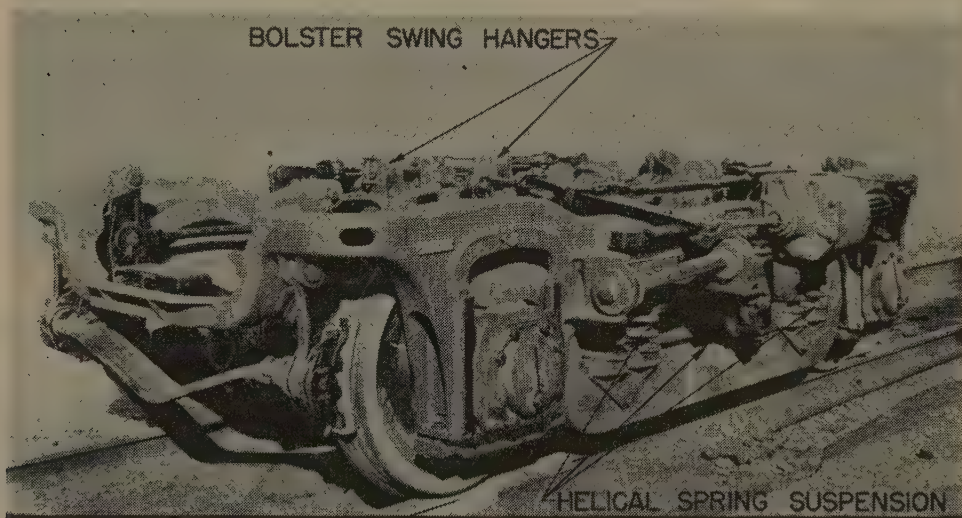

Fig. 2 New York Central Railroad Four-Wheel Passenger Car Truck

foreign matter. For this reason, springs of the elliptical form have been superseded by those of helical design and supplemented by hydraulic snubbers, two per truck, positioned vertically and designed to provide the major portion of their resistance during release action. It is here emphasized that these hydraulic devices are installed solely as a controlling or dampening means to prevent or "head off" the beginnings of harmonic action due to resonance. Therefore the almost universal reference to these instruments as "shock absorbers" is definitely a misnomer.

In addition, the four double helical springs per bolster having an outside diameter of 10 in., now being used, as compared with two triple helical springs of $13^3/_4$ in. OD, employed by Mr. Nystrom in the truck shown in his Fig. 3, were designed for low periodicity or rate of natural oscillation, which characteristic results in a definitely beneficial effect on the vertical riding performance. Although the periodicity of a spring varies inversely as the square root of the static deflection, free to working, there is a practical limit to the amount of static deflection which should be used. The figure of about 10 in., portioned approximately 60 per cent for the bolster and 40 per cent for the equalizer springs, has been found to produce very good results. Naturally high static deflection is accomplished by corresponding effect on working stresses because the outer diameter of the spring is more or less fixed, due to structural limitations. It has been proved by experience, however, that these higher stresses, if confined within reasonable limits, can be tolerated, as very good service life has been obtained with such designs. This indicates that spring failure, due to fatigue, is attributable more to wide stress reversals than to high fiber stress.

Bolster Anchor. This device provides positive longitudinal positioning of the truck bolster with respect to the frame transom, and guides the vertical and lateral movements of the bolster. All frictional drag between bolster and transom is eliminated by disposing of metallic chafing plates. However, proper adjustment of this device is important, as experience has shown that excessive precompression of the rubber insulators can result in serious impairment of the riding qualities.

Swing Hangers. The effective length of the bolster swing hanger has been increased considerably to provide a system of low natural period. This characteristic, together with the longer moment arm for overcoming frictional resistance, increases the smoothness of lateral action.

Center Plate. The new designs provide the obvious advantages of lubricant retention and the exclusion of foreign matter.

Noise-Elimination Features. The incorporation of rubber-mounted bolster anchors and composition pads at such points as equalizer feet, spring and center plate, have proved effective in isolating noise and high-frequency vibration from the car body. Improved center-plate construction has gone far to reduce and control noise from these locations to the car body.

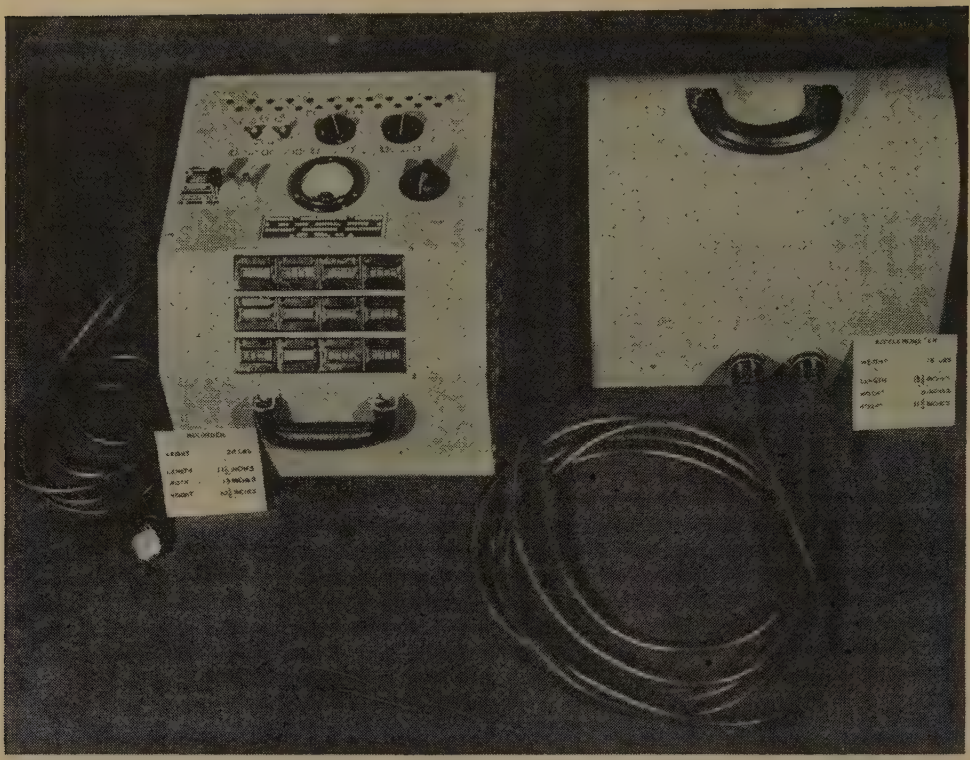

Fig. 3

Other Features. Until a few years ago, it was the general belief that a long wheel base and even the use of three pairs of wheels per truck were requisites for a good-riding truck but this theory has been disproved by the superior performance of several late design four-wheel trucks which have wheel bases ranging from 7 to 9 ft. The six-wheel truck has largely been discarded in favor of the four-wheel design for reduced weight and space occupied, except for extraordinary center-plate loads or where the braking conditions to be met are unusually severe.

For improved riding qualities of practical value, truck designs must be such as to provide high mileage continuity of operation without the necessity of constant adjustments and related attention. This feature has been improved materially during the last decade, directly by advancement in various truck detail and indirectly because of the introduction of roller bearings, and the lengthening of better wheel-service performance periods through the use of recently improved wheel-slide-control devices and metallurgical progress. Improved slack free couplers and double-acting cushioning devices for the elimination of longitudinal shocks of operation and the disturbing effects of the vertical components of such shocks, together with more logical top-supported diaphragm and buffer-plate applications for reduction of noise and friction have contributed greatly to riding comfort.

We have no "sacred standards" with respect to passenger trucks or other equipment features but rather endeavor to be constantly alert to investigate possible changes and improvements for the betterment of existing arrangements. One such problem now demanding and receiving concentrated attention relates to passenger-truck lateral action which is dependent upon a plurality of complex and variable functions, with improvement much more difficult of attainment than for the betterment of vertical action.

To this end a new type bolster controller has been produced in co-operation with one of our suppliers. This device, which is installed between the bolster and frame casting has been designed to provide double-acting but very low cushioned resistance within the range of normal bolster movement and to produce increasing build-up of such resistance beyond this range so as to prevent the occasional shock caused by bolster contact against the frame during heavy lateral surges. The equipment is now ready for trial and comparative road-test performance data will be available at a later date.

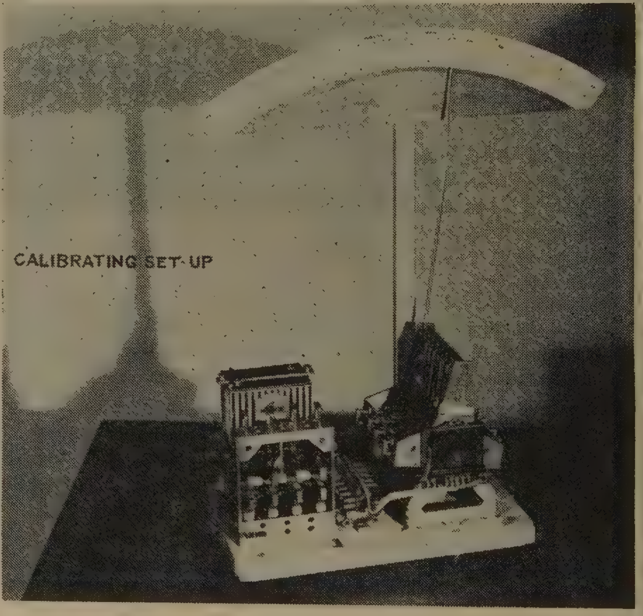

Fig. 4

Recording Equipment and Road-Testing Procedure. Progress toward improvement in riding qualities of passenger trucks and cars has been handicapped greatly by the lack of reliable meas-

uring and recording devices for the accumulation of operating data on which sound appraisals of the results of mechanical change may be based. Instruments heretofore used, which have been capable of providing the required records, have had the disadvantage of great bulk and weight, and the consequent necessity for fixed mounting and use in special test cars with the obvious limitations in scope of operation and the applicability of results.

After much discouraging experience with the instrument makers in efforts to obtain efficient portable equipment, our engineers, themselves, now have developed an accelerometer which embodies the fundamental requirements for an instrument of this kind as we see them, namely, means for continuous simultaneous measurement and registration of the vertical and horizontal force reactions in terms of gravity, when operating over tangents or curves, together with accuracy and reliability, and of size and total weight consistent with convenient portability. The accelerometer and recorder are shown in Figs. 3 and 4.

The accelerometer consists essentially of an instrument for measuring force reactions within the range of preset magnitudes. arrived at by experience in car operation, and an electrically operated recording device for counting and totaling the force reactions so measured, as they are accumulated. The measuring instrument is divided into two units, one to register the vertical accelerations, and the other a horizontal unit for measuring in both directions either lateral or longitudinal accelerations, depending upon the relative position of the instrument.

The use of counter-type recording in an accelerometer, especially for railroad work, has distinct advantages as it provides immediately a means for comparing total results over a given territory which is in contrast with the uncertainties of tape-recording, as well as the time and labor required for comprehensive analyses.

In truck development and other work on riding-quality improvements, it has long been our conviction and experience that as an engineering fundamental, a reliable "yardstick" or base must be made available at all times in the form of performance results of the then-best existing design or arrangement for simultaneous comparison with the new or experimental application, whether it be a complete truck or one or more details of consequence which have been changed. Hence the indispensable need for a companion base car operated with the unit under test, and reliable recording equipment placed in both cars with which the required records may be obtained. Thus numerous variables are eliminated; such as those brought about by incidental changes in weather, roadbed conditions, track alignment, running speeds, and the effects of acceleration and deceleration. This is the practice we follow when making road-test comparisons, for which any two cars when coupled together in any revenue or special train may be used at any time in any territory. It should be apparent that the value and integrity of the results are dependent first of all upon the character and reliability of the recording equipment used.

In conclusion, it is desired to emphasize that the present discussion relates solely to riding qualities for car-occupant reaction as recorded inside the car. This is accented because the strains and stresses set up in truck and associated running-gear parts, resulting from the succession of dynamic loadings of operation to which they are subjected, is another important phase of the general subject which warrants detailed investigation in like comparative manner. Through suitable instrumentation, the magnitudes and locations of these strains should be ascertained for judgment of their relative importance, and evaluations of the different truck arrangements, not only for comparative performance as manifested thereby, but also for possible further weight reduction through refinements in design.

To date, this problem has received relatively little attention by the railroads and manufacturers, but it is on our docket for the future advancement of the art.

G. T. Wilson.[4] In this discussion it is the intention to scan briefly the early beginnings of car heating and then to outline subsequent progress in ventilation and air conditioning and carry this through the period of recent improvements, first used experimentally, then expanded in practice, and now being installed, with further refinements, on a broad scale. All this has been made possible, step by step, as a result of research, practical experiment, and the lessons learned from that stern and unrelenting teacher, experience.

Heating. In the early days of railroading, the wood or coal-fired stove, as first used for heating the interiors of passenger cars, was a welcomed comfort convenience, especially during periods of subzero temperature and other adverse weather conditions. This simple and elemental form of heating means was then superseded by the coal-fired hot-water radiator, then pressure steam, and later, by the currently used basic arrangement, consisting of low-pressure steam-heat floor radiation, supplied from the high-pressure coupled train line, charged from the locomotive. Although, since the turn of the century, development of apparatus for rail-travel purposes has kept pace with the art in the general field of heating, there still remained the highly objectionable uncertainties resulting from manual control by the train-crew members who still were relied upon.

The year 1921 marked an epoch in the control of passenger-car heating because at that time the first experimental automatic thermostatic temperature-control apparatus was introduced in the United States, with the installation made on a Michigan Central Railroad coach, in co-operation with the then Vapor Car Heating Company. Regardless of this addition of delicate mechanism to the railroad passenger car with all that it implied, there is no question about the modern development of this control being one of the most productive improvements for human comfort which subsequently has been made available to travelers by rail through having overcome the annoyance and discomfort resulting from wide range in car-interior temperature common to manual operation.

Over the past few decades, major changes in passenger-car construction and operation have taken place, such as the introduction of the all-steel body, the longer train consists, and increased speeds, all of which influence the heating performance. The leakage rate from the early designs of all-steel bodies, together with the higher velocities of movement, demand greater heating capacities both in steam supply from the train line and radiation in the respective cars. It has been our experience that provisions for comfortable and acceptable heating conditions present a more complex problem than that of cooling, discussed later.

Under conditions of geographical location commonly met, such as those on our System as one example, proper heating capacity must be provided within atmospheric temperature range on the order of plus 50 F to minus 25 F, which is approximately twice that for cooling. In predominantly north-south operations, the spread may be greater. In open-space cars, sufficient radiation for heating and protection against freezing at extremely low temperatures must be supplied which, in some instances, under the more normal atmospheric conditions, has resulted in considerable discomfort because of the necessary high surface temperatures and the larger radiation areas required. Through modulation, there are now available, three means of improving this situation, namely, the step method, throttling, and the thermostatic cycling control of steam to the radiator.

[4] Assistant Engineer Rolling Stock, New York Central System, New York, N. Y.

The heating equipment of the large number of new sleeping cars now under construction for our System will embody means for the room occupant to control both the floor and overhead heat on switch and damper, respectively, by manual selection. In these cars the cycling modulation is arranged to admit steam to the radiator in direct proportion to the temperature setting and steam-condensing rate, thereby eliminating heat surges and overruns of temperature common to the conventional thermostatic control. The overhead heat supply for the entire car will be primarily under the selective manipulation of the car porter, but is subject to further manual adjustment by the room occupant through use of the air-outlet damper in the same manner as provided for cooling, referred to later.

For the open-space cars, a semi-automatic temperature control has been devised and standardized, it being only necessary for the trainman to select either "heating" or "cooling," after which the temperature is automatically regulated.

For overhead heating the controls are arranged primarily for mild-weather conditions and during reductions in such outside temperatures the low floor heat is available, but when the freezing point is approached, a higher temperature setting takes control to compensate for the increased car-body losses.

As we all know, car-body insulation is an extremely important factor for heating as well as for cooling performance and tests have confirmed the need for ample thickness of the best material available for this purpose which, at present, is that having mineral base, with the advantage of high thermal efficiency, light weight, and other favorable characteristics.

The problem of heat delivery from the locomotive to the train is constantly becoming more serious. Steam demands are increasing, particularly for the modern-design passenger cars, because of inside length and other related dimensional features and the higher sustained operating speeds. With present steam load of approximately 300 lb per hr at or below zero temperatures, and with the multiple-angled and high frictional resistance metallic connectors now available for use between the cars with tendency to leakage and exposure to condensation effects, particularly while running over track pans, it is extremely difficult at these low exterior temperatures to supply to the rear units of trains having 15 or more cars, sufficient volume of steam for protection against freezing. Obviously, if this need is not met, the inside temperature of the rear cars cannot be maintained at acceptable or satisfactory levels.

This is a problem of long standing and in recent years has become more acute because of the wide introduction of Diesel motive power which, for the most part, has received, when built, steam-heating plants of inadequate capacity and functional characteristics. We have long believed, however, that train-heating troubles could be reduced considerably through the use of an improved form of car connector, and now have completed laboratory developments and tests of a flexible type having uniform bore and body section between the end valves and freedom from the numerous pressure joints and right-angled bends inherent in the present connectors.

It is fully realized that over the years, previous efforts in this direction have been unsuccessful but, regardless of this and because of urgent need, the further work of developing such a connector in practical and reliable form is being actively pursued, with the conviction that the use of such a connector would result in substantially reduced line leakage and pressure drops throughout the train, with corresponding benefits.

Cooling. The year 1929 marked another epoch in the fundamental advancement of rail-travel comfort. At that time the Baltimore and Ohio Railroad in co-operation with the Carrier Corporation, completed the first installation of a self-contained refrigerating plant, with related apparatus, for cooling a car interior mechanically, the application having been made and successfully operated in one of that railroad's dining cars. Thereafter it soon became the general policy of the American railroad to equip, without undue delay, as large a number of cars as practicable with the then available types of cooling apparatus, even though this was a new art. Practically all of the earlier installations were made to existing cars, which naturally placed certain limitations on what could be done, and also on performance and service results.

At that time, travelers by rail were not too critical because, like the supply of heat in cold weather, as provided in an earlier day, the primary desire was for the comforts of cooling during the seasons of hot weather.

However, when the middle 1930's had been reached, railroad equipment engineers and manufacturers recognized the necessity for research leading to refinements in performance, maintenance and serviceability of apparatus to provide more effective solution of the problem which presently became one of combined heating, ventilation, and air conditioning.

In this early stage, performance results and maintenance costs were used as the guides to show where changes would be most productive of results, and it soon became apparent that irrespective of theoretical considerations, the most important requirement was continuity of operation which could be most successfully achieved by concentrating to the extent practicable on simplicity of design and installation of equipment. When checked against acceptable standards for human comfort, it may be said without equivocation that this principle is just as valuable and essential today as it was some few years ago.

To this end, continued observations of human reaction and inquiries addressed to rail patrons have been very helpful in arriving at suitable ranges of temperatures and relative humidity for use in attaining progressively improved performance.

One of the most common complaints thus revealed pertained to supposedly high temperatures which not infrequently were found actually to have had their origins in discomfort due to high relative humidity, this being a common fault inherent in dry-bulb thermostatic control when the full cycling cooling system was used.

On this problem it was found that because of the admission of unconditioned air from the outside and recirculating air during the "off" cycle, when the dry-bulb thermostat had been satisfied, this air having a higher wet-bulb temperature, created a humid effect. Then, when the operation of the cooling system was resumed, the resulting high moisture content of the supplied air actually produced the "clammy" feeling so often complained about by the car occupants, especially when exterior temperatures and moisture contents were in the higher ranges.

For the betterment of this condition, our engineers, in co-operation with those of the air-conditioning equipment manufacturers, developed and installed in 1941, the initial application to a railroad car of a modulated cooling system. This consisted essentially of an evaporator split 60–40 per cent, in which the higher-capacity section is cycled under the thermostatic control, with the lower-capacity coil operating continuously but protected against under-cooling in mild weather by means of a low-limit thermostat. This eliminates the off cycle and provides uninterrupted but reduced cooling output, with sufficient latent capacity to maintain the desired relative humidity without decreasing the dry-bulb temperature. Thus a comparatively flat wet and dry-bulb curve is produced within the limits of the prescribed comfort zone. Further refinements in this direction could be obtained through division of the evaporator into more than two sections, but this would lead to added mechanical complications which, in our opinion and experience, as previously mentioned, should be avoided. Because of the economics of

power requirements, it is believed that two-part modulated electromechanical air-conditioning system, in conjunction with the axle-driven generator, is much more desirable than the use of reheat for moderation of relative humidity, because of respective power requirements.

The fact remains, however, that the control of cooling temperatures probably is the most common cause of unsatisfactory comfort conditions during the summer season. In the early developments of this feature, the selective automatic arrangement was in most common use, but the results obtained therewith depended upon the judgment and mental attitude of the train-crew members. On hot humid days the inclination was to use the low-temperature settings, with resulting chilling effects on the seated passengers. For the open-space cars, such as the coach, diner, and lounge, where the composite thermal characteristic of the occupants naturally vary over a considerable range, the possibilities of differential thermostat control were analyzed, using the accepted temperature relation between the inside and the outside of the car throughout the territory in which our System is operated. Although it was expected that the "northern curve" would prove satisfactory, it became necessary to introduce a limited deviation therefrom to the extent of using the "northern railroad curve," which provides for slightly lower temperature for car interior than obtained when following the generally accepted northern curve. Through the use of such cooling, uniform temperature is obtained for all like cars of a train, and the adverse effects of temperature settings selected by train-crew members, with the inevitable result, is avoided.

The cooling controls for the multiple-room car, such as the sleeper, require a different application, because here success depends more upon meeting the requirements of individuals than those of groups of car occupants.

The large number of sleeping cars now under construction for our System, previously mentioned, are receiving modulated cooling equipment, together with provision for selective automatic control by the car attendant, and the damper providing improved means for manual operation by the room occupant. With this setup, the volume of cooled air may be varied over a quite wide range for adjustment of temperatures among the various rooms. It is our belief that such an arrangement of controls should prove superior to that provided by thermostatically operated dividers, dampers, or separate reheat coils in the individual rooms. Such multiple automatic controls introduce undesired complications for maintenance and increase the liability of failure and discomfort to the passenger. Simplicity in such apparatus is a proved advantage.

Heating and Cooling. In each bedroom of the new cars, a conspicuously located plate is being provided which will contain briefly worded but comprehensive instructions to the room occupant, set forth in easily readable sized etched lettering which may be readily understood by travelers of either sex who cannot be expected to be mechanically minded.

Summary. The heating, air-conditioning, and ventilating systems being incorporated in the new cars now under construction and delivery for our System, contain the cumulative results of co-operative research and development extending over a period of several years and embody the important features of better humidity control, adequate means available to the room occupant for year-round automatic or, if the need should arise, manual regulation of temperature and ventilation to suit the individual requirement, and for protection against temporarily defective equipment anywhere in the car. Simplified and understandable instructions are posted for the guidance of the room occupant. The principal improved mechanical features, not previously mentioned but incorporated to assist in obtaining the desired improvement in performance, include a dry-type air-blown condenser with reduced head pressure and corresponding power input to the compressor, separation of compressor and condenser units to facilitate maintenance, loop-type system for steam-heat supply to radiation, reduced number of valves, regulators, traps, and related apparatus beneath the car floor to minimize discharge of condensate on running gear, and after much experimentation, the installation of the impingement-type adhesive-coated metallic filter for better service from this important detail.

Closure by K. A. Browne

Mr. G. T. Wilson gave an excellent paper on the history of development of heating and air conditioning as applied to passenger cars. His paper points out that the major development of combining the problem of heating and cooling cycles was made between the years of 1930–1934, and that since then work was limited only to the refinement of mechanical components.

Yet the problem of creating comfortable conditions was ever present as pointed out by J. D. Loftis. Realizing the foregoing situation, it was decided to break away from the railroad practice and follow the specifications set up by ASHVE for buildings.

Although we missed out on some of the requirements and the equipment used in our first installation was over-complicated, enough advantages were demonstrated to cause considerable changes in equipment currently offered the railroad.

Our overhead equipment is offered as part of the railroad comfort-air system by The Trane Company. Vapor Car Heating Company is installing convector side-wall panels in a number of currently built cars.

It was gratifying to see that the companies mentioned and men of Mr. Loftis' standing took notice of our work and applied the results in application of their equipment.

Closure by Brooks Stevens

The stimulant to this type of general discussion of the railroad car and passenger comfort is the fact that patron preferences are becoming more easily discerned in rising and falling revenues. Design and styling will influence the riding public, but not necessarily sell them tickets. "Selling the tickets" is the combined job of engineering and design more than ever before, with a high competitive and comparative standard established in the informal comforts of the home of today and the ease and luxury which the automotive and air industries have inbred into other means of overland travel.

A new train soundly conceived and tastefully executed is a success only in terms of public response. The perfection of its engineering and propriety of its interior and exterior design and styling must meet the challenge of ever faster schedules and ever improved operating efficiency—with the critical vote of the public registered at the ticket windows.

No form of travel where any distance is involved has a decided edge at this time, with all factors considered. Historically, however, the railroads have a decided advantage in the length and breadth of public service and contact. From the standpoint of prudent public relations and sales planning, this is an exclusive asset upon which they can capitalize to a greater degree.

For example, in the field of industrial design we are continually searching for new materials or adaptations of old materials which reduce the mechanical chill of transportation interiors. By using plastics, light metals, impregnated fabrics, processed woods, and protected papers a "permanent freshness" is achieved. The new paints have a very proper place in these treatments and contribute to a smart, distinctive appearance that wears equally well between Chicago and Milwaukee, or Chicago and Seattle.

Designwise, people expect more than they did in 1940, and the

tempo of their expectations and demands will increase much more rapidly with each new car, each modern innovation for the home, than ever before.

The same is true of the public's observations of engineering improvements. The same general standard-raising and appreciative education of Mr. and Mrs. Passenger gives them the insight to damn a bouncing car or a poorly conceived heating system.

The railroads have been blasted from every angle for a litt better than a decade. Despite a tariff situation that has hand capped engineering and design improvements they have moved i the right direction and have proved that fact by "selling tickets.

The next ten years will require a closer analysis of public prefe ence, and a fast-moving and proper interpretation into railwa equipment and facilities.

A New Approach to the Design of Dynamically Loaded Extension and Compression Springs

By CURT I. JOHNSON,[1] ENDICOTT, N. Y.

This paper contains formulas and derivations of a design procedure for dynamically loaded extension and compression springs which permits straightforward solutions to spring problems with minimum assumptions. It is based upon a new method of graphical representation of spring characteristics and includes the following equations

$$C_e = \sqrt{\frac{GK}{\pi S_s} \times \frac{1}{Y - 1 + T}}$$

for extension springs, or

$$C_c = \sqrt{\frac{GK}{\pi S_s} \times \frac{1}{Y - T_c}}$$

for compression springs.

$$Q_e = P\,(Y - 1 + T)$$

for extension springs, or

$$Q_c = P\,(Y - T_c)$$

for compression springs

$$d = \sqrt{\frac{8\,C^3\,Q}{G}}$$

where C is the spring index, Q is the load constant, and d is the wire diameter as determined either mathematically or graphically. These items are utilized with "spring proportion tables" (Table 1), for convenient solutions to problems. This paper also describes a method of cataloging stock springs based upon a new graphical representation.

Nomenclature

The following nomenclature is used in the paper:

C = spring index
C_c = spring index, compression springs
C_e = spring index, extension springs
D = mean coil diameter
d = wire diameter
F = total deflection
F_0 = theoretical equivalent initial deflection in extension springs
f = deflection per coil produced by load $(P - P_o)$ in extension springs or by load P, in compression springs
f_T = deflection per coil at 100,000 psi and no initial tension shown in "spring proportion tables" (Table 1)
G = torsional modulus of elasticity
i = load increase factor
K = Wahl's correction factor for stress[2]
L = active length at load P
L_1 = active length at load P_1
L_c = total coil clearance
L_i = inactive length
L_o = solid active length
n = number of active coils
OD = outside coil diameter
P = maximum working load
P_1 = minimum working load
P_T = load at 100,000 psi stress according to table
P_o = initial tension
p = correction factor for effect of initial tension or coil clearance on spring index
Q = load constant
Q_c = load constant, compression springs
Q_e = load constant, extension springs
R = spring rate
S_s = torsional stress
s = length of stroke
s/L = stroke-to-length ratio
T = initial tension factor
T_c = coil clearance factor
Y = deflection ratio

Introduction

Although the basic formulas for spring design are well known, their efficient use is limited to establishing wire sizes and coil diameters for statically loaded springs. When these formulas are applied to the solution of spring problems involving dynamically loaded springs which must meet specific requirements with respect to operating loads and spring rate, a laborious trial-and-error procedure is involved. Further complication is added to the problem because, in spite of the fact that such springs require a definite minimum volume of material for satisfactory performance, machine designs are executed often without regard to adequate space requirements for these springs. For this reason, the author began compiling data to provide the designer with more definite reference material on spring design. While investigating these data, several relationships were discovered which resulted in a more straightforward design procedure, eliminating the necessity for numerous assumptions, and it is felt that this information may be of interest to mechanical engineers and designers in general.

This material was developed from a new and more descriptive graphic portrayal of spring characteristics which reveals the presence of a "load constant" Q which remains the same as long as the wire and coil diameters are unchanged. Since these fac-

[1] Engineering Department, International Business Machines Corporation. Mem. ASME.

Contributed by the Machine Design Division and presented at the Semi-Annual Meeting, Milwaukee, Wis., May 30–June 5, 1948, of The American Society of Mechanical Engineers.

[2] "Mechanical Springs," by A. M. Wahl, Penton Publishing Company, Cleveland, Ohio, 1944.

tors make up the spring index, $C = D/d$, and since Q is determined by the conditions of the problem, it follows that C may also be found for the specific problem, eliminating the necessity for any assumption of C. Hence the coil size selected is dependent upon the maximum load P and Q, or C. Values for Q and C may be found either mathematically or graphically and used with a "spring proportion table" (Table 1), which has been developed for convenient solution to the problem.

In the material which follows, the derivation of this design procedure will be shown along with allied data developed for making preliminary space allowances for springs in mechanisms. A description is included of the spring proportion tables, and a catalog of stock springs, based on graphic representations which give the designer an opportunity to evaluate the characteristics of a spring, and to re-evaluate the characteristics of the spring when any change is made with respect to the initial tension, number of coils, or other physical dimensions.

The following three equations are considered the basic equations for spring design

$$P = \frac{\pi d^3 S_s}{8\,DK} \qquad [1]$$

$$f = \frac{\pi D^2 S_s}{d\,GK} \qquad [2]$$

$$f = \frac{8\,D^3 P}{Gd^4} \qquad [3]$$

The use of these equations is facilitated by new equations and graphs in which consideration is given to the active coils in the spring only. The reader should keep this in mind; and in establishing the maximum and minimum operating lengths, due allowance should be made for fastening devices, inactive loops, and coils.

This new approach to spring design has been used successfully for some time in the design of small mechanisms for electric accounting and bookkeeping machines, and it is the author's belief that since these procedures are based on the fundamental spring formulas, this method of obtaining spring specifications should be applicable regardless of the physical dimensions of the spring.

Graphic Representation of Extension Springs

The conventional graphic representation of extension springs, Fig. 1, has limitations because it does not lend itself to any extensive analysis of the influence of the physical spring proportions on the operating characteristics. A much more comprehensive picture of the spring proportions and operating characteristics may be had by plotting the applied load versus the extended length of the active coils as in Fig. 2.

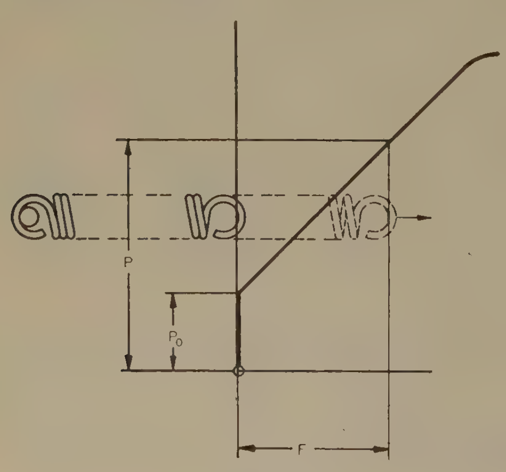

Fig. 1 Conventional Graphic Representation of an Extension Spring

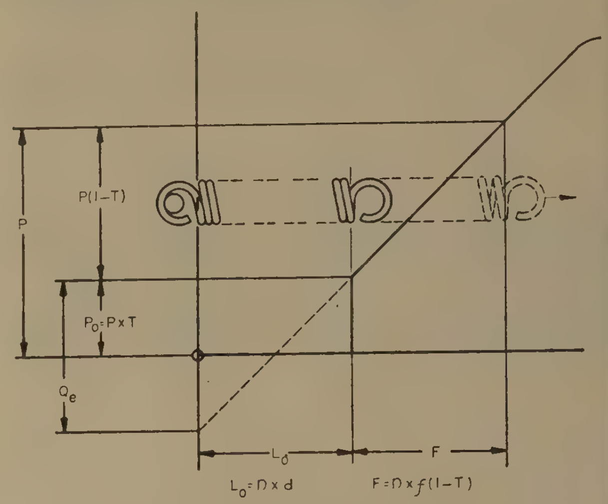

Fig. 2 New Graphic Representation of an Extension Spring

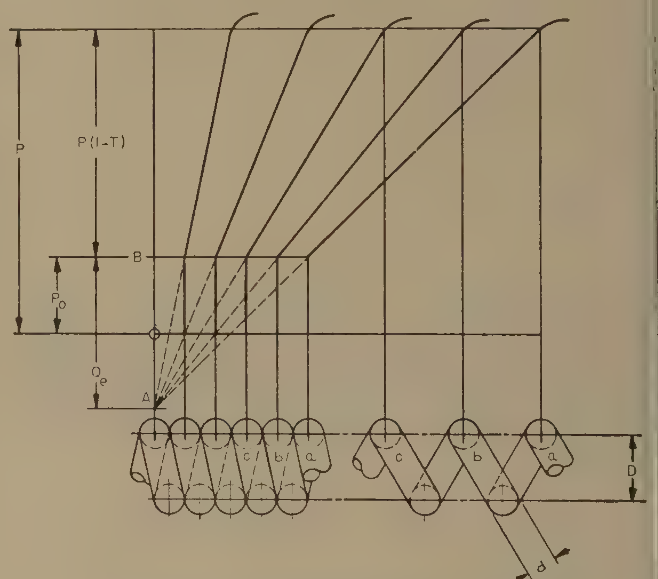

Fig. 3 $Q = Pd/f$ Remains Constant for a Specific Coil Size and Material Regardless of Number of Coils

In Fig. 3 it is interesting to note that with this method of presentation, the gradients for springs with varying numbers of active coils will converge at one point A, as long as the mean coil diameter D, wire diameter d, and initial tension P_o remain constant. The value represented by $B - A$ also remains constant for any spring with the same mean coil diameter and wire diameter and is independent of the active length of the spring. This value, called the load constant Q, may be defined as the theoretical load required to deflect the spring a distance equal to its solid active length or to produce a deflection in one coil equal to its wire diameter.

Referring to Fig. 2, if a load P causes a deflection f in each active coil of the spring

$$\frac{Q}{P\,(1-T)} = \frac{n\,d}{n\,f\,(1-T)}$$

TABLE 1 SPRING PROPORTION TABLES

Spring Index C	WIRE DIAMETER (d) = .085				WIRE DIAMETER (d) = .090				WIRE DIAMETER (d) = .095			
	Outside Diameter O. D.	Load P_T	Deflection Per Coil f_T	Load Constant Q_T	Outside Diameter O. D.	Load P_T	Deflection Per Coil f_T	Load Constant Q_T	Outside Diameter O. D.	Load P_T	Deflection Per Coil f_T	Load Constant Q_T
3.0	.340	60.980	.0132	393.569	.360	68.365	.0139	441.233	.380	76.172	.0147	491.620
3.2	.357	58.851	.0155	323.324	.378	65.978	.0164	362.481	.399	73.513	.0173	403.875
3.4	.374	56.815	.0180	268.903	.396	63.696	.0190	301.469	.418	70.969	.0201	335.896
3.6	.391	54.877	.0206	226.076	.414	61.523	.0218	253.455	.437	68.549	.0231	282.399
3.8	.408	53.038	.0235	191.904	.432	59.461	.0249	215.145	.456	66.251	.0263	239.713
4.0	.425	51.295	.0265	164.301	.450	57.507	.0281	184.199	.475	64.074	.0297	205.234
4.2	.442	49.646	.0298	141.758	.468	55.658	.0315	158.926	.494	62.014	.0333	177.075
4.4	.459	48.085	.0332	123.165	.486	53.908	.0351	138.082	.513	60.064	.0371	153.850
4.6	.476	46.608	.0368	107.692	.504	52.253	.0390	120.734	.532	58.220	.0411	134.522
4.8	.493	45.210	.0406	94.710	.522	50.685	.0430	106.180	.551	56.474	.0453	118.305
5.0	.510	43.886	.0445	83.736	.540	49.201	.0472	93.877	.570	54.820	.0498	104.597
5.2	.527	42.632	.0487	74.396	.558	47.795	.0516	83.405	.589	53.253	.0544	92.930
5.4	.544	41.442	.0531	66.396	.576	46.461	.0562	74.437	.608	51.767	.0593	82.938
5.6	.561	40.313	.0576	59.505	.594	45.195	.0610	66.711	.627	50.356	.0644	74.330
5.8	.578	39.240	.0623	53.536	.612	43.992	.0660	60.020	.646	49.016	.0696	66.874
6.0	.595	38.219	.0672	48.340	.630	42.848	.0712	54.195	.665	47.741	.0751	60.384
6.2	.612	37.248	.0723	43.797	.648	41.759	.0765	49.101	.684	46.528	.0808	54.708
6.4	.629	36.323	.0776	39.805	.666	40.722	.0821	44.626	.703	45.373	.0867	49.722
6.6	.646	35.441	.0830	36.285	.684	39.733	.0879	40.679	.722	44.271	.0928	45.324
6.8	.663	34.599	.0887	33.168	.702	38.790	.0939	37.185	.741	43.219	.0991	41.431
7.0	.680	33.795	.0945	30.398	.720	37.888	.1001	34.079	.760	42.215	.1056	37.971
7.2	.697	33.027	.1005	27.928	.738	37.026	.1064	31.311	.779	41.255	.1123	34.886
7.4	.714	32.291	.1067	25.719	.756	36.202	.1130	28.834	.798	40.336	.1193	32.127
7.6	.731	31.587	.1131	23.738	.774	35.412	.1198	26.612	.817	39.456	.1264	29.651
7.8	.748	30.912	.1197	21.954	.792	34.655	.1267	24.613	.836	38.613	.1338	27.424
8.0	.765	30.264	.1264	20.345	.810	33.929	.1339	22.809	.855	37.804	.1413	25.414
8.2	.782	29.642	.1334	18.890	.828	33.232	.1412	21.178	.874	37.027	.1491	23.596
8.4	.799	29.045	.1405	17.570	.846	32.563	.1488	19.698	.893	36.282	.1570	21.948
8.6	.816	28.471	.1478	16.371	.864	31.920	.1565	18.353	.912	35.565	.1652	20.449
8.8	.833	27.919	.1553	15.278	.882	31.301	.1645	17.128	.931	34.875	.1736	19.084
9.0	.850	27.388	.1630	14.280	.900	30.705	.1726	16.010	.950	34.211	.1822	17.838
9.2	.867	26.876	.1709	13.368	.918	30.131	.1809	14.987	.969	33.571	.1910	16.698
9.4	.884	26.382	.1790	12.531	.936	29.577	.1895	14.049	.988	32.955	.2000	15.653
9.6	.901	25.906	.1872	11.763	.954	29.044	.1982	13.188	1.007	32.360	.2092	14.694
9.8	.918	25.447	.1956	11.057	.972	28.529	.2071	12.396	1.026	31.787	.2186	13.811
10.0	.935	25.003	.2042	10.406	.990	28.031	.2163	11.666	1.045	31.233	.2283	12.998
10.2	.952	24.575	.2130	9.805	1.008	27.551	2256	10.992	1.064	30.697	.2381	12.247
10.4	.969	24.160	.2220	9.249	1.026	27.086	.2351	10.369	1.083	30.180	.2482	11.554
10.6	.986	23.760	.2312	8.735	1.044	26.637	.2448	9.793	1.102	29.679	.2584	10.911
10.8	1.003	23.372	.2406	8.258	1.062	26.202	.2547	9.258	1.121	29.195	.2689	10.315
11.0	1.020	22.996	.2501	7.815	1.080	25.781	.2648	8.762	1.140	28.726	.2795	9.762
11.2	1.037	22.633	.2598	7.404	1.098	25.374	.2751	8.300	1.159	28.271	.2904	9.248
11.4	1.054	22.280	.2698	7.020	1.116	24.978	.2856	7.871	1.178	27.831	.3015	8.769
11.6	1.071	21.938	.2799	6.663	1.134	24.595	.2963	7.470	1.197	27.404	.3128	8.323
11.8	1.088	21.607	.2901	6.330	1.152	24.223	.3072	7.096	1.216	26.990	.3243	7.907
12.0	1.105	21.285	.3006	6.018	1.170	23.863	.3183	6.747	1.235	26.588	.3360	7.518
12.2	1.122	20.973	.3113	5.727	1.188	23.512	.3296	6.420	1.254	26.198	.3479	7.154
12.4	1.139	20.669	.3221	5.454	1.206	23.172	.3411	6.115	1.273	25.818	.3600	6.813
12.6	1.156	20.374	.3332	5.198	1.224	22.842	.3528	5.828	1.292	25.450	.3724	6.493
12.8	1.173	20.088	.3444	4.958	1.242	22.520	.3646	5.559	1.311	25.092	.3849	6.193
13.0	1.190	19.809	.3558	4.733	1.260	22.208	.3767	5.306	1.330	24.744	.3976	5.912
13.2	1.207	19.538	.3674	4.521	1.278	21.904	.3890	5.068	1.349	24.405	.4106	5.647
13.4	1.224	19.274	.3791	4.321	1.296	21.608	.4014	4.844	1.368	24.075	.4237	5.398
13.6	1.241	19.017	.3911	4.133	1.314	21.320	.4141	4.634	1.387	23.755	.4371	5.163
13.8	1.258	18.767	.4032	3.956	1.332	21.039	.4270	4.435	1.406	23.442	.4507	4.941
14.0	1.275	18.523	.4156	3.789	1.350	20.766	.4400	4.247	1.425	23.138	.4645	4.732
14.2	1.292	18.285	.4281	3.631	1.368	20.500	.4533	4.070	1.444	22.841	.4785	4.535
14.4	1.309	18.054	.4408	3.481	1.386	20.240	.4667	3.903	1.463	22.552	.4926	4.349
14.6	1.326	17.828	.4537	3.340	1.404	19.987	.4804	3.745	1.482	22.270	.5071	4.172
14.8	1.343	17.608	.4668	3.207	1.422	19.740	.4942	3.595	1.501	21.994	.5217	4.005

and

$$Q = Pd/f \qquad [4]$$

Since stress, or load P, is proportional to strain, or deflection f, it follows from Equation [4] that Pd/f is constant for all springs of the same material, wire diameter, and mean coil diameter.

By substituting $Q = Pd/f$ and spring index $C = D/d$ in Equation [3], a formula is derived for calculating the wire diameter

$$d = \sqrt{\frac{8C^3Q}{G}} \qquad [5]$$

Values of C and Q are readily obtained from formulas derived later, as Equations [7] and [10], which permit d to be determined analytically and, for quick reference, practical solutions have been summarized in the graph, Fig. 5.

The ratio of the active length at maximum operating load to the theoretical deflection of a spring having no initial tension is known as deflection ratio Y.

From the geometry in Fig. 4

$$Y = \frac{L}{F + F_0}$$

$$\frac{P}{F + F_0} = \frac{P - P_1}{s} = R$$

$$F + F_0 = \frac{P}{R}$$

$$Y = \frac{LR}{P} \qquad [6]$$

Thus elimination of deflection factors shows the deflection ratio to be an important factor in the design of springs, regardless of initial tension, because the load and length components P and L establish the boundaries which locate the gradient, and the rate component establishes the slope of the gradient.

Further from Fig. 4

$$\frac{P - P_o + Q_e}{L} = \frac{P - P_1}{s} = R$$

and since

$$P_o = PT$$

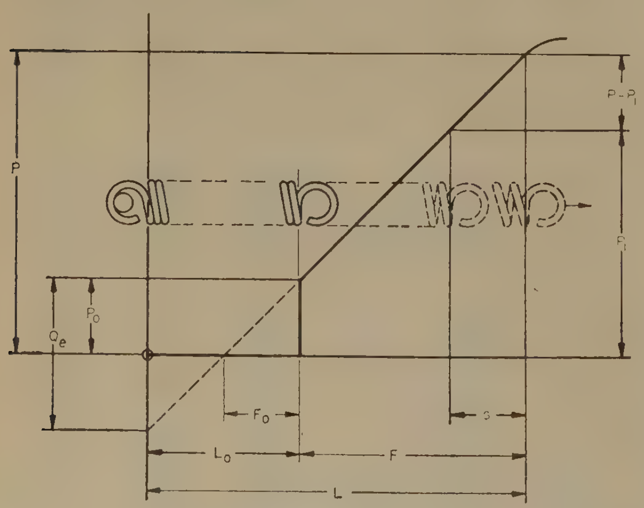

Fig. 4 Graphic Representation of Dynamically Loaded Extension Spring

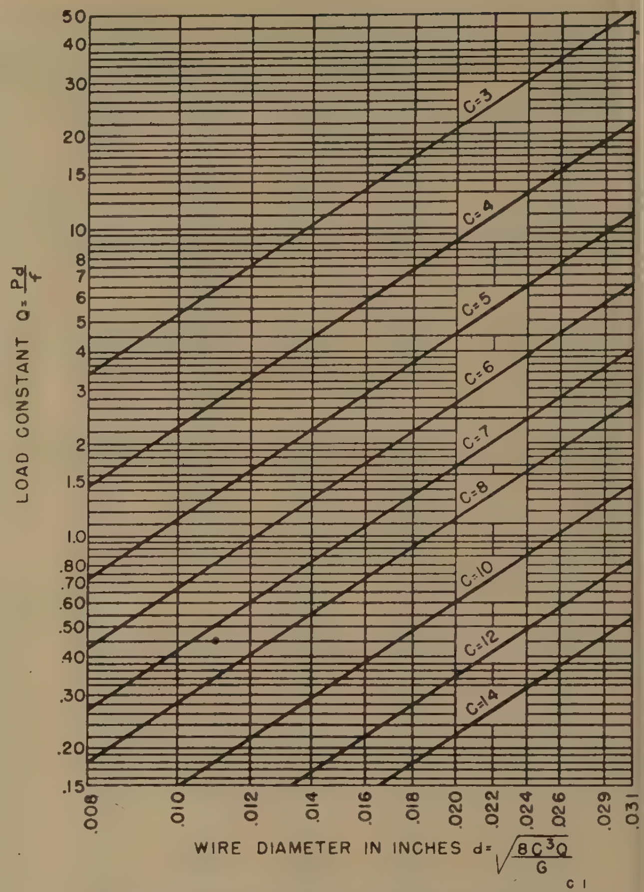

Fig. 5 Q Versus d for Determining Wire Diameter
(This figure has been modified for clarity.)

$$Q_e = LR - P(1 - T)$$

Substituting Equation [6]

$$Q_e = P(Y - 1 + T) \qquad [7]$$

Dividing by P and substituting Equation [4]

$$\frac{d}{f} = Y - 1 + T \qquad [8]$$

From Equation [2]

$$\frac{d}{f} = \frac{d^2\,GK}{\pi D^2 S_s} = \frac{GK}{\pi C^2 S_s} \qquad [9]$$

and

$$C_e = \sqrt{\frac{GK}{\pi S_s} \times \frac{1}{Y - 1 + T}} \qquad [10]$$

Graphic Representation of Compression Springs

A method similar to the one just described for extension springs may be used to analyze graphically the gradients and proportions of compression springs. In this case the active free length of the spring is plotted against the applied compressive load, as shown in Fig. 7, rather than in the conventional manner in Fig. 6. From the geometry in Fig. 7 again it is established that

$$Q = Pd/f \qquad [4]$$

From here on, the compression-spring equations depart somewhat from those derived for extension springs. One reason for

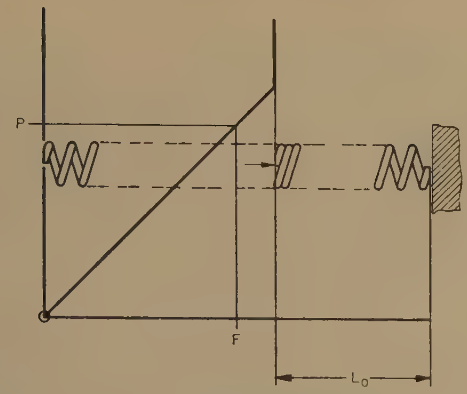

FIG. 6 CONVENTIONAL GRAPHIC REPRESENTATION OF A COMPRESSION SPRING

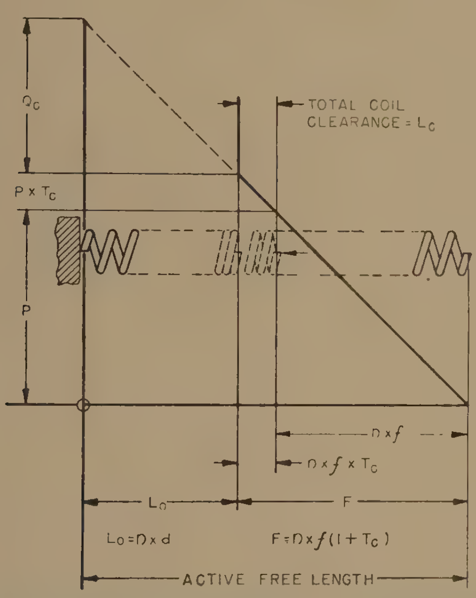

FIG. 7 NEW GRAPHIC REPRESENTATION OF A COMPRESSION SPRING

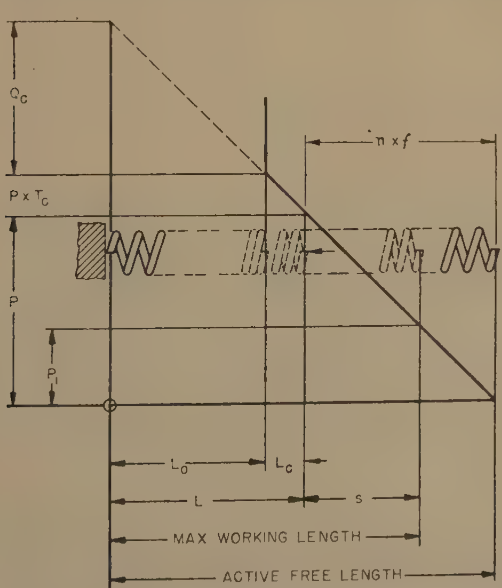

FIG. 8 NEW GRAPHIC REPRESENTATION OF A DYNAMICALLY LOADED COMPRESSION SPRING

this is the fact that compression springs do not have initial tension. Instead they require consideration with respect to coil clearance. By expressing coil clearance as a function of the compressive load P, a coil clearance factor T_c may then be used in the expression $P \times T_c$ to evaluate the additional load required to cause solid compression L_o of the spring from its minimum operating length L.

From the geometry in Fig. 8.

$$Q_c = LR - PT_c \qquad [11]$$

But from Equation [6]

$$\frac{LR}{P} = \frac{L\,(P - P_1)}{P\,s} = Y$$

Therefore

$$Q_c = P\,(Y - T_c) \qquad [12]$$

Following the procedure for formulating Equation [10]

$$C_c = \sqrt{\frac{GK}{\pi S_s} \times \frac{1}{Y - T_c}} \qquad [13]$$

The wire diameter d can now be determined from Fig. 5 or from Equation [5] where

$$d = \sqrt{\frac{8\,C^3 Q}{G}} \qquad [5]$$

using values of C and Q from Equations [12] and [13].

COMPRESSION-SPRING COIL CLEARANCE FACTOR T_c

It is a common practice in compression-spring design to allow a coil clearance of 10 per cent of the wire diameter or coil deflection, whichever is larger; but in formulating an equation for coil clearance, it is more satisfactory to allow 5 per cent of the sum of the wire diameter and coil deflection or 0.05 $(d + f)$ per coil.

By designating this percentage as p, expressed as a decimal, then, in general, the clearance per coil is $p\,(d + f)$.

Letting total coil clearance $= L_c$ and spring rate $= R$, from Fig. 8

$$PT_c = L_cR$$

or

$$P\,T_c = p\,n\,(d + f) \times \frac{P}{fn}$$

$$T_c = p\left(\frac{d}{f} + 1\right) \qquad [14]$$

$$T_c = p\left(\frac{GK}{\pi C^2\,S_s} + 1\right) \qquad [15]$$

Thus it is seen that coil clearance is a function of the spring index and can be applied to the formulas for Q_c and C_c directly by expressing it as a function of Y, and developing corrected Y values for use in Equations [12] and [13].

Solving for Y in Equation [13]

$$Y = \frac{GK}{\pi C^2 S_s} + T_c \qquad [16]$$

The difference is negligible if the coil-clearance factor T_c in Equation [16] is ignored

$$Y = \frac{GK}{\pi C^2 S_s} = \frac{d}{f}$$

Substituting in Equation [14]

$$T_c = p\,(Y + 1) \qquad [17]$$

Equations [12] and [13] become

$$Q_c = P\,[Y\,(1 - p) - p] \qquad [18]$$

$$C_c = \sqrt{\frac{GK}{\pi S_s\,[Y\,(1 - p) - p]}} \qquad [19]$$

Extension-Spring Initial Tension

Upon investigating the use of Equation [17] for determination of initial tension factor T for extension springs, it is found that by coincidence it produces very good results, and the general equations for Q_e and C_e may be written thus

$$Q_e = P\,[Y\,(1 + p) - 1 + p] \qquad [20]$$

$$C_e = \sqrt{\frac{GK}{\pi S_s\,[Y(1 + p) - 1 + p]}} \qquad [21]$$

A p value of 0.05 produces medium initial tension whereas for high initial tension 0.10 should be used where C is greater than 4.

Graphical Determination of Spring Index C

The actual use of the equations for C may be simplified considerably by plotting graphs of Y versus C. Fig. 9 is a Y versus C graph which has been prepared from Equations [10] and [13] for the design of music-wire springs. It is not necessary to plot a different set of Y versus C curves for compression springs, because solving for Y in Equations [10] and [13]

for extension springs

$$Y = \frac{GK}{\pi C^2 S_s} + (1 - T)$$

for compression springs

$$Y = \frac{GK}{\pi C^2 S_s} + T_c$$

Therefore $(1 - T)$ and T_c are increments to Y which can be taken into consideration when reading the graphs in the form of additions to or subtractions from Y and it is necessary only to plot C versus Y as determined from the equation

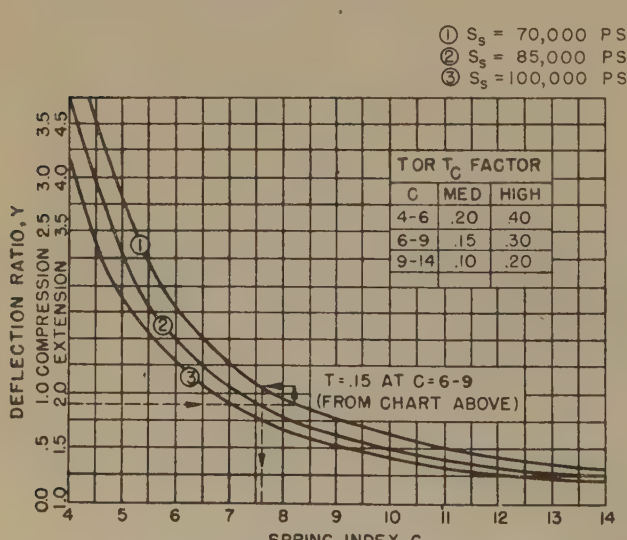

Fig. 9 Y Versus C for Selecting Spring Indexes

$$Y = \frac{GK}{\pi C^2 S_s}$$

The graph, Fig. 9, was calculated with G = 11,500,000 and S_s = 70,000 for Curve 1, 85,000 for Curve 2, and 100,000 for Curve 3. In using this graph to determine C, Y is calculated from Equation [6], and the T factor is added or the T_c factor subtracted from Y to obtain the correct spring index C. This graph is very flexible in that the corresponding spring index for any value of T or T_c may be obtained from the single curve.

Spring-Proportion Tables

The design of helical extension and compression springs can be simplified to a considerable extent by the use of properly prepared reference tables. In addition, if these tables are arranged so that they may be used in conjunction with a mathematical or graphical design procedure as outlined in this paper, springs to meet very exacting requirements can be designed with a minimum of design time.

Partly because the spring index C has such a great significance in spring calculations and partly because it produces a desirable range of outside diameters for springs, arbitrary values of C in steps of 0.2 are used in the calculation of the tables (see Table 1). For the sake of convenience, the outside diameter OD is listed in preference to the mean diameter D. The loads and deflections are calculated from the basic formulas at 100,000 psi stress, making it easy to select springs for other stresses by direct proportions.

To use the tables it is convenient to calculate Y from Equation [6] and then to determine either C or Q graphically, or from formulas included in this paper. After C or Q has been found, the table may be scanned for the desired load P_T at the established C or Q value

$$P_T = \frac{100{,}000\,P}{S_s}$$

where P is the maximum operating load and S_s is the desired maximum stress.

From the table, values may now be read for wire diameter d outside diameter OD, and deflection f_T at table load P_T. The number of active coils may be calculated from the equation

$$n = \frac{P_T \times s}{f_T\,(P - P_1)} \qquad [22]$$

where s is the operating stroke and P_1 is the minimum operating load. The solid active length L_o may be determined from the formula

$$L_o = nd$$

to which should be added the necessary inactive coils and end loops to get the final specifications for the spring.

If the operating load and length conditions of a problem are drawn to scale and represented similarly to the diagram, Fig. 4, Q may be scaled from a tentative initial tension point. and a coil of sufficient strength P_T and corresponding Q value selected from Table 1. If the Q value is not exact, this may be remedied by changing the initial tension accordingly. After the initial tension is fixed, the solid length L_o may be scaled, and the number of coils determined from the formula

$$n = L_o/d$$

In the case of compression springs, as shown in Fig. 8, L_o is measured at the final Q value. Care should be taken when making graphical solutions to insure sufficient coil clearance and initial tension within recommended ranges.

The graphical solution of spring problems is explained further and in greater detail in the section on the graphical cataloging of existing springs, where Q is utilized in conjunction with the catalog for making specifications for new springs from coil proportions of cataloged springs.

Space Considerations in Machine Designs Requiring Springs

In order to introduce well-designed springs in a mechanism, it is of primary importance to have sufficient space available to accommodate a spring of the proper physical proportions. For a statically loaded spring this is not nearly as important as for a spring subject to dynamic loadings; on the other hand, if the spring has to meet specific requirements with respect to its rate, the possible number of solutions to the problem is reduced. For this reason a guide for making spring space allowances in the early phases of a design is a welcome aid to the designer. The spring tables will serve the purpose of establishing the required outside-diameter clearance for a spring with an appropriate spring index if the approximate maximum working load has been defined.

It is quite another problem to determine the proper ratio between the active operating length L at load P and the working stroke s. This may be done by substituting the load increase factor[3] $i = P/P_1$, in Equation [6] after expressing the spring rate R in terms of loads and stroke

$$Y = \frac{LR}{P} = \frac{L\,(P - P_1)}{P_s}$$

$$Y = \frac{i-1}{i} \times \frac{L}{s} \qquad [23]$$

By solving Equation [23] for the stroke-to-length ratio s/L at various values of Y and i, the graph in Fig. 10 is produced. This graph may be used for selecting s/L and P/P_1 values which will produce a spring with reasonable proportions. Since a spring index between 6 and 9 falls within what may be considered an optimum range, it will be well to select Y-values which eventually will produce a spring whose index will fall within that range. It should be noted that Equation [23] does not include a load term P. This is a valuable asset in that it is possible to determine suitable spring proportions without knowing the final load requirements in the mechanisms

$$L = \frac{Y\,i\,s}{i-1} \qquad [24]$$

Selected Working Stress

The load-increase factor $i = P/P_1$ takes on added significance when its use in conjunction with fatigue tests is realized. Fig. 11 is a diagram showing the trend of results from fatigue tests of springs operating over various loading ranges. Failure in actual tests takes place at points above the maximum stress shown, but on the same general curve. The maximum stress has been modified to allow an adequate safety factor. Inasmuch as the torsional stress in the spring will be proportional to the applied load

$$\frac{\text{Max stress}}{\text{Min stress}} = \frac{P}{P_1} = i$$

a curve plotted with respect to max S_s versus i may be superimposed on the fatigue diagram, and used to determine safe maximum design stresses for various load-increase factors.

[3] "Helical Spring Tables—I," by Paul Klamp, *Product Engineering*, vol. 10, 1939, p. 361.

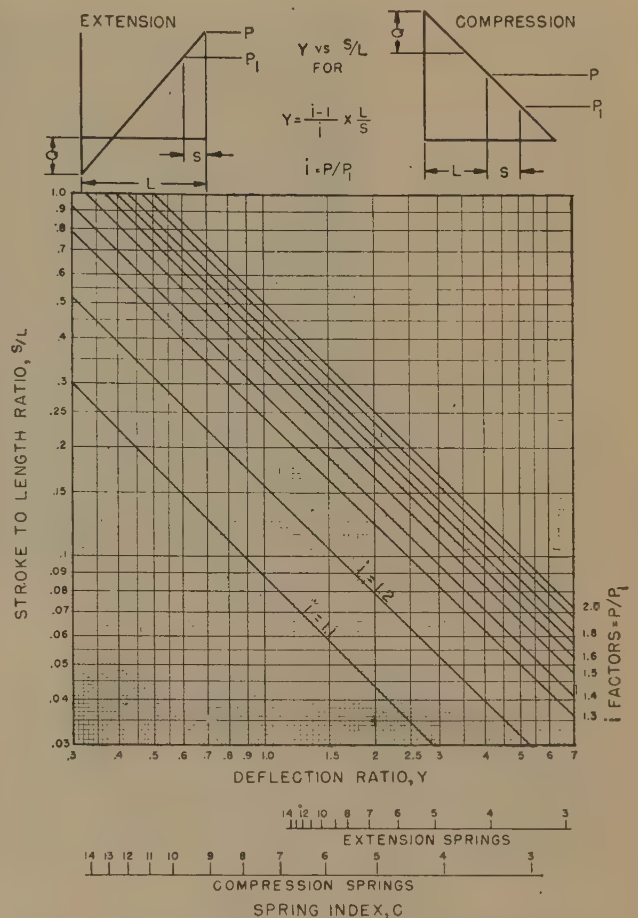

Fig. 10 Y Versus s/L and i for Making Preliminary Space Allowances for Dynamically Loaded Springs

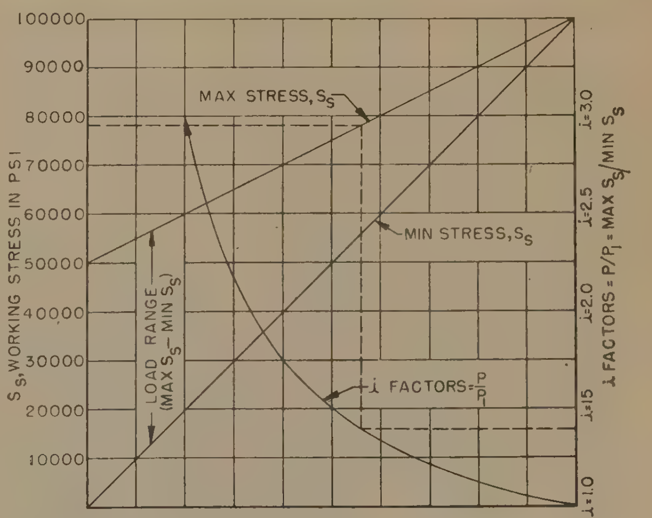

Fig. 11 Max S_s Versus i Factors for Selecting Working Stresses

Inactive-Length Allowance

The L term in the stroke-to-length ratio s/L and in Equations [6] and [23] for calculating Y, represents the active working length at maximum load P. When determining length requirements between supports early in the design of a mechanism from

Y or s/L, it is necessary to add to the active working length the approximate inactive length to avoid the necessity for severe requirements with respect to initial tension or coil clearance in the final design. Also, for the same reason, when calculating Y for a spring to operate between two previously located supports, it is necessary to subtract the approximate inactive length. Fig. 12 may be used as a guide in selecting the approximate inactive-length allowance when the maximum load is predictable. Curve 1 is for extension springs with regular machine end loops. Curves 2, 3, and 4 are for compression springs with squared, squared

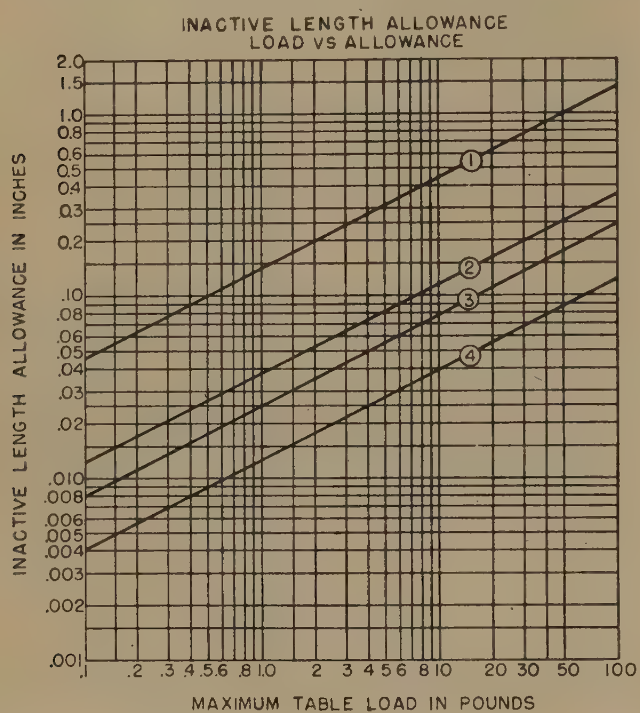

Fig. 12 L_i Versus P for Making Inactive Length Allowances

and ground, and plain ends, respectively. The actual inactive length will be calculated from the accepted formulas when the coil proportions are known.

Cataloging of Existing Springs

Manufacturers who use considerable numbers of extension and compression springs in their products are faced from time to time with the problem of selecting existing springs for changes in the machine design or for new applications. Unless sufficient data are available, it is generally easier for the designer to specify a new spring than to use one that is already released for production. Consequently new springs are often duplications of existing designs. From the standpoint of economy and speed in procurement, it is desirable to be able to select a stock spring for the new application. In order to facilitate such selection, it is possible to use the information submitted in this paper for producing a spring catalog which will reflect accurately the spring specifications and make it easy for the designer to select a spring with the desired characteristics. Furthermore, with the method of cataloging springs described in the following paragraphs, it is possible to use available spring data to set up specifications for new springs in case a suitable existing spring is not found.

Fig. 13 indicates the method used for plotting the gradients for various springs. It should be noted that the spring gradient starts at a distance L_i from the Y-axis. This distance represents the inactive coils and end loops of the spring. The inclusion of L_i makes it possible to consider the spring characteristics on the basis of the over-all dimensions of the spring rather than on the active coils alone. In the illustration, Fig. 13, showing a spring gradient, the upper end of the solid line represents the load which

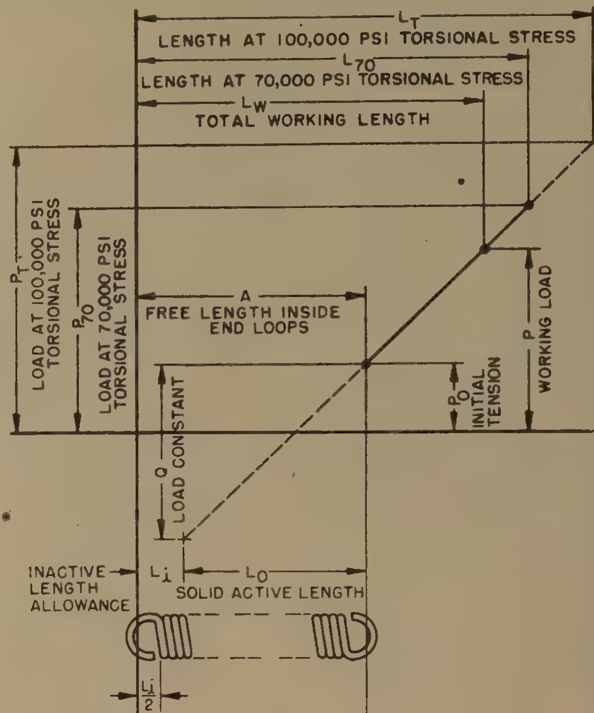

Fig. 13 Sample Graph, Extension Spring

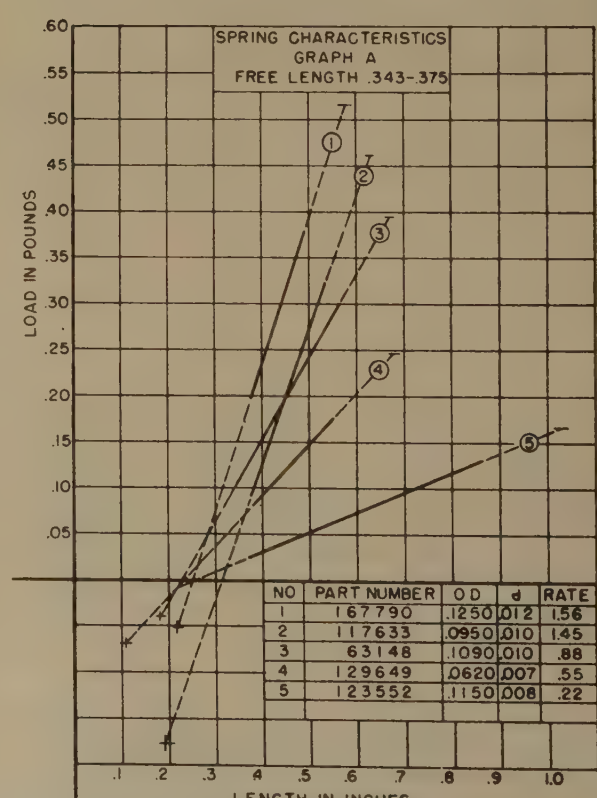

NO	PART NUMBER	O D	d	RATE
1	167790	.1250	.012	1.56
2	117633	.0950	.010	1.45
3	63148	.1090	.010	.88
4	129649	.0620	.007	.55
5	123552	.1150	.008	.22

Fig. 14 Sample Page, Graphical Spring Catalog

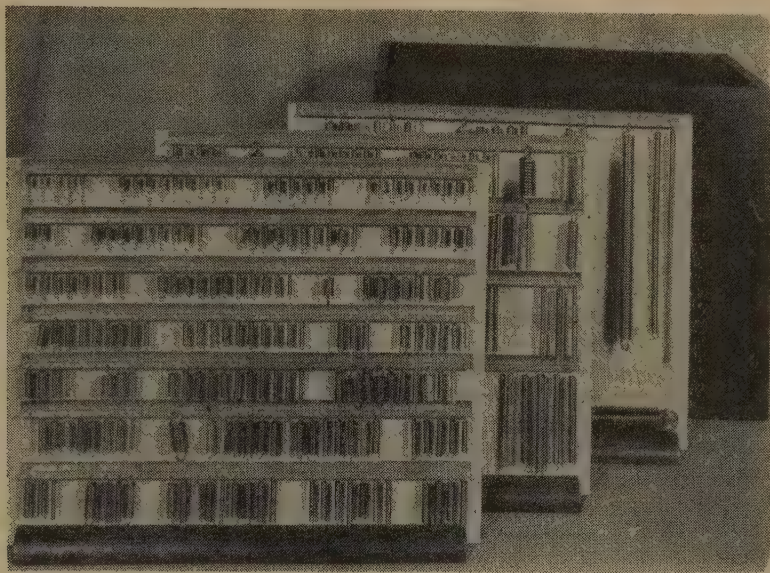

Fig. 15 Spring Display Panel

produces 70,000 lb stress, and the upper end of the broken line represents the load producing 100,000 lb torsional stress.

An actual chart of a family of gradients is shown in Fig. 14. The graphs on each chart represent springs, all of which have essentially the same free length. It is easily seen how conveniently a designer can select a spring that will give him the desired load at a definite extension, and also determine the stress at which the spring is working under those conditions. If these graphs are supplemented by a display panel as shown in Fig. 15, the designer has an opportunity to inspect the actual spring.

The spring catalog is also useful in establishing specifications for new springs when existing springs cannot be found which will meet the requirements. An example of this is shown in Fig. 16

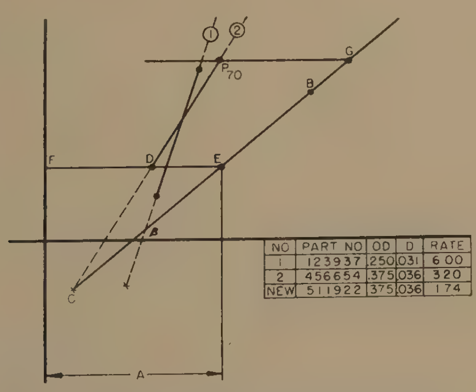

NO	PART NO	OD	D	RATE
1	123937	.250	.031	6 00
2	456654	.375	.036	3 20
NEW	511922	.375	.036	1 74

Fig. 16 Spring Design, Graphical Method

in which is depicted a required spring whose gradient should go to point B in the co-ordinate system. On the basis that an outside diameter of 0.375 will be satisfactory, a line is drawn through points B and C, since C is the terminal point for the gradient of a spring with a 0.375 diam. The line FD, representing the initial tension of spring No. 2, is extended to the new gradient at E. The new free length inside end loops is equal to the distance FE, and the rate equals the slope of the gradient. The specifications for the wire diameter and outside coil diameter were taken from the tabulated data on the graph for spring No. 2.

In a similar manner it is possible to obtain the specifications for a spring which must have a definite rate. In this case it will be necessary to plot two points in the co-ordinate system and draw a line between them, extending the line and selecting a point C which lies close to the gradient drawn. The specifications can now be obtained as in the previous example.

The procedures just described are further applications of the load constant principle and are similar to the graphical solution presented in the section on the "Spring Proportion Tables."

Acknowledgment

The author wishes to express his appreciation to Dr. W. J. Eckert and Dr. L. H. Thomas of the Watson Laboratory of Pure Science, Columbia University, for their co-operation in preparing the tables.

Discussion

A. H. Burr.[4] There would seem to be considerable merit in the author's method representing the deflection curve of a spring with the spring length included. This gives an excellent conception of the space requirements. His several constants and ratios such as Q, T, Y, and i become convenient means of introducing several design considerations into the formulas which lead to the determination of wire diameter. In regard to the over-all approach and the method of direct solution for wire diameter, it seems to the writer that only experience in their use can bring a full comprehension of their significance to spring-design practice.

Under "Nomenclature," should not f be defined as the deflection per coil produced by load P when there is no initial tension or compression? Only by this definition can the total deflection F, in terms of number of active coils n, be nf for the compression spring in Fig. 8, and $nf\,(1 - T) = nf\,(P - P_o)/P$ for the tension spring with initial tension P_o in Fig. 2.

There is an alternate proof for the statement that the load constant Q, represented by the distance BA in Fig. 3 of the paper, is constant or the same for all springs with the same mean coil diameters D, wire diameters d, and the same material. In both Figs. 2 and 7, Q is the spring rate R multiplied by the solid length

[4] Department of Machine Design, Sibley School of Mechanical Engineering, Cornell University, Ithaca, N. Y. Mem. ASME.

L_o. Spring rate R, from Equation [3], is $P/nf = (Gd^4)/(8\,D^3n.)$. Also $L_o = nd$. Hence

$$Q = RL_o = \frac{Gd^4}{8\,D^3n} \cdot nd$$

$$= \frac{Gd^5}{8D^3}$$

Q is seen to be a function of G, d, and D only. Equation [5] follows readily from this after the substitution of $C = D/d$.

In the derivation of Equation [12] does not the relationship $LR/P = Y$ follow from the definition of Y and the geometry of Fig. 8, rather than from Equation [6], as stated?

In the method the value of the spring index C is controlled by the deflection ratio $Y = LR/P$ and other factors. It is suggested in the paper that C may be kept within a desirable range of 6 to 9 by careful selection of Y-values. Can a guide for the selection of Y and of i, the ratio of maximum to minimum working loads, be given? Without a guide does the problem become one of trial and error?

It would be desirable to know the steel and its treatment on which Fig. 11 is based, also the factor of safety used in determining the working stresses.

It is not clear to the writer how the data in Fig. 12 are applied. If the author would furnish an illustrative example, a better choice could be made by a reader between this method and the more conventional trial-and-error method.

F. W. Gaskins.[5] We have here a new and different approach to the problem of spring design. The emphasis placed on the necessity for providing sufficient space for a spring having certain characteristics of load, rate, etc., and the convenient means provided for establishing the dimensions of that space should be of inestimable value to the designer. With the method described available to him, and the implied warning that if he does not provide proper space he will have to accept something less than satisfactory spring performance, we may hope that at least some of the unsound designs which are so common today will be avoided.

Undoubtedly, it was the author's desire to have his formulas mathematically correct which caused him to include the Wahl "correction for curvature" factor. It is rather startling to encounter this factor in the basic equations. Whatever its value or lack of value as a factor in establishing a safe maximum stress in any given case, its inclusion does have the virtue of tending toward conservative design from a stress standpoint. Spring manufacturers will rise up and call blessed any procedure which will accomplish that.

In the method of depicting and comparing the characteristics of springs set forth under the heading "Cataloging of Existing Springs" and illustrated by Figs. 13, 14, and 16, the designer is presented with another invaluable aid. In a plant using many springs of similar kinds the saving resulting from the prevention of duplication and near duplication should be tremendous.

H. F. Ross.[6] It is a common practice among engineers to deal with a problem from every possible angle. This paper shows a well-integrated system, conceived from certain new relationships developed by the author to establish a progressive procedure of spring selection, based upon a concept of physical dimensions as applied to the complete working range of the spring. The resulting method should prove a real contribution to facilitate the practical selection of springs for particular applications.

In order to utilize this system, two new concepts must be kept in mind. These are symbolized by the letters Q and Y, representing, respectively, the load to produce a deflection equal to the active solid length, and the ratio of the active length at maximum operating load to the theoretical deflection at that load. They may be used either for compression or tension springs, but the graphical distinction must be remembered. In addition, the representation of a clearance factor T_c, as a function of Y, and its use in modifying the value Q for compression springs, must be visualized, together with a similar modification of Q by an initial tension factor T for tension springs.

The following procedure is typical of a dynamic spring design by this method:

1 Determine mathematically the value of Y as a function of the load-increase factor P/P_1, making the value come within the limits of safe design on the stress-range chart.

2 Find C or Q graphically or mathematically by the formulas provided.

3 Extrapolate the load P at the maximum desired stress to the value P_T, the load at 100,000 psi, in order to use the spring tables provided.

4 Read values of wire diameter d, outside diameter, and deflection per coil from the tables. This is permissible since the term Q is constant for any given wire size and coil diameter.

5 Calculate the number of active coils and the active solid length of the spring.

6 Add provision for inactive wire or loops.

It has been the experience of the writer in the limited time available to become acquainted with this system, that the time required to arrive at a solution is somewhat longer than by other means. However, it is conceivable that the benefit coincident with a single solution, as opposed to trial and error, and the accumulation of a catalog file as a permanent reference for selection or modification, might prove to have an advantage over established methods.

The writer suggests that the safety factor contained in the load-increase curve used in conjunction with the fatigue diagram be defined a little more clearly, and also that separate curves be made for tension and compression springs, since tension springs do not contain the beneficial residual stress produced in compression springs by cold-setting and therefore cannot be used successfully over the same stress range in a dynamic application.

The value of shotblasting and its effect on the stress-range diagram has become increasingly recognized in the past few years. The general load-increase curve shown in Fig. 11 might well become a family of curves to facilitate this and other particular solutions not defined adequately by one curve.

The author is to be commended for a significant contribution to the literature in this field, particularly on the originality and integration of a new approach to spring design.

J. T. Wang.[7] The ordinary objectives in designing a helical spring is to keep the working stress below a harmless limit and to get desirable deflections or restoring forces under the prescribed conditions. The usual method of making a solution is by "cut and try" using the two following fundamental formulas

$$S_s = \frac{8KPD}{\pi\, d^3}$$

$$\delta = \frac{8PD^3N}{Gd^4}$$

The author's method introduces a new variable called "deflec-

[5] The General Spring Company, Cincinnati, Ohio.

[6] Research Division, United Shoe Machinery Corporation, Beverly, Mass.

[7] Professor of Machine Design, University of Che-Kiang, China. Visiting Consulting Engineer, Allis-Chalmers Manufacturing Company, Milwaukee, Wis.

tion ratio," Y. The required given conditions for solution of problems of helical spring according to his method are as follows:

1 Maximum length of the spring.
2 Minimum length of the spring.
3 Load on spring at maximum working length.
4 Load on spring at minimum working length.
5 Free length of the spring.

It will be definitely a help to the designer if he has an idea of these lengths when he starts to work the problem. On the other hand, if what he has in his mind are only the maximum force he has to handle and a desirable deflection under the given force, then he still must resort to trial-and-error methods.

Some time ago the writer had a problem of designing a helical spring with the following specifications:

1 It should have an initial compressive force of 1750 lb.
2 The working compression beyond the position of initial compression is a stroke of $1^{15}/_{16}$ in. At the end of the stroke, further compression of the spring is prevented by some kind of stop mechanism. However, at the end of the stroke of $1^{15}/_{16}$ in., the spring should not be overstressed.
3 The outside diameter of the coils should not exceed 6 in.; a smaller diameter will be preferred.
4 It should have as short a length as possible.
5 Maximum allowable shear stress is 70,000 psi.

At the start, we did not have any idea of the lengths required for the spring. If we were to use the author's method, we would have to assume some of the lengths and later improve the results by trial and error. The problem was solved with the two fundamental formulas by cut and try. The writer still feels that it is a better method than the author's. The reason is that we are more familiar with the fundamental formulas.

However, there are certain problems for which the author's method will prove to be superior. It is also the writer's opinion that when the design of springs becomes a sizable routine in a design office, special charts or formulas should be devised to facilitate the work, as the author did for his office.

F. P. Zimmerli.[8] The author and his associates have completed an immense amount of work in assembling data for their method of spring calculation. For the use to which they intend to put it, the material should help them a great deal. The author is to be congratulated on the originality of his solution of his problem.

A recent survey of spring uses in the automotive and other industries shows that 95 per cent of the helical springs used fall inside the physical specifications of the Society of Automotive Engineers.[9] These specifications are rather broad, so the fact that they cover such a usage indicates that many springs need not be extremely accurate. Because of this, we do not believe the suggested method will meet with much use by the ordinary draftsman. It appears easier to use handbook tables which are figured for constant stress. For example, "Marks Handbook" at 60,000 psi, torsion only, will give load, outside diameter, and deflection per single coil per 100-lb load. In a matter of a very few minutes the deflection for the load, number of coils needed, and wire size are available. A mistake of 100 per cent, i.e., stress of 120,000 psi will in many cases "get by" in static designs.

The few who must figure springs most of the time have slide rules laid off in third and fourth-power logarithmic scales. A glance at such a rule and slight movement of the slide brings so many springs under view that tables would not accelerate the computation but slow it down.

The incorporation of Wahl's correction into the stresses is not exactly essential for ordinary work. Actually, when one calculates a spring, Wahl's correction for curvature is necessary only when the spring must have an infinite life. The ordinary machinery used to produce springs is not efficient if D/d ratio is less than 3. At this ratio Wahl's correction can be shown to cover an area of cross section around 3 per cent. It is obvious that for long life the start of failure in this 3 per cent of the area will ruin the spring.

Many springs, however, are either static or used less than 50,000 times during their life. Such springs, being highly stressed, are more liable to fail through setting than breakage. Using the Wahl correction, a compression spring at 150,000 psi might not set much with a D/d ration of 3, but were this ratio increased to 20, the same material would lose an appreciable amount. Therefore we would not use this correction in calculating for a number of spring uses. Unfortunately, Wahl's factor overcorrects these small ratios.

In general, we believe stress calculations using the Wahl factor are essential in considering fatigue. We do not believe this correction of much use as regards setting. In considering the effect of heat on springs the correction is often used, but curves using ordinary torsion stresses are also reliable. We have used both kinds of curves but have published load-loss curves due to heat, employing corrected stresses only.

The author's idea of classifying and setting up methods to select springs for new applications from those made previously is excellent. For any one plant or product we believe this might be done with a saving to all concerned. Looking over the mechanical-spring industry as a whole, we find there are no standard springs, save die-knockout springs. This is because the over-all demand of various users is so different as to render such a standardization industry-wise impractical. The spring plant today is essentially a jobbing plant. With the present diversity of uses of springs, we are actually producing more different designs and kinds of springs than were thought of as little as 10 years ago.

Author's Closure

The several discussions submitted in conjunction with this paper offer valuable contributions to the subject. In some cases, they actually have extended the scope of the paper to include discussions on the relative merit of Wahl's correction and stress conditions in springs. Notable in this respect is Mr. Zimmerli's discussion which is very interesting. However, we do not consider ourselves qualified to offer additional comments on this phase of the subject.

Mr. Gaskins has expressed the author's ultimate objective in the preparation of this paper and the work which preceded it; namely, that of providing for machine designers a basis for a spring-design procedure that would encourage the allowance of adequate space for springs in mechanisms at the early stages of the design. A machine designer is not necessarily an expert in the design of helical springs, but with a clear concept of this design procedure, he will be influenced to provide the desirable spring space in his design.

The discussions offered by Mr. Burr and Mr. Ross indicate that these gentlemen have given the paper a very thorough review. We wish to acknowledge Mr. Burr's correction of our definition of f, which appears in the nomenclature. It is unfortunate that this error was not noted by us and we appreciate Mr. Burr's calling this matter to our attention. Mr. Burr's alternate derivation of an equation for Q is accurate and interesting.

Mr. Burr also called our attention to the need for guidance in the selection of Y- and i-values. By referring to Fig. 10 of the

[8] Chief Engineer, Barnes-Gibson-Raymond, Division of Associated Spring Corporation, Detroit, Mich. Mem. ASME.

[9] "Manual on Design and Application of Helical and Spiral Springs for Ordnance," Society of Automotive Engineers, 1943, pp. 28–29.

paper, it may be seen that appropriate Y-values may be selected by making use of the scales for spring indexes, both for extension and compression springs, which appear in that figure. With respect to i-values, it has been found that a load-increase factor approaching 1.3 is very desirable. In the event that the spring designer has great latitude in the specifications for his spring, which is often true in the early phases of a machine-design problem, he may work toward the following values in extension springs: $C = 7, i = 1.3, s/L = 0.13$. For compression springs: $C = 7, i = 1.3, s/L = 0.2$.

With this guide in mind, Mr. Wang's problem becomes one that may receive a direct approach in its solution rather than a trial-and-error method. The absence of a required rate in his problem permits us to select a load-increase factor i, of 1.3, and we can thus establish the maximum operating load at 70,000 lb as 1.3×1750. Because the condition of permissible stress and work required from the spring establishes the minimum volume of material in the spring, it follows that the shortest length of the spring is obtainable only with the largest permissible diameter. We can now refer to any reliable spring table and establish the outside diameter and wire diameter, as well as the deflection per coil at maximum operating load that is consistent with the stress condition given in the problem.

From Equation [16] we can determine with the available information the deflection ratio as $Y = (d/f) + T_c$. With a coil clearance factor T_c of 0.25, it appears that the proper deflection ratio for Mr. Wang's problem would be 1.5. Referring to Fig. 10, we can now establish the stroke to length ratio s/L and thus set up an equation for the solution of the minimum operating length of the compression spring. It is interesting to note that this procedure also closely approximates the design procedure based on the data in the paper which Mr. Ross has suggested in his discussion. Quite by coincidence, Mr. Ross' suggested procedure closely parallels one which we have submitted in the form of a recommendation to our Engineering Department. The entire and detailed procedure was not included as part of this paper because of its length. It includes a complete set of tables for wire sizes between 0.004 and 0.170, giving data for 3600 spring coils. The author will be happy to forward a complete set of these tables to anyone who is interested.

The author wishes to thank all the discussers for their contributions of time and effort which have resulted in a fuller treatment of this very interesting subject. He also wishes to acknowledge with thanks the several contributions and valuable suggestions offered by his associates in the Customer and Production Engineering Department in IBM, particularly the encouragement he has received from Mr. E. W. Gardinor and Mr. W. G. Baird's valuable review of the paper.

Centrifugal Blowers for Two-Cycle Diesel Engines

By ROBERT CRAMER, JR.,[1] MILWAUKEE, WIS.

The usual means for supplying scavenging air to two-cycle Diesel engines is by reciprocating piston pump, by engine-driven positive-displacement blower, or by motor-driven blower, either of the positive-displacement type or centrifugal type. The pressure-volume characteristics of the centrifugal blower are less favorable for engine scavenging than those of either the Roots-type blower or the reciprocating pump. In spite of its somewhat lower efficiency, the centrifugal blower offers a solution to the problem of installing maximum additional horsepower to a plant restricted in space. This paper deals with the characteristics of this type blower and its advantages for certain applications.

The Field for Centrifugal Blowers

Current practice in scavenging two-cycle Diesel engines is to supply air by reciprocating piston pump, by engine-driven positive-displacement blower, and to a lesser extent by motor-driven blower, either positive-displacement or centrifugal.

The efficiencies of these air sources vary greatly, as shown by Table 1. This efficiency is the ratio of engine power consumed by the blower and its drive to the theoretical adiabatic power, the engine power being referred to the crankshaft and including all losses of the drive.

TABLE 1 TYPICAL EFFICIENCIES OF VARIOUS BLOWERS AND DRIVES

Blower type	Blower efficiency	Drive efficiency	Combined efficiency
Reciprocating pump	0.50 to 0.68	0.95	0.48 to 0.65
Positive blower, Roots-type, gear-driven	0.80 to 0.84	0.97	0.78 to 0.82
Positive blower, Roots-type, motor driven	0.80 to 0.84	0.86[a]	0.69 to 0.72
Centrifugal blower direct motor drive	0.68 to 0.75	0.86[a]	0.59 to 0.65
Centrifugal blower gear-motor drive	0.68 to 0.75	0.84	0.57 to 0.63

[a] The product of 0.94 generator efficiency and 0.92 motor efficiency.

From this table it is apparent that the Roots-type positive-displacement blower, gear-driven from the engine crankshaft, is the most efficient source of scavenging air. The centrifugal blower of itself can be quite efficient when properly proportioned but the loss due to the combined electrical losses of the generator and motor reduces it to a level about comparable with an efficient reciprocating pump.

The pressure-volume characteristics of the centrifugal blower are less favorable for engine scavenging than those of either the Roots-type blower or the reciprocating pump. This will be discussed later.

In spite of the less favorable efficiency and pressure-volume characteristic, the motor-driven centrifugal blower has found its place in recent years for other reasons. When an additional engine is installed into an existing powerhouse, either in place of an older engine or in other available but restricted space, it has been found possible to include one or two additional cylinders in the space which would be occupied by the scavenging pump or gear-driven blower. The centrifugal blower may be located in a smaller structure outside the main powerhouse. Figs. 1, 2, and 3 are a striking example. Fig. 1 shows the interior of the municipal power plant at Carthage, Mo. The foreground engine is an 8-cylinder $21^1/_2$-in. × 29-in. two-cycle engine, rated 3200 hp at 225 rpm, scavenged by a motor-driven blower. The engine directly behind, which occupies the same floor length, is a 6-cylinder engine of slightly smaller cylinder bore, scavenged by a reciprocating pump and rated 2250 hp at the same speed. Fig. 2 is a view of the interior of the blower house showing the direct-motor-driven blower of 14,900 cfm, and Fig. 3 is an external view of the blower house showing also the intake pipe and the exhaust muffler. The left side of the blower house is a chamber housing a continuous self-cleaning air filter.

For very large engines, especially with large numbers of cylinders, a much better distribution of scavenging air is possible than with an engine-driven blower or pump located at one end of the crankshaft. Fig. 4 shows the arrangment of the scavenging-air system for a large power plant currently being built in Mexico City. The engine is one of six 12-cylinder 29-in. × 40-in. machines, the crankshaft being 57 ft long. It has been found that for engines of this length scavenging-air distribution to the cylinders becomes quite unbalanced if air is supplied through one end of the scavenging header. The arrangement shown provides even distribution and uniform scavenging for all cylinders.

For an engine of the magnitude just mentioned, which requires 45,000 cfm at a pressure rise of 3.6 psi, there are no commercially available Roots-type blowers which are suitable. Even if developed they would be extremely large and require either a large slow-speed motor or a reduction gear. A reciprocating pump would be much too large and cumbersome.

In ships where the machinery space is very crowded it has been found practical to locate the centrifugal blowers at almost any reasonable place and pipe the air to the engine. Fig. 5 shows a typical arrangement in a U. S. Maritime Commission VC2-M-AP4 Victory ship of 14,900 tons.

Air Requirements of Two-Cycle Diesel Engines

The air requirements of two-cycle engines are dependent upon so many factors that experience and experiment are the only reliable guides. Engines of the type being discussed require a scavenging-air volume 1.3 to 1.4 times the cylinder displacement, measured at atmospheric pressure. Schweitzer[2] has described methods for determining the amount of air and has shown that increasing air flow produces higher scavenging efficiency. It also improves engine cooling.

The air requirements are based upon average conditions.

[1] Assistant Chief Engineer, Nordberg Manufacturing Company. Jun. ASME.

Presented at the 20th National Oil and Gas Power Conference, St. Louis, Mo., May 20–22, 1948, of The American Society of Mechanical Engineers.

Note: Statements and opinions advanced in papers are to be understood as individual expressions of their authors and not those of the Society. Paper No. 48—OGP-2.

[2] "Porting of Two Cycle Diesel Engines, Part II," by P. H. Schweitzer, Diesel Power, Diesel Transportation, vol. 20, June, 1942, pp. 477–479.

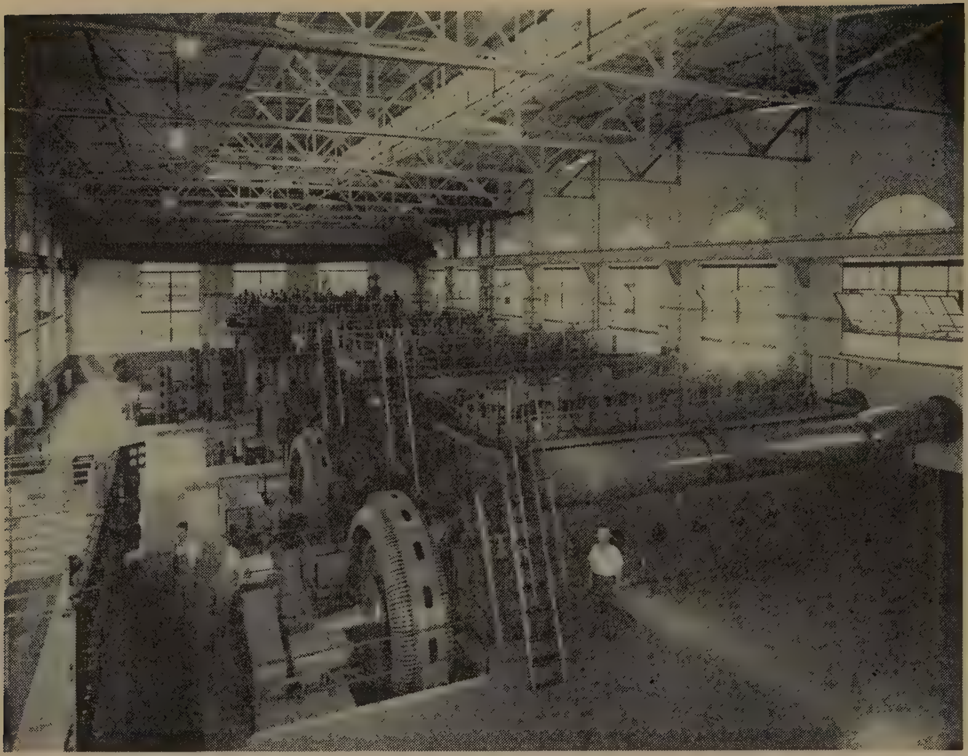

Fig. 1 Interior of Power Plant at Carthage, Mo.

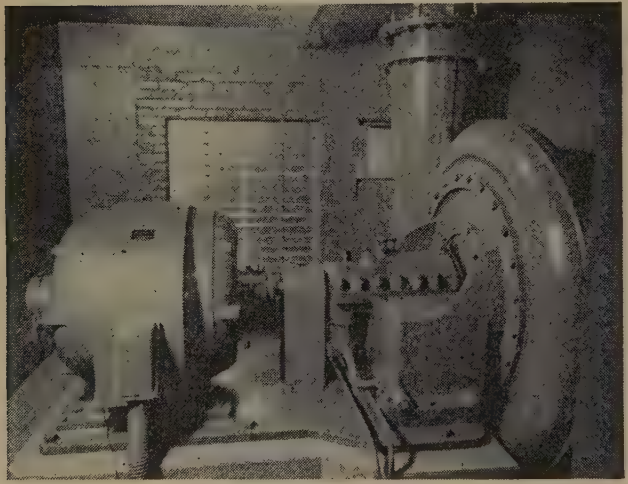

Fig. 2 Scavenging Blower Installed in the Carthage Power Plant

However, the basic variable is air density, i.e., the weight of fresh air trapped in the cylinder at the end of the scavenging period. Hence a given engine will run equally well at lower volume of high density because the trapped weight of new air is the same, and the cooling effect is also proportional to the density. Elliott[3] has shown that humidity has a negligible effect on performance and may be disregarded.

The power required to compress the scavenging air is a direct charge against the engine output, hence the air requirements are based on the minimum flow which will secure clear exhaust at

[3] "Conversion of Measurements of Power Output of Diesel Engines to Standard Atmospheric Conditions," by M. A. Elliott, Trans. ASME, vol. 68, 1946, pp. 525–539

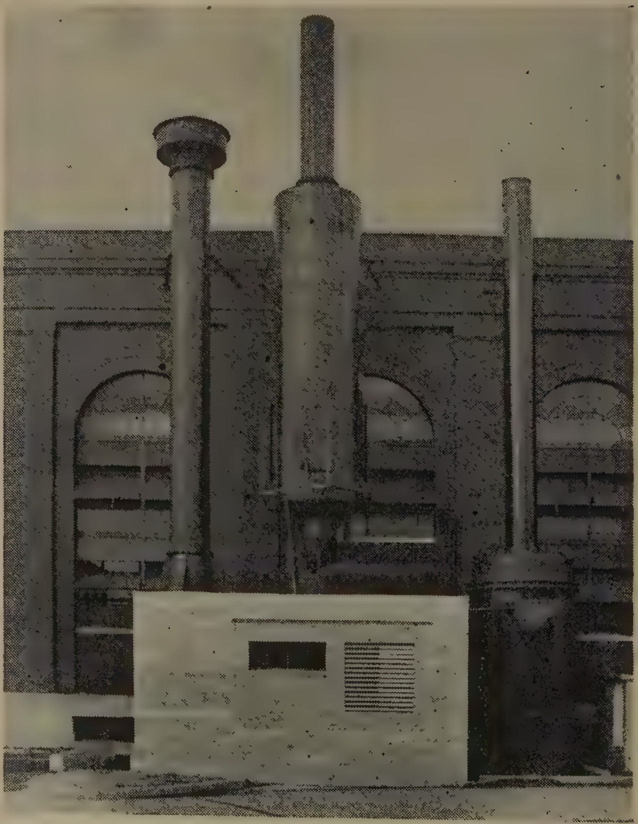

Fig. 3 Blower House at the Carthage Power Plant

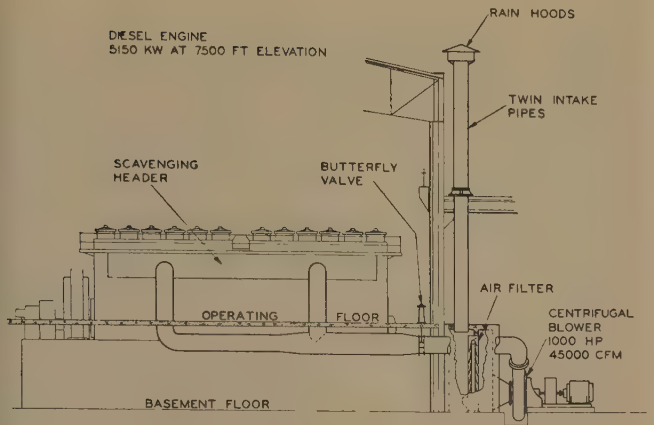

Fig. 4 Scavenging Air System for 29-In. × 40-In. 12-Cylinder Diesel Engine

blower characteristic and engine resistance on volume, the blower power may increase as much as 45 per cent from the 90 F, minimum barometer condition unless limited by blower-speed variation or throttling.

Engine Resistance Characteristics

From experimental investigations on two-cycle engines of 17.5 in., 21.5 in., and 29 in. bore, and numbers of cylinders from 5 to 10, it appears that the resistance of the engine varies very nearly as the 1.5 to 1.6 power of the volume if speed and load are held constant. Fig. 6 shows typical resistance characteristics for a 21.5-in-bore engine plotted against air volume, and also shows pressure and power characteristics of a typical centrifugal blower. These will be discussed later.

No attempt has been made to form a mathematical theory for the 1.5 to 1.6 exponent. It is thought that the resistance would vary approximately as the square of the volume if the temperature remained constant, but since increasing volume

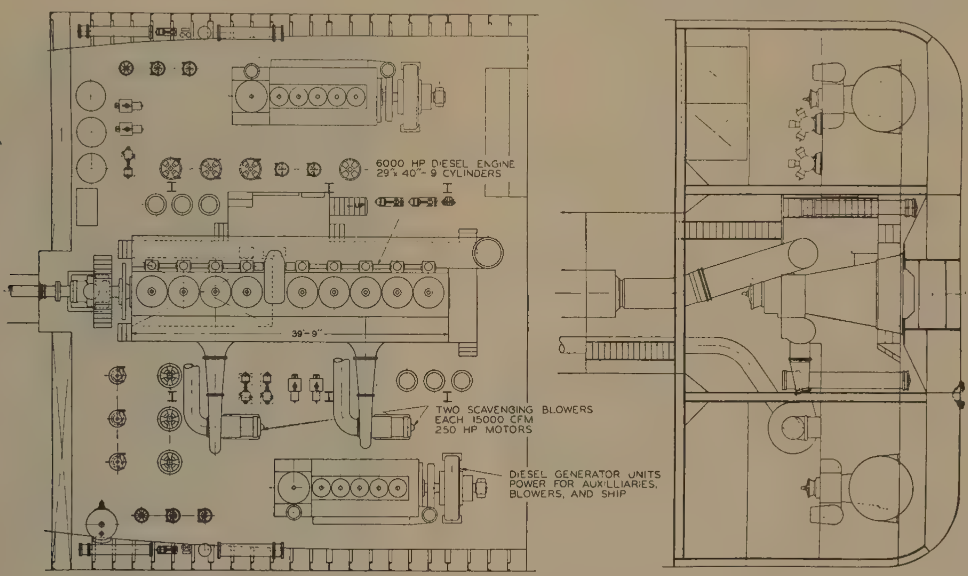

Fig. 5 Machinery Arrangement of a Vessel Propelled by a 6000-Shp Engine

the maximum load requirement and minimum atmospheric air density.

The Diesel Engine Manufacturers Association (DEMA) standards[4] for rating engines provide for no corrections up to 90 F, barometer as low as 28.25 in., and up to 1500 ft altitude. To meet guarantees, the air supply must be based upon density at 90 F and minimum barometer at the installation location. Any available type of constant-speed blower which can supply sufficient air for this condition will be oversize for any other condition of lower temperature or higher barometer.

Table 2 gives normal variation in atmospheric air density at 750 ft elevation above sea level in northern United States, and shows that any given installation may experience an increase of inlet-air density of nearly 30 per cent from the minimum requirement just described.

TABLE 2 VARIATION OF ATMOSPHERIC AIR DENSITY

Condition	Temp, deg F	Barometer, in. Hg	Density, lb per cu ft	Ratio
Extreme heat, low barometer	90	28.5	0.069	1.00
Extreme cold, high barometer	—20	29.6	0.089	1.29
Normal or average.........	60	29.0	0.074	1.07

The blower power is proportional to air density at a given volume and pressure rise. Together with the effect of the

[4] "Standard Practices for Stationary Diesel Engines," third edition, Diesel Engine Manufacturers Association, New York, N. Y., 1946.

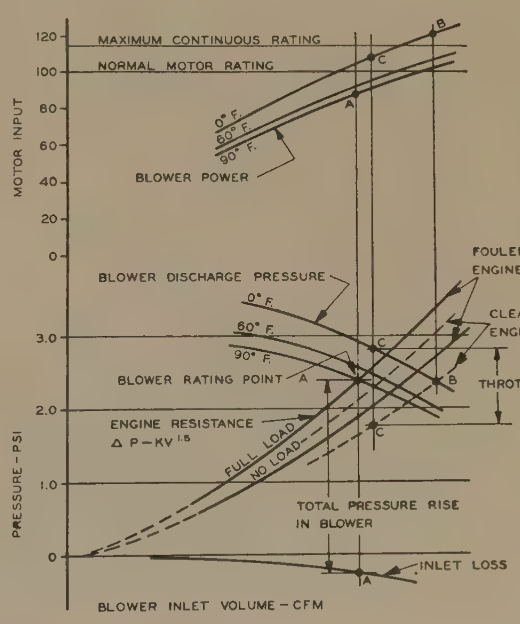

Fig. 6 Diesel-Engine and Blower Characteristics

decreases exhaust temperature and hence exhaust volume, it partially offsets the increase of resistance in the exhaust portion of the system.

There is a considerable drop in resistance as load decreases due to reduced exhaust temperature and volume. This resistance decrease may be as much as 20 to 25 per cent between full load and no load.

Accurate data are not available as to the effect of engine speed. Some limited data indicate a slight increase in resistance as speed increases, other conditions such as load and volume remaining constant.

The resistance of an engine increases gradually in operation due to carbon formation in the scavenging and exhaust ports. This may be very slight when combustion is proper but may in time increase the resistance, as shown by scavenging pressure, up to 20 per cent if the combustion is poor. In such case, cleaning of the ports becomes necessary.

The resistance also increases with increasing air density, but the pressure developed by a centrifugal blower does also, so it is not necessary to make an allowance for this except in motor horsepower.

Characteristics of Centrifugal Blowers

The general characteristics of centifugal blowers are covered adequately in the literature and textbooks and need not be reviewed here, except in so far as they are related to engine characteristics.

The practice of blower manufacturers is to supply characteristic curves based upon standard conditions at the blower inlet and constant blower speed. Several curves are usually supplied showing the characteristic at various temperatures.

In studying the interrelation of the centrifugal blower and the Diesel engine, it is important to realize that both speed and conditions at the blower inlet are variable as volume and density change. Characteristic curves must be constructed for the unit as installed, allowing for increasing resistance in the intake system with increasing volume, and also decreasing motor speed with increasing horsepower. Both of these factors increase the droop of the blower characteristic curves. Fouling of the engine, as mentioned, and fouling of the blower vanes by dust and oil must also be taken into account.

The blower discharge-pressure curves in Fig. 6 are actual curves, the pressure droop being increased due to motor speed droop as volume and, consequently, power increase. Also, they have been constructed by using the total pressure rise developed in the blower and subtracting the loss in inlet piping and filter, which increases almost as the square of the volume.

There is a small pressure loss in the blower-discharge piping which has here been included with the engine resistance.

For most efficient operation, the air volume of a two-cycle engine could decrease as the load decreases, but no available air source has this characteristic, with the possible exception of an exhaust-driven supercharger. The characteristic of positive-displacement blowers and pumps is very steep, i.e., the volume delivered is almost independent of changes in engine resistance or atmospheric conditions. The power required is affected only by atmospheric-density variations.

The characteristics of the centrifugal blower are less favorable and, because it is necessary to select the blower for the 90 F, minimum-barometer, maximum-load condition plus allowance for engine and blower fouling, it is also necessary to limit the blower power at high-density (cold air) and minimum-load conditions to maintain reasonable fuel consumption and to avoid overloading the motor. This is most conveniently done by throttling with a butterfly valve. Again referring to Fig. 6, the rating point (90 F, full load) is shown at A. If with no other changes the load drops to zero and the temperature decreases to 0 F, the volume will increase about 20 per cent and the power about 45 per cent to the point B. Accepting the premise that weight flow is the necessary criterion for proper engine performance it will be seen that any point to the right of A and above the 90 F characteristic will give better than minimum scavenging, and any throttling which does not reduce the volume below point A is not detrimental. Hence by throttling to some point such as C, the blower power may be limited to a reasonable extent.

The throttling valve may be located either in the blower suction or in the blower discharge. It is usually located in the discharge because it is more readily accessible to the engine operator, as reference to Fig. 4 will show. Automatic control has not been found necessary. Generally, the adjustment is mainly to compensate for atmospheric temperature variation, and a conveniently located ammeter to show motor current is a rough but reliable guide to throttle setting. Fig. 7 shows a typical wafer-type butterfly valve with handwheel and worm drive.

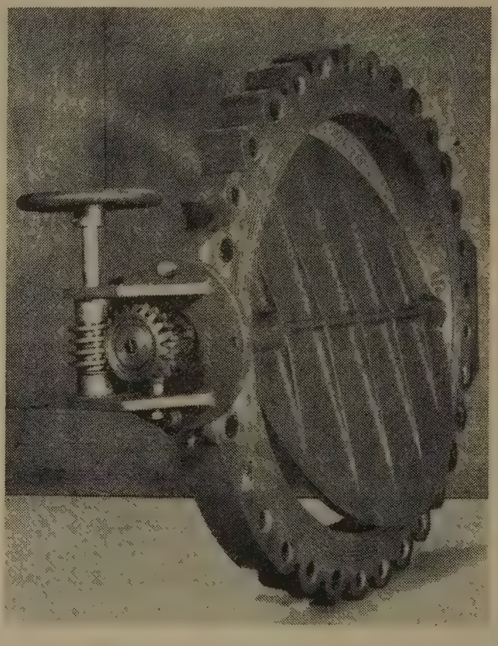

Fig. 7 Butterfly Valve

When centrifugal blowers are driven by direct-current motors, as in marine installations, some compensation for atmospheric variation may be accomplished by variable-speed control.

Starting and Control

A centrifugal scavenging blower may be started in advance of starting the engine, with normal motor-starting equipment, and in many power plants this method is used. Marine installations operating on direct current from auxiliary generating units are always started in this way. There are several important objections to this procedure in a power plant which have made it necessary to develop a method of starting engine and blower unit simultaneously and without the aid of other power.

In a typical Diesel generating plant, operating with one engine idle, the unexpected loss of one operating unit may so overload the remaining units that the blower of the idle unit cannot be added to the bus load in advance of starting the idle unit. Also, in case of shutdown of the entire system, it is desirable to be able to start any unit without the aid of outside power.

If the large blower motor, which usually operates at the same voltage as the generators, is to be started from the bus, a circuit breaker or fuses must be provided in addition to the motor-starting equipment, and this protective equipment must have interrupting capacity equal to the total generating capacity of the plant. This equipment becomes large and expensive for a system comprising several units.

Because engine resistance is very low when an engine is not running, it is necessary to reduce the volume by almost closing the throttle valve, in order to start a centrifugal blower without overloading the motor. This consumes time whenever the engine is started, and failure to do so results in tripping the blower protective device.

In order to overcome these objections in alternating-current generating plants, a motor-driven scavenging blower may be electrically connected direct to its generator and will automatically start as its engine is started. This is shown diagrammatically in Fig. 8. To reduce the delay, the field of the exciter is energized by an auxiliary source of direct current (pilot excitation), usually a storage battery of about 90 volts. No circuit breaker or other control is required for the blower motor, but a protective panel is provided to operate an alarm in case of motor overload, or to open the generator circuit breaker and generator field switch in case of a short circuit in the blower motor or its lead.

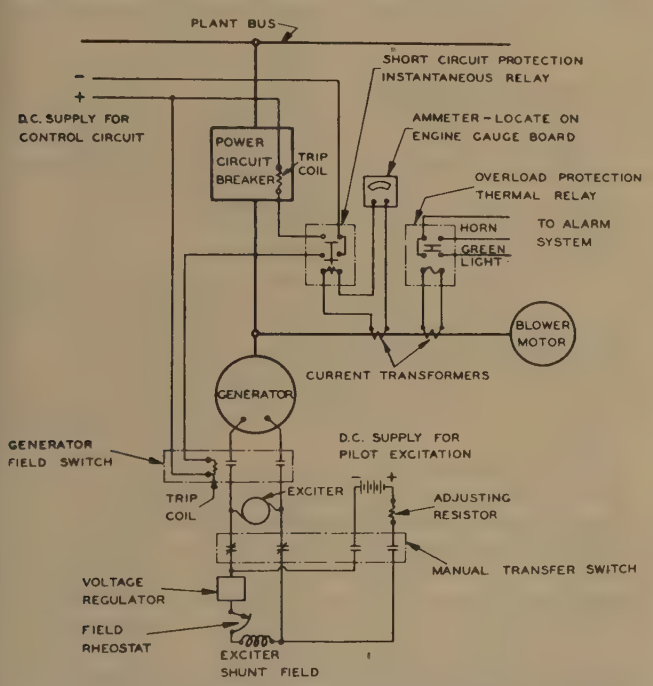

Fig. 8 Wiring Diagram for Simultaneous Starting of Engine Alternating-Current Generator and Centrifugal Blower

It will be noted in Fig. 8 that the main power leads run directly from the generator to the blower motor, there being no circuit breaker in the blower leads. Since the engine cannot run without the blower, and the generator would draw power from the bus and run as a motor in case of failure of the blower, the circuit is arranged so that, in case of failure or fault in the blower leads, the main circuit breaker, connecting the generator to the bus, is opened and the generator field switch is opened at the same time. The interrupting capacity of the generator circuit breaker is determined by the total generating capacity connected to the plant bus.

The electrical delay of the blower motor in following the generator during the starting period is substantially reduced by supplying pilot excitation from a separate direct-current source to the exciter field during the starting period. It has been determined experimentally that sufficient scavenging air is supplied to operate an engine on fuel and build up speed after the blower motor has reached approximately $^1/_6$ of its rated speed. Using pilot excitation and starting on compressed air in the normal manner, the blower motor will begin to turn in a little over 2 sec after moving the engine-starting lever to the "Start" position, and will reach $^1/_6$ speed in less than an additional second or two. Thus it is only necessary to run the engine on starting air for a few seconds before going to the "Run" position. As soon as the engine is up to speed, the manual transfer switch is used to eliminate the separate direct-current supply and return the exciter field to its normal arrangement. An adjusting resistor is necessary to provide the proper pilot current through the exciter field, the characteristics of this resistor being determined in each case by the direct-current voltage available and the characteristics of the exciter-field circuit.

On some installations, pilot excitation has been applied automatically. A limit switch on the engine control lever initiates the transfer to battery excitation as soon as the lever is moved away from the "Stop" position. The transfer back to normal excitation is initiated by a voltage-sensitive relay set to operate about 20 per cent under normal generator voltage and is usually backed up by a frequency-sensitive relay. All of these devices operate on a contactor which does the switching.

Although there is no circuit breaker directly in the motor leads, protection is provided by the protective relays shown in Fig. 8. A two-pole thermal relay, having one normally open and one normally closed contact, is arranged to act on the engine alarm system in case of motor overload. Then the operator can determine the cause of the overload and either throttle the air discharge to reduce the motor load or shut down the unit if it is due to other causes. In case of a fault in the blower circuit or in the motor, protection is afforded by an instantaneous relay which opens the power circuit breaker of the generator and also opens the generator-field switch. These relays are actuated by two sets of current transformers in the blower-motor circuit, or one set of double secondary-current transformers. In those cases where differential protection for the generator is provided, it is necessary to extend this differential protection system to include the blower motor and, in this case, the instantaneous relay is omitted.

The observed time sequence of the starting cycle for a 10-cylinder, 29-in. × 40-in. 164-rpm Diesel generating unit in the power plant of the Iowa Electric Light & Power Company at Marshalltown, Iowa, and 34,000 cfm centrifugal blower directly connected to the generator leads is shown in Fig. 9. This installation includes automatic pilot-excitation transfer equipment

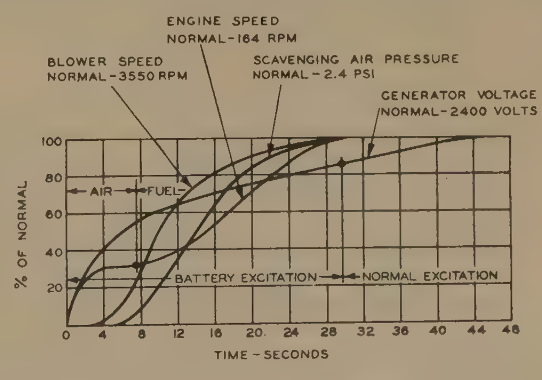

Fig. 9 Observed Starting Cycle of 10-Cylinder 29-In. × 40-In. Diesel Engine and 34,000-Cfm Centrifugal Blower

with a voltage relay set to transfer to normal excitation at about 2000 volts for a 2400-volt generator. The data for the engine-speed and blower-speed curves were recorded on the tape of a vibrograph, mechanically connected to a flat spot on the blower shaft and electrically connected to contacts on the engine camshaft. The scavenging-air pressure and generator-voltage curves were recorded by stop-watch observations. It will be noted that each of the curves builds up continuously without any hesitation or dropping off at the time of transfer from starting air to fuel, or at the time of transfer from battery excitation to normal excitation.

Conclusions

While the motor-driven centrifugal blower is not the most efficient source of scavenging air for a two-cycle Diesel engine, its use has provided one solution to the problem of installing maximum additional horsepower into a restricted space. When the blower is proportioned properly and its peculiarities are understood, it is a very satisfactory source of air.

That the motor-driven blower is economically justified is proved by the fact that the author's company has installed or has under construction, since the end of the war, Diesel-engine installations in excess of 170,000 hp employing motor-driven blowers.

Discussion

R. Tom Sawyer.[5] The writer would like to suggest that the title of this paper be changed to "Centrifugal Blowers for Two-Cycle Heavy-Duty Engines," because the locomotive designer would be way behind if he had to use this type of motor-driven compressor. The centrifugal blower we use is driven by an exhaust gas turbine which does not take any power from the generator.

E. J. Kates.[6] Referring to the high-altitude installation in Mexico City described by the author, would the author explain the factors which prevented obtaining an altitude power rating nearer the sea-level rating?

T. M. Robie.[7] In connection with the butterfly valve, and the fact that it is operated manually, with the changing labor conditions and the like, would it not be desirable to put some sort of control indicator on it? In other words, with manual operation without any pointer or dial in connection with the load and density of the air, isn't trouble likely to develop, because the operator might have the valve half shut instead of fully opened when it is supposed to be? The writer believes there is a definite danger in having a manually operated control on that butterfly valve. There should be some sort of table or chart to show in just what position it should be with varying conditions of load, and air temperature and density.

J. C. Barnaby.[8] This paper is a valuable contribution to the subject of centrifugal scavenging pumps for two-cycle engines. The author has covered the use of electrically driven centrifugal scavenging blowers and has drawn a comprehensive comparison with reciprocating and Roots-type scavenging blowers. However, he does not mention blowers of the mechanically driven or exhaust-turbine-driven centrifugal type. During a recent trip to Europe, the writer observed a number of engines equipped with gear-driven centrifugal blowers, and one unit equipped with an exhaust-gas-turbine-driven centrifugal scavenging blower. Both of these types have their advantages, especially the latter, which not only is self-compensating for load conditions on the engine, but also, under proper circumstances, may deliver scavenging air without subtracting power from the engine. The possibilities of the exhaust-driven centrifugal scavenging blower are such that it should not be overlooked in any discussion of this nature. There also have been some applications of axial-flow compressors for scavenging.

It would greatly enhance the value of the paper if the author could extend his Table 1 to include these other types, and also a discussion of their possibilities.

E. H. Codding.[9] The blower with its connecting system is certainly a necessary adjunct to these engines. The paper gives an interesting description of it and explains the economic reasons for adjusting the system for maximum efficiency.

In view of the original cost of the installation and the savings which are available through proper adjustment, it appears that instruments should be provided which will allow a complete analysis of its operation. In addition to the barometer and thermometer for atmospheric-air conditions, there should be thermometers and manometers on both the upstream and downstream sides of the air damper. A consideration of these temperatures and pressures, together with the power input to the blower, would allow adjustment for optimum operation under varying engine loads and atmospheric conditions.

Reference is made to carbon build-up in the exhaust ports. A study of the readings of the suggested instruments would allow comparisons of pressure drop through the engines, which would, in turn, indicate the condition of the ports.

Mention is made of the necessity for cleaning the vanes of the blowers and it would be interesting to know if methods other than manual have been tried for cleaning these parts during operation.

Louis Bonaventure,[10] J. M. Drabelle,[11] and H. C. Kullander.[12] Application of the motor-driven centrifugal blower for combustion-air supply for Diesel engines introduces certain operating problems in the power station. The direct starting of the motor-driven blower unit by boosted excitation on the pilot exciter has been working satisfactorily at the Marshalltown generating station since April 1, 1948, and a total of 31 starts have been made to May 17, 1948, without any difficulty or failure. With the starting of the engine, the blower starts to rotate, due to the low-frequency current of approximately 20 cycles, causing sufficient current to flow in the motor windings to develop ample torque, and the motor rapidly comes up to speed with the engine. It is a satisfactory and certain means of simplifying the electrical gear and reducing cost. The motor at Marshalltown is tied directly to the generator terminals without the interposition of any electrical gear such as oil switches. The blower is rated 600 hp, 3600 rpm. Maximum electrical input is approximately 450 kw.

The DEMA standards, mentioned in the paper, specify that the air supply should be based upon a density at 90 F, and a mini-

[5] American Locomotive Company, New York, N.Y. Mem. ASME.

[6] Consulting Engineer, Diesel Specialist, New York, N. Y. Director at Large, ASME.

[7] General Diesel Sales Division, Fairbanks, Morse & Company, Chicago, Ill. Mem. ASME.

[8] Worthington Pump & Machinery Corporation, Harrison, N. J.

[9] Tide Water Associated Oil Company, New York, N. Y. Mem. ASME.

[10] Chief Engineer of Power Station, Iowa Electric Light and Power Company, Marshalltown, Iowa.

[11] Chief Engineer, Iowa Electric Light and Power Company, Cedar Rapids, Iowa. Mem. ASME.

[12] Engineering Department, Iowa Electric Light and Power Company, Cedar Rapids, Iowa.

mum barometric pressure of 28.25 in. of mercury. Obviously, under low-temperature conditions such as exist in many parts of the country, it is possible to have entering-air temperatures of minus 20 F with a barometric pressure of, say, 30 in. At Marshalltown, a laboratory portable indicating wattmeter, in addition to an ammeter, was connected into the motor circuit and under noload condition on the engine other than supplying power to the blower at a temperature of 74 F, and a barometer of 29.18 in., electrical input to the blower motor was 358 kw. At the 74-deg temperature, 29.18 in. barometer, full load on the unit, the electrical input to the motor was 398 kw. A projection of these test points to minus 20 F, same barometer, indicates a possible load at no load on the motor of 432 kw, and full load on the unit, same temperature, 481 kw.

Table 3 herewith clearly indicates that the butterfly valve in the blower-discharge line should be adjusted as the entering-air temperature varies. It should be noted that this table is calculated for a constant barometer and a constant-volume air discharge, the only variable being the temperature of the air entering the blower suction.

TABLE 3 OBSERVED AND CALCULATED PERFORMANCE; ASSUMED BAROMETER 30 IN. HG

Temperature deg F	Air density, lb per cu ft	Power input to blower, kw — Engine load, 5000 kw	Engine load, zero
− 20	0.0900	481	432
0	0.0864	462	416
+ 20	0.0828	443	398
40	0.0795	425	382
60	0.0764	409	367
70	0.0750	401	361
74	0.07443	398[a]	358[a]
80	0.0736	394	354
90	0.0723	387	348
100	0.0710	380	341

[a] Kilowatts for this temperature observed from test; all other kilowatt requirements calculated.

NOTE: Air density based on perfect gas laws and air weight of 0.08071 lb per cu ft at 32 F and barometric pressure of 14.696 psi.

This situation therefore introduces two problems for the operator of such a unit. One is relatively simple, namely, some form of overload device to indicate overloading of motor, due to failure of operator to adjust butterfly valve properly for changing barometer, entering-air temperature, and engine loading. With the present high cost of fuel oil (roughly, at Marshalltown, 10 cents per gal for No. 5 fuel), every kilowatthour and kilowatt of demand energy that can be saved on this blower unit in the reduction of parasitic power, means a lower fuel cost per net kilowatthour generated, and additional energy available for sale.

The ammeter is not a satisfactory device for giving the operator on the floor such information. It merely indicates ampere flow to the motor and is useful only to meet the overloading situation. Based on our experience to date, we recommend that an indicating wattmeter be installed to show the actual energy input in kilowatts to the motor. A further refinement on the engine control panel would be a dial-type thermometer, for reading the entering-air temperature to blower suction, and a high-quality pressure gage to show scavenging-air header pressure, so that the operators by experience will learn to position the butterfly valve for the various hour-to-hour changes of outdoor air temperature, engine loading, and barometric pressure. This reduction in parasitic power will mean high-economy operation of the unit under the present high cost of fuel oil.

Data obtained so far indicate that, for each 1 deg F change in entering-air temperature, there is a change of power to the blower of 1 kw. The positioning of the butterfly valve is of power-saving importance.

AUTHOR'S CLOSURE

Answering Mr. Kates's question: As soon as one investigates what happens to fuel consumption as a normal two-cycle engine is boosted by raising the back pressure, without any sort of supercharging arrangement, it will be found that the effect on fuel consumption is always adverse. As the manifold pressure and back pressure are boosted, a point is soon reached where the increase in blower power is more than the increase in engine power. In this case there is a gain of about 8 per cent. In other words, the derating would be 24 per cent without manifold boost, but with the manifold boost, it is only 16 per cent, and that is about the limit. Beyond this point it will be found that the blower power increases very rapidly. The blower for the Mexico City installation requires a 1000-hp motor. The power is actually around 900 hp. If there were no boost in the power, it would only be between 600 and 700 hp, hence it is taking 200 hp to secure a gain of a little over 600 hp in the engine, and that is just about the limit of what is economical.

Replying to Mr. Robie: We have not found it necessary to make any elaborate charts for the engine-room operator; a very simple expedient has taken care of that. Inscribing two red marks on the blower ammeter, located on the engine gage board immediately adjacent to the control stand, takes care of the blower adjustment for the normal plant. The upper red line marks the danger point (overload), and the lower red line marks minimum power to secure sufficient scavenging air. The changes in atmospheric conditions usually do not occur so fast that the operators cannot keep the blower power within the proper range, especially since temperature is the main variable.

The butterfly valve, shown in Fig. 7 of the paper, does not have a pointer, but as installed, there is a pointer on the other end of the stem which shows the position of the valve.

The subject of instrumentation is mentioned; the answer is very simple. There is quite a bit of instrumentation provided in a large installation. In so far as the control of the operation of the engine is concerned, there is a manometer which shows the scavenging pressure, and this indicates quite satisfactorily the resistance in the engine-exhaust system.

Improved Techniques in the Study of Engine Firing Orders Using the Vectorscope

By G. J. DASHEFSKY,[1] BROOKLYN, N. Y.

The state of dynamic balance of an engine and the magnitude of minor orders of torsional vibration are greatly influenced by the firing sequence of the cylinders. Investigation of this problem requires the evaluation of large numbers of vector diagrams and is therefore adaptable to the use of the Vectorscope.[2] This mathematical instrument automatically and rapidly adds vector quantities with about the same accuracy as a good graphical summation. The principle and operation of the Vectorscope and its application to the solution of various vector problems were given in an earlier paper.[2] The present paper deals specifically with techniques involved in applying the Vectorscope to the study of firing orders. Methods are indicated whereby large numbers of firing orders may be examined expediently and rapidly.

Nomenclature

The following nomenclature is used in the paper:

n = number of cylinders or cranks
N_{Fo} = number of independent firing orders
F_c = centrifugal force due to unbalanced weights, lb
F_i = inertia force due to reciprocating weights, lb
F_1 = primary inertia force, lb
F_2 = secondary inertia force, lb
ΣF_c = vector sum of centrifugal forces, lb
ΣF_1 = vector sum of primary inertia forces, lb
ΣF_2 = vector sum of secondary inertia forces, lb
ΣM_1 = vector sum of primary moments, lb-in.
ΣM_2 = vector sum of secondary moments, lb-in.
N = rpm
R_c = crank radius, in.
l = length of connecting rod, in.
W_r = reciprocating weight per crank, lb
W_c = rotating weight per crank, lb
g = gravitational constant, in./sec^2 (386 in./sec^2)
d = distance between cylinders, in.
K_I = energy input from harmonic torques, in-lb
M_v = harmonic torque of cylinders, lb-in.
$\Sigma\beta$ = vector sum of relative amplitudes at cranks, deg
α = amplitude of torsional vibration at free end of crankshaft, $\pm$ deg
γ = crank angle between successively firing cylinders, deg
θ = crank displacement from reference position, deg
m = order of vibration
ϕ = phase angle between vectors for successively firing cylinders ($\phi = m\gamma$), deg
R_{I}, R_{II} = terminal points of resultant vectors
${}_nC_r$ = number of combinations of n cranks r at a time
${}_nP_n$ = number of permutations of n cranks n at a time

Introduction

The state of engine balance and the magnitude of the minor orders of torsional vibration are intimately associated with the choice of firing order. The longitudinal spacing of cylinders which may also be an important factor is discussed in a paper by Cormac.[3]

The number of firing orders possible in multicylinder engines rises very rapidly with the number of cylinders. The number of independent firing orders for in-line engines is given by

$$N_{Fo} = \frac{(n-1)!}{2} \qquad [1]$$

where n = number of cranks. The term "independent firing order" is meant to indicate that pairs of firing orders exemplified by the 7-cylinder sequence

1 7 2 4 5 3 6
1 6 3 5 4 2 7

are equivalent in so far as the magnitudes of dynamic effects produced. The time-phase relationship of the resultant is affected, but ordinarily is of no consequence. These two firing orders apply to a single crank arrangement and represent the firing orders for rotation in opposite directions.

The number of possible independent firing orders for multicylinder engines is given in the following table:

No. of cylinders.....	3	4	5	6	7	8	9	10
No. of indep. firing orders..	1	3	12	60	360	2520	20160	181440
No. of cylinders....	11	12						
No. of indep. firing orders..	1814400	19958400						

It is apparent from this tabulation that the complete investigation of engines with 8 or more cylinders requires special means to handle the great number of firing orders.

It has been found possible with the aid of the Vectorscope to handle expeditiously, yet comprehensively, engines up to 9 cylinders. The investigation of all of the firing orders of the 10-cylinder engine is believed to be feasible, although so far only some 30,000 of the 181,440 firing orders have been investigated for primary and secondary moments. The 11-cylinder engine has so many possible firing orders as to involve a prohibitive amount of work for a complete study. The Vectorscope does, however, permit the rapid selection of some better firing orders by a trial-and-error procedure. The nature of the Vectorscope is such that it serves as a visual aid in the selection of good crank arrangements, by manipulation of the weight representing the importance of the cranks.

The selection of suitable firing orders for the 12-cylinder engine

[1] Consultant Mechanical Engineer, Material Laboratory, New York Naval Shipyard.

[2] U. S. Patent No. 2,203,674. "The Vectorscope," by G. J. Dashefsky, Trans. ASME, vol. 61, 1939, pp. 403–414.

Contributed by the Oil and Gas Power Division and presented at the 20th National Oil and Gas Power Conference, St. Louis, Mo., May 20–22, 1948, of The American Society of Mechanical Engineers.

NOTE: The opinions expressed are those of the author and are not to be construed as official or reflecting the views of the Naval Service at large. Paper No. 48—OGP-1.

[3] "The Design of Dynamically Balanced Crankshafts for Two-Stroke-Cycle Engines," by P. Cormac, *Engineering*, London, England, vol. 128, October 11, 1929, pp. 458–461.

may be aided by considering the engine made up of two 6-cylinder units. By coupling the two units in suitable angular relationship, the primary and secondary forces and moments may be limited to desired values. The minor torsional vibrations are also affected, and may at times be undesirably large even though the resultant forces and moments are small. Determination of a suitable compromise is considerably simplified by use of the Vectorscope.

Lewis, Breault, and Donaldson[4] presented an ingenious scheme for evaluating the firing orders of the 9-cylinder engine. This scheme consists essentially in dividing the cranks into two groups, evaluating the resultant for each group by special charts. There result 35 charts, each bearing points representing the vector resultants for both groups of cranks. The distance between any point in one group and a point in the second group represents the magnitude of the vector resultant for a firing order combining the crank groups represented by the points.

Application of the Vectorscope to this method offers considerable advantage in speeding the process, and appears to provide a useful tool for handling this type of problem.

The "convergent" method to be described later is suggested as a means for converging rapidly the selection of those firing orders which are of importance to a particular problem, rather than a complete study of all firing orders.

Description of Vectorscope

The mathematical principle of the Vectorscope and some of its general applications to the solution of problems reducible to vector summation have been given by Dashefsky.[2] The instrument consists of a disk effectively pivoted at its center in a Cardan suspension or on a single pivot bearing, as indicated in Figs. 1 and 2. Pegs to receive weights proportional to the vector mag-

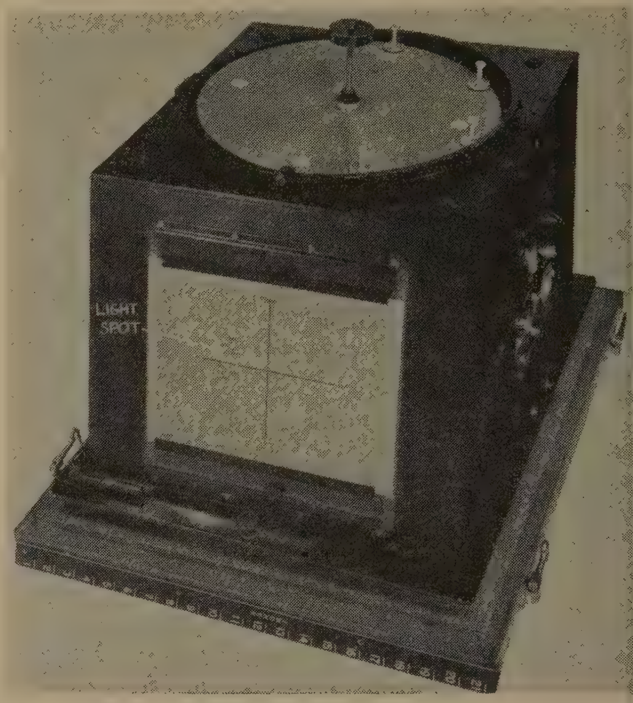

Fig. 1 The Vectorscope
(Setup with 7-cylinder disk.)

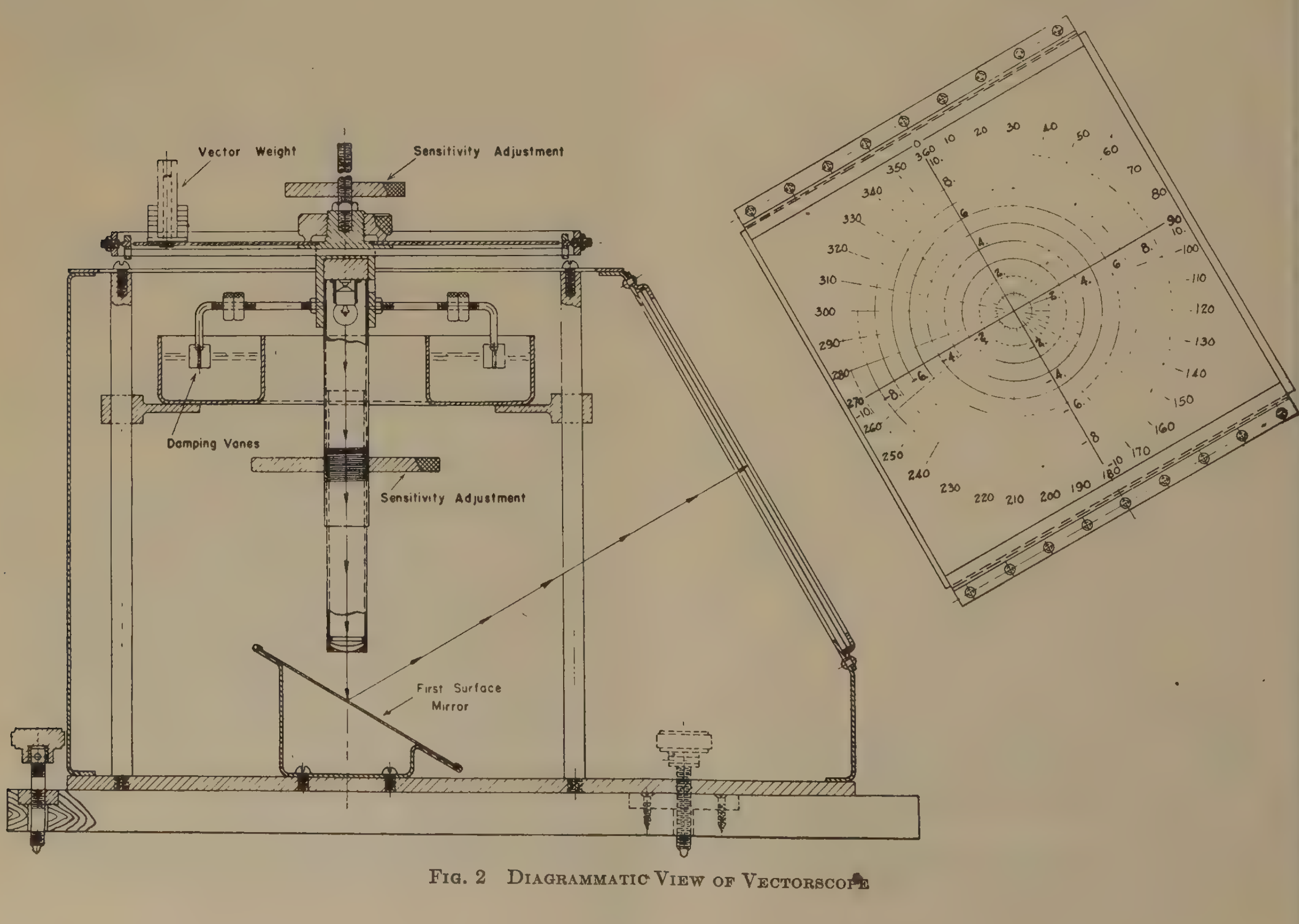

Fig. 2 Diagrammatic View of Vectorscope

[4] "The Crank Arrangement of a Nine-Cylinder Engine," by F. M. Lewis, E. E. Breault, and R. M. Donaldson, Trans. ASME, vol. 59, Sept., 1937, pp. A-128.

nitudes are distributed around the disk in the same angular orientation as the vectors to be added. An adjustable pendular weight provides the equilibrating moment for the disk-and-weight system and also a means for controlling the sensitivity of the instrument. The optical system, carried by the disk, projects a lamp filament focused as a spot of light on the screen, indicating the position of equilibrium of the disk. The displacement of the light spot from the zero position represents both magnitude and direction of the resultant vector. Use of a clear-glass screen permits marking the projected points upon translucent paper placed thereon. Adjustment and calibration of the Vectorscope are accomplished by placing a sheet of polar co-ordinate paper on the glass top. The weights representing vectors are made up by placing the weight carrier upon one of the pegs and adjusting the amount of weight to give the required deflection. The actual weight is of no importance. Sensitivity of deflection is controlled by the vertical position of the pendular weight.

Engine Balance

In the reciprocating in-line engine, the forces at each crank are as follows:

The centrifugal force due to unbalanced rotating weights

$$F_c = \frac{4\pi^2 N^2 R_c W_c}{3600\ g} \cos\theta \quad [2]$$

Inertia force due to reciprocating weights

$$F_i = \frac{4\pi^2 N^2 R_c W_r}{3600\ g}\left(\cos\theta + \frac{R_c}{l}\cos 2\theta + \ldots\ldots\right)$$

$$F_i = \frac{4\pi^2 N^2 R_c W_r}{3600\ g}\cos\theta + \frac{4\pi^2 N^2 R_c W_r}{3600\ g}\,\frac{R_c}{l}\cos 2\theta \quad [3]$$

Let

$$\frac{4\pi^2 N^2 R_c W_r}{3600\ g} = F_1 \text{ (primary force)} \quad [4]$$

$$\frac{4\pi^2 N^2 R_c W_r}{3600\ g}\,\frac{R_c}{l} = F_2 \text{ (secondary force)} \quad [5]$$

Ordinarily only the primary and secondary forces F_1 and F_2 need be considered. The 4th harmonic is occasionally of importance in high-speed engines.

Usually the cranks are equally spaced in angular relationship for which case

$$\left.\begin{aligned}\Sigma F_c &= 0\\ \Sigma F_1 &= 0\\ \Sigma F_2 &= 0\end{aligned}\right\} \quad [6]$$

Each of these sets of forces gives rise to resultant moments whose magnitudes depend upon the force at each cylinder, the longitudinal cylinder spacing (cylinder pitch) and the firing order. Fig. 3 shows the moment diagram of a 7-cylinder engine chosen as an example. Typical vector diagrams for evaluating the resultant primary and secondary moments, ΣM_1 and ΣM_2 are

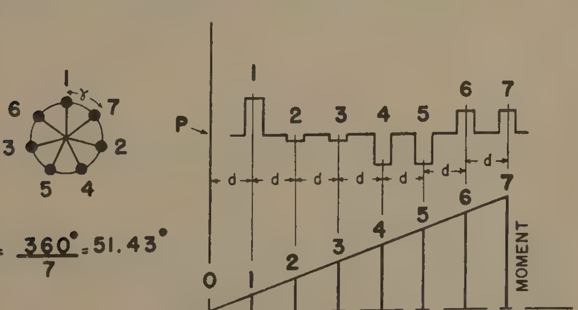

Fig. 3 Moment Diagram for 7-Cylinder 2-Cycle Engine With Firing Order 1-7-2-4-5-3-6

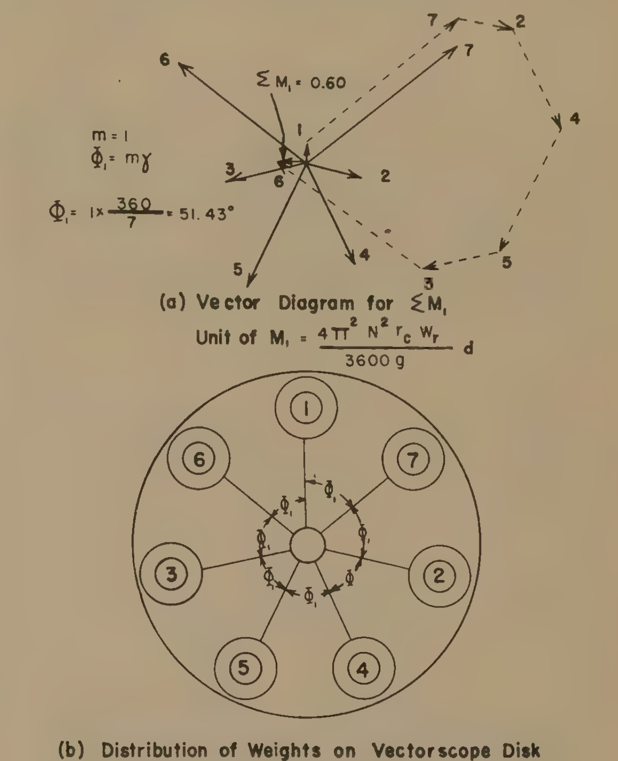

Fig. 4 Vector Summation for Primary Moments
(Applies to Fig. 3.)

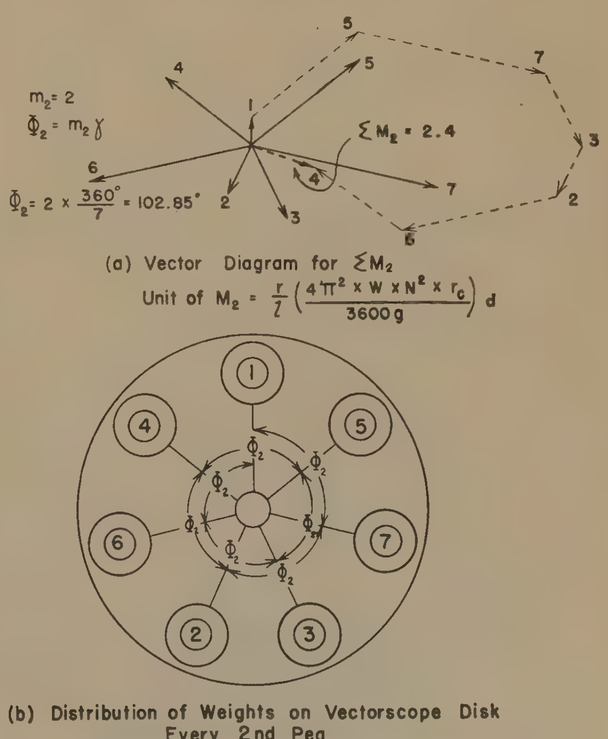

Fig. 5 Vector Summation for Secondary Moments
(Applies to Fig. 3.)

shown in Figs. 4 and 5. As a matter of convenience, moments are taken about P, a distance d ahead of crank No. 1, as shown in Fig. 3. For equal cylinder pitch, the importance of any crank in the moment diagram is expressed by the crank number. Each unit of moment vector diagram is given by $F_c d$, $F_1 d$, or $F_2 d$ as appropriate.

Torsional-Vibration Problem

The choice of firing orders profoundly affects the magnitude of the minor orders of torsional vibration. A firing order eminently suitable as regards engine balance may be found to be entirely unfavorable because a minor order torsional vibration within the operating range may be severe.

The amplitude of vibration in a multicylinder engine depends upon the energy input from the harmonic torques which may be expressed by

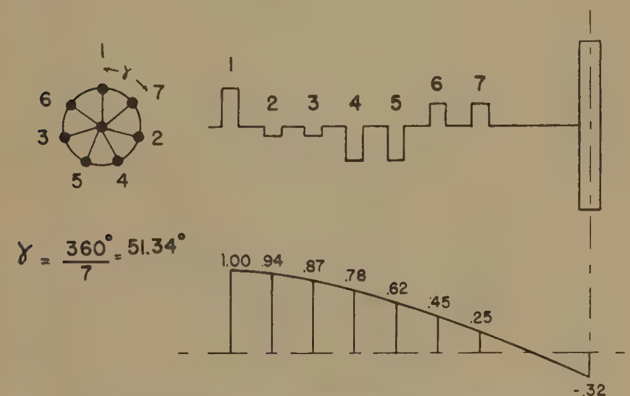

Fig. 6 Relative Amplitudes Curve
(For I-Noded torsional vibration. Firing order 1-7-2-4-5-3-6.)

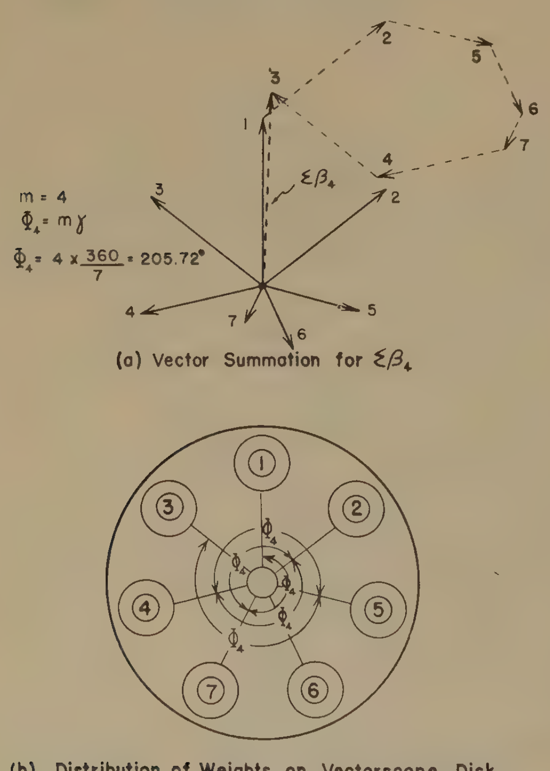

Fig. 7 Vector Summation for $\Sigma\beta$ for Minor Order
(For engine of Fig. 6.)

$$K_i = \frac{\pi^2}{180} M_v (\Sigma\beta) a \quad [7]$$

The amplitude a, at the front end of the engine is dependent upon the magnitude of energy input K_i, and the damping in the system. The quantity $M_v(\Sigma\beta)$ is therefore an index of vibration for any order. The values of $\Sigma\beta$ for the families of orders are represented by the familiar typical diagrams shown in Figs. 6 and 7.

Application of Vectorscope to Firing-Order Studies

The investigation of firing orders resolves itself into evaluating the resultants of vector diagrams representing engine-balance and torsional-vibration factors including ΣM_1, ΣM_2, and $\Sigma\beta$ for each firing order. Now $\Sigma\beta$ occurs in families for each type of engine. In a complete study of firing orders, the number of vector diagrams to be evaluated may be considerable. As an example, for each firing order of the 7-cylinder 2-cycle unit previously considered, there are involved one vector diagram for ΣM_1 and ΣM_2 and three vector diagrams for the families of $\Sigma\beta$ for the minor orders of torsional vibration. Since there are 360 independent firing orders, the total number of vector diagrams is $4 \times 360 = 1440$.

Because of the great number of vector diagrams involved in this type of study, it is necessary to devise means for reducing the labor to practicable limits.

The application of the Vectorscope to the system described by Lewis, Breault, and Donaldson,[4] can best be illustrated by an example. Consider the 7-cylinder 2-cycle engine shown in Figs. 3 and 6. Using a Vectorscope disk with 7 equally spaced pegs, shown in Figs. 4 and 5, prepare weights proportional to the moments of the cranks about P. For details as to this procedure refer to Dashefsky's paper.[2] Mark each weight carrier distinctly with its crank number.

Having prepared the weights representing the vectors, it is now necessary to tabulate the vector groups for programming on the Vectorscope. The 7 cranks are listed according to the schedule for the 7-cylinder engine listed in Table 1. Retention of cranks 1 and 2 in Combination I avoids mirror-image vector diagrams which are equivalent as regards firing order. Crank No. 1 will always be used as the reference vector. Taking Group 7 of Table 5 as an example, we deal with Combination I, cranks 1 2 4 7, and Combination II, cranks 3 5 6. Since crank No. 1 is fixed as a reference point there remain in Combination I, cranks 2, 4, and 7 which are to be permutated 6 ways

2 4 7, 2 7 4, 4 2 7, 4 7 2, 7 2 4, 7 4 2

Keeping weight No. 1 representing the moment of crank No. 1, on the Vectorscope disk in fixed reference position, the remaining weights 2 4 7 are distributed according to the foregoing permutations in the manner illustrated in Fig. 8. For each arrangement of weights corresponding to one of the permutations, the indicating spot of light of the Vectorscope moves to a position representing the resultant vector radius and direction. These are recorded by marking a sheet of paper serving as the Vectorscope screen, each point being appropriately labeled as shown in Figs. 8 and 9.

It is now necessary to obtain the resultants for permutations of Combination II, namely, cranks 3 5 6. Permutations of cranks 3 5 6 are

3 5 6, 3 6 5, 5 3 6, 5 6 3, 6 3 5, 6 5 3

The Vectorscope chart is now turned through 180 deg, as shown in Fig. 9, so as to shift the resultants for Group II through 180 deg. The weights for cranks 3, 5, and 6 are distributed so as to obtain the resultants for each permutation of Combination II, in the manner previously accomplished for Combination I. The

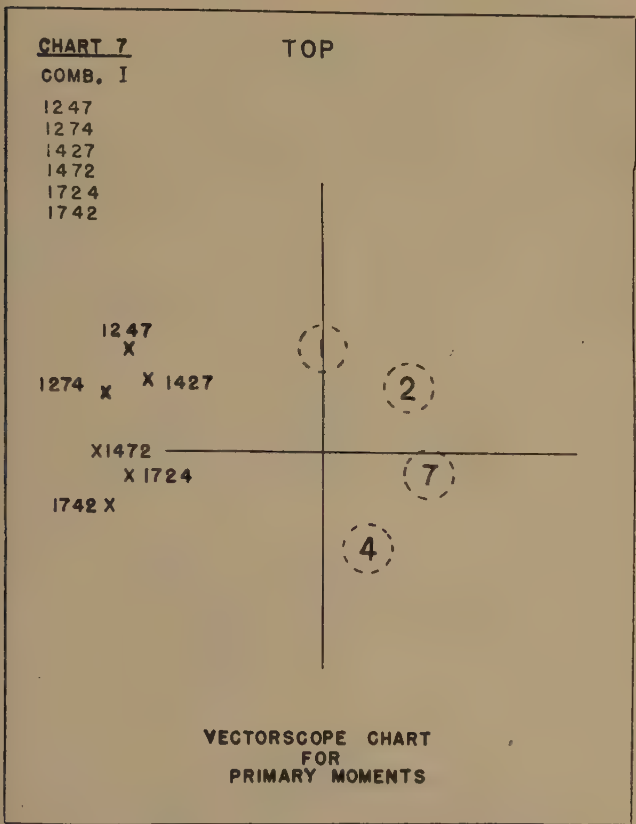

FIG. 8 STEP 1: OBTAIN RESULTANTS FOR ALL PERMUTATIONS OF COMBINATION I. POSITION OF REFERENCE CRANK REMAINS FIXED AT TOP. PERMUTATION 1 2 7 4 SHOWN

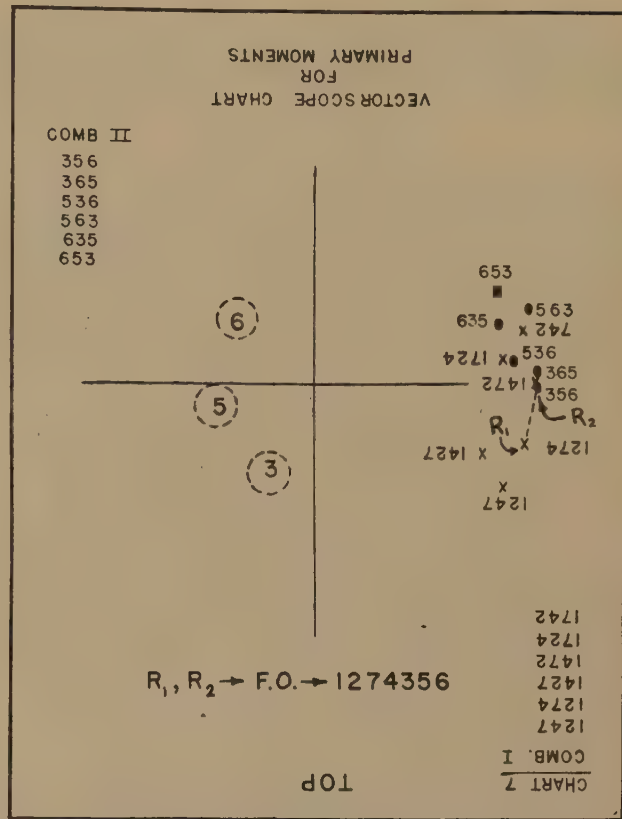

FIG. 9 STEP 2: TURN CHART THROUGH 180 DEG ON VECTORSCOPE SCREEN. RECORD RESULTANTS FOR ALL PERMUTATIONS OF COMBINATION II

distance between any point for Combination I, and Combination II represents the resultant for the firing order represented by the two groups of cylinders. For example, the resultant represented by the line R_{I}, R_{II} corresponds to the firing order 1-2-7-4-3-5-6.

The reason for shifting the vectors for Combination II through 180 deg by turning the Vectorscope chart through 180 deg is illustrated in Fig. 10. It will be noted that the sum of the two vectors is now indicated directly by the distance between the vector terminals such as R_{I}, R_{II}.

The foregoing procedure is repeated for each of the 10 groups listed in Table 1. There result 10 charts, each of which represents the resultants for 36 firing orders. Where two points such as R_{I} and R_{II} fall close together, a firing order with small unbalanced moment is indicated. Where the points are far apart large unbalance is indicated.

If complete information is required, the primary moments for all firing orders are listed. The secondary moments may also be obtained from this listing. This is illustrated by reference to Fig. 4, which represents the vector relationship for primary moments for firing order 1-7-2-4-5-3-6. Since the vectors for secondary moments have a phase angle twice that of the primary moments, the same vector diagram represents the firing order 1-2-5-6-7-4-3 for secondary moments. It must be remembered that the unit of moments for the secondary must now be used.

In investigating the values of $\Sigma\beta$, the procedure is much the same as for the determination of moments just described. Weights are prepared to represent the amplitudes at the cranks as shown in the typical relative-amplitudes curve, Fig. 6. The weights are distributed for the 1st order in the same manner as for the primary moments, obtaining two groups of points on each chart. The distance between points R_{I} and R_{II} represents the resultant for one firing order, for $\Sigma\beta_1$, that is, for the 1st order.

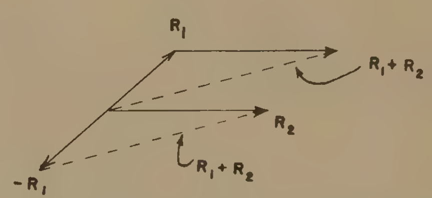

FIG. 10 TWO METHODS OF GRAPHICAL VECTOR ADDITION

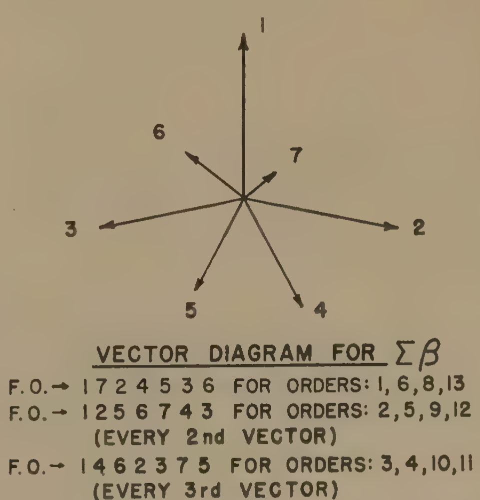

FIG. 11

As before, 10 charts are required to cover all of the firing orders. Having the values of $\Sigma\beta_1$ for the 1st order for all firing orders, it is now simply a matter of transcription to write the values of $\Sigma\beta$ for other minor orders as illustrated in Fig. 11.

"Convergent" Method

In many instances it is necessary to list only those firing orders which have desirably small primary and secondary moments and those values of $\Sigma\beta$ which are of importance to the specific problem. The following procedure has been found to work out satisfactorily. Charts are prepared for primary moments as previously described. It will be found that only a few and sometimes no desirable firing orders appear on a chart. Visual inspection is often sufficient for discarding many combinations of R_{I} and R_{II}.

Having selected and listed firing orders with suitably small primary moments ΣM_1, these relatively few firing orders are now to be evaluated for secondary moments ΣM_2. Secondary moments may be rapidly checked on the Vectorscope, using the same weights as were used for primary moments. The phase relationship for secondary moments is $(2 \times 360)/7$, corresponding to two peg spacings on the Vectorscope disk. Accordingly, to evaluate the resultant secondary moment, the weights are distributed according to firing order on every second peg. This is a simple rapid procedure for each of the relatively few firing orders. Those firing orders having large secondary moments are now discarded, leaving only those having small primary as well as secondary moments.

The values of $\Sigma\beta$ for torsional vibrations may now be investigated. If there is a particular minor order which is of importance, this should be evaluated first, so as further to eliminate firing orders which are unsuitable with regard to $\Sigma\beta$. The method for evaluating $\Sigma\beta$ on the Vectorscope has been described in detail.[2] Weights are prepared corresponding to the relative amplitudes of torsional vibration at the cranks, Fig. 6. The weights are distributed on the disk according to firing order, skipping the requisite number of pegs, depending upon the order of vibration.

The foregoing process has been found to be rapidly convergent in sifting out usable firing orders. In one problem it was advantageous to devote the first step of the study to investigation of a particularly important minor order of torsional vibration. Firing orders unfavorable with respect to this order of vibration were discarded. The remaining firing orders were investigated for primary moments, and unsuitable firing orders from this aspect, further discarded. In the next step the firing orders thus far suitable were further investigated for secondary moments. This procedure permitted examination of some 30,000 firing orders of a 10-cylinder engine with tolerable expenditure of time and labor.

Firing orders for 3, 4, 5 and 6-cylinder engines are given in Tables 1 to 4, inclusive. The study of firing orders in these engines is readily handled by direct distribution of Vectorscope weights according to the methods described by Dashefsky,[2] without necessity for operating separately on groups of cranks.

Summary

This paper has aimed to describe application of the Vectorscope to the mass investigation of firing orders. The influence of firing order upon manifolding, bearing pressures, internal bending moments, and similar properties is beyond the scope of this paper. No attempt has been made to present all of the fine points of technique. It is believed that each specific problem calls for improvisation which must be contributed by the individual investigator.

The illustrative examples in the foregoing discussion have dealt with the 2-cycle engine. It is believed, however, that application of the Vectorscope to the 4-cycle engine will be apparent as an extension of the previous discussions, and from the detailed descriptions of Dashefsky.[2]

Experience has shown that it is advantageous, when using the Vectorscope, to operate whenever convenient in such manner that the deflections for each of the two crank combinations are not extreme. This objective may be achieved by arranging the distribution of weights for each group around, rather than on one side of the disk, as suggested for the 8-cylinder engine, Table 7.

The Appendix suggests a means for guarding against possible omissions in the tabulation of the various combinations of cranks and the permutations of each such combination.

TABLE 1.
3-CYLINDER ENGINE.
INDEPENDENT FIRING ORDERS

1 2 3

TABLE 2.
4-CYLINDER ENGINE.
INDEPENDENT FIRING ORDERS.

Reference No	Firing Orders.
1	1 2 3 4
2	1 2 4 3
3	1 3 2 4

TABLE 3.
5-CYLINDER ENGINE.
INDEPENDENT FIRING ORDERS.

Reference No	Firing Orders.
1	1 2 3 4 5
2	1 2 3 5 4
3	1 2 4 3 5
4	1 2 4 5 3
5	1 2 5 3 4
6	1 2 5 4 3
7	1 3 2 4 5
8	1 3 2 5 4
9	1 3 4 2 5
10	1 3 5 2 4
11	1 4 2 3 5
12	1 4 3 2 5

TABLE 4.
6-CYLINDER ENGINE.
INDEPENDENT FIRING ORDERS.

Ref No	Firing Order	Ref No.	Firing Order	Ref. No.	Firing Order.
1	123456	21	126435	41	136425
2	123465	22	126453	42	136524
3	123546	23	126534	43	142356
4	123564	24	126543	44	142365
5	123645	25	132456	45	142536
6	123654	26	132465	46	142635
7	124356	27	132546	47	143256
8	124365	28	132564	48	143265
9	124536	29	132645	49	143526
10	124563	30	132654	50	143625
11	124635	31	134256	51	145236
12	124653	32	134265	52	145326
13	125346	33	134526	53	146235
14	125364	34	134625	54	146325
15	125436	35	135246	55	152346
16	125463	36	135264	56	152436
17	125634	37	135426	57	153246
18	125643	38	135624	58	153426
19	126345	39	136245	59	154236
20	126354	40	136254	60	154326

Tables 1 to 4, inclusive, give firing orders for engines from 3 to 6 cylinders. Suggested grouping of cylinders, distribution of Vectorscope weights for engines from 7 to 9 cylinders, and the permutations of 3, 4, and 5 cranks are given in Tables 5 to 12, inclusive.

ACKNOWLEDGMENTS

The author wishes to express his sincere thanks to Capt. H. L. Dodson, USN, Director of the Laboratory, for permission and encouragement to prepare the paper, and also appreciation to the Navy Department for authorizing its publication.

TABLE 5

7-CYLINDER ENGINE.

GROUPING OF CRANKS.

GROUP NO.	COMB. I A B C D	COMB. II E F G
1	1 2 3 4	5 6 7
2	1 2 3 5	4 6 7
3	1 2 3 6	4 5 7
4	1 2 3 7	4 5 6
5	1 2 4 5	3 6 7
6	1 2 4 6	3 5 7
7	1 2 4 7	3 5 6
8	1 2 5 6	3 4 7
9	1 2 5 7	3 4 6
10	1 2 6 7	3 4 5

TABLE 6

PERMUTATIONS $_3P_3 = 3\times2\times1 = 6$

COMB. I : BCD, BDC, CBD, CDB, DBC, DCB.

COMB. II : EFG, EGF, FEG, FGE, GEF, GFE.

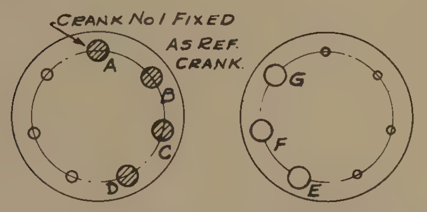

COMBINATION I COMBINATION II

VECTORSCOPE SET UP FOR 2 & 4 CYCLE ENGINES.

FIG. 12

TABLE 9.

8-CYLINDER UNIT.

PERMUTATION OF COMB II (EFGH)

$_4P_4 = 4\times3\times2\times1 = 24$

1	EFGH	7	FEGH	13	GEFH	19	HEFG
2	EFHG	8	FEHG	14	GEHF	20	HEGF
3	EGFH	9	FGEH	15	GFEH	21	HFEG
4	EGHF	10	FGHE	16	GFHE	22	HFGE
5	EHFG	11	FHEG	17	GHEF	23	HGEF
6	EHGF	12	FHGE	18	GHFE	24	HGFE

THE FOLLOWING ARE SYMMETRICAL ABOUT VERTICAL AXIS. USE OF ONLY ONE AVOIDS MIRROR IMAGE FIRING ORDERS.

1 & 24, 2 & 18, 3 & 22, 4 & 12, 5 & 16
6 & 10, 7 & 23, 8 & 17, 9 & 20, 11 & 14
13 & 21, 15 & 19.

8-CYLINDER ENGINES.

TABLE 7.

GROUP No	COMB. I ABCD	COMB. II EFGH
1	1 2 3 4	5678
2	235	4678
3	236	4578
4	237	4568
5	238	4567
6	245	3678
7	246	3578
8	247	3568
9	248	3567
10	256	3478
11	257	3468
12	258	3467
13	267	3458
14	268	3457
15	278	3456
16	345	2678
17	346	2578
18	347	2568
19	348	2567
20	356	2478
21	357	2468
22	358	2467
23	367	2458
24	368	2457
25	378	2456
26	456	2378
27	457	2368
28	458	2367
29	467	2358
30	468	2357
31	478	2356
32	567	2348
33	568	2347
34	578	2346
35	678	2345

VECTORSCOPE SET UP.
8 CYL.-2 CYCLE ENGINE.

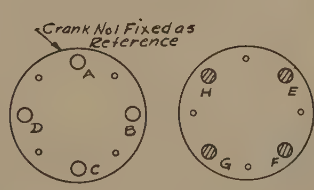

(AVOID MIRROR IMAGES)

FIGURE 13.

VECTORSCOPE SET UP.
8 CYL.-4 CYCLE ENGINE.

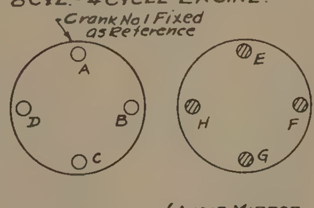

(AVOID MIRROR IMAGES)

FIGURE 14.

TABLE 8.

8-CYLINDER ENGINE

PERMUTATIONS OF COMB. I (BCD)

COMBINATION I : $_3P_3 = 3\times2\times1 = 6$

BCD, BDC, CBD, CDB, DBC, DCB

9 CYLINDER ENGINE.

TABLE 10

GROUP No	COMB. I	COMB II
1	12345	6789
2	12346	5789
3	12347	5689
4	12348	5679
5	12349	5678
6	12356	4789
7	12357	4689
8	12358	4679
9	12359	4678
10	12367	4589
11	12368	4579
12	12369	4578
13	12378	4569
14	12379	4568
15	12389	4567
16	12456	3789
17	12457	3689
18	12458	3679
19	12459	3678
20	12467	3589
21	12468	3579
22	12469	3578
23	12478	3569
24	12479	3568
25	12489	3567
26	12567	3489
27	12568	3479
28	12569	3478
29	12578	3469
30	12579	3468
31	12589	3467
32	12678	3459
33	12679	3458
34	12689	3457
35	12789	3456

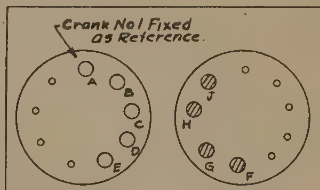

COMBINATION I. COMBINATION II.
VECTORSCOPE SET UP
FOR 2 & 4 CYCLE ENGINES.

FIGURE 15.

TABLE 11

PERMUTATIONS OF COMB. I (BCDE)

$_4P_4 = 4\times3\times2\times1 = 24$

1	BCDE	7	CBDE	13	DBCE	19	EBCD
2	BCED	8	CBED	14	DBEC	20	EBDC
3	BDCE	9	CDBE	15	DCBE	21	ECBD
4	BDEC	10	CDEB	16	DCEB	22	ECDB
5	BECD	11	CEBD	17	DEBC	23	EDBC
6	BEDC	12	CEDB	18	DECB	24	EDCB

TABLE 12

PERMUTATIONS OF COMB. II (FGHJ)

$_4P_4 = 4\times3\times2\times1 = 24$

1	FGHJ	7	GFHJ	13	HFJG	19	JFGH
2	FGJH	8	GFJH	14	HFGJ	20	JFHG
3	FHGJ	9	GHFJ	15	HGFJ	21	JGFH
4	FHJG	10	GHJF	16	HGJF	22	JGHF
5	FJGH	11	GJFH	17	HJFG	23	JHFG
6	FJHG	12	GJHF	18	HJGF	24	JHGF

Appendix

Because of the complication in tabulating the groupings for engines with 7 or more cylinders, it is desirable to have a check on the completeness of the tabulation. Taking the 7-cylinder engine as an example, the number of independent firing orders is

$$N_{Fo} = (n - 1)!/2 = 6 \times 5 \times 4 \times 3 = 360$$

Now consider the grouping of cylinders in Table 5. Crank No. 1 is fixed as a reference point, and crank No. 2 is retained in Combination I to avoid mirror-image vector diagrams. The remaining 5 cylinders are now tabulated as combinations under Combination I. The combinations of n things r at a time are given by

$$_nC_r = \frac{n(n-1)(n-2)\ldots(n-r+1)}{r!}$$

Accordingly, the number of combinations possible for Combination I is

$$_5C_2 = \frac{5 \times 4}{2 \times 1} = 10$$

Combination II in each of the groups is made up of the remaining cranks.

The cranks in Combination I, except crank No. 1, which is fixed, are to be permutated. The number of permutations of n things n at a time is

$$_nP_n = n!$$

Thus the number of permutations of the cranks in Combination I is

$$_3P_3 = 3 \times 2 \times 1 = 6$$

The number of permutations of the cranks in Combination II is also

$$_3P_3 = 3 \times 2 \times 1 = 6$$

Therefore the total number of firing orders is

$$N_{Fo} = (_5C_2) \times (_3P_3) \times (_3P_3) = 10 \times 6 \times 6 = 360$$

This is consistent with the number of firing orders indicated by the basic expression

$$(n - 1)!/2$$

The number of points to be plotted is 6 + 6 = 12 for each chart, and a total of 10 × 12 = 120 for the complete study of primary moments.

Discussion

K. J. DeJuhasz.[5] It is gratifying to note that the ingenious mathematical instrument developed by the author some years ago has been developed further and put to considerable practical use. The writer cannot offer any comments on the mathematics and geometry of engine balance, except to commend the clarity and conciseness with which the author presented this abstruse subject in this paper of limited length. However, the writer has some questions relative to the construction and possible future development of the Vectorscope as an instrument.

The complete investigation of engines, having large numbers of cylinders, for optimum firing order requires tests running into hundreds of thousands and even millions. Even with the Vectorscope, in its present construction, the execution of so many tests is beyond practical possibility. In particular, the shifting of the weights by hand appears to be a cumbersome and tedious operation, subject to errors. Perhaps this operation could be facilitated by using, instead of weights, such loading devices as springs, chainomatic devices, or solenoids. The changing of loading, then, so it would appear, could be made more rapidly by hand, or could even be performed automatically according to a prearranged program, and the resultant vector could be recorded as to its direction and magnitude. Solutions for the detail problems of such a design are probably available already in recording balances, and calculating machinery.

Probably the author has already given thought to the further development of the Vectorscope, and it would be of interest to learn of any plans which may be contemplated in these directions.

[5] Professor of Engineering Research, Pennsylvania State College, State College, Pa. Mem. ASME.

J. C. Georgian.[6] The new method of application of the Vectorscope to firing-order studies is similar to the method as given by Lewis, Breault, and Donaldson,[4] and as such is a convenient method to reduce the amount of work necessary for complete firing-order studies. The convergent method proposed is a common-sense way to select the best firing order for a specific situation. This same method may be used without the use of the Vectorscope by simple inspection. As an example, a 10-cylinder firing order is desired with a small $\Sigma\beta$ for the 5th order. This may be found by noting that the 5th order is the difference of two groups of 5 cylinders. By inspection, it may be seen what the minimum value of $\Sigma\beta$ for the 5th order will be when 1-3-6-7-10 is subtracted from 2-4-5-8-9 shown in the phase diagram, Fig. 16 of this discussion.

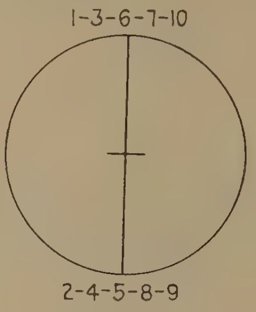

Fig. 16

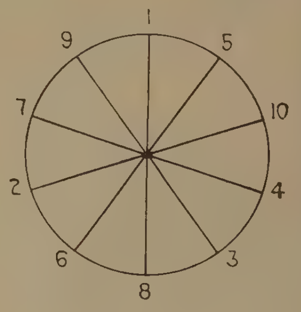

Fig. 17

With this arrangement the firing order must be such that any number on the top list of Fig. 16 must be combined with the number on the bottom list as opposite cranks in the crank diagram, and in this manner we arrive at a firing order of 1-9-7-2-6-8-3-4-10-5 as shown in the crank diagram, Fig. 17.

Thus it is possible to select the firing order without the use of a Vectorscope and without the necessity of analyzing a large number of combinations. This method is typical for engines with any number of cylinders. However, it must be admitted that the use of the Vectorscope would aid in the foregoing determination as there are still 1440 firing orders which will give the same 5th order vector sum.

The best firing order from the point of view of over-all external moments may be found by setting up symmetrical firing orders by starting at the center of the engine and placing the numbers of the cylinders in consecutive order on each side of the center in alternating order, e.g., for a 7-cylinder engine we start with No. 4 cylinder and then place Nos. 3 and 5 on each side of it as 3-4-5, the next group will be 2 and 6 but are placed in alternate order as 6-3-4-5-2, then the last are 7 and 1 and we get the firing order 1-6-3-4-5-2-7.

[6] Torsional Analyst, Nordberg Manufacturing Company, Milwaukee, Wis. Jun. ASME.

In a similar manner we may obtain firing orders for any number of cylinders. In the following tabulation we have listed firing orders to 12 cylinders:

No. of cylinders	Firing order
3	1-2-3
4	1-3-2-4
5	1-4-3-2-5
6	1-5-3-4-2-6
7	1-6-3-4-5-2-7
8	1-7-3-5-4-6-2-8
9	1-8-3-6-5-4-7-2-9
10	1-9-3-7-5-6-4-8-2-10
11	1-10-3-8-5-6-7-4-9-2-11
12	1-11-3-9-5-7-6-8-4-10-2-12

The only disadvantage of the foregoing firing orders is that the center 2 and 3 cylinders fire in succession for an even number and an odd number of cylinders, respectively. This is not serious for cylinders 3 to 8, but for 9 and above, the angles between the cranks are getting so small that there is decided unbalanced internal loading from these closely spaced cranks; if the bedplate is not stiff it will cause the engine to take an undesirable weaving action. In general, however, the firing orders from 3 to 8 are the standard firing orders used by most manufacturers of 2-cycle engines.

For 4-cycle engines, the firing orders for an even number of cylinders are such as to use balanced crankshafts and therefore this limits the number of possible firing orders and crank arrangements. For an odd number of cylinders of 4-cycle engines, the number of crank arrangements will be the same as 2-cycle engines. However, with 4-cycle engines, every other crank fires in succession.

The paper is quite valuable as it describes the most efficient use of the Vectorscope in solving firing-order problems. However, since the Vectorscope is not available for commercial use, the value of the paper would be greatly enhanced if for cylinders above 8, the best firing orders, had been tabulated with their values of ΣM_1, ΣM_2, and $\Sigma\beta$.

Alexander Goloff.[7] As the author tacitly admits in his summary, the usefulness of the Vectorscope in reducing greatly the amount of computational effort could be made more apparent if the scope of the paper were enlarged to incorporate the study of bearing loads, internal bending moments imposed on the cylinder block, and the like.

The construction of the Vectorscope is ingenious. If a comprehensive study of firing orders is to be made, the use of this instrument in the solution of problems, considered by the author, is almost a necessity. It would seem that this instrument, as well as the clever methods described, which realize many possible computational short cuts, are of particular interest to a manufacturer of larger engines. However, the writer feels that the Vectorscope can be used advantageously in studying various phenomena pertaining to smaller engines as well.

For instance, the study of torsional amplitudes or stresses in a multimass system with damping furnished by a damper, as well as internally by the engine, is greatly facilitated by the use of the mobility method. Since this method requires extensive manipulation of complex numbers, the Vectorscope should result in substantial saving of time. With very little additional effort it should be possible to add reciprocals of vectors.

The use of this device can be further extended to the solution of many electrical problems, particularly those in filter design, impedance matching, etc.

[7] Staff Engineer, Research Department, Caterpillar Tractor Company, Peoria, Ill.

J. D. Swannack.[8] The writer's comments are based upon experience with 2-cycle engines up to 12 cylinders.

The subject of firing orders is one upon which the writer would prefer to speculate rather than to calculate. It is encouraging that the author has described a method for removing much of the numerical labor normally involved in firing-order investigations. It would be useful to know the author's estimate of the time involved in obtaining and recording the primary-moment factor for a 10-cylinder firing sequence.

The writer's, and it is believed also the author's thought, is that the most useful firing-order index is one arranged in ascending order of primary-moment factor. In most cases the primary moment is of primary importance. Unless one is committed to additional mechanical complications, he is forced to select a firing order with a reasonable primary balance. The designer must of course decide what is "reasonable."

The writer would be quite pleased to possess a list of firing orders whose primary-moment factor was less than 1, for all engines up to and including 12 cylinders. Undoubtedly, for 11 and 12 cylinders this would be a long list. As the author says, it would involve a prohibitive amount of labor.

A suggested sequence of investigation is mentioned in the author's "Convergent Method." In most cases this will be the shortest path to a satisfactory firing order. The writer has found in engines of high piston speed and low over-all weight, the following approach is advantageous:

1 Consideration of primary balance.
2 Consideration of internal bending moment and effect on a flexible engine frame.
3 Investigation of secondary moment.
4 Torsional-vibration study.

It is appreciated that there might be disagreement over considering torsional vibration last. However, the calculator working on an engine of this type will shortly conclude that all firing orders are bad and resign himself to other means of dealing with this phase of the problem.

The author's interest in engine dynamics is greatly appreciated, and we sincerely hope he will continue to produce such useful contributions as the present paper.

F. P. Porter.[9] A ten-cylinder engine with equal firing intervals has 181,440 possible firing orders. If fifteen minutes were spent on calculating the balance factors for each of the firing orders, working 8 hours a day 300 days a year, it would take about 18 years for one person to work them all out. For the 12-cylinder engine it would take about 100 times as long, or about 1800 years. Thus it is apparent that the interesting device that Mr. Dashefsky has described may be used to advantage in the study of firing orders.

The subject of firing orders is really very pertinent to all engine builders, particularly where the number of cylinders increases. Of course many of the good firing orders have been identified and are being used by manufacturers at the present time. There are, however, special problems that come up that may influence the choice of the firing order. Undoubtedly many here have rather definite ideas on some of those subjects. It would be interesting if some of them would give us their points of view on this.

There is one phase of the subject that undoubtedly the Vectorscope could handle as well as it handles the usual solution. This may be stated as the problem of determining the firing order for

[8] Chief Design Calculator, Fairbanks, Morse & Company, Beloit, Wis. Mem. ASME.

[9] Consulting Engineer, American Locomotive Company, Schenectady, N. Y.

an engine that is structurally weaker than average, due to intentional design to make a light engine. Here the choice of the firing order might be influenced not only by good over-all balance but also by the requirement of minimum internal bending movement.

There is an interesting but rather insignificant detail in speaking of the number of possible firing orders and crankshafts. If the cylinders of an engine were numbered by one manufacturer from one end of the engine and by another manufacturer from the other end of a similar engine, it can happen that different firing orders for the two engines correspond identically to the same crankshaft. You can check this if you write down a few firing orders for the five-cylinder two-cycle engine. For example, consider the firing order 1-3-4-2-5. If the engine were numbered from the other end, cyl 1 = cyl 5, cyl 2 = cyl 4, etc., 3 = 3, 4 = 2, 5 = 1. Therefore the same crankshaft numbered from the other end is 5-3-2-4-1 or 1-4-2-3-5, which is a different firing order for the same crankshaft. The usual firing for this engine, namely, 1-4-3-2-5, does not show this characteristic, since numbering from the other end gives 5-2-3-4-1 or 1-4-3-2-5, which is the same firing order. It turns out that of the twelve possible firing orders for a 5-cylinder engine, there are only eight different crankshafts. For the 6-cylinder engine, there are sixty possible firing orders but only 38 different crankshafts. For the 7-cylinder engine, there are 360 possible firing orders and 192 possible crankshafts. Although this point is not very important, the writer thought it might be of interest at this time.

Author's Closure

The remarks of Professor Dejuhasz are appreciated. There are many good ways to accomplish the loading of the Vectorscope disk. Some of those suggested by Professor Dejuhasz have been considered. The present scheme is the result of the inevitable compromises which always seem to become necessary in these cases. Some effort has already gone into the design of electromagnetic loading, an automatic "permutating" device, and photographic recording, but much still remains to be done in this direction.

Mr. Georgian indicates a procedure for selecting good firing orders without use of the Vectorscope. In his example pertaining to a 10-cylinder engine, Mr. Georgian has selected the 5th order to illustrate the simple manner in which a good firing order may be selected. This results in sets of vectors differing in phase by 180 deg, and the vector sum may be arrived at by simple addition and subtraction. However, for all other orders such as the 3, 4, 6, etc., which also require investigation, the phase angle between vectors will not permit such simple manipulation. It is here that the use of the Vectorscope may be better appreciated. Any necessity for working with the 11-cylinder engine would also demonstrate the labor-saving features of the Vectorscope.

The suggested firing orders for different number of cylinders listed by Mr. Georgian are valuable as concerns engine balance but require further investigation to determine their desirability with respect to minor orders of torsional vibration and other characteristics influenced by firing order. The purpose of the present paper has been the presentation of the techniques for the use of the Vectorscope, rather than presentation of particular firing-order properties. In response to Mr. Georgian's statement that the Vectorscope is not at present available for commercial use, it is desired to indicate that arrangements for commercial availability of the instrument are being completed.

The additional uses of the Vectorscope, mentioned by Mr. Goloff, are very interesting, particularly the suggested applications of the instrument to problems involving the mobility method. In general, the Vectorscope appears to be applicable to the solution of any problem which is reducible to a vector summation. Its applicability to electrical problems will be determined in any instance by the saving of time which the Vectorscope may afford.

The author is in close agreement with Mr. Swannack as to the importance of primary balance. However, most problems result in a compromise among the several engine characteristics which are influenced by firing order. It is regretted that the listing of firing orders with small primary unbalance desired by Mr. Swannack cannot be provided at this time.

Regarding Mr. Swannack's suggested sequence of investigation, it seems to the author that in any particular problem, the factor to be considered first should be the one which would eliminate the greatest number of firing orders with minimum labor. As an example of this is the problem discussed by Mr. Georgian. Here the 5th order torsional is one of importance. This order has two sets of vectors 180 deg apart and is readily handled as a simple arithmetic process. In this problem, this would be the first step in eliminating large groups of undesirable firing orders. The next steps would be in order, primary moments, secondary moments, and the other minor-order torsional factors. It seems to the author that the sequence cannot be fixed but remains one of expedience for the particular problem in hand.

Regarding Mr. Swannack's question as to the time required to obtain and list all of the primary-moment factors for the 10-cylinder engine, the mere writing of the 181, 440 firing orders would in itself be a long job. However, if we were to limit ourselves to examining all of the firing orders, but writing down only those having a primary-moment factor less than unity, our experience thus far indicates that about 400 man-hours would be required to explore the primary, secondary, and minor-order torsional vibration factors. In this regard, the remarks on this subject offered in Mr. Porter's discussion are of interest.

Mr. Porter in his discussion contributes in too casual a manner the important and pertinent observation that a single crankshaft configuration can satisfy more than one firing order. The author was not aware of this fact, and believes that it is not generally recognized. Although Mr. Porter's observation does not invalidate any of the content of this paper, it is a most important contribution.

The author is grateful to the discussers for their contributions which have added considerable pertinent opinion and material and thus enhanced the value of the paper. It is hoped that the techniques indicated herein will provide an additional tool for handling this time-consuming problem.

Distribution of Heat Generated in Drilling

By A. O. SCHMIDT[1] and J. R. ROUBIK,[2] MILWAUKEE, WIS.

The object of this investigation was to determine the amount of heat which goes into the workpiece, chips, and drill at different cutting speeds and feeds. A tubular test bar of extruded Dowmetal was used as the workpiece, thus making the cutting action of the drill similar to that of a single-point tool. The total heat, the heat in the chips, and the heat in the drill were measured separately in a calorimeter.

PRACTICALLY all of the energy expended in cutting metal is converted into heat which manifests itself in varying amount and degree in the chips, tool, and workpiece. The energy referred to is that required at the cutting tool and does not include that energy which is necessarily dissipated as mechanical and electrical losses in the machine transmission and drive. Heat generated in a cutting operation can be determined accurately with a calorimeter, and the measurements thus obtained permit computations of work, power, chip temperatures, and tool forces (1).[3] Power data, derived from torque and thrust measurements on a carefully calibrated dynamometer, are in close agreement with calorimetric determinations (2).

It is generally accepted that the major portion of heat in a metal-cutting operation is generated in forming the chips and is carried away by them. Calorimetric tests of milling operations on steel at cutting speeds of 100 to 800 fpm indicate that the heat in the chips comprises 60 to 70 per cent of the total heat. However, since somewhat elaborate preparation and correction are needed with milling tests, simpler drilling tests were resorted to.

Drilling-Test Procedure

In a series of drilling tests the amounts of heat in the chips, tool, and workpiece were measured separately. Three different calorimetric tests were used to measure: (*a*) total heat, (*b*) heat in the tool, and (*c*) heat in the chips (see Figs. 1, 2, and 3, respectively). A $^7/_{16}$-in-diam drill with a 30-deg helix angle, 118-deg point angle, and 12-deg relief angle was used in all tests. Test bars were made from a single piece of extruded Dowmetal, 0.375 in. diam. A centrally located pilot hole 0.110 in. diam and $1^1/_4$ in. deep was machined in each bar. To insure uniform cutting conditions, each piece was countersunk at the top with a $^7/_{16}$-in. drill. All tests were performed on a Kearney & Trecker 2-C Autometric precision boring machine with variable feeds and speeds.

At each of the following peripheral cutting speeds of 9.8, 49, 98, 147, 196, and 246 fpm, the drill was operated at feed rates of 0.0022, 0.0057, and 0.0091 in. per revolution (ipr). Distilled water at room temperature was measured into the calorimeter with a pipette. Water-temperature readings were taken immedi-

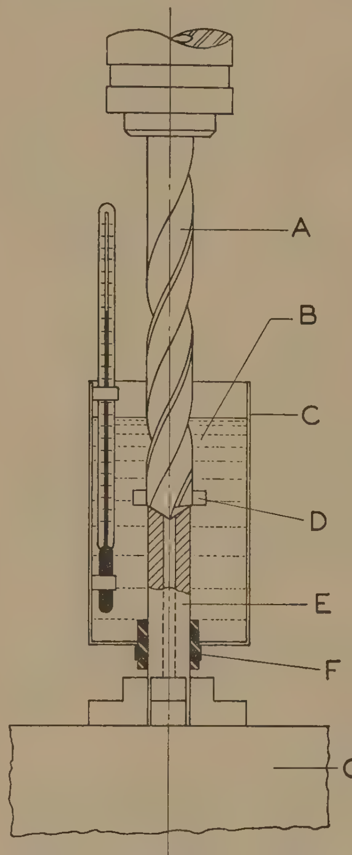

Fig. 1 (*left*) Calorimetric Apparatus for Measuring Total Heat Generated in Drilling

A drill $^7/_{16}$ in. diam
B 50 cc of water
C container
D blades on drill for agitation
E $^3/_8$-in. test bar
F rubber grommet
G three-jaw chuck

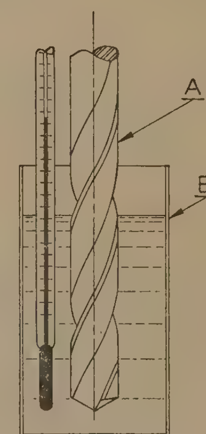

Fig. 2 Measuring Heat in Tool After Cut

A drill $^7/_{16}$ in. diam
B container with 50 cc of water

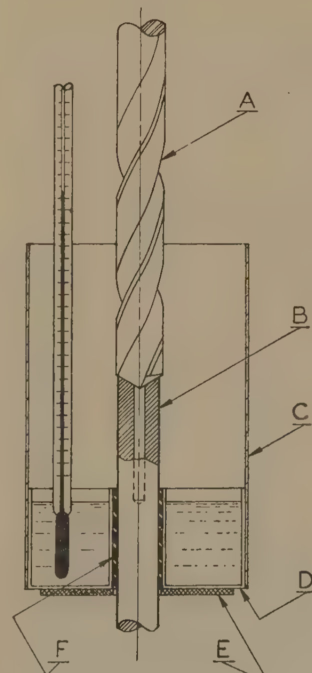

Fig. 3 (*left*) Measuring Heat in Chips
(Short chips resulting from brass point on drill fall into water.)

A drill $^7/_{16}$ in. diam
B $^3/_8$-in. test bar
C chip guard made of cardboard
D container with 50 cc of water
E insulator
F rubber grommet

[1] Research Engineer in Charge of Metal Cutting Research, Kearney & Trecker Corporation. Mem. ASME.

[2] Lecturer in Mechanics, Marquette University; and Research Department, Kearney & Trecker Corporation. Jun. ASME.

[3] Numbers in parentheses refer to the Bibliography at the end of the paper.

Contributed by the Special Research Committee on Metal Cutting Data and Bibliography and presented at the Semi-Annual Meeting, Milwaukee, Wis., May 30–June 5, 1948, of The American Society of Mechanical Engineers.

ately before cutting and after the drill had removed 1 in. from the length of the test bar. The total heat was measured by performing the drilling operation with the workpiece, chips, and tool submerged in water, see Fig. 1. The heat in the tool was determined by cutting an identical test bar dry and dropping the tool into the calorimeter immediately upon completion of cutting, see Fig. 2. Heat in the chips was obtained by noting the temperature rise of the calorimeter and water into which only the chips were permitted to fall, see Fig. 3. When drilling at 100 rpm, corrections for heat losses were made. At the higher cutting speeds the time of cutting was short and heat losses were within the reading errors. Calorimetric temperature measurements in all cases are directly comparable since the different calorimeters were designed to have the same water equivalents. Therefore each calorimeter-temperature-rise value is a uniform true index or measure of heat whether it be total heat, heat in the chips, or heat in the tool.

Test Results

Data obtained in these tests are plotted in Fig. 4. These curves indicate that for any given chip thickness the total amount of heat generated and contained in the chips, workpiece, and tool, as measured with the calorimeter shown in Fig. 1 is practically constant regardless of cutting speed, at least up to a peripheral cutting speed of 250 fpm. It can be seen that greater amounts of heat occur with the finer chip thicknesses, whether the total heat, heat in the chips, heat in the tool, or heat in the workpiece be considered. Under the conditions of these tests higher temperatures would of course accompany greater amounts of heat. Thus it may be said that at the same cutting speed, a fine feed will result in higher chip, tool, and workpiece temperatures than will a heavier feed.

It is misleading to use the peripheral cutting speed in the interpretation of these drill-test data, since this value is only a maximum and is not at all representative of the cutting speed on the smaller diameters of the drill contact with the workpiece. Use of the cutting speed on the mean diameter of the workpiece is more justifiable. If the last-mentioned values are used, it can be seen that the test data extend only to 175 fpm.

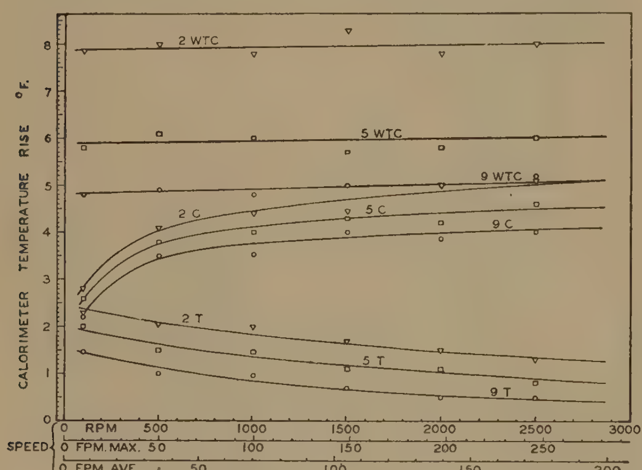

Fig. 4 Calorimeter Temperature Rise in Relation to Cutting Speed and Feed

($2WTC$ = heat in workpiece, tool, and chips at a feed of 0.0022 ipr: $2C$ = heat in chips at feed of 0.0022 ipr; $2T$ = heat in tool at feed of 0.0022 ipr; 5 and 9 denote feeds of 0.0057 and 0.0091 ipr, respectively.)

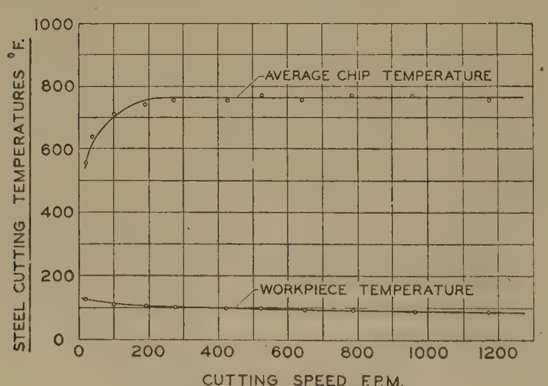

Fig. 5 Average Temperature In Milling of Steel Workpiece and Chips in Relation to Cutting Speed

(Feed per tooth 0.008 in.; depth of cut 0.125 in.; milling cutter with 6-deg negative radial rake angle. Chip temperatures measured with a calorimeter, surface temperatures of identical workpieces 1 in. diam and 2 in. long determined by Alnor low-range thermocouple. Each of foregoing values was determined with a keen cutting edge; tool wear will change cutting forces and therefore cutting temperatures also.)

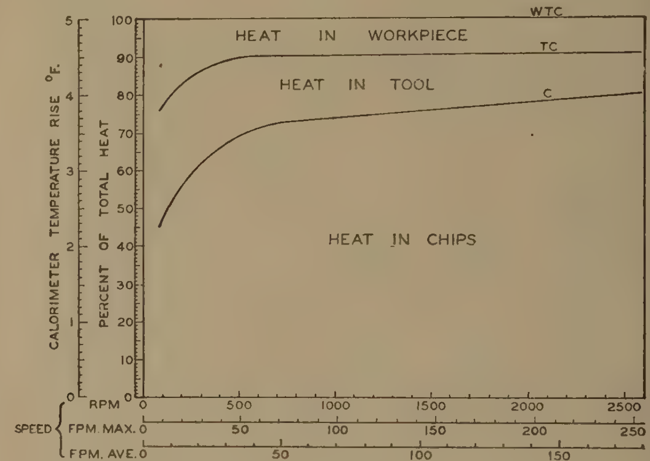

Fig. 6 Typical Distribution of Heat in Workpiece, Tool, and Chips at Various Speeds

[C, curve represents heat in chips; TC, curve represents total heat in tool and chips; WTC, curve (100 per cent) represents total heat in workpiece, tool, and chips, or simply total heat.]

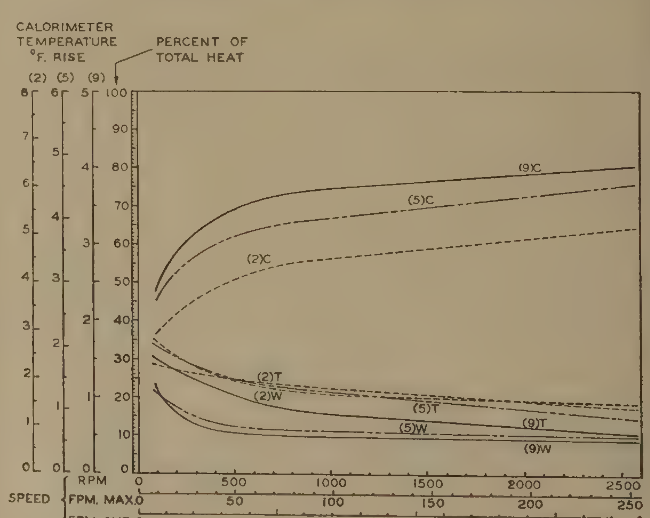

Fig. 7 Relation at Various Speeds and Feeds of Heat in Chips in Tool, and in Workpiece

[C, curves represent heat in chips; T, curves represent heat in tool; W, curves represent heat in workpiece. Number prefixes indicate feed in inches per revolution; (2), 0.0022; (5), 0.0057; and (9), 0.0091.]

Above 1000 rpm (69.4 fpm average) the slopes of the curves indicating heat in the chips have a lower value, see Figs. 4 and 6. It may be expected that the ordinates of each of these curves will attain a different constant value at some higher speed, perhaps between 3000 and 3500 rpm (208 and 243 fpm average). The basis for this statement may be found in Fig. 5 which shows that the temperature of milling chips, and therefore the heat in the chips, acquires a constant character between 200 and 250 fpm cutting speed. Chip-temperature value of course depends on the material being cut, tool angles, and thickness of chip, but remains practically constant for any given set of the foregoing conditions regardless of cutting speed above 200 fpm (2).

Data for a feed rate of 0.0091 ipr have also been plotted in Fig. 6 to show the percentages of heat in the chips, tool, and workpiece with the total heat taken as 100 per cent. In general, the chips contain the greatest proportion of the total heat with tool and workpiece following in that order. It can be seen, Fig. 7, that for the thicker chip the percentage of heat in the chips is greater, and the percentage of heat in both the tool and workpiece is less than it is for the thinner chip.

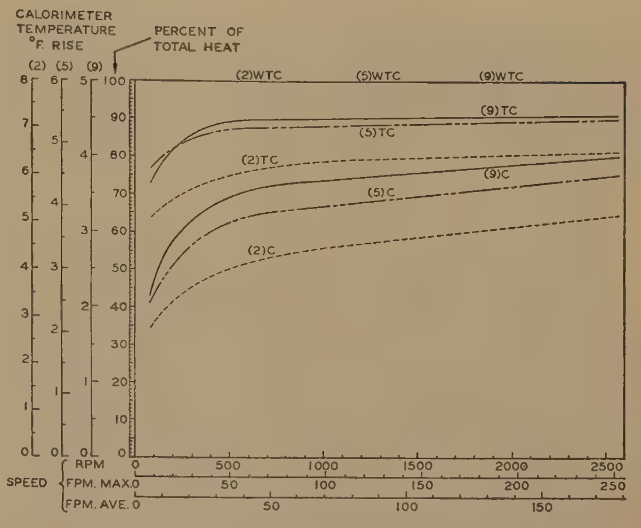

Fig. 8 Distribution of Heat in Workpiece, Tools, and Chips at Various Feeds and Speeds

[These curves are similar to those in Fig. 6 but represent three different feed rates and are placed together for comparison. The curves (9) *C*, (9) *TC*, and (9) *WTC* are the same as *C*, *TC*, and *WTC* in Fig. 6. *C* curves represent heat in chips; *TC* curves represent total heat in tool and chips; and *WTC* curves (100 per cent) represent total heat in workpiece, tool, and chips, or simply total heat or work. Number prefixes indicate feed in inches per revolution; (2), 0.0022; (5), 0.0057; and (9), 0.0091. To obtain calorimeter temperature-rise values, use vertical scale which has same number as prefix number of curve.]

Interpretation of Results

Several factors affect the heat distribution in any machining operation. Practically all of the mechanical energy is transformed into heat primarily by the deformation of the metal in the chip and to a lesser degree by the friction of the chip against the tool face. A very small portion of the mechanical energy is converted into cold work and is evidenced as strain in the machined surface to a depth of a few thousandths of an inch (4).

The amounts of heat that are conducted from the chip to the tool and workpiece depend upon the temperature differential between these elements, their masses, and the length of time in contact with one another. Heat lost to the surrounding atmosphere caused negligible error in these drill-test data because the time needed to complete each test was of only a few seconds' duration.

In view of the foregoing statements, it can be seen that data for the higher cutting speeds show greater amounts and percentages of heat in the chips because the heat has had less time to be conducted from the chip to the tool and workpiece. Thick chips have a lower temperature than thin chips, Fig. 4, but the percentage of heat in the chips is greater for thicker chips, Figs. 7 and 8. Because a thick chip has a greater mass and a lower temperature, the rate of conduction of heat away from a thick chip is less than it would be for a thin chip.

In summary, thick chips mean less total work, lower tool temperatures, and lower workpiece temperatures (3). Higher cutting speeds neither increase nor decrease greatly the work per volume of material machined when cutting conditions and tool remain identical. Of course higher cutting speeds would increase power requirements since equal amounts of work would be done in shorter time intervals. As cutting speeds increase up to about 200 fpm, they entail higher chip temperatures and lower workpiece temperatures. Above 200 fpm chip temperatures remain practically constant. Generally, tool temperatures will increase, however, if machining is continuous or prolonged, or the cutting speed is increased, since the heat in the tool will accumulate faster than it can be dissipated in most instances. For the same reason the heat in the tool will be concentrated near the cutting edge and the temperature of this portion of the tool will be considerably higher than surrounding portions. Higher cutting speed especially will tend to accentuate this condition. Chip thickness is limited by the strength of the tool, surface-finish requirements, and setup and machine limitations. Cutting speed is often limited by the ability of the tool to conduct heat away from the immediate vicinity of the cutting edge.

When only the lips of a drill are used to cut a tubular test bar the action is similar to machining with a single-point tool and therefore can be considered related to machining accomplished in planer, lathe, and many milling-machine operations (5)

Conclusions

The major portion of the heat generated in a metal-cutting operation is carried away by the chips.

Under 200 fpm cutting speed the percentage of heat in the chips will vary with cutting speed and chip thickness; the higher the cutting speed and the thicker the chip, the higher will be the percentage of heat in the chips. Above a cutting speed of 200 fpm the amount of heat in the chips, and also the chip temperature, acquire a constant character for otherwise identical cutting conditions.

At low cutting speeds (around 10 fpm) the amount of heat in the chips will be about 40 to 52 per cent of the total heat generated, depending upon the chip thickness.

At higher cutting speeds (200 fpm and above) the amount of heat in the chips will vary between 60 and 80 per cent of the total heat generated, depending upon the chip thickness. The remaining heat is distributed almost equally to the tool and workpiece. Since the workpiece is usually of larger mass than the tool, its temperature will be low while the heat in the tool is of necessity concentrated in a zone near the cutting edge which at high cutting speeds or under continuous machining will reach a high temperature. This is a frequent contributing cause of tool failure.

BIBLIOGRAPHY

1 "A Thermal-Balance Method and Mechanical Investigation for Evaluating Machinability," by A. O. Schmidt, W. W. Gilbert, and O. W. Boston, Trans. ASME, vol. 67, 1945, pp. 225–232.

2 "Measurements of Temperatures in Metal Cutting," by A. O. Schmidt, O. W. Boston, and W. W. Gilbert, Trans. ASME, vol. 68, 1946, pp. 47–49.

3 "An Investigation of Radial Rake Angles in Face Milling," by J. B. Armitage and A. O. Schmidt, Trans. ASME, vol. 66, 1944, pp. 633–643; vol. 67, 1945, pp. 507–510.

4 "X-Ray Diffraction as a Gage for Measuring Cold Work Produced in Milling," by F. Zankl, A. G. Barkow, and A. O. Schmidt, Trans. ASME, vol. 69, 1947, pp. 307–318.

5 "Correlation of Coefficient of Friction With Drilling Torque and Thrust for Different Cutting Fluids," by A. O. Schmidt, W. W. Gilbert, and O. W. Boston, Trans. ASME, vol. 64, 1942, pp. 703–709.

Discussion

O. W. Boston.[4] The authors have employed a very ingenious means of determining the proportionate amount of heat which is absorbed by the tool, the chips, and the workpiece material when drilling a material having a diameter slightly less than that of the drill, and a hole drilled through the center of the material equal to the length of the chisel edge. In this way the cutting edges of the drill have a free cutting action. This work was started at the University of Michigan a number of years ago, at which time the objective was to determine the equivalent of the power developed at the drill point by measuring the torque and thrust, and the work done by measuring the amount of heat developed as recorded by a calorimeter. In the writer's opinion, this work was successful in that a heat-work balance was obtained within an error of 2 to 3 per cent.

The present paper is a continuation of this type of work, and it is felt that the procedure is sound and that the results, although rather limited in amount, are relatively reliable. There is a question as to the time expended in drilling up to the time of taking thermal measurements, as well as a heat loss in transferring the drill to the calorimeter, Fig. 2, for determining the heat in the tool. Care must be exercised also in evaluating temperature and heat developed.

This work confirms the general belief that the major portion of the heat generated in a metal-cutting operation is carried away by the chips. This is particularly true at high speeds, as is shown.

This paper is one of several involving studies of metal-cutting temperatures and heat developed, and it is hoped that others of this nature will follow, as they all add to our knowledge on the subject of metal cutting.

W. W. Gilbert.[5] The authors' use of a calorimeter to measure the heat in the workpiece, the chips, and the drill provides a useful tool for the thermal analysis of the cutting process. The method of conducting the drilling tests as used in these experiments should promote good accuracy, since the pilot hole eliminates the rubbing action at the point of the drill. Since the bar being drilled was smaller than the outside diameter of the drill, this also eliminates the rubbing on the margin of the drill, preventing this source variation.

Since some of the tests were run with the drill surrounded with distilled water, while other tests were run dry, some question might arise as to the effect of the cutting fluid in affecting the generation of heat. Torque and thrust dynamometers have shown there is little change in torque or thrust when using water as a cutting fluid in this type of drilling.

One statement in the paper appears to be misleading owing to the misconception of the word, "temperature." A careful differentiation should be made between temperature and heat. For instance, the statement, " . . . at the same cutting speed, a fine feed will result in higher chip, tool, and workpiece temperatures than will a heavier feed." The temperature of the cutting edge is higher for heavier feeds, but, since the time required to cut a given amount of material is shorter, the total heat going into the tool will be lower.

M. E. Merchant,[6] Michael Field,[7] Norman Zlatin.[7] The information given in this paper is important and much needed. Many people, including the writers, have felt the need for such a study, as reported here, for some time, and we wish to congratulate the authors on having carried out this useful research. The calorimeter method used is particularly well-suited to obtaining information on the distribution of heat in metal cutting.

The information resulting from this study, while important and valuable, can be somewhat misleading as presented in the paper unless certain points are emphasized or are well understood by the reader. The writers would like to discuss certain of these points. The first point is one on which insufficient information appears in the paper. In making the calorimeter test for measuring total heat generated in drilling, the cutting operation takes place under water, whereas in making the calorimeter test for measuring the heat in the chips, the cutting operation takes place in the absence of water, i.e., dry.

Earlier work in our own laboratories[8] has demonstrated that under certain conditions plain water can be a fairly effective cutting fluid in reducing tool forces and power consumption, i.e., heat generation. This is particularly true at very low cutting speeds. Since this is the case, it is possible that in the present study the results obtained in the tests made for measuring heat in the chips are not strictly comparable with those obtained in the tests made for measuring the total heat generated in drilling, particularly at the lowest cutting speeds. The way to clarify this point would be to calibrate the calorimetric apparatus with a torque-and-thrust dynamometer when cutting with the drill point submerged in water, and also when drilling dry, and so to determine what difference in power consumption, if any, is caused by the presence of the water. The tests should of course be made at very low cutting speeds. The writers would like to ask the authors whether such check tests have been run and if so what results were obtained.

The next point for discussion is one on which it appears that some clarification is needed. The calorimeter tests made by the authors measure average *heat* distribution in metal-cutting rather than actual *temperature* values; therefore statements made about chip, tool, or workpiece "temperatures" in the paper should be read with certain mental reservations. The reader should realize that the heat measurements made by the authors, when interpreted in terms of temperatures, can give only *average* temperature values; these in many cases may bear little relation to the actual physical temperatures of importance in metal cutting. For instance, the reader should realize that such statements by the authors as ". . . . a fine feed will result in higher chip, tool, and workpiece temperatures than will a heavier feed." are correct only if it is understood that the *temperatures* referred to are average temperatures.

It is well known of course that the actual temperatures at the chip-tool interface *increase* with increasing feed, which is just the opposite of the behavior of the average chip and tool temperatures mentioned in the foregoing quotation. In like manner, it is well known that the actual chip-tool interface temperatures increase rapidly with increasing cutting speed rather than remaining practically constant with speed as do the average chip and

[4] Professor of Metal Processing, Chairman, Department of Metal Processing, University of Michigan, Ann Arbor, Mich. Fellow ASME.

[5] Associate Professor, Department of Metal Processing, University of Michigan, Ann Arbor, Mich. Mem. ASME.

[6] Senior Research Physicist, The Cincinnati Milling Machine Company, Cincinnati, O. Mem. ASME.

[7] Research Engineer, The Cincinnati Milling Machine Company.

[8] "Chip Formation, Friction and High Quality Machined Surfaces," by H. Ernst and M. E. Merchant, "Surface Treatment of Metals," American Society for Metals, 1941, pp. 299–378.

tool temperatures referred to by the authors. It is these actual chip-tool interface temperatures, rather than the average chip and tool temperatures, which are responsible for such important practical considerations as the fact that tool life (in terms of time) decreases with increasing feed (except at very fine feeds) and cutting speed.

Another point which the writers believe should be emphasized is the fact that the heat measurements made by the authors are based on removing a constant amount of metal at the different cutting speeds and feeds rather than on cutting for a constant length of time at the different speeds and feeds. It is quite probable that if constant cutting time had been used as the basis of comparison, rather than a constant volume of metal removal, the average tool temperature would have increased with increasing feed and speed rather than decreasing or remaining constant as in the present tests. The trends of the average chip and workpiece temperatures should remain about the same in either case.

The final point for discussion is the paradox which is apparently raised by the findings reported in this paper. Why should the average chip temperature decrease or remain constant with increasing feed and speed while the actual chip-tool interface temperature increases with increasing feed and speed? The answer lies in the mechanism of chip formation and heat generation in metal cutting. There are two major sources generating heat in the cutting of metals.[9] In the process of chip formation, the metal is first deformed plastically in shear on a plane extending ahead of the cutting tool from the cutting edge to the surface of the workpiece. The deformation of the metal on this "shear plane" is the first major source of heat generation. This deformation forms the chip which then slides over the face of the tool, encountering frictional resistance as it slides. This frictional resistance on the tool face is the second major source of heat generation in metal-cutting. The deformation on the shear plane raises the average temperature of the chip more or less uniformly; the friction on the tool face makes the chip-tool interface temperature soar above this average value. The average temperature rise of the chip due to the deformation at the shear plane is controlled by the ratio of the length of the shear plane to the value of the feed per revolution. It is evident that this ratio would remain constant with changing feed if the angle between the shear plane and the path traveled by the cutting edge remained constant. However, it is found that this shear angle increases considerably with increasing feed.[10] As a result the average temperature rise resulting from deformation on the shear plane is less for large feeds than for small. Thus it is because the shear angle increases with increasing feed that the average chip temperature decreases with increasing feed.

On the other hand, it is evident that with a heavy feed the chip is pressed against the tool face with greater force than with a light feed. As a result, more frictional heat is generated at the chip-tool interface at high feeds than at low. It is for this reason that the chip-tool interface temperature increases with increasing feed in spite of the fact that the average chip temperature decreases.

As regards the effect of cutting speed, it has been found that the shear angle changes only slightly with normal changes in speed (except at very low cutting speeds or where negative rakes are used).[10] Therefore the average temperature rise of the chip due to deformation on the shear plane varies little if any with cutting speed. On the other hand the sliding speed of the chip over the tool face increases directly with increasing cutting speed. Thus the rate at which heat is generated at the chip-tool interface increases with increasing speed and so the temperature at that interface does likewise, despite the fact that the average chip temperature remains practically constant. Such facts as these help to resolve the apparent paradox raised by the paper.

[9] "Basic Mechanics of the Metal-Cutting Process," by M. E. Merchant, *Journal of Applied Mechanics*, Trans. ASME, vol. 66, 1944, p. A-168.

[10] "Mechanics of the Metal Cutting Process I, Orthogonal Cutting and a Type 2 Chip," by M. E. Merchant, *Journal of Applied Physics*, vol. 16, 1945, pp. 267–275.

V. Paschkis.[11] The calorimetric test used by the authors yields of course mean temperatures. If the authors' claim, that the heat losses are negligible, is correct, then the independence of the value of WTC from speed (fpm) is understandable.

However, from a heat-transfer viewpoint, the following comments may be made:

(*a*) It would be misleading to apply the findings of the experiments lasting only a few seconds to a production problem where an operation may last several minutes, and heat losses therefore would count.

(*b*) Were any experiments carried out which would show that the height of the water level in the container C (Figs. 1 and 2 of the paper) was sufficient? Heat is of course conducted in the drill A away from the cutting edge and, if the level is not high enough, part of the heat would not be measured.

(*c*) The arrangement, Fig. 3, may give erroneous results if the rubber grommet F is not thick enough to prevent heat flow from the test bar B into the water. Either experimental or mathematical proof that this source of error is negligible would be welcome.

(*d*) In the last sentence of the conclusions the authors point out the danger of tool failure by excessive temperatures. The determination of the temperature at the cutting face is extremely difficult, if not impossible. But with data as presented in this paper as a basis, the cutting-edge temperature could possibly be determined with a reasonable degree of accuracy by the electric-analogy method.

K. J. Trigger.[12] This interesting paper presents a clear picture of the heat distribution when a constant volume of metal is removed by drilling over a range of speeds and feeds. That a fine feed should increase the amount of heat in the chips, tool, and workpiece per unit volume of metal removed is consistent with both theory and practice. However, the paper contains statements which, unless interpreted properly, are apt to be misunderstood. Under the heading "Test Results" it is stated:

"Thus it may be said that at the same cutting speed, a fine feed will result in higher chip, tool, and workpiece temperatures than will a heavier feed." The writer will agree to this statement under the conditions of the tests reported, i.e., when a 1-in. length is machined from the test bar. However, it is possible that the statement may be misinterpreted to mean the effect of feed when analyzed on the basis of the rate of metal removal. In this case an entirely different picture is obtained. At constant speed the feed is a direct measure of the rate of metal removal. To illustrate this interpretation, compare the effect of feed at some constant cutting speed.

The tables at top of page 250 are derived from Fig. 4 of the paper, and compare the extremes of feed at a speed of 1500 rpm.

It is apparent that if a comparison is made upon the basis of the rate of metal removal, an increase in feed results in an increase in the amount of heat in the chips, tool, and workpiece. This is shown by the temperature rise, degrees F per minute, in which the rate of metal removal is directly proportional to the feed. On this basis the time variable in the quantity of heat transferred to

[11] Heat and Mass Flow Analyzer Laboratory, Columbia University, New York, N. Y. Mem. ASME.

[12] Professor of Mechanical Engineering, University of Illinois, Urbana, Ill. Mem. ASME.

Feed, ipr	Approx temp rise deg F when 1 in. is drilled	Time to drill 1 in. length, min	Temp rise, deg F per min
	Heat in Tool		
0.0022	1.65	0.303	5.45
0.0091	0.67	0.073	9.18
	Heat in Chips		
0.0022	4.68	0.303	15.45
0.0091	3.85	0.073	52.7
	Heat in Workpiece		
0.0022	1.59	0.303	5.25
0.0091	0.45	0.073	6.17

the chips, tool, and workpiece is eliminated. The principal factor affecting the quantity of heat involved is then the temperature at the interface of the chip and the tool. This tool-chip interface temperature, not to be confused with average chip temperature, has been found to be a function of feed at constant cutting speed.

Figs. 9 and 10 of this discussion present the results of a series of tests which compose part of an extensive investigation on tool-chip interface temperatures. Fig. 9 shows the effect of speed upon tool-chip interface temperature (denoted cutting temperature) for a range of feeds. Each cutting temperature was obtained in essentially the same total cutting time, namely, 10 sec.

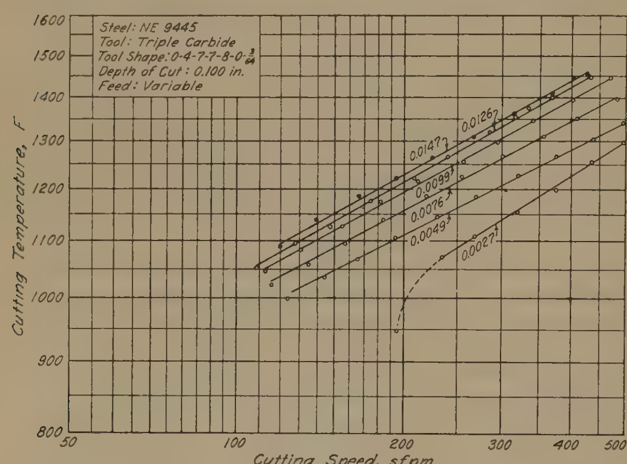

Fig. 9 Cutting Speed Versus Cutting Temperature

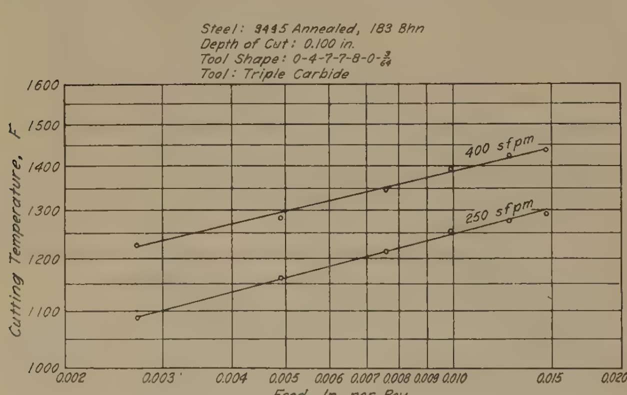

Fig. 10 Effect of Feed Upon Cutting Temperature

Fig. 10 compares the effect of feed upon cutting temperature at two cutting speeds (points obtained from Fig. 9), namely, 250 sfpm and 400 sfpm. The relationships are straight lines on logarithmic co-ordinates and of the form $T = Cf^n$ in which T = cutting temperature, deg F; C = const; f = feed in. per revolution; and n is an exponent. The equation of the lines in Fig. 10 are $T = 2013 f^{0.1038}$ and $T = 2175 f^{0.0976}$ for the 250 and 400 sfpm lines, respectively.

The interpretation of the summary statment that "thick chips mean less total work, lower tool temperatures, and lower workpiece temperatures" must then be based upon the premise of unit volume of metal removed.

Authors' Closure

All the comments appearing in the discussion are greatly appreciated. Professors Boston and Gilbert who have collaborated in a number of previous investigations of this kind must have had these tests in mind when preparing their discussions. Previous papers, listed in the Bibliography, should be taken into consideration for a clearer understanding of the foregoing report which is but one of a series.

Measurements taken with this calorimetric arrangement become more accurate with a decrease in cutting time. In order to minimize heat losses at the low cutting speeds, such as at 100 rpm, the cutting time was decreased by machining only $^1/_2$ in. of the workpiece material. The temperature values obtained in this manner were multiplied by 2 to give results equal to those which would be obtained in machining 1 in. of the test bar. This procedure was also resorted to in measuring the heat in the drill.

A number of good questions were raised and partially answered by Messrs. Merchant, Field, and Zlatin. When a cutter machines identical workpieces or cuts test bars of equal dimensions at various feeds and speeds, the distribution of the heat generated in machining one workpiece, that is, in removing specific equal amounts of material each time, will be similar to the curves illustrated in Fig. 4 of the paper. In continuous cutting for specific equal periods of time at various feeds and speeds, the distribution of heat generated will be similar to the curves shown in Fig. 11 of this closure. The values of heat in the chips and total heat, which are directly proportional to those given in Fig. 11 are to be expected since more material will be removed at the higher speeds and feeds during equal times of cutting, and hence more work will be done and more heat will be generated. The

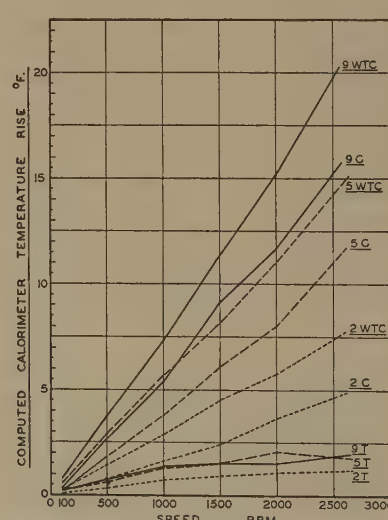

Fig. 11 Calorimeter Temperature Rise in Relation to Speed at Constant Cutting Time

(Constant cutting time = 10 sec; 9 WTC = heat in workpiece, tool, and chips at a feed of 0.0091 ipr; $9C$ = heat in chips at a feed of 0.0091 ipr; $9T$ = heat in tool at feed of 0.0091 ipr; 2 and 5 denote feeds of 0.0022 and 0.0057 ipr, respectively. Curves should be used for comparison of heat values only.)

upper six curves in Fig. 11 cannot be used directly for average temperature comparisons since different amounts of material are involved at each speed and feed.

In previous, similar tests carried out with a dynamometer (5), when using only the cutting edge of a drill to machine a tubular test bar, no measurable difference in torque or thrust at the same feeds and speeds could be discerned whether the cutting was done dry or with the drill submerged in water or other coolants. The cutting speeds and feeds used in those tests were similar to the speeds and feeds mentioned in the paper. For example, the lowest peripheral speed used in previous tests of this nature was 13 fpm, as compared to 10 fpm reported herein. Since no difference in torque or thrust, and hence no difference in work or power, could be found with a dynamometer between cutting dry and cutting with coolants, the values obtained with the calorimeter in measuring only the heat in the chips or the heat in the tool (cutting dry) should be directly comparable to those obtained in measuring the total heat (cutting under water).

Calorimeter temperature-rise values in these tests may be interpreted in terms of heat, work, power, and average temperature rise of the chips, workpiece, and tool. Average temperature rises rather than localized, instantaneous temperatures are obtained with the calorimeter since these temperatures must be determined by heat-balance computations in which the temperature gradients that exist in the chips, workpiece, and tool during cutting and for some time after do not enter or are not considered.

The actual temperature reached during the cutting operation by the tool tip itself, that is, by the cutting edge and the immediately surrounding tool material, is of primary interest because the ability of the tool edge to stand up will decrease with increasing temperatures. Frequently it has been observed from a comparison of chip-temper colors that the temperature of the chip on the side away from the tool was higher than on the side which rubs against the tool. Also, it has been observed frequently that the temper color of the chip on the rough surface away from the tool was formed before the temper color on the shiny surface which has rubbed against the tool face. This would indicate that the heat on the rough side was more intense than the heat on the shiny side and actually caused a rise in the temperature of the shiny side to a value high enough to produce a temper color after the heat had had time to flow through the width of the chip.

For example, the temper colors on chips of SAE 1020 steel, 180 Bhn, removed at a cutting speed of 450 fpm and a feed per tooth of 0.020 in. with a milling cutter having 0 deg axial rake, 6 deg negative $\times$ 0.030 in. primary and 30 deg positive secondary radial rake, and 15 deg corner angle, indicated 500 F on the rough side and 450 F on the shiny side. These temper colors may not provide an accurate method of temperature measurement under these conditions, but the comparison of chip-temper colors may be used in determining that one temperature is lower than another.

The average chip temperature, as measured with a calorimeter is therefore greater than the temperature of the chip at the tool-chip interface. At the higher cutting speeds the temperature of the chip is much lower than the temperature of the tool at the tool-chip interface. This difference in temperatures will affect the interpretation of data on tool-chip interface temperatures obtained with a tool-work thermocouple arrangement. Tool-chip interface temperatures may represent approximately the temperature of the tool but not the temperature of the chip at the tool-chip interface.

Tool life in terms of time means very little unless it is also expressed in amount of material removed or number of workpieces finished. An increase in feed per tooth (undeformed-chip thickness) generally will be accompanied by an increase in number of pieces finished before tool failure, and these pieces also will be finished in shorter time intervals. This tendency holds true until the feed per tooth (undeformed-chip thickness) becomes large enough to cause fracture of the tool or edge by virtue of excessive force. An increase in cutting speed, especially to very high values, generally will cause a decrease in tool life whether expressed in terms of time or number of pieces finished.

Because, in actual shop operations, workpieces of similar dimensions are machined, it was thought more appropriate to choose a uniform length of test bar as a standard condition of these tests rather than a uniform period of cutting time. This choice also greatly simplified the experimental setup and apparatus, test procedure, and interpretation of data.

If constant cutting time had been used as the basis of comparison, the trends of the average chip and workpiece temperature as given in this paper would remain unchanged. However, the average tool temperature would increase with increasing feed and speed as indicated by the lowest three curves in Fig. 11 herewith. This result must be expected since more chip material will rub against the tool face in a given period of time with either an increase in feed or an increase in speed.

The authors would certainly welcome an investigation by Dr. Paschkis into tool temperatures by means of an electrical analogy. It is only for purposes of accuracy of measurement that an attempt has been made to minimize heat losses. Heat losses are negligible in those cases in which the cutting speeds are high or the operation performed takes but a few seconds. Of course the amounts of heat in the chips, tool, and workpiece will be affected by heat losses over periods of time encountered in production

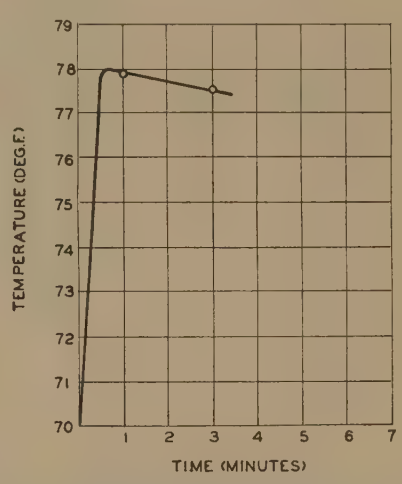

Fig. 12 Heat Loss in Calorimeter Fig. 1
(Rate of fall of temperature at 77.75 F = 0.15 deg F per min.)

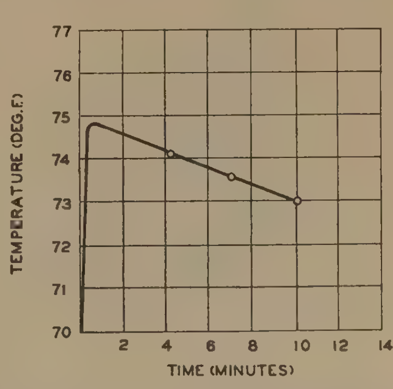

Fig. 13 Heat Loss in Calorimeter Fig. 3
(Rate of fall of temperature at 73.5 F = 0.35 deg F per min.)

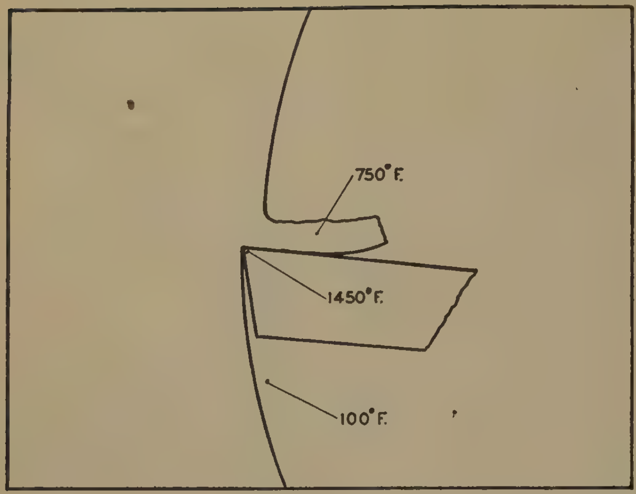

Fig. 14 Diagram of Temperatures in Steel Cutting at 400 Fpm Cutting Speed

(Temperatures of workpiece, 100 F, and chip, 750 F, taken from Fig. 5. Tool-tip temperature, 1450 F, based upon tool-chip interface temperature measurements by Trigger.)

operations, but the amounts of heat distributed to the chips, tool, and work per unit of time or per unit of volume remain fairly constant under a given set of conditions. In order to measure the maximum average temperature of the chips and the heat, work, or power absorbed by the chips, heat losses must be minimized or corrections be applied to the calorimeter data. What happens to the heat in the chips a half-minute or minute after they have been formed has little importance in the problem. However, the heat in the tool generally will increase with prolonged cutting until the tool reaches a point of balance at an elevated average temperature at which it can dissipate the heat as fast as it is acquired.

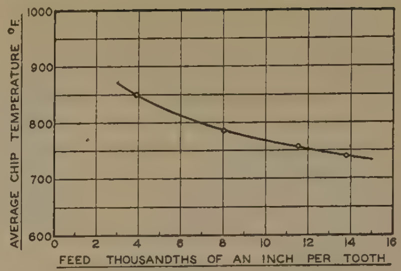

Fig. 15 Effect of Feed on Average Chip Temperature

(These chip temperatures were measured with a calorimeter when machining 1-in-diam test bars of SAE 1055, normalized steel, with a 2-in-diam face mill which had two tungsten-carbide tips of 6-deg negative radial rake. Depth of cut 0.125 in.; speed 285 fpm. The curve shown will remain approximately the same at higher speeds.)

In order to confine the heat of cutting to the lower part of the drill as much as possible, only $^1/_2$-in. length of the test bar was machined. Values obtained in this manner were multiplied by 2 to have them correspond to the rest of the data. At the low temperatures and with the short intervals of time involved no significant heat flow occurred in the test arrangement illustrated in Fig. 3 of the paper (see Figs. 12 and 13 herewith).

The discussion of Professor Trigger points out other important factors in relation to this paper. The cutting temperatures plotted in Figs. 9 and 10 of his discussion, represent, most probably, temperatures of the tool near the cutting edge. Temperature of the steel workpiece and chips measured in milling are plotted in Fig. 5 of the paper. Based upon these tests and data provided by Professor Trigger, the temperatures in a steel-cutting operation will be similar to Fig. 14 of this closure. The effect of feed upon average chip temperature is opposite in nature to the effect the feed has on the cutting-edge temperature (Fig. 10 of Professor Trigger's discussion). Typical average chip temperatures, as affected by feed are plotted in Fig. 15 herewith.

Thermal Contact Resistance of Laminated and Machined Joints

By A. W. BRUNOT[1] and FLORENCE F. BUCKLAND[2]

Values of thermal contact resistance are reported for two types of joints: (1) the joint between two blocks of laminated steel, either in direct contact or separated by cement or shims of steel, aluminum, or aluminum foil; (2) the joint between two blocks of cold-rolled steel with various surface finishes. The resistance as measured amounts to 0.3 to 8 in. of additional material, depending upon the configuration. Results are also given in terms of contact resistance.

Introduction

Some years ago the authors' company instituted a test program to determine thermal contact resistance for several types of production joints, in order to evaluate this resistance more closely for use in the calculation of the temperature rise of various components of electrical equipment. In so far as was known, work previously done by others did not cover the particular materials or surfaces in which the company was interested. The results of this program are presented in this paper.

If surfaces of two dry metal blocks are placed in contact, there remains a considerable resistance to heat flow from one block to the other, unless the surfaces are bonded together by a solid metal bond as in welding, brazing, or soldering. This thermal resistance, known as "contact resistance," is due to the dead air and sometimes also oxide layers, in the space between the surfaces. Contact resistance is present in addition to the usual thermal resistances of the materials themselves, as indicated in the thermal circuit, Fig. 1. The resistance of the contact may be

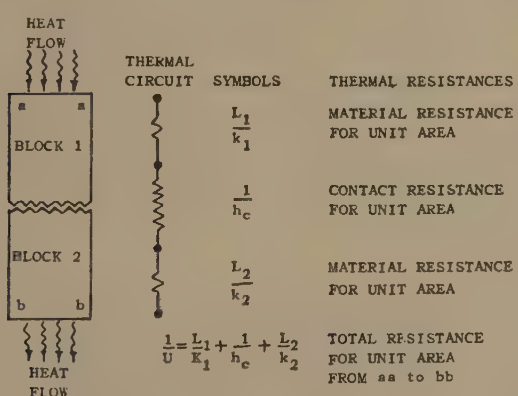

Fig. 1 Thermal Circuit for Contact Resistance

large compared with the other resistances, and should rarely be neglected.

Thermal contact resistance $1/h_c$ may vary widely, depending upon smoothness, contact pressure, and thermal conductivity of the metal and of the gas between the metal surfaces.

Types of Joints

Tests were made on joints in two types of blocks which are shown in Fig. 2. One consisted of the joint between two laminated steel blocks, each made up of packages of 25-mil sheets of silicon steel, now designated as AISI type M27. The chemical composition of a typical ladle analysis of this steel is given in terms of maximum values as follows: Si-2.5 to 3.0; C-0.10; Mn-0.5; P-0.05; S-0.05. Slots were cut in the two center laminations as shown to provide space to insert the thermocouples, and then the laminations were stacked on a flat plate and welded together. Each block had one end ground flat to fit the heater or the cooling pad. These blocks were either in direct contact or separated by cement or shims of steel, aluminum, or aluminum foil.

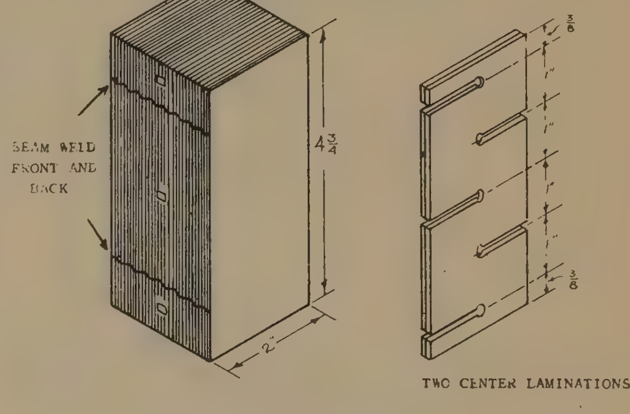

LAMINATED TEST BLOCK

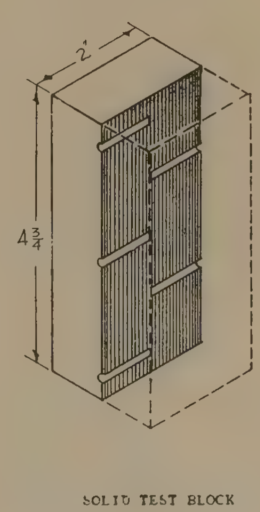

SOLID TEST BLOCK

Fig. 2 Test Blocks

[1] Thomson Laboratory, General Electric Company, West Lynn, Mass. Mem. ASME.

[2] General Engineering and Consulting Laboratory, General Electric Company, Schenectady, N. Y.

Contributed by the Heat Transfer Division and presented at the Semi-Annual Meeting, Milwaukee, Wis., May 30–June 5, 1948, of The American Society of Mechanical Engineers.

Note: Statements and opinions advanced in papers are to be understood as individual expressions of their authors and not those of the Society. Paper No. 48—SA-27.

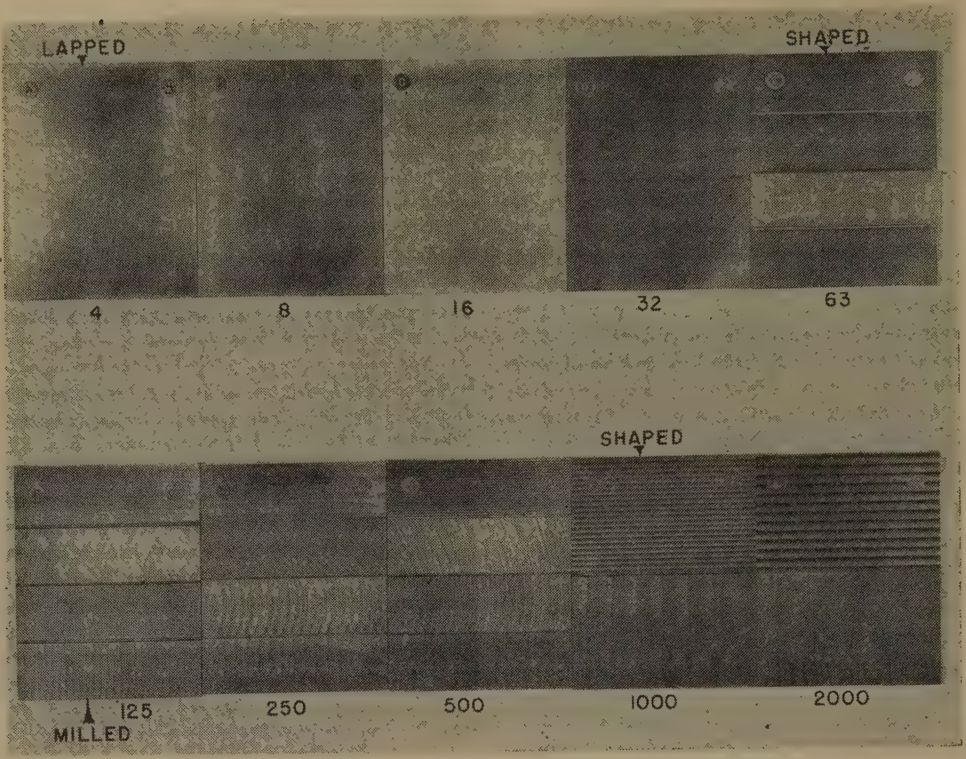

Fig. 3 Surface Finishes of Cold-Rolled Steel Specimens Tested
(Numbers refer to average roughness in microinches.)

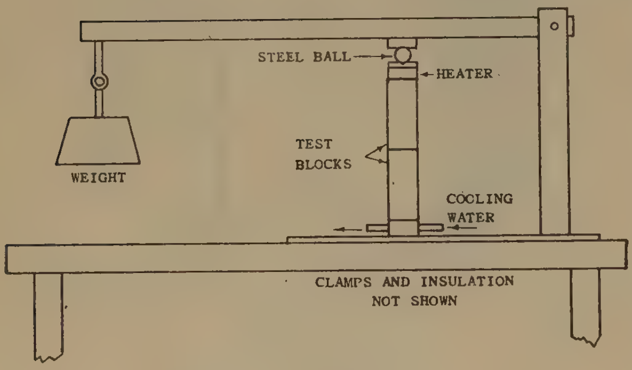

Fig. 4 Test Setup

The other tests were made on the joints between two cold-rolled steel blocks having machined surfaces in contact, with the heated and cooled ends finished as in the preceding paragraph. One way to define a machined surface finish is by "average" roughness,[3] in accordance with ASA standards. The average value of roughness is the average deviation from a center line on a profile contour of the surface, expressed in microinches. Fig. 3 indicates the surface finishes which were tested in the program. Actual roughness in microinches was not measured; the surfaces were cut to match the standard specimens.

Procedure

Copper-copnic thermocouples were soldered in the holes or slots shown in Fig. 3 to insure good thermal contact. The cold junction of the thermocouples was kept at 32 F.

The heater consisted of a copper block in which two cartridge-type heaters were embedded. This heater was supplied by a bank of storage batteries to insure a constant rate of heat generation. The cooling pad was a lead casting containing water coils through which tap water was circulated.

In order to minimize heat losses, the heater, test block, and cooling pad were all enclosed by a heavy layer of cotton waste.

The apparatus arranged for testing is shown in Fig. 4. The system was designed to keep uniform pressure between the blocks. A recess was cut in the top plate above the test blocks to insure the centering of the steel ball. The loads were varied by varying the weight on the end of the beam. The testing procedure was to set the weight, turn on the heater and the tap water, and run until a steady state had been reached. At that time, usually about 3 hr after the start of the test, the ten thermocouples were read.

Analysis

Plotted in Fig. 5 to a reduced scale, are the results of a typical test, giving the temperature distribution in the blocks as a function of distance from the heated end. The discontinuity in the curve measures the temperature drop through the joint, while the temperature gradient gives the density of heat flow. The gradients were linear and substantially equal on opposite sides of the joint, which indicates that transverse heat flow was negligible. From the plot of the data the temperature gradient at each side of the joint is determined and the average taken as the basis for calculating heat flow.

The heat flow is given by the following equation

$$q = -k\frac{dt}{dx} = -\frac{k\,\Delta t}{b} \qquad [1]$$

Rewriting this equation to obtain the equivalent length explicitly

[3] "Determining Surface Roughness," by Walter Mikelson, *Mechanical Engineering*, vol. 69, 1947, pp. 391–393.

$$b = \frac{\Delta t}{(dt)/(dx)} \quad [2]$$

The equivalent length may be expressed in terms of a contact resistance, $1/h_c$ by dividing by the conductivity, or

$$\frac{1}{h_c} = \frac{b}{k} \quad [3]$$

where

q = heat density, watts per sq in.

k = thermal conductivity of the metal, $\frac{\text{watts per sq in.}}{\text{deg C per in.}}$

$\frac{dt}{dx}$ = average temperature gradient, deg C per in.

b = equivalent length of metal, in.

Δt = temperature difference at joint, deg C

$\frac{1}{h_c}$ = thermal resistance of joint per unit area, sq in. deg C per watt

The temperature difference used in these relations is the temperature drop between the surfaces of the test blocks as determined from the curves. This temperature drop therefore represents the effect of one joint when the laminations are in direct contact, and two or more joints when shims are used.

Results of Tests

Fig. 6 shows the variation of contact resistance with pressure for laminated steel blocks in direct contact or separated by shims.

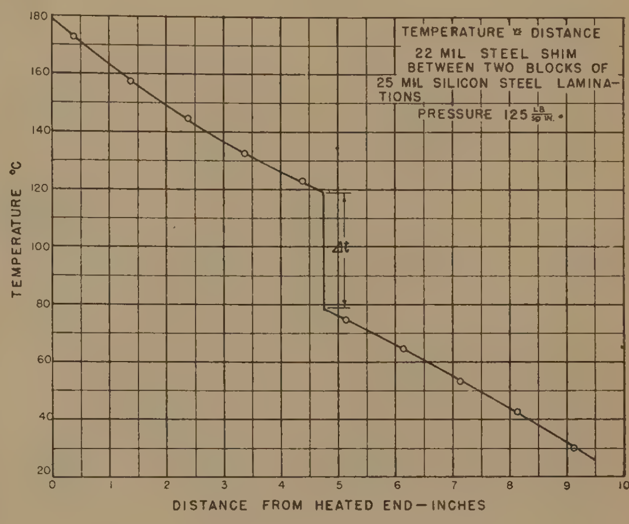

Fig. 5 Typical Test Curve

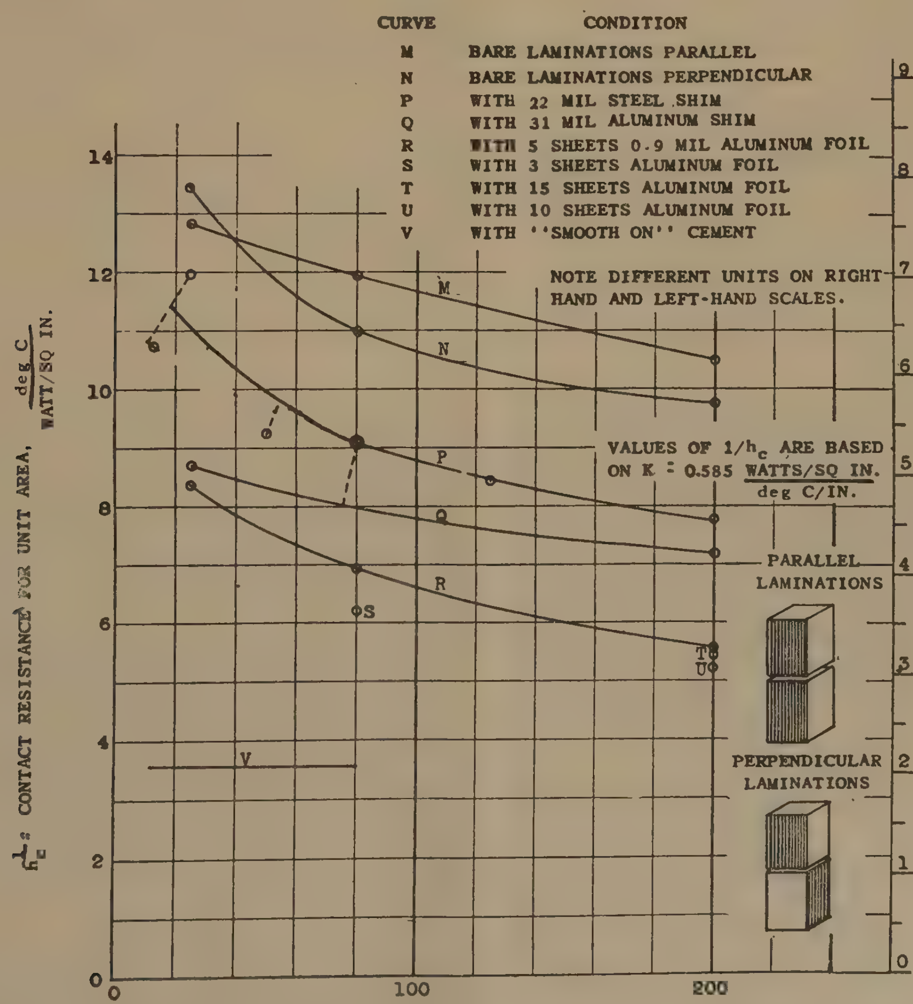

Fig. 6 Contact Resistance Versus Contact Pressure for Laminated Blocks

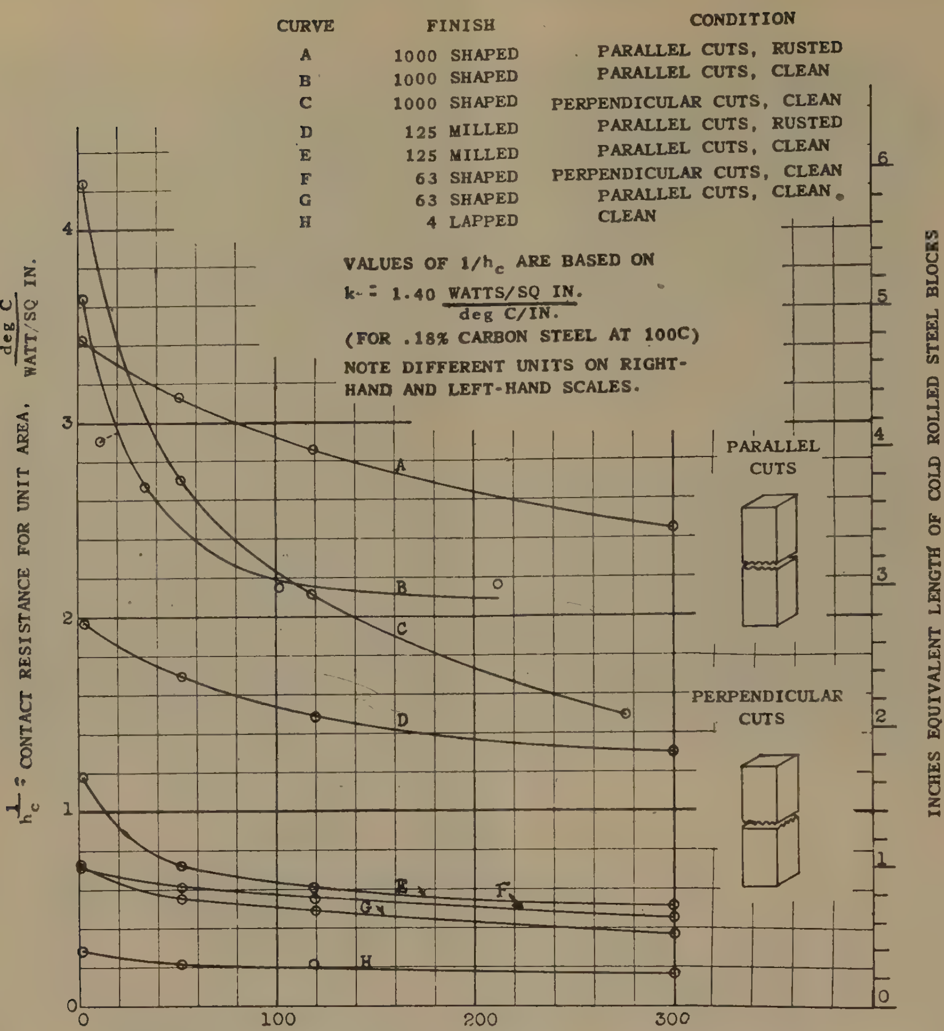

Fig. 7 Contact Resistance Versus Contact Pressure for Cold-Rolled Steel Blocks

Fig. 7 shows the variation of contact resistance with pressure for cold-rolled steel blocks with various surface finishes.

The numerical values in these two figures are obtained from the test data, using Equation [2] to calculate the equivalent length of the laminations on the steel blocks. These values are converted to the general form $1/h_c$ by using Equation [3], with $k = 0.585$ (watts per sq in.)/(deg C per in.) for 2.75 per cent silicon steel and $k = 1.40$ (watts per sq in.)/(deg C per in.) for cold-rolled steel. The values of k for silicon steel were determined in the company's laboratory. For cold-rolled steel k was obtained by interpolation for 0.18 per cent carbon steel at 100 C between the data of references.[4,5] If the results are needed in terms of Btu, hr, ft, deg F units, divide $1/h_c$ by 273 to convert to hr (sq ft) deg F/Btu.

Conclusions

The tests on laminated steel blocks indicate that if a thick metal shim is used between the two surfaces, the hardness of the shim metal has little effect. If aluminum foil is substituted, the resistance is lowered as pressure is increased. This is probably due to the fact that the laminations are embedded deeper in the foil. For more than five layers of foil the effect seems to be slight, and the resistance may be increased as the number of layers becomes large due to the resistance between the layers of foil.

The tests on solid steel blocks with various degrees of smoothness indicate that the smoother the surface the lower the resistance. This may be due to the thinner layer of air or the larger area of contact encountered. This latter idea may be substantiated by observing that the variation of resistance with pressure is greater for the rough blocks, where the pressure may make the rough spots indent the surface of the other block and thus allow more projections to come in contact.

If the gas between the surfaces is other than air, the resistance may be expected to increase or decrease, according to the greater or less resistivity of the gas, as compared with air. The effect of changing the gas has not been investigated. The amount of increase or decrease in surface resistance probably depends upon the roughness of the surface in contact as well as upon the thermal conductivity of the gas.

Acknowledgments

This paper covers the work done by J. R. Outt and W. L. Knaus using packages of laminations, and the work of B. R. Prentice and W. C. Johnson using solid steel blocks.

[4] "Thermal Conductivity of Some Irons and Steels Over the Temperature Range 100 C to 500 C," by S. M. Shelton, U. S. Bureau of Standards, *Journal of Research*, vol. 12, April, 1934, pp. 441–450.

[5] "Die Wärmeleitfähigkeit von reinem Eisen und technischen Stählen," by F. Bollenrath and W. Bungardt, *Archiv. für das Eisenhüttenwesen*, vol. 9, November, 1935, pp. 253–262.

Discussion

J. D. Keller.[6] Comparing Figs. 6 and 7 of the paper, it is interesting although not surprising that the thermal resistance of the contact between the surfaces of laminated blocks, whether the laminations are parallel or crossed, is about 5 times as great as that of even the roughest solid-block surfaces tested.

Comparing the thermal conductances in Btu per (sq ft) (hr) (deg F) for steel contact surfaces at about 212 F, and a pressure of 10 psi, with those found by Weills and Ryder[7] under the same conditions, the authors' figures are about 400 for a surface roughness of 63 microinches and 1050 for 4 microinches; whereas the Weills-Ryder values are about 200 for a surface roughness of 50 to 100 microinches and 1700 for 10 microinches, or only one half as great for the rough surfaces, but 60 per cent greater for the smooth surfaces. These discrepancies do not point to any error in either set of tests, but to variation in the character of the surface roughness not indicated by the root-mean-square roughness figures.

In the writer's opinion, it is not merely the rms roughness but more especially the height of the highest peaks of the surface above the mean level, which largely determines the thermal conductance through the air film between the surfaces. This was explained in a paper by the writer,[8] on the basis of which analysis it is probable that at least 95 per cent and likely 98 per cent of the conductance in the authors' tests was due to the air film, and only 5 per cent to 2 per cent to actual metallic contact. In view of this it would have been interesting if the authors' tests could have been repeated, first in vacuo and second with a gas of high thermal conductivity, such as hydrogen, filling the space between the contact surfaces.

Myron Tribus.[9] The contact resistance should consist essentially of three parallel resistances as shown in Fig. 8 of this discussion. A measure of the variations of R_{III} with pressure

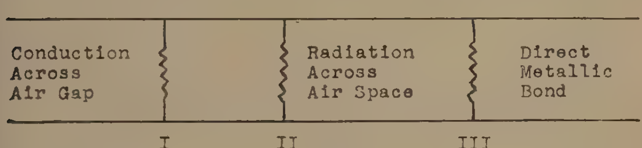

Fig. 8

can be obtained by measuring the electrical resistance simultaneously with the thermal resistance using the apparatus already designed by the authors.

As a first approximation the writer considered that perhaps R_{III} and R_{II} would be very large in comparison with R_I for, say, sample A of Fig. 7 of the paper. Therefore the contact resistance should be

$$\frac{1}{h} = \frac{2 \times \text{roughness}}{\text{conductivity of air}} = \frac{2 \times 10^{-3}}{12 \times 0.014} = 1.2 \times 10^{-2}$$

deg F (sq ft) (hr)per Btu

$$= 3.28 \text{ sq in. deg C per watt}$$

This is in general agreement with the intercepts for samples A, B, and C.

The application of the same analysis to the other samples did not produce this sort of agreement.

Authors' Closure

The comments of Messrs. Keller and Tribus help to clarify the meaning of the data presented. The variation of contact resistance with the character of the surface is seen to be substantial, and the question would seem to be whether root-mean-square roughness is a suitable criterion. The authors attempted to clarify this point in so far as these particular tests were concerned by the inclusion of a photograph of the surfaces. This indicated which particular machining, all varieties of which resulted in rms roughness of, say, 63, was used in the sample. Two other ways of evaluating the surface according to ASA standards are average peak-to-valley and maximum peak-to-valley. Each of the first two definitions give the same value for all types of machining, i.e., ground, profiled, shaped, and milled are all 63 for average, and all 220 for average peak-to-valley. The maximum peak-to-valley roughness undoubtedly would have different values for the different types of machining, and these maximum points must be the only ones in contact at the low pressures. Therefore if the data of this paper were to be used for other types of surfaces than the ones specifically described, it would be desirable to compare the maximum peak-to-valley roughness with the maximum peak-to-valley roughness of the actual kind of machining that was tested.

The concept of parallel resistances to heat flow across a contact area is extremely useful. If R_1 is defined as b/A_1k_a, R_2 as $1/h_rA$ and R_3 as $b/(k_2A_2)$, where k_a and k_2 are thermal conductivities of air and metal, respectively, A_1 and A_2 are areas not in contact and in contact, respectively, and b is average or maximum roughness, the basis of Mr. Tribus' first approximation becomes clear. His calculated value of 3.28 sq in. deg C per watt is slightly less than that shown on the curve. Since the total resistance must be less than any of the component resistances, then, in order to make the resistance across the air gap larger, the 1000 rms microinches should be replaced by some larger value corresponding to maximum peak-to-valley roughness.

Since application of Mr. Tribus' analysis to the smoother samples did not produce the same sort of agreement, it is worth while to speculate about the reason. A similar calculation for the 4-rms roughness gives 0.0131 sq in. deg C per watt. As this is only 5 per cent of the test value, it would seem that some other resistance now dominates, such as the oxide film over the entire surface. Another possibility is that the maximum peak-to-valley roughness may be far in excess of the average for these very smooth surfaces.

[6] Consulting Engineer, Pittsburgh, Pa. Mem. ASME.

[7] "Thermal Resistance Measurements of Joints Formed Between Stationary Metal Surfaces," by N. D. Weills and E. A. Ryder. Published in this issue of Trans. ASME, pp. 259 to 267.

[8] "Heat Conduction in Strip Coil Annealing," by J. D. Keller, Association of Iron and Steel Engineers, Yearbook, 1948.

[9] Research Engineer, University of California, Los Angeles, Calif. Jun. ASME.

Thermal Resistance Measurements of Joints Formed Between Stationary Metal Surfaces

By N. D. Weills[1] and E. A. Ryder[2]

Results are presented of the measurements of the thermal resistance of dry and oil-filled joints formed between two flat surfaces of various metals. Experimental apparatus consisted of two test blocks, 3 in. diam × 3 in. long, stacked axially on one another, in contact with an inductively heated copper block at one end and with a water-cooled copper block at the other, all placed between the platens of a hydraulic press. The thermal conductance of the joint formed between the two test blocks was obtained from the measured heat flow and temperature gradient through the blocks and studied as a function of temperature, pressure, and surface finish. The temperature at the joint ranged from 300 to 500 F, the thermal current across the joint from 10,000 to 130,000 Btu/(hr)(sq ft), the temperature drop across the joint from 1 to 100 F, and the pressure on the joint from 2 to 8000 psi. The thermal resistance, interpreted by analogy to the concept of electrical spreading resistance, is decreased by increasing the temperature and pressure, by the inclusion of oil, or by plating the surfaces with a soft metal.

Introduction

This paper describes experimental work conducted at the Beacon Laboratories of The Texas Company, in evaluation of the thermal resistance of joints formed between stationary metal surfaces. This work was a portion of a comprehensive program[3] conceived by Dr. Charles E. Lucke of the Mechanical Engineering Department, Columbia University, and organized by Pratt & Whitney Aircraft, to make possible the control of the metal temperatures of high-duty aircraft engines by analysis and study of the resistances to the dissipation of combustion heat. However, the thermal-resistance data reported in this paper apply equally well to all classes of machinery in which heat transfer across joints, formed between metal surfaces not in relative motion, is a factor.

Joint-Conductance Mechanism

The close analogy between thermal and electrical conduction is well known. Much study has been given to the phenomena controlling electrical resistance or conductance, in contrast to the paucity of information on the thermal resistance of joints.[4] In particular, R. Holm (1)[5,6] has published a large amount of experimental and qualitative theoretical material which forms a good foundation for the explanation of the behavior of the electrical properties of metallic contacts. The concept of spreading resistance developed through study of the electrical contacts has been adapted for the interpretation of the behavior of the resistance presented by a joint between flat surfaces in a thermal circuit.

In these experimental measurements the thermal conductance of the joints was observed primarily as a function of the pressure or load on the joint. It is possible, at sufficiently high pressures, or for sufficiently smooth and flat surfaces, for the entire surface area of each end face to be in contact with that of the other. The resistance of the joint then would be zero. At usual pressures, however, these faces are in contact over only a fraction of their total area. This total contact area is made up of the sum of a large number of separate small contact areas distributed more or less uniformly over the surface of each face in a manner depending upon the roughness and flatness of the surfaces. When it is assumed that air fills the "void" spaces, the dominant flow of heat across the joint is through these contact areas, due to the high resistance offered by the parallel path through the air, whose thermal conductivity is about one thousandth that of the metal. The resistance to the flow of heat is thus mainly associated with the metal-to-metal contacts, and can be discussed simply by use of the concept of spreading resistance.

As shown schematically in Fig. 1, the term "spreading resistance," or "spreading conductance," expresses the concept

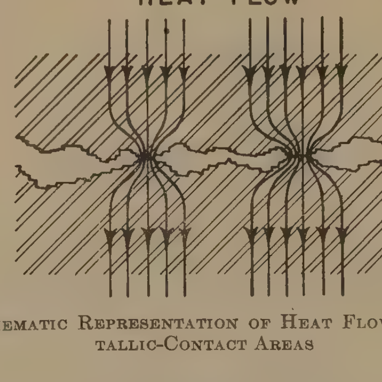

Fig. 1 Schematic Representation of Heat Flow Across Metallic-Contact Areas

that the lines of flow of heat must fan or spread out after passing through a contact area which is smaller in size than the boundaries of the solids in contact. It is a measure of the fact that not all of the volume of the solids in contact is equally available for the conduction or flow of heat.

A calculation has been performed[7] in which the spreading conductance of a contact was derived in the idealized case, in which the contact area is a circle centered in the lower contact surface of a right circular cylinder. It was possible to calculate the change in the spreading conductance, or what is the same thing, the joint conductance, if one neglects the effect of air in the region not in

---

[1] Chemical Engineer, Beacon Laboratories, The Texas Company, Beacon, N. Y. Present address, Cornell Aeronautical Laboratory, Inc., Buffalo, N. Y.

[2] Consulting Engineer, Pratt and Whitney Aircraft, East Hartford, Conn.

[3] The results of one phase of this work have been published: "Heat Transfer From a Baffled-Finned Cylinder to Air," A. W. Lemmon, Jr., A. P. Colburn, and H. B. Nottage, Trans. ASME, vol. 67, 1945, pp. 601–612.

[4] Reference (9)[5] was the only one found which was concerned with the study of the thermal resistance of metallic contacts.

[5] Numbers in parentheses refer to the Bibliography at the end of the paper.

[6] Also reference (2).

Contributed by the Heat Transfer Division and presented at the Semi-Annual Meeting, Milwaukee, Wis., May 30–June 5, 1948, of The American Society of Mechanical Engineers.

Note: Statements and opinions advanced in papers are to be understood as individual expressions of their authors and not those of the Society. Paper No. 48—SA-43.

[7] L. C. Roess, personal communication.

contact, in this ideal case as a function of the relative area of the contact region and the boundary cylinder. Since the area in metallic contact is directly proportional to the load during plastic deformation and to the two-thirds power of the load during elastic deformation (3), the variation of the joint or spreading conductance of this ideal type of joint with contact area, and thus with pressure, can then be used as a basis for thinking about the way in which the conductance of the actual joint, composed of many contact regions which are neither circular nor surrounded by circular boundary cylinders, can be expected to vary as the load is changed. Qualitatively, the general trend of the spreading conductance with pressure for the ideal case agrees with the experimental curves to be discussed.[8]

The presence of a film of oxide or other foreign material of low thermal conductivity could contribute to the thermal resistance of the joint (1). However, calculations show that except at very low pressures the oxide resistance appears to account for only a small part of the total resistance.

Experimental Apparatus and Procedure

Apparatus. The experimental apparatus used most in this investigation is shown in Fig. 2. The test gap was formed between the end faces of two 3-in-diam × 3-in-long metal bars or blocks, D and E. Heat was supplied to the test blocks from a copper heater block C, inductively heated in a high-frequency electromagnetic field. Removal of the heat flowing across the test gap was accomplished in a copper coolant block F. Through this block water flowed at a controlled rate, and inlet temperature, approximately room temperature, in a closed system containing a rotary pump and a heat exchanger. The flow of heat was determined from the measurements of the rate of coolant-water flow and its temperature increase. The latter measurement was made with the aid of a multijunction differential thermocouple, which was a composite of ten differential copper-constantan elements in series and was accurately calibrated by two Beckmann thermometers.

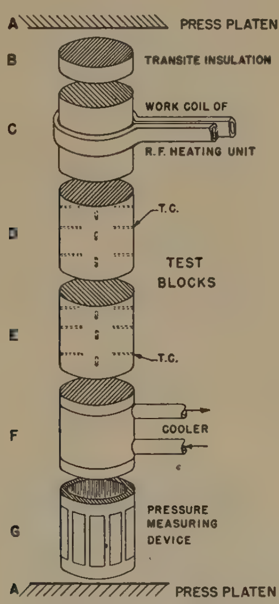

Fig. 2 Test Apparatus

The assembly of blocks stacked axially on one another, with the addition of transite insulation B above the heater block, and a pressure-measuring device G below the coolant block, was placed between the platens A of a 100-ton hydraulic press which permitted pressures on the test gap as high as 25,000 psi. A precision Bourdon-tube gage indicated hydraulic pressures corresponding to pressures on the blocks greater than 1000 psi. Below 1000 psi, the pressure required to overcome the friction of the press ram made it necessary to use an independent measuring device in this region. This pressure-measuring device consisted of a hollow aluminum cylinder on which were mounted wire strain gages arranged in a simple bridge circuit. The test blocks were insulated by a layer of glass wool about 1 in. thick and covered with a shell of Foamglas which was 2 in. thick.

An earlier test apparatus used only at very low pressures (2 to 150 psi) was similar to the one just described with the exception that heat was supplied from a calrod cast in a copper block, and pressure was applied through a simple lever system.

Thermocouple Technique. Temperatures at chosen locations in the test blocks were measured with iron-constantan thermocouples placed in small holes (0.04 to 0.06 in. diam) drilled radially to a depth of $^3/_4$ in. to 1 in. The use of small wires (B & S gage Nos. 28 and 30) reduced conduction errors. A copper dental cement served as a heat conductor and secured the thermocouples in the holes. This thermocouple technique[9] and the measurements of thermocouple locations with a traveling microscope permitted the measurement of the temperature gradient through the test blocks with a precision of about 1 per cent.

Temperature Gradient. In each test block, the thermocouples were located in axial rows of three to four thermocouples. In the early apparatus, two rows of thermocouples diametrically opposite were installed. In the induction-heated apparatus it was necessary to include two more rows of thermocouples making four in all, spaced 90 deg apart, to average out the effect of asymmetrical heat flow caused by the inability to get precise central loading.

From the temperature and the measured location of each junction, the temperature gradient in each test block was determined by the method of least squares. In all cases the gradient was found to be linear in the region of the test gap, indicating no measurable radial heat flow which would cause warping of the surfaces bounding the joint.

Thermal Conductance. The temperature at each surface bounding the joint was determined by extrapolating the temperature-distance curve, as shown in Fig. 3. The thermal conductance of the gap then was calculated from the following expression

$$h = (q/A)/\Delta t \qquad [1]$$

where q/A is the thermal current or heat flow per unit cross section of area expressed in Btu/(hr)(sq ft), and Δt is the temperature drop across the gap in deg F.

Metal Surfaces. The metals used are described in Table 1. The test surfaces were ground in one of two roughness ranges, 10 microinches (rms) was considered smooth and 50 to 100 microinches (rms) was chosen as the range for a rough surface. Roughness measurements were made either with a profilometer or a Brush surface analyzer.

The flatness of the surfaces was checked by comparison with a standard surface plate, and was found to be within the accuracy of the dial gage employed or ± 0.0001 in.

Experimental Procedure. Before testing freshly ground blocks the test surfaces were pressed together at room temperature under the maximum anticipated load as a preliminary treatment designed to smooth out unusual high spots on the surfaces which

[8] A more complete discussion of the spreading-resistance concept, as used in the interpretation of the experimental data, is beyond the scope of this paper.

[9] Developed by Dr. H. D. Baker of Columbia University.

TABLE 1 DESIGNATION, CHEMICAL COMPOSITION, HARDNESS, AND APPLICATION OF AIRCRAFT-ENGINE METALS TESTED

Metal	No.	Alcoa no.	AMS no.	SAE no.	C	Mn	P	S	Ni	Cr	Si	Mo	Fe	Cu	Mg	Zn	Sn	Pb	Hardness[a]	Application
Steel	..	..	..	4140	0.43	0.82	0.015	0.022	0.08	1.05	0.21	0.17	..	..	..	..	..	..	370	Cylinder barrel
Aluminum	1	A-51-S	4125-A	..	..	..	..	..	..	0.26	0.82	..	0.27	0.1	0.65	..	..	..	50	Forged muffs
Aluminum	2	18-S	...	..	..	0.2	..	..	1.78	0.1	0.40	..	0.46	4.41	0.63	0.25	..	..	90	Forged heads
Aluminum	3	32-S	4145-A	..	..	..	..	..	0.83	..	12.31	..	0.62	0.96	1.03	..	..	..	..	Forged piston
Aluminum	4	142-T61	..	..	..	..	..	..	2.0	..	0.39	..	..	4.9	1.05	..	..	..	..	Cast heads
Aluminum	5	17-S	4030-A	..	..	0.5	..	..	..	..	..	..	..	4.0	0.5	..	..	..	..	..
Bronze	..	..	4846	..	..	..	0.05	...	..	..	..	..	0.65	84–89	..	1–3	9–13.5	1	110	Valve guides

[a] Numbers from Shore monotron hardness indicator.

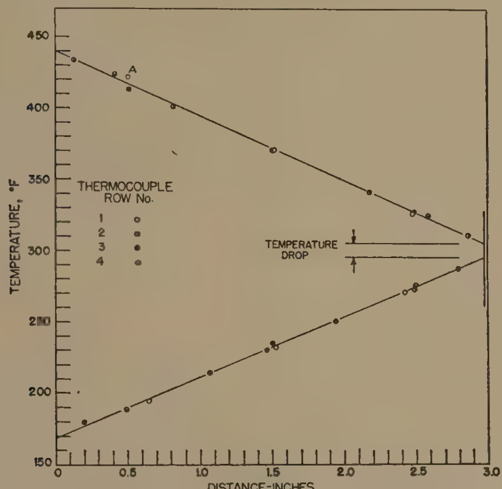

Fig. 3 Typical Temperature-Distance Gradients Through Test Blocks

would produce an abnormally high resistance. Following this pretreatment, the test surfaces were cleaned with an organic solvent and placed together to form the joint. After applying a light load, the test joint was brought up to a predetermined steady temperature, and measurements of temperature, heat flow, and pressure were recorded. Without disturbing the test joint and while maintaining the temperature, the pressure was increased by definite increments, and the recording of measurements repeated after each increase of pressure. On occasions measurements were made likewise upon successively decreasing the pressure without disturbing the joint, but normally the joint was broken following the highest pressure reading, and the sequence of measurements repeated starting again at low pressure. The second and subsequent assemblies of the same joint provide the mating surfaces with new areas of metal contact as no provision or attempt was made to match the surfaces in the same way twice.

Roughness measurements, following the room-temperature pretreatment, indicated a maximum smoothing of the surfaces of about 20 per cent. An additional decrease in roughness was usually found following normal operation at the test temperature. In the data which follow, the roughness values recorded are those measured just prior to the initial conductance measurements of a given joint.

Precision of Measurements. The errors associated with the experimental measurement of temperature, thermocouple location, thermal current, and pressure are small compared with the variation due to asymmetrical heat flow caused by not having perfectly uniform loading over the cross section of all the joints and the variations due to changes in the metals themselves. The effects of asymmetrical heat flow are noted in Fig. 3 which shows typical temperature-distance curves through the test blocks and the temperature drop across the joint. The individual temperature points shown on the curves are classified according to the axial thermocouple rows in each block. Although in one instance, the highest point in row No. 1 (point A), the experimental temperature deviates as much as 5 deg F from the mean linear least-squares line, this same point varies only 0.5 deg F from the mean of the measurements in its row. Evidently the heat flow is nearly constant in any one axial path but varies somewhat from point to point over the joint area. These data, which show the asymmetrical heat flow to be more pronounced near the heater, were taken at 70 psi. At higher pressures all four rows agree much better with the mean curve.

The standard error in the thermal conductance of the joint is related to that of the thermal current and that of the temperature drop across the joint as follows

$$\left(\frac{\sigma_h}{h}\right)^2 = \left(\frac{\sigma_{q/A}}{q/A}\right)^2 + \left(\frac{\sigma_{\Delta t}}{\Delta t}\right)^2 \ldots\ldots\ldots\ldots [2]$$

The extrapolation to the test-joint surface of each block produces a standard error in the temperature drop of about 2 deg F. The standard error in the thermal conductivity of the test blocks, to which the temperature gradients are inversely proportional, is less than 4 per cent. The estimated standard error in the thermal current is 2 per cent.

The experimental measurements which are presented in the next section show large differences depending upon the metal or the conditions at the joint. These differences, although they remain for the most part unexplained, are definitely outside the range of the standard error in the thermal conductance, based upon the precision of the experimental measurements.

Equivalent Thickness of Aluminum. To help in visualizing the scale of conductance values, a quantity D_0, called the equivalent thickness of aluminum, is introduced. This is the thickness of aluminum which would present to the flow of heat a resistance equivalent to that of the joint having a given thermal conductance, the aluminum having the same area as the joint. It seems reasonable that a joint having a D_0 value less than 0.25 in. will have little effect on heat flow in an engine. This represents a conductance of 5600 Btu/(hr)(sq ft)(deg F) and is indicated on some of the figures giving experimental data.

Experimental Results

Low-Pressure Data. In Figs. 4(a) and 4(b) are shown curves of the measured joint thermal conductance versus pressure for joints formed between surfaces of steel and No. 1 aluminum. The measurements were made with the low-pressure apparatus and extend only to about 100 psi. In the region below about 10 psi, the conductance varies with a power of the pressure which is less than unity, while beyond this pressure the experimental curves are essentially linear up to the maximum pressure reached.

An estimate of the area in metal contact at about 10 psi indicated that less than 1 per cent, and possibly even less than 0.1 per cent, of the total area is actually in metallic contact. This

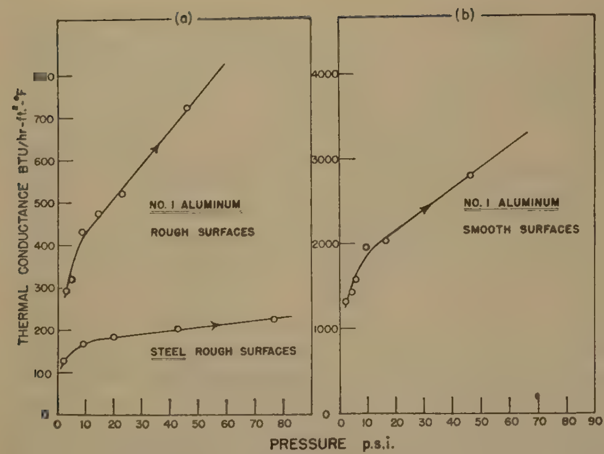

FIG. 4 TYPICAL DRY-JOINT THERMAL-CONDUCTANCE DATA OBTAINED AT LOW PRESSURE

small contact area suggests that the dominant thermal conductor in this pressure region is the air in the void space. This conclusion is further supported in the later discussion of the effect of surface roughness and type of metal on the conductance in this region. The shape of these curves may then be due to the decrease, with increase of pressure, in the proportion of heat flowing across the void space, becoming small relative to that through the metal contacts somewhere in the beginning of the linear region.

High-Pressure Data. In the pressure region beyond 10 psi there is no doubt that the larger fraction of heat flows through the metal-contact areas. The experimental conductance versus pressure curves follow the pattern predicted by the spreading-resistance concept when the area of metal contact is proportional to the pressure, i.e., when plastic flow pertains. Plastic flow was realized since the experimental h versus P curve, measured on increasing the load on a given joint, was not reproduced when the load on the undisturbed joint was then decreased. This latter curve was always higher than the loading curve. Likewise the marking of one surface by another at the areas of metal contact was observed and noted to be uniformly distributed over most of the surface.

Experimental curves of thermal conductance versus pressure representing joints formed between clean dry surfaces and measured with the induction-heated apparatus are shown in Fig. 5. In Fig. 5(a) are shown curves for joints between smooth and rough surfaces of steel at mean temperatures at the joint of 300 and 500 F. The curve of the rough joint at 300 F represents the mean of several different assemblies of the joint, measurements having been made only with increasing pressure as indicated by the arrow. The experimental points fell very near the mean line which is linear up to the maximum pressure of 8000 psi. In this sense this curve is said to be reproducible. At 500 F, the rough-joint curve is parallel to and somewhat higher than the preceding curve. Again this curve was reproducible.

The slope of the smooth-joint curves is steeper, reflecting a larger contact area. A mean curve for this joint at 300 F is shown bisecting the hatched area, which is bounded by two experimental curves each representing a different assembly of the joint. The dotted curves, bracketing the mean line, show the limit of the standard error in the thermal conductance represented by the mean line. Since the experimental curves are within the scope of the dotted lines, their differences are believed to be due only to experimental uncertainty. The curve at 500 F represents only one assembly, but with more measurements a similar spread would be expected.

Figs. 5(b) and (c) show thermal conductance-pressure curves for smooth and rough surfaces of No. 1 aluminum at 300 and 500 F, respectively. Again, the hatched area shows the spread in the experimental curves, each representing a new assembly of the joint. The expected experimental error (dotted lines) is much less with aluminum than with steel for a given thermal conductance and joint temperature. To establish the same joint temperature for aluminum as for steel, more heat must flow through the test blocks, so that the temperature drop across the joint is greater and more accurately measurable. For aluminum, the estimated experimental error does not begin to account for the difference between the curves. This difference is rather small at about 10 psi and increases with pressure. Although the reason for this difference is not understood thoroughly, it is believed to be associated with changes in the condition of the metal surfaces bounding the joint. It is expected that the aluminum contact areas would deform plastically by different

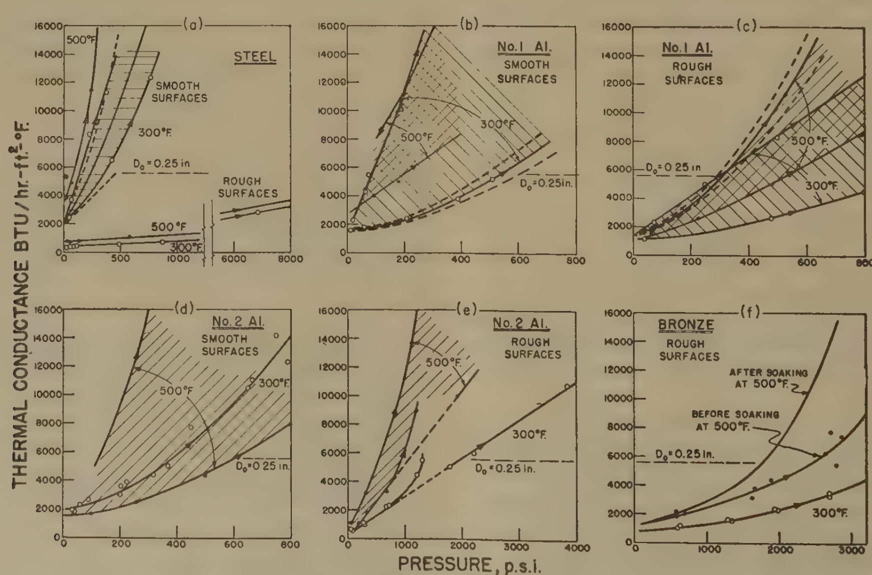

FIG. 5 TYPICAL DRY-JOINT THERMAL-CONDUCTANCE DATA FOR ROUGH AND SMOOTH SURFACES OF STEEL, ALUMINUM, AND BRONZE

amounts, depending upon the degree of previous work-hardening, crystal growth, and degree of resoftening.

Fig. 5(*d*) shows experimental curves for a joint formed between smooth surfaces of No. 2 aluminum. The curve at 300 F is reproducible within experimental error, but at 500 F there is a large spread in the data similar to that observed with the No. 1 aluminum. A similar effect is noted in Fig. 5(*e*) which represents a joint formed between rough surfaces of No. 2 aluminum. An additional contribution to the surface-condition error of these curves may be changes in hardness due to precipitation or solution of copper which is a constituent of the No. 2 alloy.

With the rough joint anomalous results were obtained in the region from 1000 to 2000 psi. An attempt was made to trace in detail the shape of the curve in the irregularity, but reproducibility was not obtained. The results of these measurements, which were all made without breaking the joint, are shown in Fig. 6. The letters refer to the sequence in which each curve was obtained, the arrows to the direction of pressure, and the dotted lines serve to connect each curve. This irregularity was likewise observed for the same joint filled with oil as will be shown.

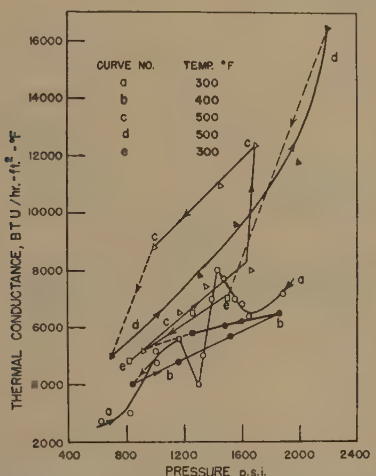

Fig. 6 Detailed Study of Irregularity in Thermal Conductance of Joint Formed Between Rough Surfaces of No. 2 Aluminum
[See Fig. 5(*e*).]

Fig. 5(*f*) shows reproducible curves at 300 F and 500 F, for joints formed between rough surfaces of bronze, measured in the usual way. However, when a given load was allowed to remain on the joint for a time at 500 F, the thermal conductance increased markedly, approaching a nearly constant value after about 5 hr. The upper curve represents a line drawn through the final mean of the conductance values, obtained by soaking at each of several pressures and at 500 F. The change with time is attributed to creep of the metal-contact areas. No attempt was made to measure the change of conductance of this joint during soaking at 300 F. Soaking the No. 2 aluminum at 500 F, and at several low pressures, revealed no measurable change of conductance during periods up to 6 hr.

Temperature. It will be noted that the curves in Fig. 5, which represent the conductance of the joints at 500 F, generally are higher than the corresponding curves at 300 F. This is particularly true at low pressures of the order of 10 psi, where reproducibility is best. Table 2 compares the conductance values for each joint at 500 F with those at 300 F at this low pressure. The average ratio of the conductance at 500 F to that at 300 F is 1.5.

It was suggested that at low pressures the dominant flow of heat was across the void space which was presumed to be filled with air. Here the thermal conductance of the joint is proportional to the thermal conductivity of air, and inversely proportional to the thickness of the void space. The thermal conductivity of air increases by 20 per cent with increase in temperature from 300 to 500 F.[10]

At a given pressure the thickness of the void space should be a function of the modulus of elasticity or hardness of the metal depending upon whether elastic or plastic deformation is considered. Upon increasing the temperature from 300 to 500 F, these quantities are reduced in a ratio of 1.4 for the elastic modulus (5), and 1.8 for hardness (6), which is in general agreement with the conductance measurement.

At the higher pressures, where the dominant heat flow is through the metallic contacts, the decrease in hardness should tend to increase the contact area and therefore to increase the joint conductance.

In Fig. 7 are shown curves of conductance versus the mean temperature of the joint at 10 psi. It is noted that the roughness of the surfaces appears to influence the relation between the conductance and temperature.

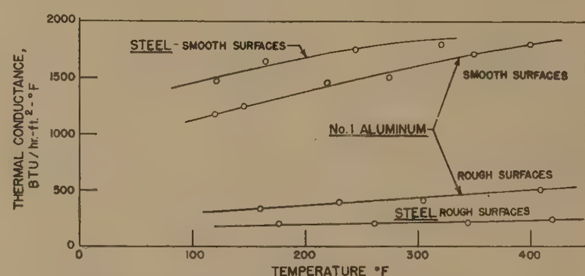

Fig. 7 Effect of Temperature on Conductance of Dry Joint at 10 Psi

Metal. The thermal conductance of a joint is also influenced by the kind of metal forming the joint. It may be shown that the slopes of conductance-pressure curves, each representing a different metal at a similar roughness and at the same mean temperature, increase in the same sequence as the hardness values shown in Table 1.

Hysteresis. When a joint is loaded progressively and then unloaded without being disturbed, the thermal conductance, observed upon increasing the load, is not reproduced upon unloading. The conductance on the unloading portion of the cycle is always higher than that obtained on loading. Examples are given in Fig. 8. The loops *a*, *b*, and *c* in Fig. 8(*a*) were measured in sequence without disturbing the joint. Since curve *c* at 500 F is higher than the curves representing this temperature shown in Fig. 5(*f*), some smoothing of the joint surfaces probably occurred at 300 F, producing a better fit for this measurement at 500 F.

Two different assemblies of the aluminum-steel joint are represented in Fig. 8(*b*). The difference in the curves is characteristic of the behavior observed previously for the No. 1 aluminum.

The steel-steel joint shown in Fig. 8(*c*) represents only one assembly of the joint, the pressures being increased successively, then decreased several times without disturbing the joint. After the initial loading of this joint, the curves are reproduced tolerably well. These curves indicate that the metal-contact areas behave elastically, following an initial plastic deformation.

Surface Roughness. A rough correlation showing the dependency of the conductance upon surface roughness is given in Fig. 9 for joints formed between dry surfaces at 300 F and at 10 psi.

[10] Reference (4), p. 391.

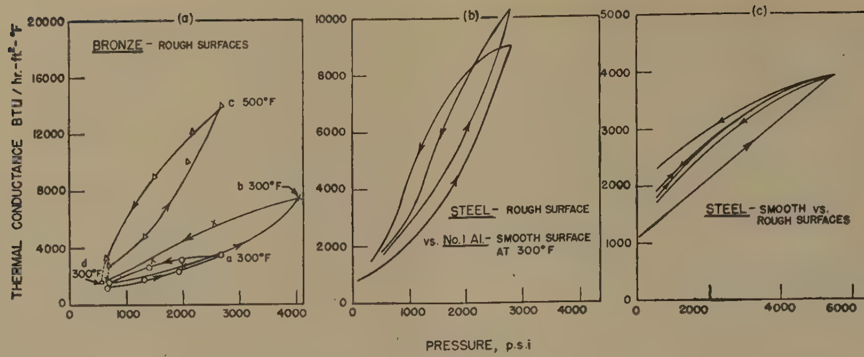

Fig. 8 Hysteresislike Variation of Thermal Conductance With Pressure

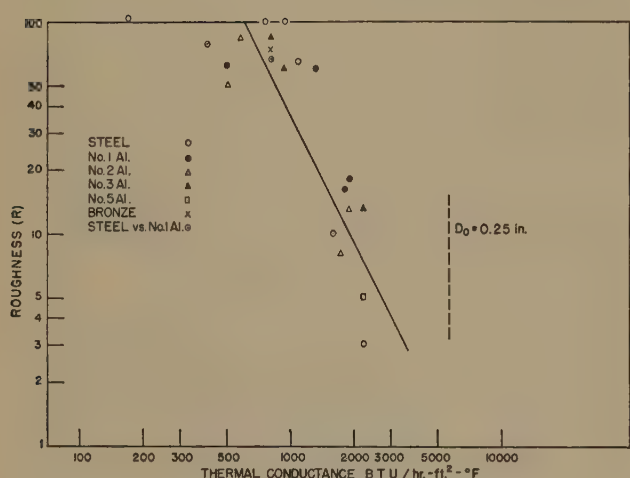

Fig. 9 Effect of Surface Roughness on Conductance of Dry Joints at 300 F and 10 Psi

$\left(R = \sqrt{\dfrac{R_1^2 + R_2^2}{2}}\right.$ where R_1 and R_2 represent roughness of bounding surfaces in rms microinches.$\Big)$

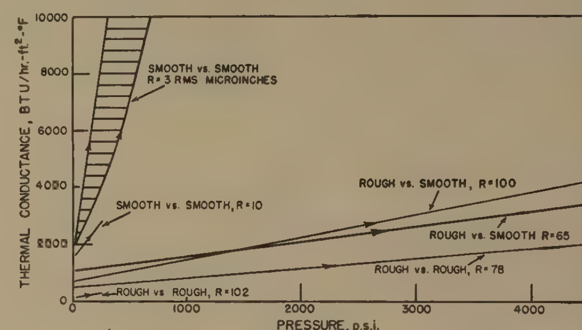

Fig. 10 Effect of Roughness on Conductance of Dry Steel Surfaces Bounding Joint at 300 F

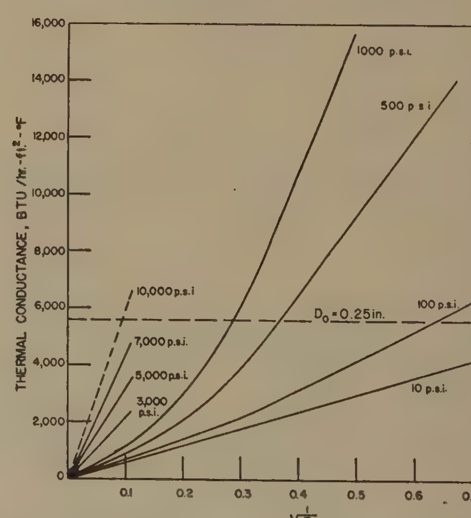

Fig. 11 Approximate Correlation Between Conductance, Roughness, and Pressure for Dry Steel Joints at 300 F

Although the spread of the data is rather large, it is not as great as would be expected if the dominant flow of heat at this pressure were across the metallic contacts. The thermal conductivity, to which the spreading conductance is proportional, of aluminum is 4 to 5 times that of steel, and its hardness, to which the conductance is inversely proportional, is about one third that of steel. Thus at a given roughness, the conductance of aluminum could be of the order of 10 to 15 times that of steel. As the spread of the data is not this large, it is assumed that the dominant conductor under these conditions is the air-filled space. A similar plot (not included) for higher pressure showed large differences between the conductance of steel and aluminum.

Likewise, the spread of the data in Fig. 9 is evidence that a measure of the roughness does not fully describe a joint formed between any one metal. This is brought out in Fig. 10 which shows curves of joints formed between surfaces of the same steel at 300 F, produced by a similar surface-grinding operation. Marked inconsistency is shown. Despite this, an approximate correlation between the conductance, roughness, and pressure at 300 F for dry joints formed between steel surfaces, taken from Figs. 9 and 10, is shown in Fig. 11. The uncertainty in the values is large, but the trend is clearly indicated.

Oil-Filled Joints. The thermal conductance of oil-filled joints, measured in the same way as the dry joints, was found to be a function of both the pressure and the temperature, as shown in Fig. 12.[11] In Fig. 12(*a*), the rate of change of the slope of the curve is small down to pressures as low as 2 to 3 psi, in contrast to the observation with the dry joint, Fig. 4, in which an abrupt change in curve shape occurred at about 10 psi. The behavior of these curves at high pressure is shown in Figs. 12(*b*) and 12(*c*).

Where oil instead of air fills the void spaces in the joint, more heat flows across the oil-filled areas and less across the metal contacts than in the dry joint. The proportion of the heat flowing through the oil decreases with increase in pressure and metallic

[11] No retaining sleeve was placed around the joint in these measurements.

TABLE 2 COMPARISONS OF THERMAL-CONDUCTANCE MEASUREMENTS AT 10 PSI

	Joint	Surface roughness—rms, microinches: Surface 1	Surface 2	Mean	Thermal conductance, Btu/(hr) (sq ft) (deg F): Dry 300 F	Dry 500 F	Dry 500 F / Dry 300 F	Oil 300 F	Oil 300 F / Dry 300 F
Steel	Smooth vs. smooth surfaces	3	3	3	2200	3600	1.6		
	Rough vs. rough surfaces	70	85	78	400	800	2.0	1350	3.4
No. 1 Aluminum	Smooth vs. smooth surfaces	16	17	16	1800	3500	1.9		
	Rough vs. rough surfaces	60	60	60	1300	1500	1.2	2000	1.5
No. 2 Aluminum	Smooth vs. smooth surfaces	15	10	13	1900	2500	1.3		
	Rough vs. rough surfaces	50	50	50	500	650	1.3	1600	3.2
Bronze	Rough vs. rough surfaces	70	80	75	800	1200	1.5	1200	1.5
No. 1 Aluminum	Smooth surface vs. rough steel surface	15	90	66	800	..	...	1600	2.0
						Average	1.5	..	2.3

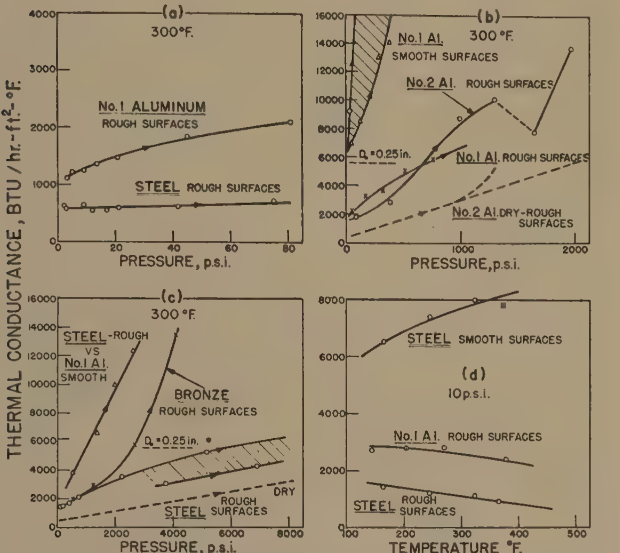

Fig. 12 Typical Oil-Filled-Joint Thermal-Conductance Data for Rough and Smooth Surfaces of Steel, Aluminum, and Bronze

contact area up to a point beyond which the flow of heat is predominantly through the metal.

The joint formed between rough surfaces of bronze is most characteristic. Here the flow of heat across the oil can be said to dominate up to about 2000 psi. Beyond this pressure the contact areas control, producing a curve of shape similar to that of the corresponding dry joint. The experimental curves, representing rough surfaces of steel, show that the conductance of oil-filled joints is not so easily reproduced as that of dry joints. Again the irregularity characteristic of the No. 2 aluminum dry joint is present in the oil-filled-joint curve.

Continued soaking at 500 F of an oil-filled, rough, steel-steel joint caused some decomposition of the oil which lowered the conductance progressively.

The effect of temperature on the conductance of an oil-filled joint at low pressure is shown in Fig. 12(*d*). The inconsistency in general slope of these curves is unexplained.

Table 2 shows the conductance of oil-filled joints to be about twice that of dry joints at 10 psi and 300 F. The effect of the oil is also noted in Figs. 12(*b*) and 12(*c*), where both dry and oil-filled-joint curves are compared.

Thermal Conductivity of Oil. Although Texaco AEO-120 oil was used exclusively in this investigation, thermal conductivity and other measurements were made on a wide variety of commercial aviation oils. Table 3 shows that little difference in thermal conductance of joints filled with different oils would be expected.

Insertion of Soft Metal in Joint. A rough-surfaced steel disk, 0.23 in. thick and plated with a thin layer of copper,[12] was inserted in the joint between two steel surfaces. Without disturbing the joint, successive conductance measurements were made at increasing and then decreasing pressures. Conductance values, corrected to represent only one joint and taken both before and after copper-plating the disk, are shown in Fig. 13. Qualitatively, the increased conductance following copper-plating is to be expected.

[12] The copper-plating was done through the courtesy of Thompson Products, Inc.

TABLE 3 PROPERTIES OF COMMERCIAL AIRPLANE-ENGINE OILS

Number of oil	Temp, deg C	Thermal conductivity,[a] Cal/cm²-sec (deg C/cm), divide nos. by 10^6	Specific gravity, 60 F/60 F	Viscosity in Saybolt sec at 100 F	210 F	Viscosity index
1	50	381	0.8838	1560	120.4	103
	90	374				
2	50	360	0.8916	1574	117.3	99
	90	356				
3	50	357	0.8893	1682	119.3	97
	90	356				
4	50	349	0.8916	1558	118.2	101
	90	357				
5	50	378				103
	90	370	0.8871	1525	118.6	104
6	50	373	0.8871	1571	121.7	
	90	369				
7	50	398	0.9639	1364	99.3	87
	90	393				
8	50	275	0.9548	4588	116.9	—45
	90	271				
9	50	360	0.8899	1589	123.7	105
	90	372				
10	50	334				
	90	345	0.8967	1954	121.3	87

[a] Measurements of thermal conductivity made by Dr. O. Kenneth Bates. at St. Lawrence University, Canton, N. Y.

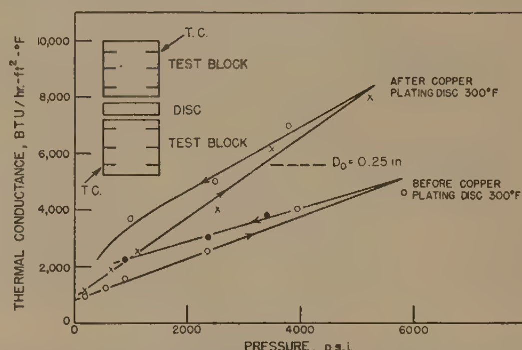

Fig. 13 Increase in Thermal Conductance by Copper-Plating One Steel Surface

Thermal Conductivity of Metals. The measurements made in these experiments also were used to calculate the thermal conductivities of the metal bars employed. Although these data are not included here, it is noted that the standard error in the thermal conductivity-temperature curve for each metal was in the range from 1 to 4 per cent.

A check with handbook values (7) was obtained for No. 1 and No. 2 aluminum in an annealed condition as shown in Table 4.

Conclusion

If the parameters governing the thermal and mechanical behavior of a metal joint were completely known, the data presented here would permit the prediction of its thermal resistance

with a practically useful accuracy. Due to these unknowns and to the incompleteness of this study, no attempt was made to correlate all the observed variables by means of relationships which might be obtained by means of dimensional analysis. An example of this method has been given by J. F. Alcock (8). Variations of the sort reported in this paper may be expected to occur in practice, particularly with metals such as aluminum.

TABLE 4 COMPARISON OF THERMAL CONDUCTIVITY FOR NO. 1 AND NO. 2 ALUMINUM WITH ALCOA HANDBOOK VALUES AT 212 F IN ANNEALED CONDITION; BTU/HR-SQ FT-(DEG F/FT)

Aluminum no.	Experimental	Alcoa (7)
1	118	A-51-S-O 120
2	102	18-S-O 109

Based on the experimental observations, the following specific conclusions are drawn:

1 The thermal conductance of a dry joint increases with pressure; linearly for steel, and generally exponentially for aluminum and bronze.

2 The thermal resistance of both dry and oil-filled joints decreases with a decrease in the roughness of the surfaces.

3 At a given temperature, pressure, and roughness, the thermal resistance of both dry and oil-filled joints decreases in the order of steel, bronze, and aluminum.

4 The thermal resistance of a dry joint decreases as the temperature increases. For oil-filled joints, no consistent relationship has been found.

5 The thermal resistance is about one half as great for oil-filled joints as for dry joints at 10 psi. The effect of the oil decreases at higher pressures. The thermal resistance is decreased by copper-plating one surface of a steel joint.

6 Large variations in the general slope of the thermal conductance-pressure relation are characteristic of the No. 1 aluminum at 300 and 500 F, and of the No. 2 aluminum at 500 F.

7 A hysteresis-like loop in the thermal conductance-pressure relation is obtained when the pressure is decreased following an increase.

8 The ability to measure thermal conductivities of the metals with a standard error of less than 4 per cent confirms other estimates of the precision attained in the experimental data generally.

ACKNOWLEDGMENT

The authors wish to extend acknowledgment to Dr. C. E. Lucke of Columbia University, under whose direction the complete investigation of engine cooling was carried out; to Dr. L. C. Roess for considerable aid in interpretation of joint conductance mechanism and preparation of manuscript, Mr. Neil MacCoull, Mr. W. W. Johnson, Dr. J. J. Mitchell, and Mr. George Raymond of The Texas Company; to Mr. E. D. Brown and Mr. W. R. Wykoff of Pratt and Whitney Aircraft; and to Dr. H. Dean Baker of Columbia University.

BIBLIOGRAPHY

1 "Electrical Contacts," by R. Holm, Hugo Gebers Forlag, Stockholm, Sweden, 1946.

2 "The Area of Contact Between Stationary and Between Moving Surfaces," by F. P. Bowden and D. Tabor, Proceedings of the Royal Society of London, England, series A, vol. 169, December, 1938–March, 1939, pp. 391–413.

3 "A Treatise on the Mathematical Theory of Elasticity," by A. E. H. Love, Dover Publications, New York, N. Y., 1944, p. 196.

4 "Heat Transmission," by W. H. McAdams, McGraw-Hill Book Company, Inc., New York, N. Y., second edition, 1942, p. 380.

5 "Mechanical Properties of Aluminum Casting Alloys at Elevated Temperatures," by R. L. Templin, C. Braglio, and K. Marsh, *Iron and Steel*, vol. 50, 1928, pp. 25–36.

6 "Testing Aluminum Parts for Working Temperatures," by R. G. Anderson, *Product Engineering*, vol. 14, 1943, pp. 736–789.

7 "Alcoa Aluminum and Its Alloys," Aluminum Company of America, Pittsburgh, Pa., 1941, p. 86.

8 "Communications on a Review of Recent Progress in Heat Transfer," by J. F. Alcock, Proceedings of The Institution of Mechanical Engineers, vol. 149, 1943, p. 126.

9 "Thermal Conductance of Metallic Contacts," by R. B. Jacobs and C. Starr, *The Review of Scientific Instruments*, vol. 10, 1939, pp. 140–141.

Discussion

J. D. Keller.[13] This paper represents a very great advance in the knowledge of this little-studied subject. The test methods and apparatus and the scope of the investigation are all admirable, and it is only to be regretted that the authors did not succeed in determining definitely the relative magnitudes of the gas-film component and the true contact component of the total conductance. The present discussion is in no way intended as a criticism of this excellent work, but has the object of clarifying certain points.

Referring to Fig. 3 of the paper and accompanying text, it is a possible objection to the temperature-gradient method that a small change of slope could cause considerable error in the apparent temperature drop across the contact. The temperature drop in the example of Fig. 3, apparently was only 10 or 12 deg F, and in this case an error of 2 deg F would mean almost 20 per cent difference in the conductance. However, apparently a sufficient number of readings were taken for each test to give a much greater accuracy than this would indicate.

Although at low pressures the true metallic conductance constitutes only a minor part of the total, nevertheless, it may be well to point out that the contact conductance apparently is not related to the unit pressure but to the total force exerted on the contacting surfaces. Holm, on the basis of his own work and that of Bowden and Tabor, concluded that the number of microscopic contact points ranged between 4 and 10, entirely independent of the macroscopic contact area. It is well known that the resistance of electrical contacts is determined by the total force pressing them together, and has no relation to the pressure per unit area. (An exception would be that of contacts thin enough to be flexible.) As to the fraction of the macroscopic area which is in actual metallic contact, Bowden and Tabor found, on the basis of electrical-resistance measurements, that this fraction was $^1/_{10,000}$ for smooth steel surfaces under a pressure of $13^1/_2$ psi, for contacts of a certain size.

The metallic conductance through the few actual contact points of microscopic size can be estimated from the tests of Jacobs and Starr, in which the contacts were placed in an evacuated chamber so that the air-film conductance was absent. A transient-heat-flow method was used in these tests, but the technique was such that the results can hardly be questioned. Jacobs and Starr tested contacts of copper, silver, and gold, but not steel or aluminum. However, the conductance for each metal should be proportional to its thermal conductivity, and for steel contacts at 10 psi and 77 F, the conductance in Btu/(sq ft) (hr) (deg F) calculated from Jacobs and Starr's tests of copper would be 13.4; on the tests of silver, 45.5; on the tests of gold, 65.8. The discrepancy is considerable, but taking a mean value of about 30, the metallic-contact conductance would be about 2 per cent of the total conductance of 1420 found by the authors for the same conditions. The surfaces tested by Jacobs and Starr were polished to approximately optical flatness, hence must have been considerably smoother than the authors' smooth surfaces.

It would have been of great interest if at least some of the authors' tests could have been repeated with the contacts in a vacuum, and again, with the gap between the surfaces filled with a

[13] Consulting Engineer, Pittsburgh, Pa. Mem. ASME.

gas of much higher thermal conductivity than air, such as hydrogen or helium; or if even the electrical conductance could have been determined at various pressures, which would have eliminated the effect of the gas film. By these expedients, after due allowance had been made for radiation, the relative magnitude of each of the two conductances could have been determined definitely.

As regards the gas-film conductance, in the writer's opinion this would not be determined by the root-mean-square roughness of the surfaces alone. Profilometer measurements show that in addition to the more or less regular surface variations of sine-wave or saw-tooth form, there are occasional individual peaks projecting considerably higher, as indicated in Fig. 14 of this discussion. It is on the tops of these peaks that metallic contact occurs. The gas-film conductance depends not only upon the rms roughness but also upon the height of these peaks above the surface surrounding their base. As discussed in the writer's recent study of heat conductance in strip-coil annealing,[14] the air-film conductance varies from about $1^1/_4$ to as much as $3^1/_2$ times that which would exist if the air-film thickness were entirely uniform.

The authors seem to feel that the similarity of form of the experimental conductance versus pressure curves to those derived from calculation of the true conductance of a single contact (both curves becoming concave upward at higher pressures), if it does not prove, at least indicates almost certainly that the true contact conductance far outweighs the gas-film conductance at high pressures. While the latter is probably true, the similarity of the curves cannot be considered as proof of it; for the air-film conductance curve can also become concave upward at higher pressures, as will be clear from the following reasoning. As the contact peaks, Fig. 14 of discussion, are squashed down under the increased pressure, not only does the average thickness of the air

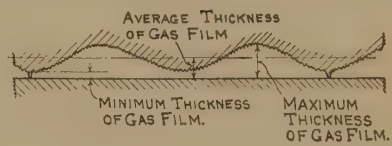

FIG. 14

film decrease and the film conductance increase as its reciprocal but the "form-factor" multiplier would increase toward the higher value mentioned as the height of the crushed peaks approached zero. The combined effect could result in the air-film conductance also increasing at a higher rate than the pressure, just as the authors show that the true contact conductance must do.

[14] "Heat-Transmission in Strip-Coil Annealing," by J. D. Keller, Association of Iron and Steel Engineers, Yearbook, 1948.

AUTHORS' CLOSURE

The authors acknowledge, with appreciation, the discussion by Mr. Keller. Certainly much information is desired for an accurate interpretation of the joint resistance mechanism. Although recognized as being of great interest, a study with various gases and liquids in the joint was not permitted in the time allowed for this project.

Since preparation of this paper, two studies in this field, in addition to Mr. Keller's, have been presented.[15,16]

[15] "Thermal Contact Resistance of Laminated and Machined Joints," by A. W. Brunot and Florence F. Buckland, presented at the Semi-Annual Meeting, Milwaukee, Wis., May 30–June 4, 1948, of The American Society of Mechanical Engineers.

[16] "Thermal Resistance of Metal Contacts," by W. B. Kouwenhoven and J. H. Potter, presented at the National Metal Congress, Philadelphia, Pa., Oct. 25–29, 1948, American Welding Society.

Cavitation Characteristics and Infinite-Aspect-Ratio Characteristics of a Hydrofoil Section

By J. W. Daily,[1] Cambridge, Mass.

This paper describes "two-dimensional" tests in a water tunnel of a profile identical to the 4412 airfoil section of the National Advisory Committee for Aeronautics. The tests included photographic observations of the inception and growth of cavitation as influenced by velocity, pressure (submergence), and angle of attack, and measurements, during cavitation-free operation, of the hydrodynamic forces and moments as functions of Reynolds number and angle of attack. The relation between the angle of attack and the value of the cavitation parameter at which inception occurs is shown for each face of the hydrofoil. The effect of profile geometry in causing cavitation, and the significance of distinctly different types of cavitation obtained with change in variables are discussed. Convenient curves are given showing the submergence required to avoid cavitation for different velocities and angles of attack. The measured hydrodynamic characteristics are presented in graphical form and are also compared with previously existing data from wind-tunnel tests of a finite-aspect-ratio span. The experimental procedure and its reliability in indicating true infinite-aspect-ratio characteristics are discussed.

Nomenclature

The following nomenclature is used in the paper:

α_0 = angle of attack between hydrofoil and mean flow of water, in degrees

d_0 = drag force per unit length of hydrofoil span in pounds

l_0 = lift force per unit length of hydrofoil span in pounds

$m_{a.c.}$ = pitching moment per unit length of hydrofoil span in foot pounds, measured about the aerodynamic center

V_0 = relative velocity between the water and the hydrofoil in feet per second

ρ = density of water in slugs per cubic foot

μ = absolute viscosity of water in pound-seconds per square foot

c = chord of hydrofoil section in feet

b = span of hydrofoil test unit in feet

b/c = aspect ratio

ac = aerodynamic center, the point about which the pitching-moment coefficient is independent of the angle of attack or lift coefficient

CP = center of pressure, the point at which the resultant of all the hydrodynamic forces acting on the hydrofoil is applied

Section drag coefficient

$$c_{d(0)} = \frac{d_0}{\rho \frac{V_0^2}{2} c}$$

Section lift coefficient

$$c_{l(0)} = \frac{l_0}{\rho \frac{V_0^2}{2} c}$$

Section moment coefficient (about aerodynamic center)

$$c_{m(a.c.)} = \frac{m_{a.c.}}{\rho \frac{V_0^2}{2} c^2}$$

Reynolds number

$$\mathsf{R} = \frac{V_0 c \rho}{\mu}$$

Cavitation parameter

$$K = \frac{P_0 - P_{vp}}{\rho \frac{V_0^2}{2}}$$

Where, in addition to terms defined

P_0 = absolute pressure in undisturbed flow, psf

P_{vp} = pressure in cavitation bubble (taken as equal to vapor pressure of water for these tests), psf

Introduction

The usefulness of a profile as a hydrofoil depends upon its susceptibility to cavitation and its behavior when cavitating, as well as its hydrodynamic characteristics when cavitation is absent. In the past, the bulk of the basic hydrofoil performance data have been determined either in wind tunnels, where cavitation cannot be produced, or in towing tanks where cavitation, if produced, cannot be examined conveniently. Therefore not only have there been very little data available showing the cavitation characteristics of hydrofoil shapes, but there have been only a few very limited descriptions of how cavitation begins and grows on a hydrofoil surface.

In 1943 a test program was undertaken in the high-speed water tunnel of the California Institute of Technology (1),[2] which provided an opportunity for making a detailed study of the characteristics of a hydrofoil that included cavitation as well as the normal hydrodynamic data. This program was initiated at the request of the David Taylor Model Basin with the objective of investigating, in general, the testing of small-scale hydrofoils in a water tunnel of the Cal-Tech type under both cavitating and noncavitating conditions.

[1] Assistant Professor of Hydraulics, Massachusetts Institute of Technology. Formerly Hydraulic Engineer at the Hydrodynamics Laboratory of the California Institute of Technology. Mem. ASME.

Contributed by the Hydraulic Division and presented at the Semi-Annual Meeting, Milwaukee, Wis., May 30–June 4, 1948, of The American Society of Mechanical Engineers.

[2] Numbers in parentheses refer to the Bibliography at the end of the paper.

For these experiments, the test installation in the water tunnel was arranged to provide as nearly as practical two-dimensional flow so that all observations and measurements would correspond to the infinite-aspect-ratio condition. The actual investigations included the following:

1 Visual and photographic observations of the cavitation on the hydrofoil as it appeared, developed, and disappeared, as functions of both velocity and angle of attack.

2 Measurements of the hydrodynamic forces and moments acting on the hydrofoil, also as functions of velocity and angle of attack. For reasons to be discussed, the force measurements were limited to the noncavitating conditions. The results of both categories of tests are presented here, together with a discussion of the test procedures used.

Experimental Equipment and Installation

The Hydrofoil Profile. Test units with profiles identical to the NACA 4412 airfoil section were supplied for these experiments by the David Taylor Model Basin. The profile of this section is shown in Fig. 1, together with a tabulation of its coordinates. It is one of the four-digit-series shapes of the National

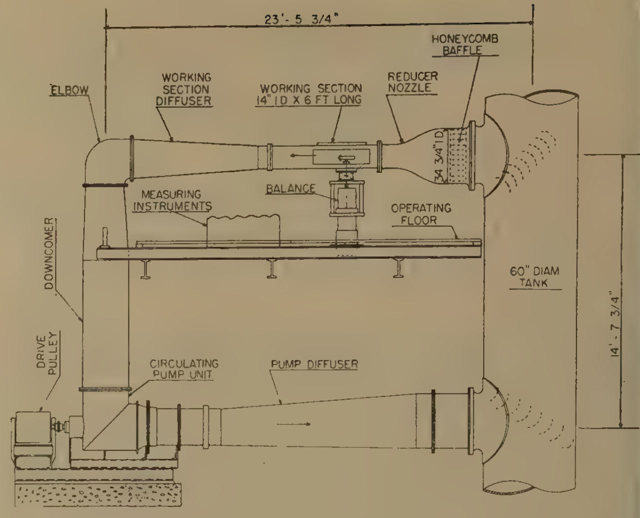

Fig. 2 High-Speed Water Tunnel at California Institute of Technology

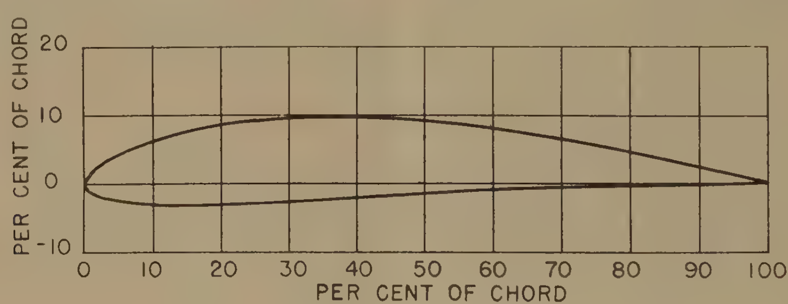

Fig. 1 Dimensions of NACA 4412 Hydrofoil

Advisory Committee for Aeronautics described in references (2, 3, 4, 5). It has a 12 per cent thickness ratio with a 4 per cent camber. The hydrodynamic characteristics, including surface pressure measurements, had been determined previously by wind-tunnel tests and were available for comparing with the water-tunnel data.

The Water Tunnel. A diagram showing the Cal-Tech water tunnel (1) as it was when used for these experiments is given in Fig. 2.[3] The tunnel is a closed-circuit type with an enclosed jet working section. The absence of any free surface limits experiments to those simulating conditions at great depths. In this tunnel water is circulated (counterclockwise in Fig. 2) with a variable-speed pump to give a wide range of velocities in the cylindrical working section. The working-section diameter is 14 in. and its length is 72 in. Visual and photographic observations can be made through transparent lucite windows whose inner faces conform to the cylindrical shape of the tunnel. A system of pressure regulation permits the fluid pressure in the working section to be controlled independently of the velocity, so that cavitation can be produced or avoided as desired. The tunnel is equipped with a three-component balance for measuring the hydrodynamic forces and moments acting on a test body. The balance system is shown schematically in Fig. 3. A rigid vertical spindle is supported near its mid-point in such a way that it is free to rotate about any axis but cannot translate. One end projects into the working section to receive the test unit upon which

[3] For a description of the high-speed water tunnel as recently revised see, "The Hydrodynamics Laboratory at the California Institute of Technology," by R. T. Knapp, Joseph Levy, J. P. O'Neill, and F. B. Brown Trans. ASME, vol. 70, 1948, pp. 437-457.

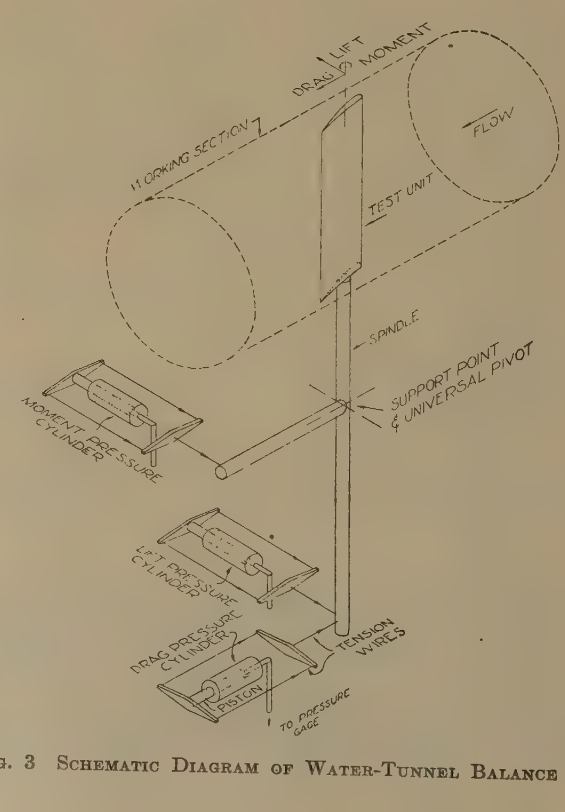

Fig. 3 Schematic Diagram of Water-Tunnel Balance

certain hydrodynamic forces and moments act. The other end is restrained from moving by the application of external forces and couples. By measuring the magnitudes of the restraining forces the corresponding hydrodynamic forces acting on the test unit are obtained. In this balance the restraining forces are created by hydraulic pressure acting on a piston-and-cylinder assembly. The pressure, which is measured by precision weighing-type pressure gages, is proportional to the force applied. Provisions are incorporated in the spindle structure for rotating the upper portion of the spindle about its own geometric axis so that the angle of attack of the test unit can be changed during tests.

Test Installation. Since the so-called infinite-aspect-ratio characteristics were desired in these experiments, two-dimensional flow was approximated by having the test unit completely span the working section. In this instance, the circular cross section of the stream was modified by inserting panels at top and bottom of the working section to form parallel walls, as shown in Fig. 4.

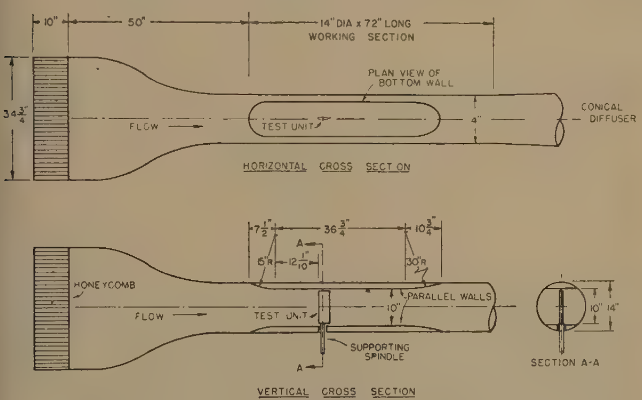

FIG. 4 HYDROFOIL TEST INSTALLATION

In the approximately rectangular section which resulted, the test unit was mounted spanwise between the two plane walls. This type of installation causes approximately a uniform effect of the hydrofoil on the fluid along the full length of the test span. The span was supported at one tip by the balance spindle and cantilevered into the stream. The hydrofoil angle of attack was changed by rotating the spindle. Referring to Fig. 1, a positive angle signified a clockwise rotation of the hydrofoil. Measurements of drag, lift, and pitching moment were obtained as reactions of the pressure cylinders shown in Fig. 3.

In addition to the desirability of having a large span-to-chord ratio, the proportions of the hydrofoil test unit depended upon the physical capacity of the balance and force measuring apparatus, and the structural rigidity of the test unit itself. In order to remain within the capacity range of the balance, it was necessary to reduce the size of the test unit, and hence its rigidity in the lift direction. Thus if the cantilevered hydrofoil completely spanned the working section, severe deflections were obtained at high lifts. As a result, two installations were provided as shown in Fig. 5. In one the test unit spanned the entire 10-in. distance between top and bottom walls except for small clearance gaps at either end. In the other the test unit spanned one half the 10-in. space up to the center line of the tunnel.

A dummy section extending from top down composed the remainder of the span. A small gap at the lower wall and at the center line of the tunnel between the ends of the two semispans served to isolate the lower half during measurements. An angle-indexing device permitted the angle of attack of the upper half to be changed simultaneously with the lower. With this arrangement the forces transmitted to the balance were cut in half, permitting an extension of the range of test velocities. Furthermore, the maximum deflection of the hydrofoil for any particular velocity and angle of attack was reduced by a large factor.

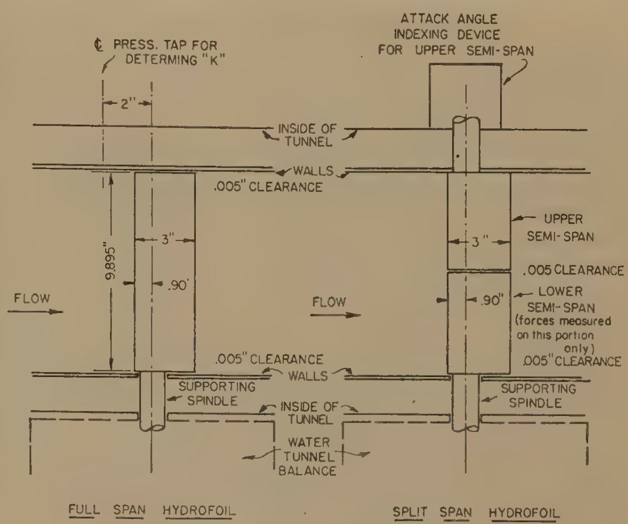

FIG. 5 DETAILS OF TEST UNITS

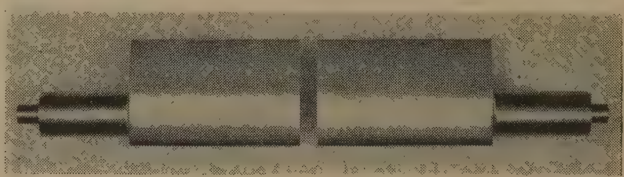

FIG. 6 UPPER AND LOWER SEMISPAN TEST UNITS

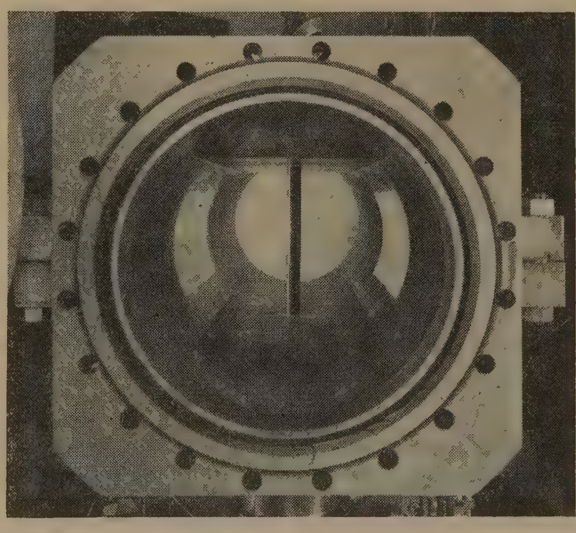

FIG. 7 VIEW LOOKING DOWNSTREAM INTO WORKING SECTION WITH HYDROFOIL IN PLACE
(Note transparent windows opposite test span.)

With the 3-in. chord dimension finally selected as a compromise between the several factors, it was possible to obtain measurements for Reynolds numbers of nearly 1,000,000. The 3-in. size resulted in a good chord-to-span ratio (3.33), and was also large enough to permit an accurate shaping of the profile. Fig. 6 shows the two semispans used, and Fig. 7 is a view into the end of the working section, showing the parallel walls and the test unit in place.

Cavitation Characteristics

Definition of Cavitation. The word "cavitation" is used to signify either the hydrodynamic phenomenon of the formation of vapor-filled bubbles or "cavities" at low pressures and the subsequent collapse of such bubbles, or the physical damage to materials which form the boundaries of the fluid passages in which this bubble formation and collapse occur. In this paper attention is limited to the phenomenon itself. By this usage, an object such as a projectile, a hydrofoil, or a pump blade is said to "cavitate" if such vapor bubbles are formed, even though no physical damage occurs.

It is generally assumed that cavitation will occur whenever the pressure at some point in the fluid becomes equal to the vapor pressure. Local "boiling" results in vapor-filled cavities which grow so long as they are in a low-pressure environment, but collapse when carried by the relative flow into a zone of high pressure. Assuming the beginning or "inception" of cavitation occurs when the pressure equals the vapor pressure exactly, implies that the fluid will not support a tension and ignores the possibility of dissolved gases being released to cause premature cavitation at pressures higher than the vapor pressure. Nevertheless, there is considerable experimental information to indicate that with water containing ordinary amounts of impurities and dissolved air, cavitation does occur at pressures that are very close to the vapor pressure.

The Cavitation Parameter. A relative flow between an immersed object and the surrounding fluid results in a variation in pressure along the surface of the object. At any point on the object the difference between the pressure at that point and the pressure in the undisturbed fluid at some distance from the object is proportional to the square of the relative velocity, or

$$\frac{P_0 - P}{\rho \dfrac{V_0^2}{2}} = \text{const}$$

where P_0 and V_0 are the pressure and velocity for the undisturbed fluid, P is the pressure at the surface of the object, and ρ is the density of the fluid. At some point on the object P will be a minimum and

$$\frac{P_0 - P_{\min}}{\rho \dfrac{V_0^2}{2}}$$

will have a definite value. In the absence of cavitation (and neglecting Reynolds number effects) this value will depend only upon the shape of the object. Now it is easy to imagine a set of conditions such that $P_{\min}$ becomes equal to the vapor pressure of the liquid. This could be accomplished by increasing the relative velocity V_0 for a fixed value of the pressure P_0, or by continuously lowering P_0 with V_0 held constant. Either procedure will result in a lowering of the absolute values of all the local pressures on the surface of the object. If carried to the point that $P_{\min}$ equals the vapor pressure, incipient conditions are said to exist and cavitation should begin.

This beginning will mean the appearance of tiny cavities at or near the place on the object where the minimum pressure is obtained. If a pressure less than the vapor pressure is not possible (which is assumed), then continual increase in V_0 (or decrease in P_0) will mean that the pressure at other points along the surface of the object will become equal to the vapor pressure. Thus the zone of cavitation will extend from its original inception point.

Up to the inception point the value of the fraction

$$\frac{P_0 - P_{\min}}{\rho \dfrac{V_0^2}{2}}$$

remains fixed. For conditions beyond the inception point the value decreases since $P_{\min}$ is identically equal to the vapor pressure, whereas V_0 is increasing (or P_0 is decreasing). Thus the value of this fraction becomes an index of the stage of advancement or "degree" of cavitation.

Written with the vapor pressure replacing $P_{\min}$, thus

$$\frac{P_0 - P_{vp}}{\rho \dfrac{V_0^2}{2}} = K$$

this fraction can be used as a cavitation parameter to relate the conditions of flow to the possibility of cavitation occurring, as well as to the degree of cavitation once the phenomenon begins. Thus for any system where the relative velocity is V_0 and the pressure in the fluid is P_0, K will have a definite value. Cavitation will occur only if the shape of the immersed object is such that

$$\frac{P_0 - P_{\min}}{\rho \dfrac{V_0^2}{2}} \geqq K$$

For the particular case of

$$\frac{P_0 - P_{\min}}{\rho \dfrac{V_0^2}{2}} = \frac{P_0 - P_{vp}}{\rho \dfrac{V_0^2}{2}} = K$$

the value is known as K_i (K for inception of cavitation) on the particular object.

By adjusting the flow conditions so K is greater than, equal to, or less than K_i, the full range of possibilities can be established from no cavitation to advanced stages of cavitation.

The immersed object referred to in the foregoing discussion can be actually a body such as a hydrofoil, or the solid boundary of the passage such as the throat of a Venturi meter.

Test Procedure. The procedure used during cavitation tests was to vary the pressure while all the other factors were held constant. Thus for a given angle of attack, α_0, at any velocity, the pressure was reduced in steps until cavitation appeared and then became well developed, that is, until K became equal to, and then less than K_i. The cavitation parameter for each step was calculated from simultaneously measured values of the velocity and pressure. Measurements were taken as α_0 was varied from —10 to +16 deg. Flow velocities ranged up to 45 fps. During these experiments the inception and development of cavitation was photographed through the transparent windows. These photographs were made with high-voltage flash lamps having a flash duration of about 20 microseconds.

Inception of Cavitation Versus Angle of Attack. In Fig. 8 the value of the cavitation parameter at which cavitation first appears on the hydrofoil is plotted as a function of the angle of attack. Two curves are shown, one marking the incipient cavitation on the upper surface of the hydrofoil and one on its lower. In the area above the curves, cavitation did not occur, while below the curves it existed in varying degrees. These two curves cross at α_0 = —1.4 deg, where cavitation appeared simultaneously on top and bottom surfaces. For any other angle, cavitation occurred on one surface before the other.

Furthermore, the lowest value of K at which cavitation appeared is at —1.4 deg. As already mentioned, the inception point depends upon the shape of the object presented to the flow. Fig. 1 shows that with the chord of the foil (line joining leading and trailing edges) parallel to the flow, the upper surface will cause a greater deflection of fluid, higher local velocity, and should cause a lower pressure than will the lower surface.

Fig. 8 indicates that this is true. For $\alpha_0 = 0$ deg, cavitation was visible first on the upper side at $K = 0.7$ and later on the lower side at $K = 0.42$. As the hydrofoil was pitched into the stream, with either positive or negative angles, the flow had to pass around the sharply curved leading edge. This resulted in increased accelerations and lower pressures so that cavitation occurred earlier (at higher K values). The lowest pressure was on the lower surface of the hydrofoil if α_0 was negative, but on the upper surface if α_0 was positive.

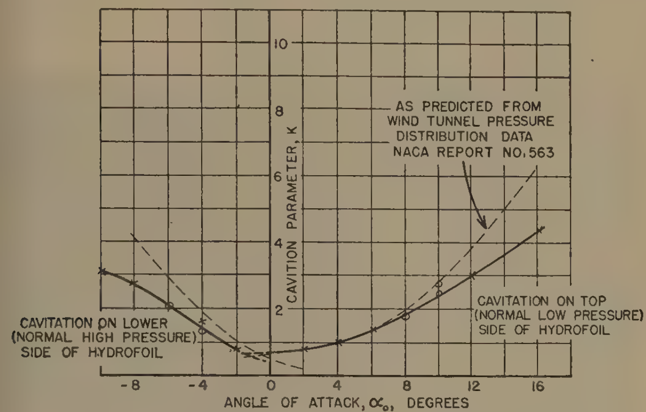

FIG. 8 VALUES OF K_i AT WHICH CAVITATION BEGINS VERSUS ANGLE OF ATTACK

As α_0 was changed from zero the surface which was pitched into the stream was subjected to extra dynamic pressure. At first this merely delayed cavitation on this surface, but eventually the pressure became so large that cavitation did not occur on this side at all. Thus, for example, for positive angles, cavitation was not obtained on the underside of the foil for angles greater than about $2^1/_2$ deg.

K_i From Wind-Tunnel Pressure-Distribution Data. If the distribution of static pressure over the surface of a body is known for noncavitating flow, the fraction

$$\frac{P_0 - P_{\min}}{\rho \dfrac{V_0^2}{2}} = K_i$$

can be evaluated. Pressure-distribution measurements have been made in the wind tunnel for the NACA 4412 airfoil (3), and values of K_i calculated from these data are compared in Fig. 8 with the values obtained in the water tunnel.

Good agreement is shown for the upper side of the hydrofoil up to an angle of about 7 deg. Beyond this, K_i as predicted from the wind tunnel is higher than the water-tunnel values. Similarly, for the lower surface, best agreement is shown near zero angle, with increasing deviation at large negative angles. Several factors are of possible importance in explaining the discrepancies. At attack angles away from zero the sharply curved leading edge of the hydrofoil is presented to the flow. Small errors in formation of the profile here will result in large errors in the minimum pressures. In fact, this indicates that extreme care must be taken in the manufacture of models, particularly small-scale ones, if accurate and consistent results are to be expected. Another factor is that for both the wind tunnel and the water tunnel the greatest deviations from infinite-aspect-ratio conditions are at large angles of attack. The effect of the proximity of the walls (particularly those parallel to the pitching axis of the hydrofoil) becomes a significant variable (6). One further possibility is that ordinary water will support a tension under dynamic loading, despite impurities and turbulence. If this is so, a cavity will not form unless the fluid is subjected to the low-pressure environment for a definite length of time. With a sudden drop and sharp rise in pressure, such as the flow experiences as it passes over the leading edge of the hydrofoil at large angles of attack, the fluid may pass through the low-pressure zone before a cavity develops. Thus the first cavitation would appear only at reduced values of K, where the low-pressure zone is extended. This latter question is one of the important unanswered questions about the mechanics of cavitation.

Submergence to Prevent Cavitation. In many applications of hydrofoils the static pressure is measured in terms of submergence, the vertical depth of the unit below the water surface. The data in Fig. 8 have been replotted in Fig. 15 to show the submergence necessary to prevent complete cavitation on the hydrofoil. The submergence is given in the left-hand diagram as a function of velocity for certain angles of attack, and in the right-hand diagram as a function of angle of attack for fixed velocities. In both diagrams all points below the constant α_0 or constant V_0 curves are for cavitation-free operation. Note that the minimum submergence is required when $\alpha_0 = -1.4$ deg; for all other angles it is greater. Note also that, at a given velocity, the range of angles is limited. For example, at 70 fps and 30 ft submergence, cavitation-free operation is possible only within the limits of -2.2 deg and $+2.4$ deg.

It should be emphasized that the method of obtaining these data corresponds to conditions expected at appreciable depths below the free surface. If the hydrofoil is but slightly submerged there results a production of waves at the surface and a change in the relative flow pattern near the hydrofoil itself. This will change the values of K_i for the hydrofoil and hence the accuracy of the data for shallow submergences in the two diagrams in Fig. 15.

Zone of Cavitation. The behavior of a cavitating hydrofoil depends upon how the cavitation forms and grows and how these cavities affect the flow. In Figs. 10 to 14, inclusive, are shown the appearance of cavitation on one or both surfaces of the hydrofoil at several stages of development. Each figure is for a fixed attack angle and velocity of flow. The variation in K, and hence degree of cavitation, was obtained by changing the pressure in the working section. (The semispan installation was in use when these photographs were taken, and the horizontal joint,

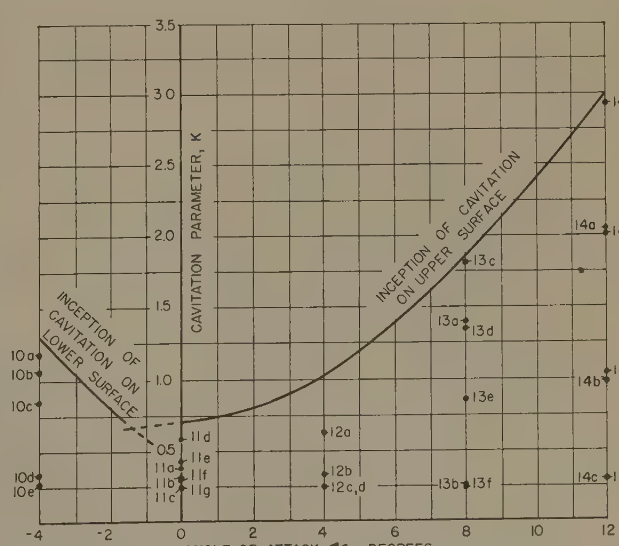

FIG. 9 DIAGRAM SHOWING CAVITATION TEST CONDITIONS FOR EACH VIEW IN FIGS. 10 TO 14, INCLUSIVE

marking the division between the two halves, can be seen in some cases.) Fig. 9, which will be useful in discussing these photographs, is another diagram of K_i versus α_0, on which have been indicated numbers corresponding to the several photographs in Figs. 10 to 14. Each number is located on the diagram at the value of K and at the angle of attack at which the photograph was taken. Thus the relationship between conditions for inception of cavitation and the conditions for each photograph is shown graphically.

The relative susceptibility to cavitation on the two surfaces of the hydrofoil is shown in the views in Fig. 11 which were taken with zero angle of attack. In Fig. 11(a, b, c), in the left-hand

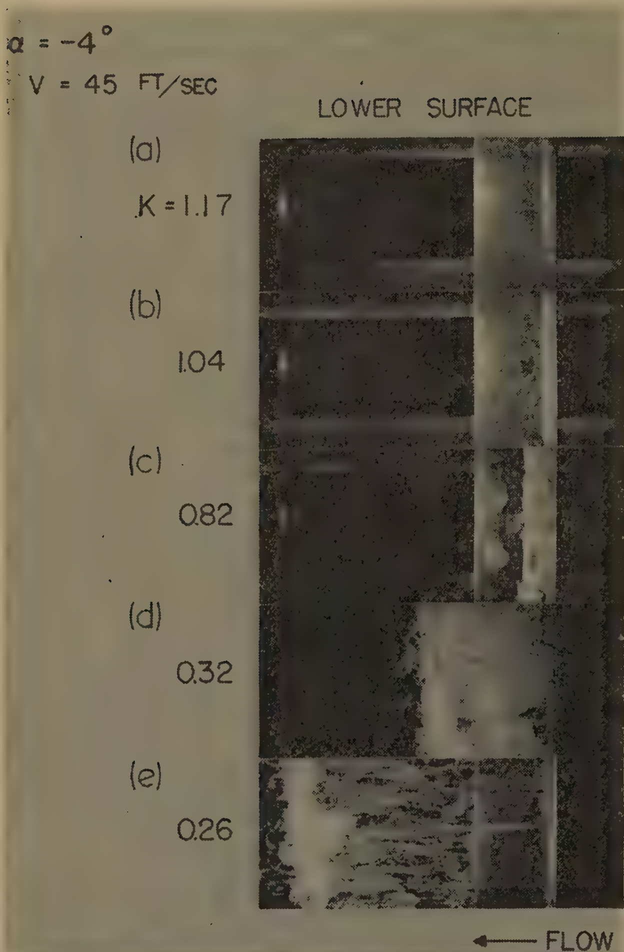

Fig. 10 Cavitation on Lower Surface of Hydrofoil; Angle of Attack = −4 Deg

(Exposure time for each photograph in Figs. 10 to 14, inclusive, is approximately 20 microsec.)

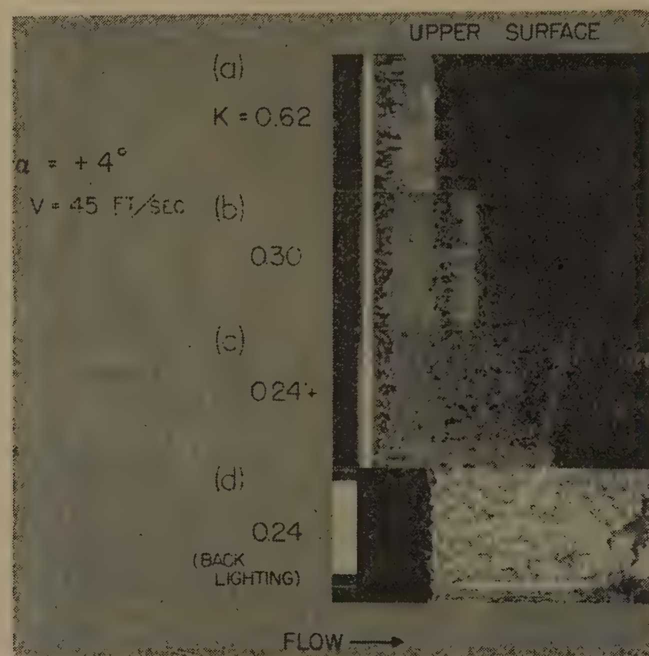

Fig. 12 Cavitation on Upper Surface of Hydrofoil; Angle of Attack = +4 Deg

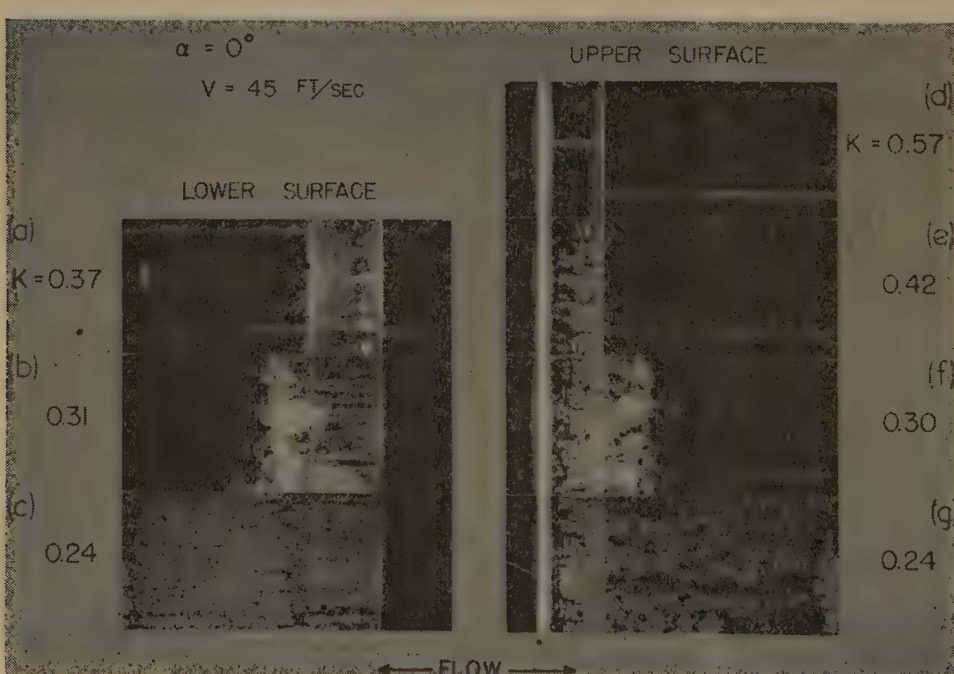

Fig. 11 Cavitation on Lower and Upper Surfaces of Hydrofoil; Angle of Attack = 0 Deg

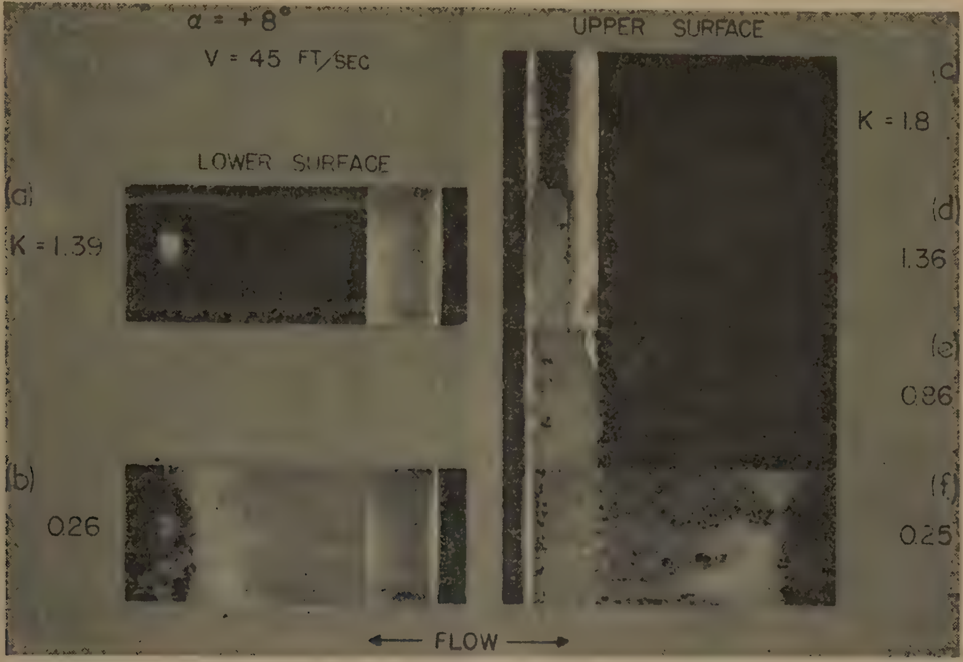

Fig. 13 Cavitation on Upper Surface of Hydrofoil as Viewed From Both Sides of Test Unit; Angle of Attack = +8 Deg

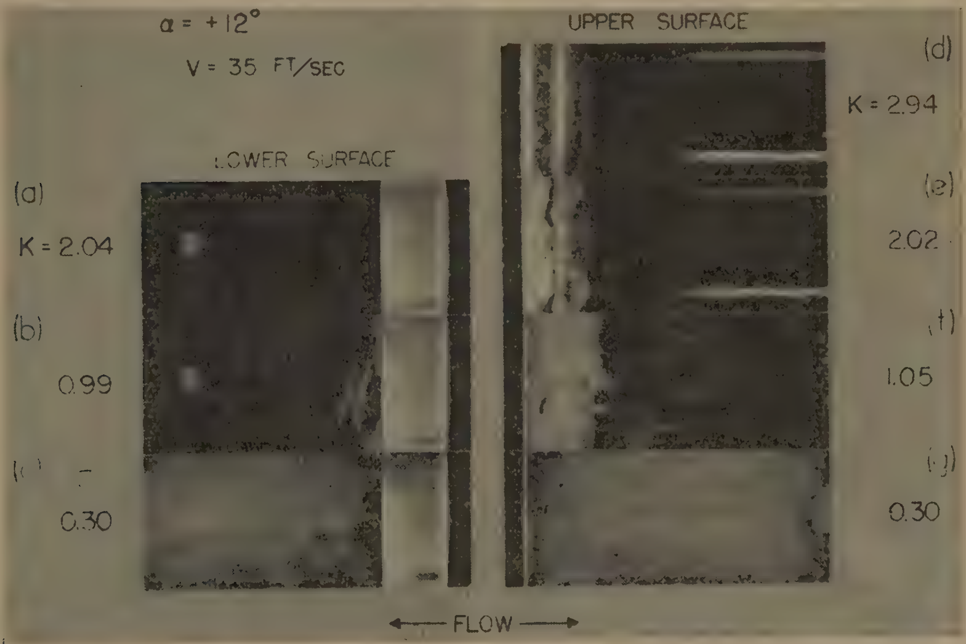

Fig. 14 Cavitation on Upper Surface of Hydrofoil as Viewed From Both Sides of Test Unit; Angle of Attack = +12 Deg

column are views of cavitation on the lower (normally high-pressure) surface of the hydrofoil. For these views, the relative flow over the surface is from right to left. In Fig. 11(d, e, f, g), in the right-hand column, cavitation is shown on the upper surface. The relative flow is from left to right. Reference now to Fig. 9 shows that cavitation first appears on the upper surface at K = 0.7, approximately, for α_0 = 0 deg. Cavitation does not appear on the lower surface until K is reduced to about 0.41. In Fig. 11 the first view for the upper surface is at K = 0.57. Even at this value cavitation does not occur over the entire length of the span continuously, but rather intermittently in any one local area. Other views taken at the same K would show patches of cavitation in other positions along the span. As K is reduced, cavitation becomes more general and more extended. In the meantime, cavitation on the lower surface shows a less advanced stage compared to that on the upper at approximately the same K values. Thus at K = 0.37, cavitation on the lower surface is very little more general than on the upper at K = 0.57. In fact, the relative degree of cavitation is shown clearly in Fig. 11(a), where tail wisps of cavitation on the upper side can be seen extending past the trailing edge.

Similar observations are obtained from Figs. 13 and 14, for α_0 =

+8 deg and +12 deg, except that in both these cases no cavitation appears on the lower surface for the range of the experiments. The pitch is such that the extra dynamic pressure prevents vaporization on this side. On the other hand, at α_0 = —4 deg, the upper surface, which was pitched into the stream, was cavitation-free.

As K is reduced, cavitation first appears as a narrow zone of small cavities which apparently originate, grow, and finally collapse on or near the surface of the hydrofoil. In the early stages, at least, the extent of the zone of cavities is an indication of the extent of the low-pressure zone, an idea that has been substantiated for certain three-dimensional bodies (13). A clean example of such an expanding low-pressure zone is shown in Fig. 10(a, b, c).

The determination of the location and extent of the low-pressure zone by water-tunnel tests, such as these, has an important application in the development of high-speed airfoils. The occurrence of cavitation at the minimum-pressure point with liquids is analogous to the occurrence of sonic velocities and shock waves at the minimum-pressure point with compressible fluids.

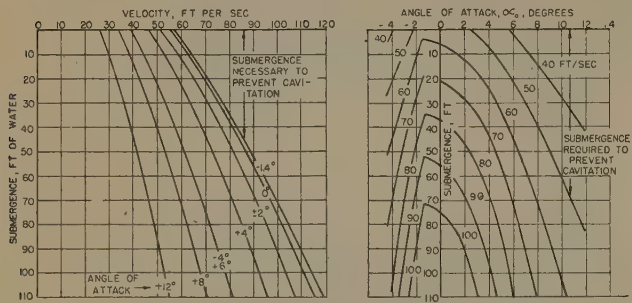

Fig. 15 Submergence Necessary to Prevent Cavitation on Hydrofoil

Advanced Stages and Entrainment Process. With continued reduction in K, a stage is reached where the collapse actually occurs in the fluid downstream from the hydrofoil itself. In fact, there exists a growing tendency for groups of cavities to be separated from the general mass and carried well beyond the hydrofoil and the main zone of cavitation before collapsing. Examples of this are shown in Figs. 10(c) and 14(e),(f). Professor Knapp has pointed out that this is an "entrainment" process whereby the main flow of fluid is acting as an entrainment pump. It is an essential feature in the mechanics of maintaining the presssure at the boiling point for the advanced stages of cavitation. For extremely advanced stages, apparently the bulk of the vapor is entrained and swept away before collapsing.

Under some conditions the individual cavities in the very advanced stages of cavitation coalesce to form a single enveloping bubble with transparent walls over a portion of its length. One example is in Fig. 10(e) where such a transparent bubble envelops the near side of the hydrofoil. In Figs. 11(c) and 11(g) the flow is on the verge of changing over to this transparent-bubble condition. The transparent walls are an indication that very little vaporization is occurring. The vapor supply must be from the zone of turbulent boiling near the downstream end of the envelope. The interior of the envelope is at the vapor pressure and is maintained at this pressure by the "pumping" action of the relative flow past the hydrofoil.

Fine Versus Coarse-Grain Cavitation. A general examination of the illustrations shows two "types" of cavitation to exist. In one, such as shown in Fig. 12, individually identifiable cavities appear. In the other, such as in Fig. 10 or 13, the cavities are very small and closely spaced, giving a sudsy appearance. Professor Knapp has termed these "coarse-grain" and "fine-grain," respectively. It will be noted that these types are associated with the curvature of the profile presented to the flow. A sharp curvature with its sudden reduction in pressure results in the fine-grain type. With a more gentle curvature the coarse-grain bubbles appear. These views show that as the hydrofoil is given larger and larger angles of attack in either direction, the minimum pressure point moves toward the sharply curved leading edge, and fine-grain cavitation is produced.

Rate of Growth and Life of a Cavity. In many of the illustrations the growth of individual cavities can be observed for a short distance after their formation. Some measurements made for α_0 = 0 deg, V_0 = 45 fps, and K = 0.25, showed a rapid growth, for the first quarter-chord length of travel, up to 60 to 75 per cent of what appeared to be the final diameter. Beyond this, growth was considerably slower until individual cavities interfered with their neighbors and then lost their identity. The growth of the cavities probably is the result of the continued vaporization into the "void," until the cavity itself is swept into a higher-pressure zone. For an example of the rapidity of the process, the life of the cavities shown in Fig. 11(e), is approximately $^1/_{200}$ sec. In this short interval the cavity grows to a diameter of approximately $^5/_{16}$ in. and then collapses.

Hydrodynamic Behavior With Cavitation. These illustrations show instantaneous samples of an unsteady phenomenon. The average or so-called "steady-state" condition obtained for a given K value represents a balance between the rate of vapor formation and the rate of annihilation, whether the latter is by collapse as in the early stages, or by entrainment as in the later stages. For any K the extent of the cavitation zone grows until this balance is obtained. Successive samples at the same velocity and pressure will have the same general appearance, but will differ in detail. This unsteady character results in fluctuating hydrodynamic forces on the hydrofoil, the well-known cause of the vibration of cavitating ships' propellers or centrifugal pumps. With increased cavitation, these fluctuating forces (and hence vibrations of the hydrofoil) were observed to grow to dangerous magnitudes. However, with the formation of the transparent enveloping bubble just mentioned, the forces became essentially steady, and the vibrations nearly ceased. Under these conditions, apparently the fluctuations normally associated with cavity formation and collapse were limited to the neighborhood of the collapsing cavities themselves and not carried back upstream to the hydrofoil proper.

The hydrodynamic forces and moments acting during cavitation were not measured during these experiments for two related reasons: (a) The water-tunnel balance, which was designed for essentially steady-force measurements, would not resolve the unsteady forces encountered with cavitation over most of the range of the studies. (b) It was observed, by noting the deflections of the hydrofoil unit, that even though the drag increased with the onset of cavitation, the lift (and pitching moment) dropped off. Low average values combined with fluctuating forces further complicated measurements of these. The effect of cavitation on the hydrodynamic behavior of the hydrofoil depends upon the extent to which the cavitation alters the flow around the unit. The existence of cavitation means that the streamlines must conform to the shape of a new "body" and that the velocity and pressure distribution is changed from that without cavitation. As the cavitation zone grows, less and less fluid is given a net deflection normal to the direction of motion and the lift drops off. This effect is similar to that encountered when airfoils stall at excessive angles of attack. At the same time, the drag goes up because cavitation increases the effective thickness of the body, resulting in a larger change in momentum of the fluid parallel to the flow direction.

Cavitation and Damage. While these experiments were not concerned with cavitation damage, it might be noted that it is the initial stages of cavitation which are probably responsible for cavitation erosion. In the early stages the cavity collapse takes place on or near the hydrofoil surface. At later stages, the collapse is in the liquid body well away from the solid surface. Since it is generally recognized that it is the collapse which results in damage, it must be the early stages that are dangerous. This is an important consideration in dealing with propellers and pumps often operating near conditions for incipient cavitation.

Significance of This Profile. These cavitation data are presented principally as a study of the cavitation process in the inception, growth, and collapse of cavities or bubbles. The use of this particular profile for the experiments was convenient because of the existence of the previously measured wind-tunnel data. Otherwise this shape has no particular merit as a hydrofoil in so far as cavitation is concerned. Other shapes exist which are far more "resistant" to the occurrence of cavitation. However, their other hydrodynamic characteristics are also different from those for this shape. In the selection of a profile for an application the requirements of both types of characteristics must be considered.

Infinite-Aspect-Ratio Characteristics

Significance of Infinite-Aspect-Ratio Data. The hydrodynamic properties of airfoil and hydrofoil shapes are reported as "infinite-aspect-ratio" or "section" characteristics because in this form they depend only upon the shape of the profile. The characteristics of a hydrofoil or airfoil of finite span differ from those for an infinite span because of "leakage" of fluid at the span tips from the high-pressure to low-pressure surface. This flow around the ends acts to reduce the lift and increase the drag at given angles of attack. These are called "induced" effects (7, 8), and their magnitude depends upon the aspect ratio, plan form, and twist of the particular hydrofoil. Infinite-aspect-ratio data are important in the design of lifting devices, such as wings, rudders, or stabilizing fins, as well as various pumping devices such as propellers, fans, and centrifugal pumps. Methods are available for converting these data to the equivalent performance of actual devices having arbitrary geometrical proportions, (8, 9, 10).

Experimental Methods. Infinite-aspect-ratio data can be obtained from tests of finite-span sections by correcting the measured forces and moments for induced velocity effects and for tunnel-wall interference, and support-interference effects. In an effort to eliminate the uncertainty of the various corrections, which may become large with respect to the measured forces, particularly drag, the trend has been toward two-dimensional tests. In these the attempt is made to cause the hydrofoil to act uniformly along its span as it deflects the passing fluid, by having the test unit span the stream completely. If this is achieved, the resulting flow differs from the ideal sought only by the effect of the presence of the tunnel walls.

As already described, the test installation for these experiments was designed to give essentially two-dimensional flow past the hydrofoil. The clearance gaps at the ends of the test span, which were necessary to isolate the unit while measuring forces, were small to make the tip leakage unimportant.

The hydrodynamic forces acting on a hydrofoil need not be measured directly but may be determined indirectly by evaluating the change in momentum of the fluid as it passes the test span and by measuring the reaction pressures created on the tunnel walls as a result of the fluid being deflected. These wake-survey and wall-pressure-survey methods (11, 12) require less elaborate test equipment because the force-measuring balance is eliminated, and the test unit need not be supported independently of the tunnel structure as is necessary for direct measurement of the forces acting on the hydrofoil. On the other hand, where the balance is available, its use for direct measurements is extremely convenient and, with the proper provisions, should permit better accuracy. One objective of this study was to investigate the adaptation of the single-spindle three-component balance to two-dimensional testing.

Measured Characteristics. The measured data were obtained over the range of Reynolds number from $\mathbf{R} = 287{,}000$ to $903{,}000$. The experimental procedure was to measure the lift, drag, and pitching moment as functions of the angle of attack for the several Reynolds numbers. In each case the pressure was maintained high enough to prevent cavitation.

The experimental results are shown graphically in Figs. 16 and 17, where lift, drag, and pitching-moment coefficients, and center of pressure are plotted versus angle of attack. In Fig. 18 angle of attack and drag, and pitching-moment coefficients are plotted with the lift coefficient considered as the independent variable. The terms and symbols used are defined in the nomenclature. In each figure, curves are given for four values of Reynolds number. All the results plotted here were obtained with the split-span installation, which permitted the measurement of the forces on one half the total span. Even so, it will be noted that the maximum lift could not be reached at the higher Reynolds numbers because of the excessive magnitude of the forces developed. Measurements with the full 10-in. span, which were in the lower Reynolds number range, gave similar results to those shown and are not included here. In Table 1 the magnitudes of the important variables for both the semispan and full-span installations are listed for each Reynolds number.

As Reynolds number increases, certain consistent changes in performance will be noted. The slope of the lift-coefficient curve, and the maximum value of the lift coefficient increase, while the drag coefficient decreases. Also, the angle for zero lift shifts to slightly lower values. The moment coefficient is figured about the aerodynamic center, the point about which the pitching moment is essentially constant for a wide range of angles of attack. Up to about 5 deg, the coefficient is constant and independent of Reynolds number. Up to 8 deg, the coefficient is within 15 per cent of a constant value. The center of pressure is also nearly independent of $\mathbf{R}$, with deviations occurring near $\alpha_0 = 0$ deg, where accuracy in calculating the center-of-pressure position is low.

TABLE 1 PRINCIPAL SECTION CHARACTERISTICS OF NACA 4412 HYDROFOIL FROM TWO-DIMENSIONAL TESTS IN WATER TUNNEL

	Tests Reynolds number	Attack angle for no lift, $\alpha_{l(0)}$ (deg)	Lift-curve slope, a_0 (per deg)	Maximum lift coefficient, $c_{l(max)}$	Minimum drag coefficient, $c_{d(0)(min)}$	Pitching moment, $c_{m(a.c.)}$	Aerodynamic center: Ahead of $c/4$ (per cent c)	Aerodynamic center: Above chord (per cent c)
Semispan installation....	287000	—3.95	0.098	1.36	0.014	—0.102	5.47	—0.26
	563000	—4.05	0.102	1.39	0.013	—p.101	4.92	—4.52
	730000	—4.15	0.104		0.0105	—0.102	5.53	—3.84
	903000	—4.25	0.106		0.011	—0.101	5.39	1.68
Full-span installation	299000	—4 (approx)[a]	0.098	1.38	0.014	—0.100	5.12	—0.38
	388000	—4 (approx)[a]	0.101		0.014	—0.102	5.12	—0.39
Theoretical values for infinite aspect ratio		—4.58	0.120			—0.137	0	0

[a] These values for $\alpha_{l(0)}$ are obtained after correction for error in initial alignment of hydrofoil chord with tunnel axis.

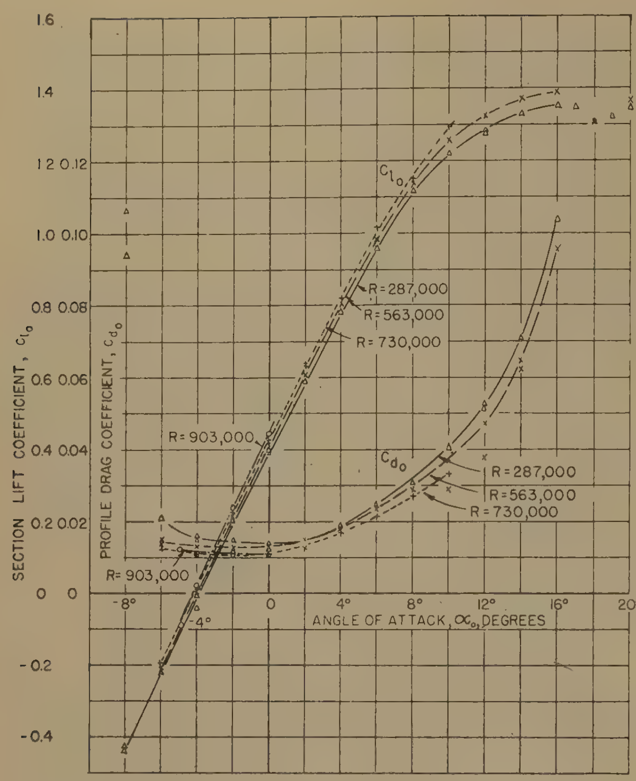

FIG. 16 INFINITE-ASPECT-RATIO CHARACTERISTICS VERSUS ANGLE OF ATTACK

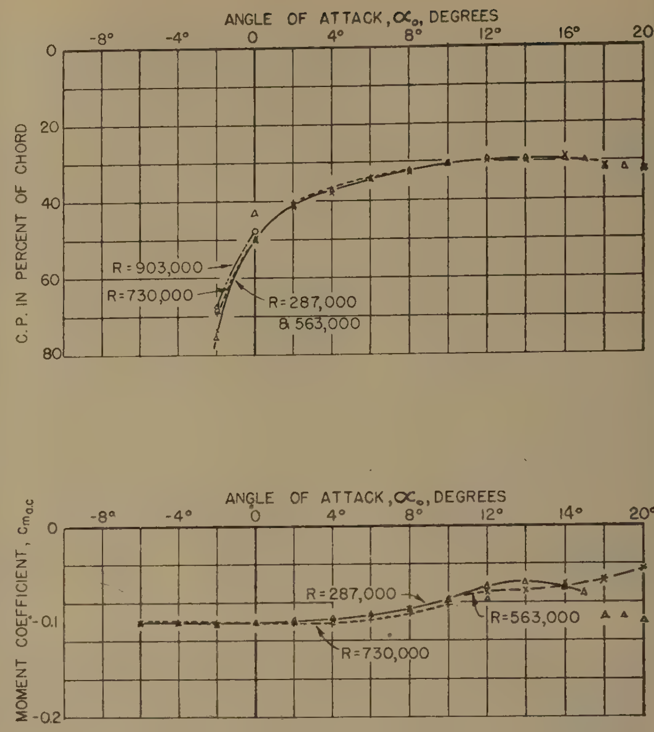

FIG. 17 INFINITE-ASPECT-RATIO CHARACTERISTICS VERSUS ANGLE OF ATTACK

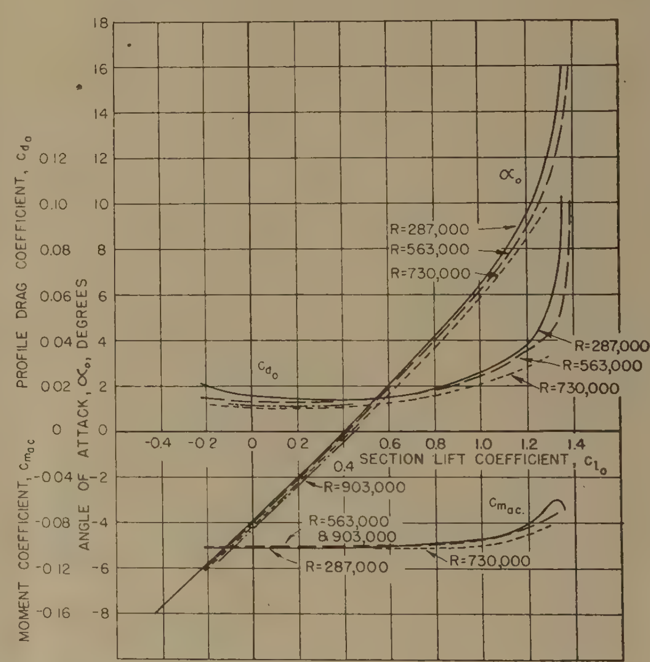

FIG. 18 INFINITE-ASPECT-RATIO CHARACTERISTICS VERSUS LIFT COEFFICIENT

Experimental Limitations on Results. The experimental arrangement used for these tests introduced the following factors causing deviation of the flow from truly two-dimensional conditions:

1 The entire span was not subject to a uniform velocity, but experienced lower velocities in the boundary-layer zone near the tunnel walls.

2 There was the possiblity of flow through the clearance spaces between the ends of the test span and the tunnel walls, or between the two halves of the split-span section.

3 There was a possibility of interference because of the proximity of the tunnel walls to the test section.

A nonuniform velocity distribution will tend to make all the coefficients numerically high. However, as shown in Fig. 4, the test span was located only about one tunnel diameter from the final contraction of the flow. In this short distance the boundary layer should occupy only a small percentage of the width of the working section so that most of the span should experience the full velocity. It should be noted also that while the velocity distribution was known to be uniform in the circular section just ahead of the final contraction caused by the addition of the two parallel walls to the working section, it was not measured in the plane of section *AA*, Fig. 4, where the hydrofoil was mounted. Good evidence of uniformity at the hydrofoil was obtained from an examination of the cavitation photographs. In these, cavitation appeared to form at the same value of K_i at all points along the span and grow uniformly along the span, with no consistent deviations. (The intermittent patches of cavitation in the early stages as shown in some cases are thought to be evidence of the unsteady nature of the phenomenon.)

Any leakage through the clearance spaces at the ends of the test span will tend to reduce the actual angle of attack at the hydrofoil at high lifts. In these tests the clearance was held to 0.005 in. to keep a high resistance to flow through the gap. At small angles of attack, the influence on the measured forces and moments should be small. However, as the angle increases and the pressure difference through the gap increases, the leakage will increase. This is an error that could be reduced by using end plates recessed into the tunnel wall, but these, in turn, would complicate the drag measurements. The magnitude of the clearance gap is important. Increasing the gap from 0.005 to 0.023

in. caused an 8 per cent increase in drag and a 4 per cent decrease in lift. The moment was not affected appreciably. If it is assumed that the error is proportional to the leakage and therefore, for laminar flow, is proportional to the clearance, the maximum error in drag is about 2 per cent with a 0.005-in. gap. It is likely that the error increases at a faster rate as the clearance is enlarged, so the error at 0.005 in. is even less. The error in lift from this cause is correspondingly less.

The tunnel walls confine the water flow and change the streamline pattern around the hydrofoil from that in a free stream. For two-dimensional flow it is particularly important that the walls parallel to the pitching axis are as far removed as possible. In this installation the maximum dimension of the water-tunnel cross section normal to the hydrofoil axis was kept at the full 14 in. as shown in Fig. 4. Wall interference, including the so-called "blocking" or actual restriction of the passage by the hydrofoil itself, is negligible at small angles of attack (low lifts) but increases with angle (6). The actual magnitude of this effect was not evaluated for these tests. The degree of fluid turbulence in the water tunnel was not determined because suitable instruments were not available for measuring it directly, as can be done readily with the hot-wire anemometer in the wind tunnel, and because indirect measurements, such as the determination of the critical Reynolds number for a sphere, required test setups involving uncertain support-interference errors. The turbulence has an important effect on the measured drag and maximum lift. Without more definite knowledge of the turbulence, measurements of these two items must be considered primarily as comparative.

Accurate measurement of the minimum drag was handicapped by the very small magnitudes of this component (approximately 4 lb total for $\mathbf{R} = 903{,}000$). Nevertheless, the decreasing trend with increasing Reynolds number already noted is in the proper direction and is a good indication that the tests give reliable comparative results.

In summary, it appears that with this method of testing, accurate results should be obtained at small angles of attack. This is in the low-lift range and the range of many hydrofoil applications. At larger angles the accuracy of the results is reduced somewhat. Nevertheless, good comparative results should be obtainable.

Theoretical Characteristics. A simple set of equations for the characteristics of hydrofoils in a frictionless fluid can be derived theoretically by the method of conformal transformation (8). Using the Joukowsky transformation, the relationships for small angles of attack are

$$\text{Lift coefficient} = c_{l(0)} = 2\pi\left(1 + 0.77\,\frac{\text{thickness}}{\text{chord}}\right)\frac{[\alpha_0 - \alpha_{l(0)}]}{57.3}$$

$$\text{Zero-lift angle} = \alpha_{l(0)} = 2\,\frac{\text{camber}}{\text{chord}} \times 57.3$$

$$\text{Slope of lift curve} = a_0 = 2\pi\left(1 + 0.77\,\frac{\text{thickness}}{\text{chord}}\right)\frac{1}{57.3}$$

$$\text{Pitching moment coefficient} = c_{m(\text{a.c.})} = \frac{\pi}{2}\left(1 + 0.77\,\frac{\text{thickness}}{\text{chord}}\right)\frac{\alpha_{l(0)}}{57.3}$$

It will be noted that for a given thickness ratio the lift coefficient is proportional to the angle of attack, the angle for zero lift is proportional to the amount of camber, and the moment coefficient is constant about the quarter-chord point. It will also be noted that because a frictionless fluid is assumed, all of these values are independent of Reynolds number and the drag is zero.

For the 4412 hydrofoil the numerical values are

$$c_{l(0)} = 0.120\,[\alpha_0 - \alpha_{l(0)}]$$
$$\alpha_{l(0)} = -4.6 \text{ deg}$$
$$a_0 = 0.120 \text{ (per deg)}$$
$$c_{m(\text{ac})} = -0.137$$

These values appear also in Table 1 where they are seen to be slightly greater (numerically) than the measured quantities.

Comparison With Finite-Aspect-Ratio Tests. Previously published data for this profile were obtained from NACA tests of wing section with aspect ratio of 6. The data were corrected to give infinite-aspect-ratio characteristics. In Fig. 19 curves from NACA wind-tunnel tests are compared with the water-tunnel measurements. The principal characteristics are given in Table

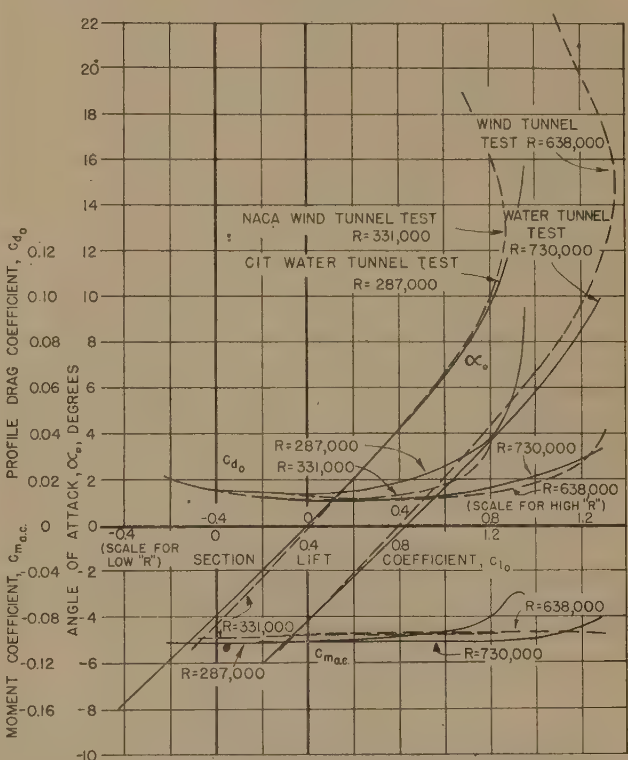

Fig. 19 Comparison of Water-Tunnel Results With Wind-Tunnel Data From Tests on a Finite-Span Unit of Aspect Ratio 6

TABLE 2 PRINCIPAL SECTION CHARACTERISTICS OF NACA HYDROFOIL FROM WIND-TUNNEL TESTS OF RECTANGULAR AIRFOILS WITH ASPECT RATIO = 6

Test Reynolds number	Attack angle for no lift, $\alpha_{l(0)}$ (deg)	Lift-curve slope, a_0 (per deg)	Maximum-lift coefficient, $c_{l(max)}$	Minimum-drag coefficient $c_{d(0)(min)}$	Pitching moment, $c_{m(a.c.)}$	Aerodynamic center: Ahead of $c/4$ (per cent c)	Aerodynamic center: Above chord (per cent c)
331000	—4.35	0.094	1.27	0.011	—0.096	1.1	—8.0
638000	—4.25	0.094	1.36	0.012	—0.094	1.0	—1.0

Note: Wind-tunnel data were taken from Fig. 7, ref. (4), and corrected by methods outlined on pages 17 and 18 of that reference to give so-called second-approximation characteristics.

2. These wind-tunnel data were taken from reference (4)[4] and corrected by the methods outlined,[5] to give so-called "second-approximation" characteristics. They apply at the test Reynolds numbers. All corrections to infinite aspect ratio are included, except the effect of support interference on drag, and certain secondary effects of variations in c_l and $c_{d(0)}$ along the finite test span at high lifts. They are not corrected for turbulence or scale effects and should not be confused with final characteristics presented in references (4) and (5), which have been extrapolated to full-scale aircraft flight Reynolds numbers.

When comparing the two sets of data from different sources, the fact should be kept in mind that most likely different degrees of turbulence existed in the two tunnels. As already noted, this factor would affect the drag and magnitude of the maximum lift attainable. The other characteristics should not be affected appreciably. In this case the water-tunnel two-dimensional tests gave values for the slope of the lift curve, the moment coefficient, the minimum-drag coefficient and the maximum-lift coefficient which were roughly 10 per cent greater in magnitude than shown by the wind-tunnel data. The drag curves for the two sets of data differ widely in spite of the reasonable agreement of the minimum-drag values. The reason for this discrepancy is not known.

Application of Results

In testing with artificial fluid streams, the degree of turbulence is invariably different from that encountered in the actual application. The higher the turbulence, the higher will be the maximum-lift coefficient. The turbulence also affects the transition in the boundary layer on a given body and hence the drag. Methods have been suggested for compensating for tunnel turbulence. These have their main value in adjusting the maximum-lift coefficient.

The range of Reynolds number covered by the tests (up to approximately 1,000,000) includes many hydrofoil applications. If the data are to be applied outside this range, some correction should be made. Wind-tunnel tests have shown that for Reynolds numbers up to 3,000,000 the slope of the lift curve increases only about 1 or 2 per cent above its value at 1,000,000. The pitching moment and the angle for zero lift are also nearly unaffected. On the other hand, the maximum-lift coefficient increases from 10 to 20 per cent. The profile drag decreases at nearly the same rate as turbulent skin friction on flat plates. It is felt that the useful range of the test results reported here can be extended considerably by careful application of rules such as these.

It should be emphasized again that the data apply to situations where there is no free surface in the neighborhood of the hydrofoil. For operation at an inappreciable submergence, the formation of waves on the liquid surface will modify the characteristics measured by tests such as these.

Acknowledgment

This paper presents the results of an investigation conducted at the high-speed water tunnel of the Hydrodynamics Laboratory at the California Institute of Technology. The high-speed water tunnel was built and operated by the California Institute of Technology under Contract OEM-sr207 with the Office of Scientific Research and Development. Division 6, Section 6.1 of the National Defense Research Committee was the sponsoring agent of the OSRD during the establishment and initial four-year operating period of the water tunnel. The Hydrodynamics Laboratory and the water-tunnel research program are under the immediate direction of Robert T. Knapp, Associate Professor of Hydraulic Engineering.

These experiments were undertaken as a part of a general program of hydraulic investigations made for the armed services during the period of NDRC sponsorship. This particular investigation was conducted on request from the United States Navy Department, the David Taylor Model Basin, and on authorization from Dr. E. H. Colpitts, chief of Section 6.1 of the NDRC. The material included here originally appeared in Report No. 6.1-sr207-1273 submitted to the NDRC of the OSRD.

In the design of the two-dimensional test installation described here, helpful suggestions were obtained from Prof. Theodore von Kármán of the California Institute. Mr. Robert E. Carr, who was in charge of the water-tunnel test crew, was responsible for execution of actual tests. The excellence of the large quantity of photographic material is due to the efforts of Mr. Hugh Stevens Bell of the water-tunnel staff. Mr. Haskell Shapiro was responsible for the lighting and miscellaneous electronic equipment auxiliary to the experimental setup.

Bibliography

1 "The Water Tunnel as a Tool in Hydraulic Research," by J. W. Daily, Proceedings of the Third Hydraulics Conference (1946), University of Iowa. Studies in Engineering, Bulletin No. 31, p. 169.

2 "The Characteristics of 78 Related Airfoil Sections From Tests in the Variable Density Wind Tunnel," by E. N. Jacobs, K. E. Ward, and R. M. Pinkerton, NACA TR No. 460, 1933.

3 "Calculated and Measured Pressure Distributions Over the Midspan Section of the NACA 4412 Airfoil," by R. M. Pinkerton, NACA TR No. 563, 1936.

4 "Airfoil Section Characteristics as Affected by Variations of the Reynolds Number," by E. N. Jacobs and A. Sherman, NACA TR No. 586, 1937.

5 "Airfoil Section Data Obtained in the NACA Variable-Density Tunnel as Affected by Support Interference and Other Corrections," by E. N. Jacobs and I. H. Abbott, NACA TR No. 669, 1939.

6 "An Investigation of Fluid Flow in Two Dimensions," by A. Thom, ARC Reports and Memoranda No. 1194, November, 1928.

7 "Aerodynamics of the Airplane," by C. B. Millikan, John Wiley & Sons, Inc., New York, N. Y., 1941, pp. 39–54.

8 "Aerodynamic Theory," vol. 2, edited by W. F. Durand, Julius Springer, Berlin, Germany, 1934.

9 "Determination of the Characteristics of Tapered Wings," by R. F. Anderson, NACA TR No. 572, 1936.

10 "The Design of Propeller Pumps and Fans," by M. P. O'Brien and R. G. Folsom, University of California Publications in Engineering, University of California Press, vol. 4, no. 1, 1939.

11 "The Measurement of Profile Drag by the Pitot Traverse Method," by B. M. Jones, ARC Reports and Memoranda, No. 1688, 1936.

12 "The Effects of Roughness at High Reynolds Numbers on the Lift and Drag Characteristics of Three Thick Airfoils," by F. T. Abbott, Jr., and H. R. Turner, Jr., NACA Wartime Report L-46. (Wake survey and wall pressure techniques were used for the two-dimensional tests described in this report.)

13 "Pressure Distribution and Cavitation on Submerged Boundaries," by J. S. McNown, Proceedings of the Third Hydraulic Conference (1946), University of Iowa. Studies in Engineering, Bulletin No. 31, pp. 192–208.

Discussion

R. G. Folsom.[6] Fundamental data of the type presented by the author are necessary for the design of a hydraulic machine using airfoil or hydrofoil sections. It is hoped that investigations will be continued to include other shapes and to determine the reasons for the differences in wind and water-tunnel results.

Similar data on hydrofoils shaped like airfoils, developed for Mach numbers near unity, should provide information suitable for design of hydraulic machines with minimum sensitivity to cavitation.

[4] Reference (4), fig. 7.

[5] Ibid., pp. 17, 18.

[6] Professor of Mechanical Engineering, University of California, Berkeley, Calif. Mem. ASME.

In Fig. 8 of the paper the information has been plotted against the geometrical angle of attack α_0. It would be helpful to include corresponding values of the lift coefficient C_L, since C_L is proportional to α_0 throughout most of the useful range. The minimum pressure reduction occurs at about —1.4 deg but this corresponds to a lift coefficient of about 0.25. It should be noted that the angle of attack for zero lift does not correspond with the condition for minimum pressure reduction. In designing an axial-flow hydraulic machine when cavitation is important, the vanes and head produced should be adjusted to operate at the minimum pressure-reduction point.

Cavitation tests on complete axial-flow pumps indicate that the tendency toward cavitation is not quite as pronounced as would be inferred from the author's tests. The reason for this action is not self-evident, but it may be due to radial flow across the face of the blade. Further differences may be due to rising or falling pressure gradients associated with pump or turbine operation. A publication[7] by the writer has suggested a lower average cavitation-parameter magnitude be used for pump design.

R. T. KNAPP.[8] It is interesting to note that the results of determining the lift, drag, and moment characteristics of this particular shape in the water tunnel agree very closely over a wide range of angle of attack with those determined in a wind tunnel under quite different test conditions. This is good confirmation of an assumption that is commonly made, i.e, that wind tunnels and water tunnels can be used interchangeably to determine the hydrodynamic forces acting on bodies completely surrounded by flowing fluid as long as the velocities are within the range where it may be assumed that the fluid is incompressible. The other necessary assumption is that only a single phase of the fluid is involved if the test facilities are interchanged. For example, cavitation forces cannot be studied in wind tunnels because both the liquid and gas phases of the fluid are involved in the cavitation phenomenon. An important conclusion often overlooked which arises out of this universality of force coefficients is that the vast body of experimental data that have been accumulated in the field of aeronautics on the force coefficients of various-shaped airfoils and bodies of revolution are equally applicable to the fields of hydraulic structures and hydraulic machinery.

In regard to the cavitation characteristics, the writer wishes to emphasize the significance of Fig. 9 presented by the author. Here is presented the over-all picture of the resistance to cavitation of this particular shape. It should be noted that each different shape of hydrofoil would have different properties. The application of such information to the design of hydraulic machinery is of obvious importance. For example, the particular shape tested shows very little change in the conditions for incipient cavitation as the angle of attack is varied from —2 deg to +2 deg. However, the lift coefficient varies from about 0.2 at —2 deg to 0.6 at +2 deg, a 3:1 ratio. It is unfortunate that these tests do not include force measurements made under cavitating conditions. They do, however, extend our knowledge into this little-known zone through the presentation of photographic record of the appearance of cavitation as a function of the cavitation parameter. This was an important forward step, and it is hoped that it can soon be followed by force measurements as well.

J. S. MCNOWN.[9] For a given boundary geometry, it is well known that gas flow is similar to liquid flow for the same Reynolds number if compressibility effects are unimportant for the gas, and if vapor cavities do not form in the liquid. Hence this paper is significant in that it indicates not only the general similarity of air and water flow, but also specific differences between them. The degree of success in predicting conditions for incipient cavitation from wind-tunnel observations is particularly interesting.

As is pointed out in the paper, from the dimensionless pressure distribution around a given object it is possible to estimate conditions for incipient cavitation if the minimum pressure is assumed equal to the vapor pressure; the accuracy of this assumption of course determines the reliability of the result. A comparison of experimental with assumed values is possible, since the incipient cavitation number K_i can be determined by direct observation. There are various ways, both direct and indirect, of determining K_i for a given flow pattern. Visual or photographic observation of the vapor pocket, sonic detection of the bubble collapse, and observation of the effect of cavity formation on the pressure distribution are probably the most effective techniques now in use. The last-named is particularly well-suited to checking the afore-mentioned assumption, because knowledge of the pressure distribution for all stages of cavitation is available for direct comparison.

Pressure distributions have been determined for a number of head forms with and without cavitation in the water tunnel at the Iowa Institute of Hydraulic Research.[10] Two distinctly different conditions of incipient cavitation were observed: 1, For bodies which normally yielded zones of flow separation, cavities first formed in the vortexes at the boundary of the separation zone, and hence the first influence of cavitation occurred while the pressure around the body was everywhere considerably greater than vapor pressure; 2, for well streamlined bodies the cavities first formed in the immediate vicinity of the body and hence at boundary pressures approximately equal to the vapor pressure. These occurrences are clearly indicated in Fig. 20 of this discussion, for a series of rounded head forms mounted on a cylindrical shaft. For the blunt or zero-caliber head, K_i is 175 per cent or more than one velocity head greater than $(h_0 - h_{min})/(V_0^2/2g)$, whereas for the heads with radii of curvature of $D/2$ or lower, the difference is much smaller, being approximately 10 per cent of assumed value. Even for the well streamlined forms, the existence of a slight degree of separation or the presence of small vortexes in the boundary layer yields experimentals values of K_i which are greater than the assumed.

In a similar comparison of the author's results, Fig. 8, values of K_i were obtained which are less than those predicted from the

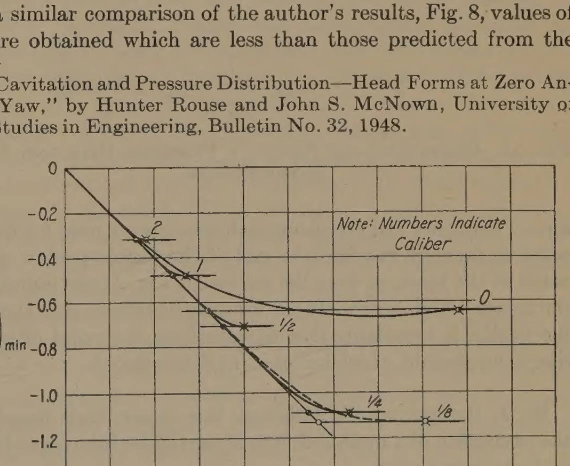

FIG. 20 VARIATION OF MINIMUM PRESSURE WITH CAVITATION NUMBER FOR ROUNDED-HEAD FORMS

[7] "The Design of Propeller Pumps and Fans," by M. P. O'Brien and R. G. Folsom, University of California Publications in Engineering, vol. 4, no. 1, 1939.

[8] Director, Hydrodynamics Laboratories, California Institute of Technology, Pasadena, Calif. Jun. ASME.

[9] Research Engineer, Iowa Institute of Hydraulic Research, State University of Iowa, Iowa City, Iowa.

[10] "Cavitation and Pressure Distribution—Head Forms at Zero Angle of Yaw," by Hunter Rouse and John S. McNown, University of Iowa Studies in Engineering, Bulletin No. 32, 1948.

wind-tunnel pressure distributions, a direct contrast to the results of the studies shown in Fig. 20 herewith. An amplification of the possible causes of error presented in the paper might explain the discrepancy. The combined effect of the vane and the near-by wall is to decrease the quantity of flow and to increase the pressure on the low-pressure side. Consequently, the tendency toward cavitation, and hence the value of K_i, would be reduced for the water-tunnel studies. Furthermore, in the studies at the University of Iowa, cavitation has never been seen or photographed until K has been reduced somewhat below K_i. Although the photographic technique used in the Caltech experiments is greatly refined by comparison, the definite possibility exists that initial stages of cavitation may be microscopic and still produce measurable effects.

Reference is made to the degree of correlation between location of the region of low boundary pressures with that occupied by the vapor cavity. Recent studies have shed further light on both the qualitative and quantitative agreement to be expected. From ultra-high-speed motion pictures of individual bubbles, Knapp and Hollander[11] have shown that the bubbles continue to expand for a brief interval of time after passing out of the zone of lowest pressure, because of the inertia of the water surrounding the cavity. Hence the ultimate collapse is delayed by the time required for this further expansion as well as for the contraction of the bubble. The lag has also been observed in the cavitation studies at the University of Iowa.[10] Silhouette photographs were used to obtain outlines of the vapor pockets for various values of K, as shown in Fig. 21 of this discussion, for the hemispherical head

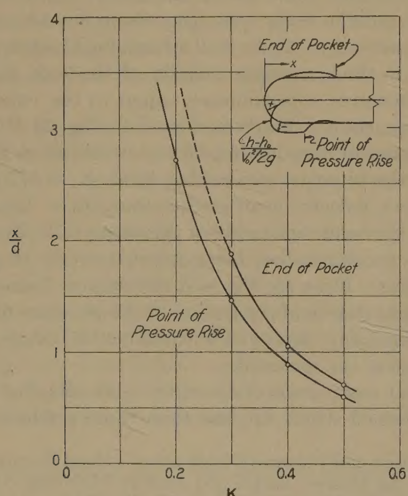

Fig. 21 Comparison of Point of Pressure Rise and End of Vapor Pocket

form. Arbitrary but consistent definitions were used for both the point of pressure rise and the end of the visible pocket, as indicated in the inset, so that the curves in Fig. 21 are indicative of the trends which occur. It can be seen therefrom that the end of the pocket is invariably downstream from the point of pressure rise by an amount which increases as K is reduced.

W. J. Rheingans.[12] Although this paper deals largely with the cavitation of a hydrofoil, it is of particular interest to hydraulic-turbine engineers.

The author, in defining "cavitation," states that it is used to signify either the phenomenon of the formation of a cavity at low pressures, or the physical damage to materials due to bubble formation and collapse in the vicinity of such cavities.

For many years hydraulic-turbine engineers have been trying to establish the definition of cavitation as applying only to the phenomenon of cavity formation. The damage to material due to the collapse of the bubbles formed in cavitation areas, has generally been known as "pitting." It is felt that there is a real need for a definite distinction between the two, because cavitation does not always result in damage to material, and can have very objectionable features other than such damage. This can best be accomplished by giving the cause and one of the possible results different names. It is hoped that such a distinction will be made in engineering fields other than those of hydraulics.

One of the interesting features mentioned by the author is the cavitation parameter defined as

$$K = \frac{P_0 - P_{vp}}{pV_0^2/2}$$

For water as the liquid, this can be written as

$$K = \frac{H_0 - H_{vp}}{V_0^2/2g}$$

where

H_0 = absolute pressure head available, ft of water
H_{vp} = vapor pressure of water, ft
V_0 = velocity of water, fps

In 1923 Dr. Thomas of Munich developed a specialized form of this cavitation-parameter formula, for use specifically with hydraulic turbines. He called this sigma, and defined it as follows

$$\sigma = \frac{H_b - H_s - H_v}{H}$$

where

H_b = barometric pressure, ft of water
H_s = static suction head on bottom of turbine runner, ft of water
H_v = vapor pressure of water, ft of water
H = head on turbine, ft

The similarity of the two formulas is apparent when it is considered that the static pressure on the bottom of a turbine runner is the atmospheric pressure H_b minus the static suction head H_s. If the runner is set below tail-water elevation, H_s is negative, and the pressure available becomes $H_b - (-H_s) = H_b + H_s$. The quantity $H_b - H_s$ therefore is the same as the H_0 or P_0 in the author's formula for cavitation parameter.

Since $V^2/2g$ is closely related to the available head H on the turbine, and since it varies as this head H, the similarity of these two formulas is quite evident. This special type of cavitation-parameter formula, used in hydraulic-turbine design and designated as sigma, is of great importance to hydraulic-turbine engineers. It is used constantly to determine the setting of reaction-type hydraulic turbines, and reference is made to it not only in engineering literature but also in specifications for hydraulic turbines.

Another interesting observation by the author is that since water will probably support a tension under dynamic loading, despite impurities and turbulence, a cavity might not form unless the fluid is subjected to low-pressure environment for a definite length of time. This theory seems to be in line with the experience on hydraulic-turbine runners. Statistical data gathered over a period of many years and covering hundreds of hydraulic-

[11] "Laboratory Investigation of the Mechanism of Cavitation," by R. T. Knapp and A. Hollander, Trans. ASME, vol. 70, July, 1948, pp. 419–435.

[12] Assistant Manager, Hydraulic Department, Allis-Chalmers Manufacturing Company, Milwaukee, Wis. Mem. ASME.

turbine installations seem to indicate that severe pitting is confined largely to the large-size runners. Since the low-pressure area on a small runner is relatively smaller than on a large runner of homologous profile, the time element required to form the cavities could account for the difference in observed damage to the metal.

It would be of great interest to hydraulic engineers if this feature of the mechanics of cavitation could be further investigated.

G. F. Wislicenus.[13] The paper reports on an experimental investigation of the high standard of quality for which the Hydraulic Machinery Laboratory of the California Institute of Technology has become well known. One immediate reaction to this paper is, obviously, a strong desire that the force measurements be extended to cover the behavior of the hydrofoil in the state of cavitation. This would seem valuable even if only a time average of the force action can be obtained.

The present test results as well as force measurement with cavitation should be compared with the results by Walchner and Martyrer.[14] These earlier investigations include force measurements with cavitation, but the photographic work as published does not seem to compare in quality with the photographic work reported by the author. The connection of photographic or visual observations with force measurements during cavitation would seem to constitute the most valuable immediate goal of further work of this type.

Development engineers in the field of hydrodynamic runners unquestionably are awaiting with eagerness the extension of the author's investigation to other profile forms, in order to obtain new information on the relations between the form of the profile and its cavitation resistance.

Regarding the comparison with wind-tunnel data, this writer believes that the agreement is closer than necessary for the majority of practical applications. It is to be expected that variations of a higher order of magnitude will result from the interaction between vanes in a system as well as from the three dimensionality of the flow in axial-flow runners.

The writer was particularly glad to see the question of a possible time or scale effect upon cavitation mentioned in this paper. This question should remain before us until the mechanism of cavitation is recognized in sufficient detail to permit a dependable answer. Reference is made to a paper by Knapp and Hollander[11] on "Laboratory Investigation of the Mechanism of Cavitation" which is certainly significant with respect to this problem.

Author's Closure

Laboratory investigations are of value if their results either contribute new information to our general store of knowledge about physical happenings or supply information of a specialized nature that can be used for design purposes. It was felt that in some measure these hydrofoil studies contributed in both ways, and it is gratifying to have the discussers indicate their general agreement.

As to application of the information to design, Professor Folsom suggested the inclusion of a diagram of K_i versus lift coefficient as an aid, and commented as to the relation between the condition for minimum pressure reduction and the lift coefficient. Professor Knapp, in a similar vein, pointed out that the rather wide range of lift coefficient over which there is very little change in the conditions for incipient cavitation. Fig. 22 of this closure shows K_i versus the value of the lift coefficient obtained in the water tunnel before cavitation appeared. Since the lift coefficient depends upon Reynolds number, the values for $\mathbf{R} = 730{,}000$ were arbitrarily selected for this graph. Within the range and accuracy of the experiments, K_i for each angle of attack was independent of $\mathbf{R}$. In addition to the points mentioned by Professors Folsom and Knapp, the graph illustrates clearly the sacrifice necessary if high lift operation is wanted.

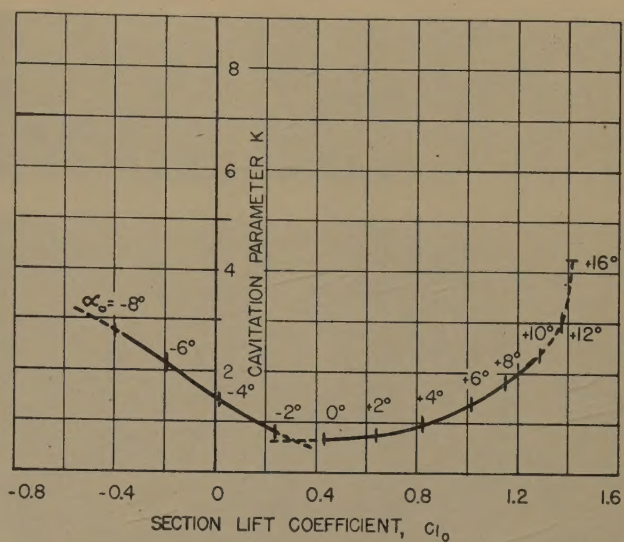

Fig. 22 Values of K_i at Which Cavitation Begins Versus Lift Coefficient Obtained Without Cavitation at $\mathbf{R} = 730{,}000$

In the process of applying this information, Mr. Rheingans' remarks on the relationship between the cavitation number and sigma are important. Maximum usefulness requires a complete understanding of their similarity.

Professor Folsom suggests that a lower average cavitation parameter magnitude be used for pump design than indicated from the tests of single hydrofoils. Turning to the reference,[7] cited by Professor Folsom, it appears that this suggestion is based partially at least upon experience with pumps which apparently operated satisfactorily even though computations of pressure reduction at the blade tips gave pressures below absolute zero. The author believes that this indicates the actual presence of cavitation. R. E. B. Sharp[15] has photographed cavitation in propeller-type turbines and established that some degree of cavitation can exist without impairing the hydraulic behavior of the machine. It is generally agreed that this is true also for centrifugal pumps. It would seem, however, that as long as the zone of cavitation is such that collapse of the individual cavities occurs on the blade surface, continued operation would result ultimately in damage to the blade. It is the author's opinion, therefore, that a blanket rule about the design figure for K_i would be unjustified. While sometimes damage is of no consequence, more frequently trouble-free operation is worth a premium.

Professors Wislicenus and Knapp both stress the desirability of obtaining measurements of forces during cavitation. Such information is of undoubted importance both for design purposes and for rounding out our general knowledge about the cavitation phenomenon and its effects. The effort to obtain force measurements at the time was abandoned reluctantly in the face of "higher priority" jobs. Professor Wislicenus mentions the works of Walchner and Martyrer,[12] which to the author's knowledge is the best information published on hydrofoil forces during cavitation. It should be noted also that many other investigators

[13] Mechanical Engineering Department, Johns Hopkins University, Baltimore, Md. Mem. ASME.

[14] "Hydromechanische Probleme des Schiffsantriebs," edited by Dr. Ing. G. Kempf and Dr. Ing. E. Foerster, Hamburg, Germany, 1932, pp. 256 and 268.

[15] "Cavitation of Hydraulic Turbine Runners," by R. E. B. Sharp, Trans. ASME, vol. 62, 1940, pp. 567–575.

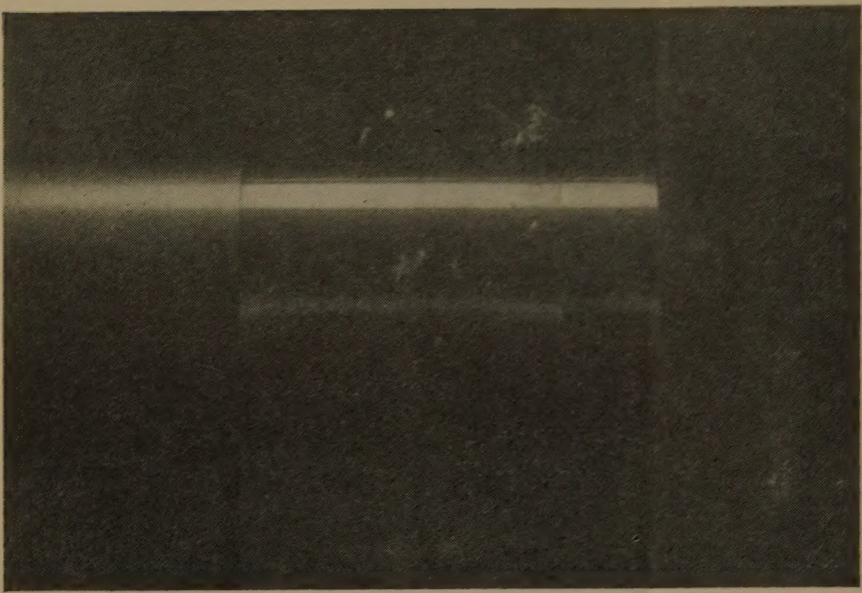

FIG. 23 SINGLE FLASH PHOTOGRAPH SHOWING CAVITATION IN VORTICES AT BOUNDARY OF SEPARATION ZONE FOR ZERO-CALIBER HEAD AT $K = 2.09$
($V_0 = 40$ fps; model diameter = 2 in. Flow from right to left past body.)

have photographed cavitation in various stages, including Mueller who reported in the same volume with Walchner and Martyrer, but it is felt that the series of pictures presented here represent the most complete description of the beginning and growth of cavitation yet published.

The importance of the degree of agreement of results with those predicted from wind-tunnel measurements was mentioned by several discussers. Interest here lies not so much in agreement between noncavitating performance coefficients, but in the degree of success in predicting the inception of cavitation from the noncavitating pressure-distribution data, which in this instance happened to be obtained in the wind tunnel. As Professors Knapp and McNown emphasize, the noncavitating coefficients should be interchangeable between fluids. Hence, a disagreement is a result only of differences in experimental conditions or procedures. As regards agreement between predicted and measured K_i, the author agrees that there is room for improvement. However, over the range of probable design values of angle of attack or lift coefficient, the agreement is good, and as Professor Wislicenus states, the effects of three-dimensionality and interference between blades undoubtedly will cause higher order deviations than the disagreements shown here.

On the other hand, as Professor McNown emphasizes, the observed deviations raise again the question of what conditions actually exist at the inception of cavitation. Professor McNown's data and remarks support the suggestion that the inception of cavitation is on a microscopic scale and occurs always at K greater than would be predicted from the noncavitating pressure distribution over the surface of the body. The visually determined K_i values reported here either agree with the predicted K_i or are lower. Involved here, in one sense, is the definition of inception of cavitation (and perhaps even of cavitation per se). As a practical matter in the application to design, it is yet to be shown that invisible cavitation has any significance, so it would seem that limitations based on K_i at which bubbles actually can be seen or photographed are more realistic. In a more scientific vein, however, these seemingly consistent series of results may hold the key to a final physical explanation of the entire cycle of happenings as K is reduced. While Professor McNown's suggestions in this respect may be entirely correct, the author has purposely withheld a definite conclusion, among the reasons for which are the following:

As mentioned in the paper and amplified by McNown, the difference in testing arrangements indicates that wall interference at high angles of attack affects the water-tunnel results. Also, as mentioned in the paper, the deviations in measured and predicted K_i values occur when cavitation is forming at a point of high curvature of the body profile. The local pressure and hence the observed K_i will be extremely sensitive to small errors in profile in these zones.

Further, the author's experience has not coincided exactly with the results presented by Professor McNown. For example, in the case of blunt bodies, Fig. 21 indicates K_i, as measured by a deviation in the pressure-distribution curve, is 1.75 for the "zero-caliber" head, and it is stated that no visual evidence of cavitation appeared until K was reduced below 1.75. Experiments at Cal-Tech, however, produced sufficient cavitation on the same shape head to see clearly at $K = 2.1$. An example appears in Fig. 23. This discrepancy may be caused by a Reynolds number effect since the Cal-Tech observations were at higher **R** than the Iowa tests. On the other hand, since the separation occurs at a sharp corner and should be independent of **R**, it would seem that the pressure distributions should be the same for the two experiments.

Finally, it is known[16] that the presence or absence of gas nuclei in a liquid will encourage or inhibit appearance of "cavitation" cavities. The role this plays in permitting cavitation near a body in a flow with variable amounts of air and various microscopic solid impurities is completely unknown. For example, it may account for the discrepancies in experience just noted, and it may be a factor in the "premature" inception obtained in the Iowa experiments. This would also support the possibility that, under favorable conditions, the water will support a tension and introduce a "scale effect" or time lag between exposure to the low pressure and formation of a cavity.

As to scale effect, it should be noted that if cavitation does originate in vortices in the boundary layer, the size of the body will affect the inception also. Mr. Rheingans' remarks are certainly another indication of the probability of scale effect.

The author is indebted to Professor McNown for correcting the unintended impression that the extent of the zone of cavities coincides "exactly" with the low-pressure zone along the surface of the hydrofoil. Agreement here was meant to be only qualitative. Since a vapor pocket will not collapse until after it passes into a high-pressure zone, it is clear there must be a "time of reaction" and, hence, some displacement between the point where the bubble passes into the high-pressure zone and the point of collapse. The amount of the displacement is not known exactly. Professor McNown's Fig. 21 distinguishes clearly between these two points and supersedes the information in his earlier publication (13).

In closing, the author wishes to express his appreciation for the interest taken by each of the discussers in this paper.

[16] "On Cavity Formation in Water," by E. Newton Harvey, W. D. McElroy, and A. H. Whiteley, *Journal of Applied Physics*, vol. 18, February, 1947, pp. 162–172.